國立臺灣大學生態學與演化生物學研究所博士論文

Institute of Ecology and Evolutionary Biology
National Taiwan University

對囊蕨屬與單葉對囊蕨多倍體化之生物地理及親緣地理學研究

Polyploidy and biogeography in genus *Deparia* and phylogeography in *Deparia lancea*

郭立園

Li-Yaung Kuo

指導老師：王俊能 博士 與 邱文良 博士

Advisor：Dr. Chun-Neng Wang & Dr. Weng-Liang Chiou

中華民國 104年 6月

June, 2015

國立臺灣大學博士學位論文
口試委員會審定書

論文中文題目

對囊蕨屬與單葉對囊蕨多倍體化之生物地理及親緣地理學研究

論文英文題目

Polyploidy and biogeography in genus *Deparia* and phylogeography in *Deparia lancea*

本論文係郭立園君（學號F97B44008）在國立臺灣大學生態學與演化生物學研究所完成之博士學位論文，於民國104年4月15日承下列考試委員審查通過及口試及格，特此證明

口試委員：

國立臺灣大學生態學與演化生物學研究所 王俊能 博士 王俊能

國立臺灣大學生態學與演化生物學研究所 胡哲明 博士 胡哲明

行政院農委會林業試驗所植物園組 邱文良 博士 邱文良

行政院農委會林業試驗所植物園組 徐嘉君 博士 徐嘉君

國立臺灣師範大學生命科學系 廖培鈞 博士 廖培鈞

國立自然科學博物館生物學組 黃俊霖 博士 黃俊霖

東海大學生命科學系 劉少倫 博士 劉少倫

所長 高文發 （簽名）

誌謝

單葉對囊蕨的多倍體親緣地理學是我最早專注的題目，最早採集紀錄距今近九年了，能有今日的研究成果不單來至一個人的努力，還來至於許多現任與前任研究室夥伴與朋友們的鉅大貢獻，以及親人在背後無私的支持與奉獻。所有三千多個日子裡的來至他人幫忙太多太多了。如今自己能回饋大家的就是希望讓大家看到一份驕傲的作品，但願不久的未來你我共同分享這份喜悅與榮耀。

這裡容我用有限的空間首先致謝兩位恩師與幾位研究夥伴。特別感謝邱文良老師與王俊能老師在這段時間於指導學生研究的用心良苦與所有奧援，我們蕨類研究的好夥伴: 海老原淳博士(Dr. Atsushi Ebihara)、正為大大、德妍大大、怡姍姐姐、佳文姐姐、天銓大大、北卡金城武、威廷大大、俊銘哥哥、資棟大大、建文學長還有碧鳳姐長久以來的採集與實驗協助，還有我們的實驗室小老闆阿 Mo 學長長期維持研究室的運作與成長。感謝秉宏、延威與培鈞學長給予族群遺傳與親緣地理分析的建議。感謝嘉君學姊在棲位模擬分析的指導與建議。感謝仁育在統計分系上的建議與協助。感謝我的高中同學老菜與杰翰在 GIS 分析軟體上的協助。感謝胡哲明老師、劉少倫學長、黃俊霖學長在論文上給予許多寶貴的意見。感謝以下許多國內外學者在這些研究提供的材料與研究資訊: 梁慧舟學長、張和明學長、毛鍋鍋學

長、劉以誠學長、胡馬度大大、朱泯寬先生、Dr. Carl J. Rothfels、Dr. Leon R. Perrie、Dr. Hank Oppenheimer、Dr. Masahiro Kato、Dr. Xian-Chun Zhang (張憲春博士)、Dr. Edmond Grangaud、Bin-Jie Ge (葛斌傑)、Duo-Qing Lin (林鐸清)、Fumikiyo Kasetani、Dr. Hong-Mei Liu (劉紅梅博士)、Hui Shang (商輝)、Kazuoki Yamaoka、Dr. Su-Kung Wu (武素功博士)、Xin-Ping Qi (齊新萍)、Yasuhiko Inoue、Dr. Yue-Hong Yan (嚴岳鴻博士)、Dr. Yu-Kun Wei (魏宇昆博士)、Dr. Yun-Fei Deng (鄧雲飛博士)、Yun-Tao Cai (蔡雲濤)、Zheng-Wei Wang (王正偉)、Dr. Sadamu Matsumoto, Dr. Goro Kokubugata、Dr. Wataru Shinohara、Dr. Remco Bouckaert、Dr. Tom A. Ranker、Dr. Germinal Rouhan、Dr. Kenneth R. Wood。感謝 MO、PNH、PE、P、TI、TNS、TAIF、TAIE、HAST、RYU 標本館與 KBCC 保種中心在材料上的協助。最後感謝中華發展基金與國科會 (NSC 96-2815-C-054 -001 -B)給予金費上的補助。

回想一起出去採集的日子真是美好，當年我高中畢業不久還留著長頭髮，這九年過雖然得過快同時留下許多大家寶貴的回憶，很開心如今的我們熱情依舊。

摘要

多倍體化(polyploidization)是一種真核生物中普遍的現象。在維管束植物中，多倍體化在蕨類演化中扮演非常特殊的角色，創造現生蕨類基因與物種多樣性。除了蕨類中常見的多倍體事件，相較於開花植物蕨類的核基因組有偏好多倍體演化的趨勢。此外，過去研究暗示多倍體類群在蕨類中有較高的拓殖能力。然而，關於蕨類多倍體的演化建立與生物地理研究相當之少。就族群建立與擴展的角度來說，成功的多倍體演化可能與歷史因子(如：年輕的演化歷史)、生態因子(如：氣候棲位偏移)、生殖因子(如：自交)有關，其中可能伴隨相關的演化適應降低了多倍體類群與二倍體親本之競爭而被滅絕的風險。為了回答蕨類多倍體如何建立與擴展族群的一系列問題，本研究論文使用對囊蕨屬(*Deparia*, Athyriaceae, Eupolypod Ⅱ, Polypodiales)的多倍體類群做為研究對象。尤其是單葉對囊蕨(*Deparia lancea*)的六倍體，本論文針對其相關因子之效應做深入的探討。對囊蕨屬的生物歷史地理與多倍體化演化重建顯示一種內的地理擴展的案例皆與多倍體化有關；但在同屬物種間的尺度，多倍體與二倍體類群的遠離散播速率並無發現有顯著之差異。在單葉對囊蕨的多倍體中(即有性的四倍體與六倍體)，歷史因子包括年輕的演化歷史與更新世氣候變遷與地質事件並非這些多倍體地理擴展的限制因子。反之，更新世早期的東亞島弧的

海洋隔閡的建立可能為這些多倍體建立的促進因子。此外，這兩個有性之多倍體推斷皆有高於二倍體之傳播速率，暗示這些多倍體都要較高之拓殖能力。在單葉對囊蕨的廣泛六倍體類群中，提升的自交能力是來至於配子器自交之偏向表現與高自交容忍度；相較於氣候棲位擴張，此自交能力的提升應為推動其族群建立與地理擴展的主要角色。此自交能力的提升讓這些六倍體拓殖能力提高，並幫助其氣候區位與實際生態區位的探索擴張。最後，依據推斷之地理分布與起源，提出單葉對囊蕨多倍體形成與建立之生物地理假說此假說，相似於“從源至匯” (source-to-sink)之種化過程。

關鍵字：生物地理，氣候棲位偏移，對囊蕨屬，單葉對囊蕨，東亞，傳播，自交 蕨類，遠距傳播，多倍體。

Abstract

Polyploidization is a universal phenomenon among eukaryotes. Among vascular plants, polyploidy in ferns play an especially important role greatly contributing to their current genetic and species diversity. This is not only because there is a high occurrence of polyploidy speciation in ferns, but also, at genomic aspects, they have evolved under a much polyploid-preferred manner than flowering plants. In addition, fern polyploids are potentially better colonizers with higher dispersal ability than diploids as implied by many previous studies. Despite these, there has scarce empirical study understanding evolutionary establishment and biogeography of fern polyploids. Regarding to establishment and subsequent expansion, the evolutionary success of a polyploid taxon should be related to different factors that are reproductive (e.g. inbreeding), ecological (e.g. climatic niche shift), in which some adaptation can reduce their extinction risk due to outcompeting by the diploid progenitors, and historical (e.g. young evolutionary age). To answer a series of questions about how ferns polyploids naturally establish and subsequently expand their population, this thesis focused on the polyploid taxa in a terrestrial fern genus *Deparia* (Athyriaceae, Eupolypod II, Polypodiales), and surveyed the relating factors associating with polyploid establishment and expansion in *Deparia lancea*, especially for its hexaploids. The reconstructions of historical biogeogeophy and polyploidy evolution based on the whole *Deparia* phylogeny revealed that all species exhibited infraspecific range expansions concurrent with polyploidization. At the species level, no significant differences of long-distance dispersal rates was detected between polyploid and diploid lineages. In *Deparia lancea* polyploids (sexual tetraploid and hexaploid), the historical factors, including young evolutionary age and recent climatic/geographical event, seem less limit their range expansion. Instead, I implied the historical event of sea barrier formation isolating East Asia Archipelago during the Early Pleistocene had possibly facilitated their successful establishments. In addition, both sexual polyploidy cytotypes were inferred with higher dispersal rates than diploids suggesting an increased colonization ability in these polyploids. In the widespread line hexaploid of *D. lancea*, I further demonstrated that an increased inbreeding ability, including inbreeding tending gender

expression and higher inbreeding tolerance, rather than broaden climatic niche might play a rather important and primary role for their successful population establishment and subsequent expansion. This increased inbreeding ability should be the major cause contributing to the high oversea colonization ability in these hexaploids, and, thus, assist their exploration in climatic niche as well as potential distribution. Finally, based on inferred distribution and origins, I proposed a biogeographical scenario for the polyploidy formation/establishment in *Deparia lancea*, which was hypothesized to be similar as a source-to-sink speciation process.

Keywords: biogeography, climatic niche shift, *Deparia*, *Deparia lancea*, East Asia, dispersal, ferns, inbreeding, long-distance dispersal, polyploid.

ACKNOWLEDGEMENTS i ii
ABSTRACT (Chinese) iii iv
ABSTRACT (English) v vi
CONTENTS vii viii

Chapter 1. General introduction of polyploidy evolution and dispersal in ferns.....1
Polyploidy in plants……1
Dispersal and polyploidy in ferns……2
Aims in this thesis……4
References……5

Chapter 2. Historical biogeography and polyploidy evolution in the genus *Deparia*……9
Abstract……9
Introduction……9
Materials and methods……10
Results……14
Discussion……16
References……19
Figures……25
Tables……34

Chapter 3. The rapid geographical range expansions and oversea dispersals of polyploid lineages in *Deparia lancea*……43
Abstract……43
Introduction……43
Materials and methods……44
Results……49
Discussion……51
References……57
Figures……62
Tables……70

Chapter 4. The phylogeography and population genetics of the *Deparia lancea* hexaploids……74
Abstract……74
Introduction……74

Materials and methods……75
Results……79
Discussion……83
References……87
Figures……88
Tables……95

Chapter 5. Inbreeding reproductive biology associating with autopolyploidization in the *Deparia lancea* hexaploids……104
Abstract……108
Introduction……108
Materials and methods……110
Results……112
Discussion……115
References……121
Figures……124
Tables……130

Chapter 6. Do climatic niche shifts facilitate geographical range expansions in the *Deparia lancea* hexaploids?……134
Abstract……134
Introduction……134
Materials and methods……136
Results……139
Discussion……141
References……143
Figures……147
Tables……153

Chapter 7. Summary and synthesis……157
Establishment and range expansion of *Deparia* polyploids……157
Historical factor and formation/establishment of *Deparia lancea* polyploids……158
Biogeography of *Deparia lancea* polyploid formation/establishment ……160
References……162

Protocols……165

Chapter 1.

General introduction of polyploidy evolution and dispersal in ferns

Polyploidy in plants

Polyploidization, or called whole genome duplication (WGD) with doubling one or more sets of nuclear genomes, is a universal phenomenon among eukaryotes and an important evolutionary force leading to their diversification. Polyploidy is particularly prevalent in vascular plant, and around 95% of extant species can be regarded as paleopolyploids, which have undergone at least one ancient WGD episode during early diversification (Nakazato *et al.* 2008; Barker & Wolf 2010; Jiao *et al.* 2011). On the other hand, nearly 35% species in vascular plants can be revealed with neopolyploids, which have undergone one or more recent WGD episode during their infrageneric diversification (Wood *et al.* 2009) (in the following I referred "polyploids" only for those neopolyploids). This high proportion of polyploids in vascular plant is associated with the frequent occurrence of unreduced gametes (i.e. genome not reduced) (reviewed in Ramsey & Schemske 1998). In addition, the polyploidization *per se* is an instant speciation mechanism providing an inherent post-zygotic reproductive isolation with diploid progenitors. Despite high occurrence of unreduced gametes and post-zygotic reproductive isolations, the natural establishment of a polyploid taxon is an evolutionary processes under selection, and the majority of nascent polyploid lineages is, however, predicted to be evolutionary dead ends during their initial formation (Parisod *et al.* 2010; Mayrose *et al.* 2015; also see Soltis *et al.* 2014a).

The success of establishment and subsequent expansion of polyploid populations might be confronted by historical, ecological, and/or reproductive factors (Arrigo & Barker 2012). Regarding to historical factors, natural distribution of polyploids can less expand due to their relatively young evolutionary age, and can be limited by the recent geographical/climatic events, such as glaciation. Compared to diploids, polyploid population can be less genetically diversified due to fewer accumulated mutations within a relatively short evolutionary time. Such

limitation of genetic diversity could also affect the long-term establishment success of a polyploid taxon. Regarding to ecological and reproductive factors, evolving with a pre-zygotic isolating mechanism with diploid progenitors avoid their extinction due to outcompeting by diploids (i.e. minority cytotype exclusion rule; Parisod *et al.* 2010; Arrigo & Barker 2012; Ramsey & Ramsey 2014). Therefore, especially when polyploid is initially minor while diploids are the majority in the same population, it is also critical for polyploids to evolve a mechanism preventing to be affected by inter-cytotype hybridization, such as ecological niche shift and assortative mating. For instance, different ecophysiological tolerances between diploid and tetraploid in *Chamerion angustifolium* (L.) Holub (Onagraceae) are likely to contribute to their potential distribution differentiation, which presumably enhance their assortative mating (Thompson *et al.* 2014). In flowering plants, the differentiation in the pollinators can also provide a premating mechanism for different cytotypes (Husband & Schemske 2000; Thompson & Merg 2008).

Nonetheless, polyploid lineages can expand their genetic variation within/among populations via other mechanisms. A polyploid taxon can increase genetic diversity by integration of multiple independent origins arisen from diploids, and can increase genotype polymorphism at individual level via intergenomic homoeologous recombination (Soltis *et al.* 2014b). In addition, the generality of invasiveness and expanded geographical range of polyploidy plants implied their increases in colonization ability for subsequent expansion, and these are always considered to link to an increased inbreeding tolerance and/or broaden ecological niche (te Beest *et al.* 2012; Buggs *et al.* 2014; Ramsey & Ramsey, 2014).

Dispersal and polyploidy in ferns

Ferns, species-richest lineage among extant seedless vascular plants, mostly utilize wind-dispersed spores to establish their natural populations, and produce only homosporous spores, that develop into the haploid gametophytes, which potentially generate egg from archegonium and sperms from antheridium. They display different biogeographical patterns than flowering plants, in part because of the higher dispersability and bisexuality potential of spores compared to seeds (Kessler 2000; Qian 2009; Kreft *et al.* 2010; Patiño *et al.* 2014, 2015). For example, ferns

comprise a greater percentage of oceanic island floras compared to mainland floras, presumably because of their greater dispersal ability (Kreft *et al.* 2010). Despite the high dispersability and bisexuality potential of fern spores, successful colonization may be hampered by inbreeding depression, especially if the colonizing founder is a single haploid gametophyte. Reproductive success of sexual species in the resulting haploid gametophyte would depend on the ability of the gametophyte to become bisexual and to self-fertilize. Such intragametophytic selfing (i.e. selfing by an egg and a sperm from the same gametophyte) would produce a completely homozygous sporophyte, which is likely suffer from inbreeding depression and unlikely to found a new population (e.g. see Ranker & Geiger, 2008, and references therein). On the other hand, species that evolve with an increased inbreeding ability or that are apomictic will stand a better chance of founding new populations from a single, colonizing gametophyte. Fern polyploids are usually found with higher inbreeding tolerances in compared to conspecific or closely related diploids, as indicated by their greater ability to produce new sporophytes via intragametophytic selfing (Masuyama & Watano 1990; Ranker & Geiger, 2008; Testo *et al.* 2015). In addition, the evolution of apomixis in ferns is usually accompanied by polyploidization (Haufler 2002). Gametophytes generated from polyploid spores of both sexual and apomictic species are better able to produce viable sporophytes because deleterious alleles are masked by heterozygosity. Thus, fern polyploids are potentially better colonizers than diploids as indicated by many previous studies (Trewick *et al*. 2002; Flinn 2006; Chen *at al*. 2014; Korall & Pryer 2014).

In ferns, polyploidy also play an especially important role greatly contributing to their current genetic and species diversity. This is not only because there is a surprising high occurrence of polyploids in ferns, but also, of genomic aspects, they have evolved under a much polyploid-preferred evolutionary manner than flowering plants. Evidence comes from the survey indicating that fern polyploids are less affected by genome downsizing and gene loss after polyploidization (i.e. processes of diploidizatio; Nakazato *et al.* 2006, 2008; Bainard *et al.* 2011; Henry *et al.* 2014), which are the post-polyploidization phenomena often observed in angiosperm (Soltis *et al.* 2003). In addition, ferns have the highest frequency of polyploidy-speciation, which is estimated double as that in the flowering plants (Otto & Whitton 2000; Wood *et al.* 2009). The

maintenances of large genome size, high gene redundancy, and high polyploidy speciation rate in ferns imply polyploidization plays a much important role in their adaptation than it in flowering plants.

Aims in this thesis

Despite exploration of cytogeography and reproductive biology, the evolutionary mechanism of establishment and subsequent expansion of fern polyploids was poorly understood, especially for the how high abundance of fern polyploids link to their biogeographical pattern. These unexplored areas are centered by three questions: comparing with diploids, (1) Do fern polyploids more frequently associate with long-dispersal and geographical range expansion? (2) Do fern polyploids have higher dispersal/colonization ability? (3) Do (3.1) historical, (3.2) ecological, or (3.3) reproductive factors affect evolutionary establishment and subsequent expansion in fern polyploids? To answer these questions, this thesis focused on a series of biogeography, phylogeography, and reproductive studies of the polyploids and their diploid close relatives in the fern genus *Deparia* Hook. & Grev. (Aythyriaceae, Eupolypod II, Polypodiales). In Chapter 2, I aimed on the historical biogeography and polyploidy evolution in the genus *Deparia*, and applied these reconstructions of ancestral states to answer the 1st question. In Chapter 3, I narrowed down the focal species with only *Deparia lancea* (Thunb.) Fraser-Jenk., in which both sexual diploids and polyploids are present. Based on the reconstruction of cytogeography and continuous phylogeography of this species, I tackled the 2nd and 3.1 questions. In Chapter 4 to 6, I further narrowed the focus on only the hexaploids in *D. lancea*. In Chapter 4, I studied population genetics and phylogeography in *D. lancea* hexaploids. By understanding the phylogeographical origins and revealing the *F*-statistics, I answered the 3.1 and 3.3 questions. In Chapter 5, I aimed on the reproductive biology of both diploids and hexaploids in *D. lancea*. By inferring their gametangium ontogeny and their inbreeding tolerances, I answered the 3.3 questions. In Chapter 6, I answered the 3.2 question by analyzing the climatic niche breadths and prefernces in both diploids and hexaploids in *D. lancea* based on niche modeling. After answering these questions, I concluded the most possible and important factors shaping the biogeography and facilitating evolutionary establishment and subsequent expansion in these *Deparia* polyploids in the final chapter. In addition, I also proposed the

biogeographical scenario of *Deparia lancea* polyploids.

References

Arrigo N, Barker MS (2012) Rarely successful polyploids and their legacy in plant genomes. *Current Opinion in Plant Biology*, **15**, 140–146.

Bainard JD, Henry TA, Bainard LD, Newmaster SG (2011) DNA content variation in monilophytes and lycophytes: large genomes that are not endopolyploid. *Chromosome Research*, **19**, 763–775.

Barker MS, Wolf PG (2010) Unfurling fern biology in the genomics age. *BioScience*, **60**, 177–185.

Buggs RJA, Wendel JF, Doyle JJ *et al.* (2014) The legacy of diploid progenitors in allopolyploid gene expression patterns. *Philosophical Transactions of the Royal Society B: Biological Sciences*, **369**, Doi: 10.1098/rstb.2013.0354.

Chen CW, Ngan LT, Hidayat A *et al.* (2014) First insights into the evolutionary history of the *Davallia repens* complex. *Blumea*, **59**, 49–58.

Flinn K (2006) Reproductive biology of three fern species may contribute to differential colonization success in post-agricultural forests. *American Journal of Botany*, **93**, 1289–1294.

Haufler CH (2002) Homospory 2002: an odyssey of progress in pteridophyte genetics and evolutionary biology. *BioScience*, **52**, 1081–1093.

Haufler CH (2014) Ever since Klekowski: testing a set of radical hypotheses revives the genetics of ferns and lycophytes. *American Journal of Botany*, **101**, 2036–2042.

Henry TA, Bainard JD, Newmaster SG (2014) Genome size evolution in Ontario ferns (Polypodiidae): evolutionary correlations with cell size, spore size, and habitat type and an absence of genome downsizing. *Genome*, **57**, 1–12.

Husband BC, Schemske D (2000) Ecological mechanisms of reproductive isolation between diploid and tetraploid *Chamerion angustifolium*. *Journal of Ecology*, **88**, 689–701.

Jiao Y, Wickett NJ, Ayyampalayam S *et al.* (2011) Ancestral polyploidy in seed plants and angiosperms. *Nature*, **473**, 97–100.

Kessler M (2000) Elevational gradients in species richness and endemism of selected plant groups in the central Bolivian Andes. *Plant Ecology*, **149**, 181–193.

Korall P, Pryer KM (2014) Global biogeography of scaly tree ferns (Cyatheaceae): evidence for Gondwanan vicariance and limited transoceanic dispersal. *Journal of Biogeography*, **41**, 402–413.

Kreft H, Jetz W, Mutke J, Barthlott W (2010) Contrasting environmental and regional effects on global pteridophyte and seed plant diversity. *Ecography*, **33**, 408–419.

Masuyama S, Watano Y (1990) Trends for inbreeding in polyploid pteridophytes. *Plant Species Biology*, **5**, 13–17.

Mayrose I, Zhan SH, Rothfels CJ et al. (2015) Methods for studying polyploid diversification and the dead end hypothesis: a reply to Soltis *et al.* (2014). *New Phytologist*, **206**, 27–35.

Nakazato T, Jung MK, Housworth EA, Rieseberg LH, Gastony GJ (2006) Genetic map-based analysis of genome structure in the homosporous fern *Ceratopteris richardii*. *Genetics*, **173**, 1585–1597.

Nakazato T, Barker MS, Rieseberg LH, Gastony GJ (2008) Evolution of the nuclear genome of ferns and lycophytes. In: *Biology and evolution of ferns and lycophytes* (eds. Ranker TA, Haufler CH), pp. 175–197, Cambridge University Press, New York.

Otto SP, Whitton J (2000) Polyploid incidence and evolution. *Annual Review of Genetics*, **34**, 401–437.

Parisod C, Holderegger R, Brochmann C (2010) Evolutionary consequences of autopolyploidy. *New phytologist*, **186**, 5–17.

Patiño J, Carine M, Fernández-Palacios JM *et al.* (2014) The anagenetic world of spore-producing land plants. *New Phytologist*, **201**, 305–311.

Patiño J, Sólymos P, Carine M *et al.* (2015) Island floras are not necessarily more species poor than continental ones. *Journal of Biogeography*, **42**, 8–10.

Qian H (2009) Beta diversity in relation to dispersal ability for vascular plants in North America. *Global Ecology and Biogeography*, **18**, 327–332.

Ramsey J, Ramsey T (2014) Ecological studies of polyploidy in the 100 years following its discovery. *Proceedings of the Royal Society B: Biological Sciences*, **369**, Doi: 10.1098/rstb.2013.0352.

Ramsey J, Schemske DW (1998) Pathways, mechanisms, and rates of polyploid formation in flowering plants. *Annual Review of Ecology and Systematics*, **29**, 467–501.

Ranker TA, Geiger JMO (2008) Population genetics. In: *Biology and evolution of ferns and lycophytes* (eds. Ranker TA, Haufler CH), pp. 107–133. Cambridge University Press, New York.

Soltis D, Segovia-Salcedo M, Jordon-Thaden I *et al.* (2014a) Are polyploids really evolutionary dead - ends (again)? A critical reappraisal of Mayrose *et al.* (2011). *New Phytologist*, **202**, 1105–1117.

Soltis DE, Visger CJ, Soltis PS (2014b) The polyploidy revolution then...and now: Stebbins revisited. *American Journal of Botany*, **101**, 1057–1078.

Soltis D, Soltis P, Bennett D, Leitch I (2003) Evolution of genome size in the angiosperms. *American Journal of Botany*, **90**, 1596–1603.

te Beest M, Le Roux JJ, Richardson DM *et al.* (2012) The more the better? The role of polyploidy in facilitating plant invasions. *Annals of Botany*, **109**, 19–45.

Testo W, Watkins Jr J, Barrington D (2015) Dynamics of asymmetrical hybridization in North American wood ferns: reconciling patterns of inheritance with gametophyte reproductive biology. *New Phytologist*, **206**, 785–795.

Thompson KA, Husband BC, Maherali H (2014) Climatic niche differences between diploid and tetraploid cytotypes of *Chamerion angustifolium* (Onagraceae). *American Journal of Botany*, **101**, 1868–1875.

Thompson J, Merg K (2008) Evolution of polyploidy and the diversification of plant-pollinator interactions. *Ecology*, **89**, 2197–2206.

Trewick S, Morgan-Richards M, Russell SJ *et al.* (2002) Polyploidy, phylogeography and Pleistocene refugia of the rockfern *Asplenium ceterach*: evidence from chloroplast DNA. *Molecular Ecology*, **11**, 2003–2012.

Wood TE, Takebayashi N, Barker MS *et al.* (2009) The frequency of polyploid speciation in vascular plants. *Proceedings of the National Academy of Sciences of the United States of America*, **106**, 13875–13879.

Chapter 2.

Historical biogeography and polyploidy evolution in the genus *Deparia*

Abstract

In this chapter, the associations between dispersal and ploidy within a phylogenetic context in the terrestrial fern genus *Deparia* were examined. Phylogenetic trees of 53 *Deparia* taxa and 13 outgroup taxa were inferred from four plastid DNA sequences (*matK, rbcL, rps16-matK* IGS, and *trnL-L-F*) generated from 53 ingroup (covering ca. 80% of the species diversity) and thirteen outgroup taxa. The origin of the genus *Deparia* was estimated to be about 27.7 Ma in continental Asia/East Asia, well after the breakup of Gondwana and its separation from Laurasia. There were multiple independent long-distance dispersals to other regions, including Africa/Madagascar, Southeast Asia, south Pacific islands, Australia/New Zealand, and the Hawaiian Islands. In addition, there were five species showing recent infraspecific range expansions. For ancestral ploidy reconstruction, 10 historical polyploidization events were inferred. All the *Deparia* species exhibited infraspecific range expansions concurrent with polyploidization. At the species level, however, no significant differences of dispersal rates were detected between polyploid and diploid lineages.

Introduction

This chapter focused on historical biogeography and polyploidization of the terrestrial fern genus *Deparia* Hook. & Grev. (Athyriaceae). This genus comprises 60–70 species. It is most species rich in Asia but is also found in Africa and islands of the western Indian Ocean (mostly in Madagascar), Australia, northeast North America, the Hawaiian Islands, and various south Pacific islands (Kato, 1984, 1993a, b). Chromosome counts have been obtained for more than one-third of *Deparia* species, and half of those have been obtained from two or more individuals (see the references in Table S2.1). Polyploids represent 52% of these reported species and 26% have conspecific diploids (Table S2.1). In addition, four

species with triploid cytotypes exhibit apomixis (Table S2.1). This information allowed current study to conduct an investigation of the relationship between biogeography and ploidy in *Deparia*. This study first conducted molecular phylogenetic analyses to produce a dated molecular phylogeny based on cpDNA regions. Because to my knowledge there is no developed methodology allowing to tackle both cytotype and geography traits to assess their possible phylogenetic correlation, I reconstructed ancestral states of geographical distribution and ploidy separately, and revealed the associations between historical biogeography and polyploidization events in *Deparia* based on these reconstructions.

Materials and methods

Species sampling and molecular dataset

Fifity three taxa in *Deparia* were sampled, which cover 75–88% of the described species and subspecies. Putative sterile hybrids were not included [e.g. *D. tomitaroana* (Masam.) R. Sano and *D. lobatocrenata* (Tagawa) M. Kato]. This ingroup sampling covered all major geographical regions occupied by the genus. The outgroup taxa included eleven species representing all of the other genera in Athyriaceae (Rothfels *et al.* 2012a) and two species from Onocleaceae and Blechnaceae. I obtained sequences of four plastid DNA regions, including two non-coding regions, *rps16-matK* intergenic spacer (IGS) and *trnL-L-F* (i.e. *trnL* intron + *trnL-F* IGS), and two coding regions, *matK* and *rbcL*, for phylogenetic analyses. In addition to previously published studies (Kuo *et al.* 2011; Li *et al.* 2011; Rothfels *et al.* 2012a), 127 new sequences of *Deparia* and outgroup species were obtained in this study.

The DNA extraction procedures were detailed in Protocol 1 and 2. PCR conditions and PCR primer sets used followed Li *et al.* (2011) and Rothfels *et al.* (2012a). For several *Deparia* samples extracted from herbarium materials, newly designed primers were applied to amplify and sequence shorter DNA fragments. Primer information is in Table S2.2. Voucher information and GenBank accession numbers are in Table S2.3 and S2.4.

For a molecular dating analysis of *matK* + *rbcL* (see below), additional 38 outgroup taxa were included, especially from Eupolypod II, mostly following Kuo *et al.* (2011) and Rothfels *et al.* (2012a). Among them, 33 outgroup species represented all Eupolypod II families, and

another three and two species were from Eupolypod I and pteroids, respectively, were included (Table S2.4). However, *Deparia tenuifolia* was excluded due to the unavailability of a *matK* sequence.

Phylogenetic analyses

DNA sequences were aligned with ClustalW implemented in BioEdit (Hall 1999) and the alignments were further edited manually. Gaps were treated as missing data in maximum likelihood (ML) analyses (see below). To infer the appropriate nucleotide substitution model for the phylogenetic analyses, jModelTest (Posada 2008) was employed, and the model was selected based on the Akaike information criterion (Akaike 1974). Garli 2.0 (Zwickl 2006) was used to conduct ML phylogenetic analyses. The proportions of invariant sites and state frequencies were estimated by the program. The "genthreshfortopoterm" and the "collapsebranches" options were set to 20,000 and 0, respectively. To infer ML bootstrap support (BS) trees, 500 replicates were run under the same criteria. For the dated-phylogeny based on *matK* + *rbcL* (see below), a constrained topology based on the phylogenetic structure at the Eupolypod II family level as inferred by Rothfels *et al.* (2012a) [i.e. the same as the well supported family phylogenetic structure shown in Fig. 4 of Rothfels *et al.* (2012b)] was applied to avoid strong topological uncertainty during the tree search due to inadequate character information. To infer ML bootstrap phylograms of this dataset, 250 replicates were run.

Divergence time estimates

For estimates of lineage divergence times within *Deparia*, two molecular dating analyses with ML trees were conducted based on different datasets using penalized rate smoothing: (1) *matK* + *rbcL* and (2) *rps16-matK* IGS + *matK* + *rbcL* + *trnL-L-F* (referred to as the first and second analyses, respectively, in the following text). The program r8s (Near & Sanderson 2004) was employed for molecular dating using the penalized rate smoothing algorithm. The goal of the first analysis was to infer the date of origin of Athyriaceae and origin of the genus *Deparia*. For the first analysis, both the most likely ML tree and 250 ML BS trees were used, which were inferred from coding regions to avoid branch length uncertainty due to potential missing data resulting from alignment of non-coding regions. In this analysis, I applied one fixed-age and two

minimum-age constraints: Euploypod II = 103.1 Ma (Schuettpelz & Pryer 2009), *Cyclosorus* ≥ 33.9 Ma (Eocene; Collinson 2001), and *Onoclea* ≥ 55.8 Ma (Paleocene; Rothwell & Stockey 1991). The position of calibration nodes can be seen in Fig. S2.1 (i.e. node A B C). The second molecular dating analysis aimed to infer node ages within *Deparia* based on more DNA regions, which included two additional variable non-coding regions (i.e. *rps16-matK* IGS and *trnL-L-F*). I used both the most likely ML tree and 500 ML BS trees in an analysis with two fixed-age constraints: the node of Athyriaceae and of *Deparia*. These two age constraints were obtained from the result of the first molecular dating analysis. The dating results of ML BS trees were finally summarized by TreeAnnotator (Drummond *et al.* 2012) using the topology of the most likely ML tree.

Biogeographical analyses

For the biogeographical analyses, eight biogeographical regions were defined, including (A) continental Asia/East Asia (including South Asia), (B) northeast North America, (C) Southeast Asia (including the Philippines, Malaysia, Indonesia, and New Guinea), (D) south Pacific islands (including Fiji and French Polynesia), (E) Central and South America (only for the outgroup taxa - *Athyrium skinneri* T. Moore and *Diplazium bombonasae* Rosenst.), (F) Africa/Madagascar (including La Réunion, Comoros, and Mauritius), (G) Australia/New Zealand, and (H) the Hawaiian Islands (Fig. 2.1A). The geographical distributions of *Deparia* species were mostly scored following the monographic work of Kato (1984, 2001), except for *D. boryana* (Willd.) M. Kato. In the current study, *D. boryana* was referred to an African/Madagascan species (including La Réunion, Comoros, and Mauritius), for which the type was collected from La Réunion, whereas the *D. boryana* regarded by Kato (1984) was actually *D. edentula* (Kunze) X. C. Zhang, as referred to here. For some Chinese *Deparia* and other Athyriaceae species, which were not included in Kato (1984), distributions were obtained from other sources (Kato 1993b; Mickel & Smith 2004; Wang *et al.* 2013).

To infer the ancestral distribution within *Deparia*, analyses both from Lagrange v.20120508 (Ree *et al.* 2005; Ree & Smith 2008) and S-DIVA (RASP v2.1b, Yu *et al.* 2010) were performed. For both analyses, no dispersal constraints were enforced, and the maximum area number was set to four to avoid an underestimation of vicariance events, since the

maximum number of biogeographical regions of *Deparia* taxa was four (Table S2.1). Blechnaceae and Onocleaceae were removed from all ML trees or chronograms due to an inability to resolve the relationships of the outgroups by ML analyses. For Lagrange, the chronogram resulting from the second molecular dating analysis was applied, but, according to the topology of the original ML phylogram, the collapsed branches on polytomy nodes within this chronogram was "resolved" (i.e. being bifurcated with zero branch length), which were resulted from r8s and not allowed for the input of Lagrange. Other optimizations followed the default setting of the online configuration tool (http://www.reelab.net/lagrange). The S-DIVA analysis was used to consider topological uncertainty on ancestral distribution reconstruction; the original 500 ML BS phylograms was applied, and the results were summarized using the topology of the most likely ML tree.

Spore size measurements

For several species for which cytotype information was not available, spore sizes (100 spores per sample) were measured to infer ploidy by comparison with those of known diploid relatives (voucher information given in Table S2.5).

Ancestral ploidy reconstruction

The cytological data of *Deparia* (Table S2.1) and the re-calibrated chronogram of Athyriaceae (i.e. the same as for the Lagrange analysis) were used to infer ancestral ploidy via ChromEvol v1.3 (Mayrose *et al.* 2010, 2011). This program was used to estimate the probability of chromosome number on phylogenetic branches via a likelihood function. With a few adjustments of the default settings, the following procedure with ChromEvol was used to infer ancestral ploidy: (1) infraspecific polyploidization was ignored and, therefore, only the record of the lowest chromosome number for each species was adopted, (2) the basic number equal to 40 (x = 40) was uniformly applied to replace 41 in *Diplazium* and some *Cornopteris* records, (3) the inferred gametic chromosome number from reports of sporophytic numbers (i.e. half the number for apomictic taxa) was applied, and (4) only one constant rate parameter to infer polyploidization was allowed (i.e. duplConstR was estimated, demiPolyR = -2, while the others were set to -999).

Dispersal rate variation in diploid and polyploid lineages

To understand the effects of the phylogenetic uncertainty of branch length on the significance of inferred differential dispersal rates between diploids and polyploids, I adopted the following approach. The chronograms of 500 ML BS trees were randomly and equally divided into ten subsets (i.e. each subset had 50 chronograms). For each subset, a new chronogram was summarized with TreeAnnotator (Drummond *et al.* 2012) using the topology of the most likely ML tree. Based on the results of biogeographical analyses and ancestral ploidy reconstruction (see above), dispersal rates (i.e. dispersal events/total branch lengths) for diploid and polyploid lineages were inferred from these ten new chronograms. A *t*-test was applied to test for significant differences between the dispersal rates of diploid and polyploid lineages.

Results

Phylogenetic relationships and divergence times

The ML phylogeny of *Deparia* was shown in Figs. 2.1B, 2.2 and S2.2. The inferred relationships were consistent with previous studies (Sano *et al.* 2000a, b; Ebihara 2011) but provided greater resolution of species clusters, with seven highly supported clades (Figs. 2.1 and S2.2). The chronogram inferred by penalized rate smoothing is shown in Fig. 2.2. The molecular dating of several important nodes inferred with biogeographical events (see below) was summarized in Table 2.1. Compared to the dating inferred by previous studies (Schuettpelz & Pryer 2009; Rothfels *et al.* 2015) for the divergence time of *Deparia* (24.7 and 21.6 Ma), the estimate in this study was earlier (i.e. node 0 or the crown group of *Deparia*: 27.68–33.99 Ma). Estimates of molecular dating using the penalized rate smoothing algorithm with the ML phylogeny of *matK* + *rbcL* (i.e. the first molecular dating analysis) were shown in Fig. S2.1.

Historical biogeographical patterns

The results inferred by Lagrange and S-DIVA were mapped on the *Deparia* phylogeny (Fig. 2.1). Compared to Lagrange, S-DIVA tended to infer more ancestral areas on the internal branches, which may have been due to its vicariance-biased computation (Clark *et al.* 2008; Kodandaramaiah 2010; Wen *et al.* 2013). Despite this, the most likely ancestral area on most branches (i.e. with the highest probability) was identical between the results of the two analyses. *Deparia* was inferred to

have originated on continental Asia/East Asia (node *0* in Fig. 2.1). Several historical dispersals were inferred (Fig. 2.1), including dispersal to Africa/Madagascar (node *a* in clade DR), dispersal to northeast North America (node *d* in clade LU), dispersal to the Hawaiian Islands (node *e* in clade DE), dispersal to south Pacific islands (node *g* in clade AT), dispersal to Southeast Asia (node *i* in clade AT), and dispersal to Australia/New Zealand (the descendent branches of node h). There were also several infraspecific range expansions from continental Asia/East Asia to Southeast Asia (*Deparia lancea* and *D. edentula*), Southeast Asia + south Pacific islands (*D. subfluvialis*), and south Pacific islands + Australia/New Zealand (D. *petersenii* subsp. *deflexa*), and from continental Asia/East Asia + Southeast Asia to Africa/Madagascar (*D. petersenii* subsp. *petersenii*). These large range shifts undoubtedly resulted from long-distance dispersals since their divergence times were estimated to be much younger (Fig. 2.2) than the breakup of Gondwana and its separation with Laurasia. The dispersal and extinction events inferred by Lagrange were mapped on the chronogram in Fig. 2.2.

Cytology and ancestral ploidy reconstruction

The ploidies of four *Deparia* species were inferred by their spore sizes by comparison with species of known cytotype in the same phylogenetic clade. All species examined here possessed 64-spored sporangia, suggesting that all are sexual species. For *D. glabrata* and *D. parvisora*, spore sizes were within the range of other diploid species in clade DR (Table S2.5), and suggested that both were diploids. For *D. fenzliana* and *D. prolifera*, spore sizes were significant larger than the other diploid species in clade DE (*t*-test P values < 0.001). This suggested that both are sexual polyploids. To avoid overestimation of polyploidization events in this analysis, *D. fenzliana* and *D. prolifera* were assumed as tetraploids since this cytotype is the lowest ploidy among all known sexual polyploids in *Deparia*. The results of ancestral ploidy reconstruction via ChromEvol are shown in Fig. 2.1. In total, ten historical polyploidization events [including demiploidization (e.g. from diploid to triploid)] were inferred (Table 2.2). These polyploidization events were also mapped on the chronogram in Fig. 2.2. In sum, the total tree lengths in units of year of diploid and polyploid lineages were 308.19 and 42.97 Ma, respectively (Table 2.2). By comparing the inferred ploidies of ancestral nodes to those of terminal taxa, 13 species with

infraspecific polyploidization were detected (i.e. polyploidization after speciation; Fig. 2.1 and Table 2.2).

Dispersal rate in diploid and polyploid lineages

Current analyses could not discern polyploidization occurred prior to long-distance dispersal if both kinds of events occurred on a single branch, and there was only one phylogenetic branch coupled with both dispersal and a polyploidization event (i.e. branch leading to Hawaiian species; Fig. 2.2). Even under the assumption of polyploidization prior to dispersal, the mean dispersal rate of polyploid lineages ($2.328 \pm 0.142 \times 10^{-2}$ Ma^{-1}) was not significantly different from that of diploid lineages ($2.323 \pm 0.043 \times 10^{-2}$ Ma^{-1}) (mean ± one standard deviation; *P* value = 0.46, *t*-test).

Discussion

Dispersal events in Deparia

My results support an origin of *Deparia* on continental Asia/East Asia at 27.68 Ma (27.68–33.99 Ma for 95% Highest Posterior Density), well after the breakup of Gondwana that was initiated at about 180 Ma (Table 2.1), with a long-distance dispersal from continental Asia/East Asia to Africa during the Miocene to Pliocene (Fig. 2.2). Such long-distance dispersals have been inferred in other fern taxa of varying ages (Wang *et al.* 2012). In addition, a recent diversification of Madagascan endemics from African lineage(s) was inferred (node *c* in Fig. 2.1B and Table2.1) similar to those found in scaly tree ferns (Janssen *et al.* 2008; Korall & Pryer, 2014). Further investigation based on more comprehensive sampling is needed to confirm the biogeographical scenario of African/Madagascan *Deparia*. The dispersal of *Deparia* species from continental Asia/East Asia to northeast North America could have been via the Bering land bridge, which connected the two continents at least until the Quaternary (Tiffney & Manchester 2001). This possibility is also implied by the divergence time estimate results, which showed the northeast North American endemic *D. acrostichoides* splitting from continental Asia/East Asia relatives during the Miocene (Figs. 2.1B and 2.2; node *d* in Table 2.1). Thus, vicariant speciation due to the loss of the land bridge and/or past climate change, rather than trans-oceanic, long-distance dispersal, might account for the distribution of *D. acrostichoides*. A similar scenario has been suggested for other cases of

East Asian-northeast North American disjunctions of ferns and seed plants (Kato 1993a; Wen 1999; Tiffney & Manchester 2001; Lu *et al.* 2011; Xiang *et al.* 2015).

For the endemic *Deparia* taxa on south Pacific islands and the Hawaiian Islands, long-distance dispersals from continental Asia/East Asia during the Miocene to Pleistocene were inferred (nodes *e* and *g* in Fig. 2.1B and Table 2.1). Interestingly, the estimated divergence time of the Hawaiian lineage splitting from continental Asian relatives (node e in Fig. 2.1B and Table 2.1; i.e. > 7 Ma) was older than the age of the oldest current high Hawaiian island of Kauaʻi (5.1 Ma; Neall &Trewick 2008). The most likely scenario is that an ancestral species colonized a geologically older island with subsequent dispersals down the island chain as new islands were produced by the volcanic hot spot. A similar situation was found in the Hawaiian endemic diellia lineage of *Asplenium* species (Schneider *et al.* 2005). In addition to these historical dispersal events, there were several recent infraspecific range expansions, including those in *D. subfluvialis*, *D. edentula*, *D. lancea*, *D. petersenii* subsp. *deflexa*, and *D. petersenii* subsp. *petersenii*, which showed increased biogeographical areas after speciation (Figs. 2.1B and 2.2). These species expanded from continental Asia/East Asia or continental Asia/East Asia + Southeast Asia and further dispersed to adjacent areas, including Southeast Asia, south Pacific islands, Australia/New Zealand, and Africa/Madagascar (Fig. 2.1B).

Relationship between biogeography and polyploidy

The number of branches relating to dispersal and to polyploidization were summarized in Table 2.2. Within *Deparia* species phylogeny, no dispersal event was confirmed after polyploidization (Fig. 2.2 and Table 2.2). Only one dispersal event was coupled with polyploidization and this proportion (i.e. 1/10; dispersal coupled with polyploidization/total polyploidization events; Table 2.2), although superficially higher than the proportion of dispersals retaining diploidy (7/76 = 1/10.9), was not significantly different even if this polyploidization is assumed to be occurred earlier than the dispersal event. Besides, these phylogenies resulted from cpDNA dataset and could only inferred partial parent lineages for those taxa with hybrid origin, such as allopolyploids. Consequently, the ancestral distribution and ploidy reconstruction based on these phylogenies could not fully represent the evolutionary history of

allopolyploids, and a similar analyzing limitation was also mentioned in Soltis *et al.* (2014) and Mayrose *et al.* (2015). This single dispersal event coupled with polyploidization was the long-distance dispersal from continental Asia/East Asia to the Hawaiian Islands (Fig. 2.1B). The earliest derived species among the Hawaiian taxa, *D. fenzliana*, seems to be of allopolyploid origin based on a low-copy nuclear marker phylogeny (see Chapter 3). Similarly, dispersal(s) of polyploids was also revealed in the terrestrial fern genus *Polystichum* to the Hawaiian Islands. The Hawaiian endemic tetraploid *P. haleakalense* Brack. and endemic octoploid *P. bonseyi* W. H. Wagner & R. W. Hobdy are most closely related to *P. wilsonii* Christ, which is a tetraploid species in continental Asia/East Asia (Driscoll & Barrington 2007). However, long-distance colonizers in ferns also include diploids, and, for example, the African/Madagascan *Deparia* and Hawaiian endemic *Polystichum hillebrandii* (Driscoll & Barrington 2007). Polyploids have usually been estimated to comprise 40–75% of the fern flora of oceanic islands (Walker 1984; Wagner 1995), which is generally greater than what has been estimated for continental fern floras (e.g. 23–36% in the Himalayan region in continental Asia, Walker 1984; ca. 38% in Australia, Tindale & Roy 2002; 42% in North America, Bogonovich 2012). Further research should address if these differences are the result of higher dispersal rates of polyploids and/or higher polyploid diversification rates on oceanic islands.

In contrast to the results inferred from the species-level phylogeny, the infraspecific range expansions in *Deparia* were associated with polyploidy, which occurred in all of the five geographically expanding taxa - *D. subfluvialis*, *D. edentula*, *D. lancea*, *D. petersenii* subsp. *deflexa*, and *D. petersenii* subsp. *petersenii* (Fig. 2.1B and Table 2.2). Although the current cytological data are still insufficient to examine the potential dominance of polyploids in most biogeographical regions (Table S2.1), cytogeographical studies in two of these *Deparia* species provide further evidence supporting range expansion of polyploids: the broadly distributed sexual polyploids of both *D. petersenii* subsp. *petersenii* and *D. lancea* originated from geographically restricted diploids (Fig. 2.3; Shinohara *et al.* 2006; Kuo *et al.* 2008; also see in Chapter 3). In addition, the apomictic triploid *D. unifurcata* seems to be more abundant, and are found in many places (Honshu in Japan and Yunnan and Guizhou in China; Kato *et al.* 1992; Takamiya 1996; Nakato personal

communication), whereas the sexual diploid is only known from Sichuan, China (Cheng & Zhang, 2010). This suggests that polyploids in these three *Deparia* species are potentially better dispersers/colonizers than their sexual diploid relatives. It has been also suggested in several other fern groups due to the likelihood that polyploid gametophytes are better able to successfully self fertilize or to be apomictic than haploid gametophytes (Trewick *et al.* 2002; Flinn 2006; Korall & Pryer 2014; Chen *at al.* 2014).

References

Akaike H (1974) A new look at the statistical model identification. *IEEE Transactions on Automatic Control*, **19**, 716–723.

Bogonovich MD (2012) Broad-scale geographical evolution of ferns. Ph.D thesis, Indiana University, U.S.A.

Chen CW, Ngan LT, Hidayat A *et al.* (2014) First insights into the evolutionary history of the *Davallia repens* complex. *Blumea*, **59**, 49–58.

Cheng X, Zhang SZ (2010) Index to chromosome numbers of Chinese Pteridophyta (1969-2009). *Journal of Fairylake Botanical Garden*, **9**, 1–58.

Clark JR, Ree RH, Alfaro ME *et al.* (2008) A comparative study in ancestral range reconstruction methods: retracing the uncertain histories of insular lineages. *Systematic Biology*, **57**, 693–707.

Collinson M (2001) Cainozoic ferns and their distribution. *Brittonia*, **53**, 173–235.

Driscoll H, Barrington D (2007) Origin of Hawaiian *Polystichum* (Dryopteridaceae) in the context of a world phylogeny. *American Journal of Botany*, **94**, 1413–1424.

Drummond AJ, Suchard MA, Xie D, Rambaut A (2012) Bayesian phylogenetics with BEAUti and the BEAST 1.7. *Molecular Biology and Evolution*, **29**, 1969–1973.

Ebihara A (2011) *RbcL* phylogeny of Japanese pteridophyte flora and implications on infrafamilial systematics. *Bulletin of the National Museum of Nature and Science. Series B, Botany*, **37**, 63–74.

Flinn K (2006) Reproductive biology of three fern species may contribute to differential colonization success in post-agricultural forests. *American Journal of Botany*, **93**, 1289–1294.

Hall T (1999) BioEdit: a user-friendly biological sequence alignment editor and analysis program for Windows 95/98/NT. *Nucleic Acids Symposium Series*, **41**, 95–98.

Janssen T, Bystriakova N, Rakotondrainibe F *et al.* (2008) Neoendemism in Madagascan scaly tree ferns results from recent, coincident diversification bursts. *Evolution*, **62**, 1876–1889.

Kato M (1984) A taxonomic study of the athyrioid fern genus *Deparia* with main reference to the Pacific species. *Journal of the Faculty of Science Section Ⅲ*, **13**, 371–430.

Kato M, Nakato N, Cheng X, Iwatsuki K (1992) Cytotaxonomic study of ferns of Yunnan, southwestern China. *The Botanical Magazine*, **105**, 105–124.

Kato M (1993a) Biogeography of ferns: dispersal and vicariance. *Journal of Biogeography*, **20**, 265–274.

Kato M (1993b) *Deparia* and *Athyrium*. In: *Flora of North America, Vol. 2.*, pp. 254–258. Oxford University Press, New York.

Kato M (2001) *Deparia cataracticola* (Woodsiaceae), a new species from Hawaii. *Acta Phytotaxonomica et Geobotanica*, **52**, 1–9.

Kodandaramaiah U (2009) Use of dispersal-vicariance analysis in biogeography - a critique. *Journal of Biogeography*, **37**, 3–11.

Korall P, Pryer KM (2014) Global biogeography of scaly tree ferns (Cyatheaceae): evidence for Gondwanan vicariance and limited transoceanic dispersal. *Journal of Biogeography*, **41**, 402–413.

Kuo LY, Chiou WL, Wang CN (2008) Cytogeography and polyploidy evolution in *Deparia lancea* group. Poster in conference *Botany 2008*, Vancouver, Canada.

Kuo LY, Li FW, Chiou WL, Wang CN (2011) First insights into fern *matK* phylogeny. *Molecular Phylogenetics and Evolution*, **59**, 556–566.

Li FW, Kuo LY, Rothfels CJ *et al.* (2011) *RbcL* and *matK* earn two thumbs up as the core DNA barcode for ferns. *PLoS one*, **6**.

Lu JM, Li DZ, Lutz S *et al.* (2011) Biogeographic disjunction between eastern Asia and North America in the *Adiantum pedatum* complex (Pteridaceae). *American Journal of Botany*, **98**, 1680–1693.

Mayrose I, Barker MS, Otto SP (2010) Probabilistic models of chromosome number evolution and the inference of polyploidy. *Systematic Biology*, **59**, 132–144.

Mayrose I, Zhan SH, Rothfels CJ *et al.* (2011) Recently formed polyploid plants diversify at lower rates. *Science*, **333**, 1257.

Mayrose I, Zhan SH, Rothfels CJ *et al.* (2015) Methods for studying polyploid diversification and the dead end hypothesis: a reply to Soltis *et al.* (2014). *New Phytologist*, **206**, 27–35.

Mickel JT, Smith AR. 2004. *The pteridophytes of Mexico*. The New York Botanical Garden Press, New York.

Neall VE, Trewick S a (2008) The age and origin of the Pacific islands: a geological overview. *Philosophical Transactions of the Royal Society B: Biological Sciences*, **363**, 3293–3308.

Near TJ, Sanderson MJ (2004) Assessing the quality of molecular divergence time estimates by fossil calibrations and fossil-based model selection. *Philosophical Transactions: Biological Sciences*, **359**, 1477–1483.

Ranker TA, Geiger JMO (2008) Population genetics. In: *Biology and Evolution of ferns and Lycophytes* (eds. Ranker TA, Haufler CH), pp.

107–133. Cambridge University Press, New York.

Ree R, Moore B, Webb C, Donoghue M (2005) A likelihood framework for inferring the evolution of geographic range on phylogenetic trees. *Evolution*, **59**, 2299–2311.

Ree RH, Smith S A (2008) Maximum likelihood inference of geographic range evolution by dispersal, local extinction, and cladogenesis. *Systematic Biology*, **57**, 4–14.

Rothfels CJ, Larsson A, Kuo LY *et al.* (2012a) Overcoming deep roots, fast rates, and short internodes to resolve the ancient rapid radiation of eupolypod II ferns. *Systematic Biology*, **61**, 490–509.

Rothfels CJ, Sundue MA, Kuo L-Y *et al.* (2012b) A revised family-level classification for eupolypod II ferns (Polypodiidae: Polypodiales). *Taxon*, **61**, 515–533.

Rothfels CJ, Windham MD, Pryer KM (2013) A plastid phylogeny of the cosmopolitan fern family Cystopteridaceae (Polypodiopsida). *Systematic Botany*, **38**, 295–306.

Rothwell GW, Stockey R A. (1991) *Onoclea sensibilis* in the Paleocene of North America, a dramatic example of structural and ecological stasis. *Review of Palaeobotany and Palynology*, **70**, 113–124.

Sano R, Takamiya M, Ito M, Kurita S, Hasebe M (2000a) Phylogeny of the lady fern group, tribe Physematieae (Dryopteridaceae), based on chloroplast *rbcL* gene sequences. *Molecular Phylogenetics and Evolution*, **15**, 403–413.

Sano R, Takamiya M, Kurita S, Ito M, Hasebe M (2000b) *Diplazium subsinuatum* and *Di. tomitaroanum* should be moved to *Deparia* according to molecular, morphological, and cytological characters. *Journal of Plant Research*, **113**, 157–163.

Schneider H, Ranker T a, Russell SJ *et al.* (2005) Origin of the endemic fern genus *Diellia* coincides with the renewal of Hawaiian terrestrial life in the Miocene. *Proceedings of the Royal Society B: Biological Sciences*, **272**, 455–460.

Schuettpelz E, Pryer KM (2009) Evidence for a Cenozoic radiation of ferns in an angiosperm-dominated canopy. *Proceedings of the National Academy of Sciences of the United States of America*, **106**, 11200–11205.

Shinohara W, Hsu TW, Moore SJ, Murakami N (2006) Genetic analysis of the newly found diploid cytotype of *Deparia petersenii* (Woodsiaceae: Pteridophyta): evidence for multiple origins of the tetraploid. *International Journal of Plant Sciences*, **167**, 299–309.

Soltis D, Segovia-Salcedo M, Jordon-Thaden I *et al.* (2014) Are polyploids really evolutionary dead - ends (again)? A critical reappraisal of Mayrose *et al.* (2011). *New Phytologist*, **202**, 1105–1117.

Tiffney BH, Manchester SR (2001) The use of geological and paleontological evidence in evaluating plant phylogeographic hypotheses in the northern hemisphere Tertiary. *International Journal of Plant Sciences*, **162**, S3–17.

Tindale M, Roy S (2002) A cytotaxonomic survey of the Pteridophyta of Australia. *Australian Systematic Botany*, **15**, 839–937.

Trewick S, Morgan-Richards M, Russell SJ *et al.* (2002) Polyploidy, phylogeography and Pleistocene refugia of the rockfern *Asplenium ceterach*: evidence from chloroplast DNA. *Molecular Ecology*, **11**, 2003–2012.

Wagner JW (1995) Evolution of Hawaiian ferns and fern allies in relation to their conservation status. *Pacific Science*, **49**, 31–41.

Walker TG (1984) Chromosomes and evolution in pteridophytes. In: *Chromosomes in evolution of eukaryotic groups. Vol. 2*, pp. 103–141. CRC Press, Boca Raton.

Wang L, Schneider H, Zhang XC, Xiang QP (2012) The rise of the Himalaya enforced the diversification of SE Asian ferns by altering the monsoon regimes. *BMC Plant Biology*, **12**, 210.

Wang CR, He ZR, Kato M (2013) Athyriaceae. In: *Flora of China Vol. 2-3.*, pp. 418–534. Science Press, Beijing.

Wen J (1999) Evolution of eastern Asian and eastern North American disjunct distributions in flowering plants. *Annual Review of Ecology and Systematics*, **30**, 421–455.

Wen J, Ree R, Ickert-Bond S, Nie Z, Funk V (2013) Biogeography: where do we go from here? *Taxon*, **62**, 912–927.

Xiang JY, Wen J, Peng H (2015) Evolution of the eastern Asian-North American biogeographic disjunctions in ferns and lycophytes. *Journal of Systematics and Evolution*, **53**, 2–32.

Yu Y, Harris AJ, He XJ (2010) S-DIVA (Statistical Dispersal-Vicariance Analysis): a tool for inferring biogeographic histories. *Molecular Phylogenetics and Evolution*, **56**, 848–850.

Zwickl DJ (2006) Genetic algorithm approaches for the phylogenetic analysis of large biological sequence datasets under the maximum likelihood criterion. Ph.D thesis, The University of Texas, Austin.

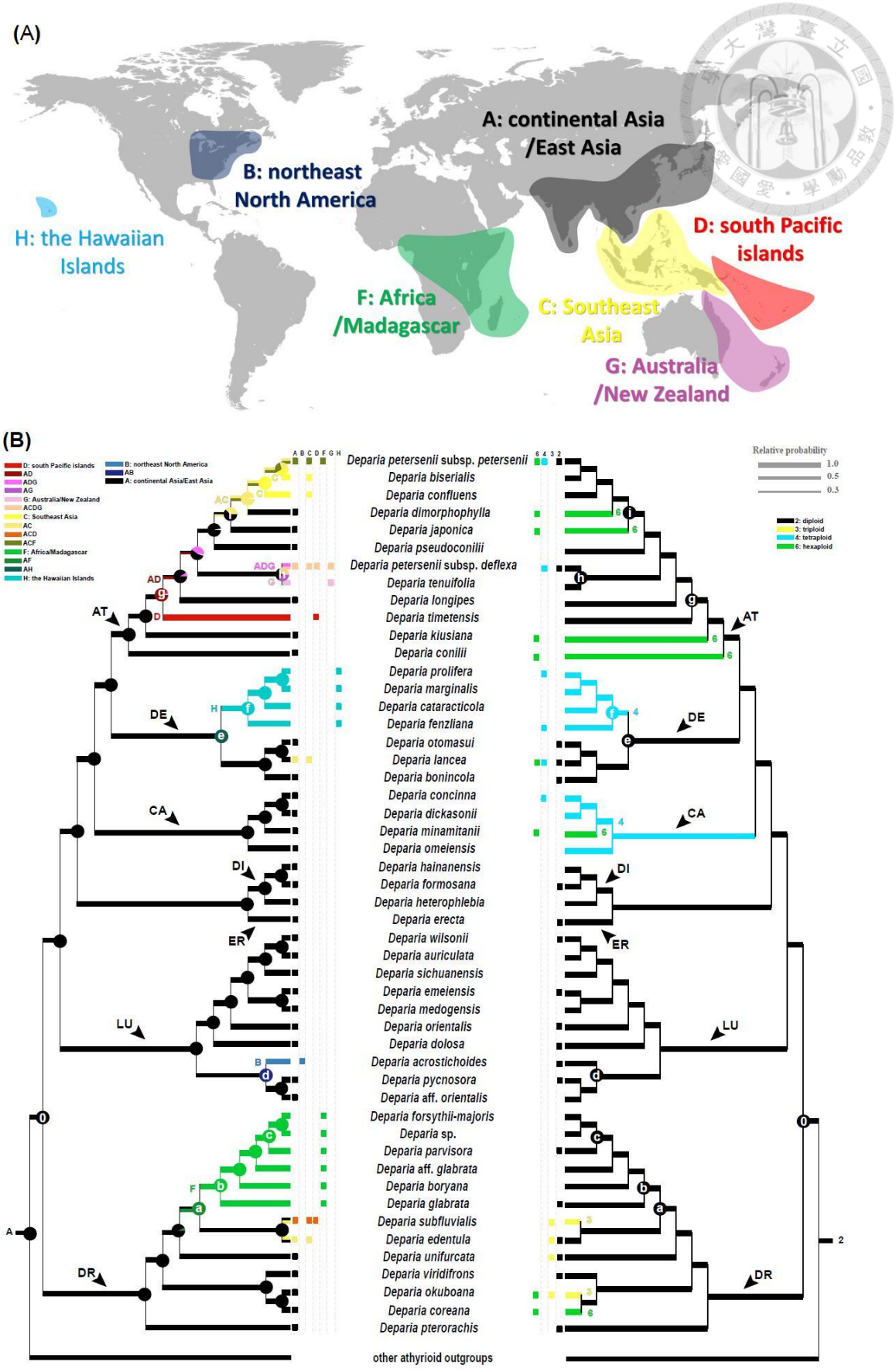
(A)
A: continental Asia
/East Asia
B: northeast
North America
H: the Hawaiian
Islands
D: south Pacific
islands
F: Africa
/Madagascar
C: Southeast
Asia
G: Australia
/New Zealand
(B)
D: south Pacific islands
AD
ADG
AG
G: Australia/New Zealand
ACDG
C: Southeast Asia
AC
ACD
ACF
F: Africa/Madagascar
AF
AH
H: the Hawaiian Islands
B: northeast North America
AB
A: continental Asia/East Asia
A B C D F G H
6 4 3 2
Relative probability
1.0
0.5
0.3
2: diploid
3: triploid
4: tetraploid
6: hexaploid
Deparia petersenii subsp. petersenii
Deparia biserialis
Deparia confluens
Deparia dimorphophylla
Deparia japonica
Deparia pseudoconilii
Deparia petersenii subsp. deflexa
Deparia tenuifolia
Deparia longipes
Deparia timetensis
Deparia kiusiana
Deparia conilii
Deparia prolifera
Deparia marginalis
Deparia cataracticola
Deparia fenzliana
Deparia otomasui
Deparia lancea
Deparia bonincola
Deparia concinna
Deparia dickasonii
Deparia minamitanii
Deparia omeiensis
Deparia hainanensis
Deparia formosana
Deparia heterophlebia
Deparia erecta
Deparia wilsonii
Deparia auriculata
Deparia sichuanensis
Deparia emeiensis
Deparia medogensis
Deparia orientalis
Deparia dolosa
Deparia acrostichoides
Deparia pycnosora
Deparia aff. orientalis
Deparia forsythii-majoris
Deparia sp.
Deparia parvisora
Deparia aff. glabrata
Deparia boryana
Deparia glabrata
Deparia subfluvialis
Deparia edentula
Deparia unifurcata
Deparia viridifrons
Deparia okuboana
Deparia coreana
Deparia pterorachis
other athyrioid outgroups
AT
DE
CA
DI
ER
LU
DR

Fig. 2.1. Current distribution map (A) and ancestral distribution and ploidy reconstruction (B) of *Deparia*. In the current distribution map of *Deparia* (A), seven biogeographical regions, A-H, are defined; A = continental Asia/East Asia, B = northeast North America, C = Southeast Asia, D = south Pacific islands, F = Africa/Madagascar, G = Australia/New Zealand, and H = the Hawaiian Islands. In the left cladogram (B), the different colors represent the different geographical regions. The pie charts on internal branches show the probabilities reconstructed by S-DIVA. The thickness of colored branches represent the relative probabilities inferred by Lagrange. In the right cladogram (B), different colors represent different ploidies; 2 = diploids, 3 = triploids, 4 = tetraploids, and 6 = hexaploids. The thickness of colored branches represents relative probabilities inferred by ChromEvol. The arrowheads indicate seven highly-supported clades in the *Deparia* phylogeny. The nodes *a-i* correspond to the nodes mentioned in the main text and Table 2.1.

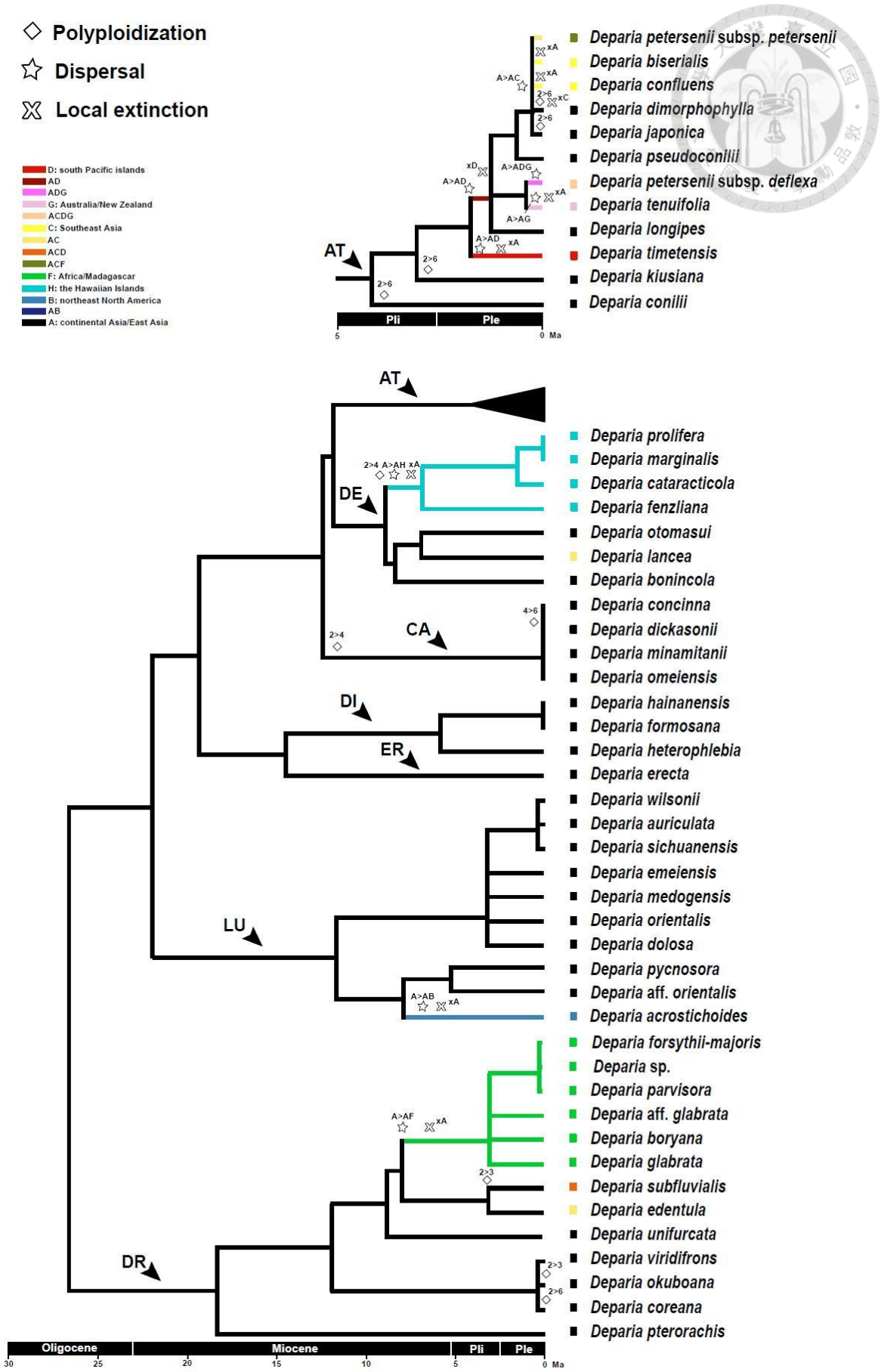
Polyploidization
Dispersal
Local extinction
D: south Pacific islands
AD
ADG
G: Australia/New Zealand
ACDG
C: Southeast Asia
AC
ACD
ACF
F: Africa/Madagascar
H: the Hawaiian Islands
B: northeast North America
AB
A: continental Asia/East Asia
Deparia petersenii subsp. petersenii
Deparia biserialis
Deparia confluens
Deparia dimorphophylla
Deparia japonica
Deparia pseudoconilii
Deparia petersenii subsp. deflexa
Deparia tenuifolia
Deparia longipes
Deparia timetensis
Deparia kiusiana
Deparia conilii
AT
Pli
Ple
5
0 Ma
Deparia prolifera
Deparia marginalis
Deparia cataracticola
Deparia fenzliana
Deparia otomasui
Deparia lancea
Deparia bonincola
Deparia concinna
Deparia dickasonii
Deparia minamitanii
Deparia omeiensis
Deparia hainanensis
Deparia formosana
Deparia heterophlebia
Deparia erecta
Deparia wilsonii
Deparia auriculata
Deparia sichuanensis
Deparia emeiensis
Deparia medogensis
Deparia orientalis
Deparia dolosa
Deparia pycnosora
Deparia aff. orientalis
Deparia acrostichoides
Deparia forsythii-majoris
Deparia sp.
Deparia parvisora
Deparia aff. glabrata
Deparia boryana
Deparia glabrata
Deparia subfluvialis
Deparia edentula
Deparia unifurcata
Deparia viridifrons
Deparia okuboana
Deparia coreana
Deparia pterorachis
DE
CA
DI
ER
LU
DR
Oligocene
Miocene
Pli
Ple
30
25
20
15
10
5
0 Ma

Fig. 2.2. The chronogram of the *Deparia* phylogeny inferred by the penalize rate smoothing. Different colors on branches indicate the most likely ancestral distribution inferred by Lagrange; A = continental Asia/East Asia, B = northeast North America, C = Southeast Asia, D = south Pacific islands, F = Africa/Madagascar, G = Australia/New Zealand, and H = the Hawaiian Islands. The dispersal and local extinction events suggested by biogeographical patterns from Lagrange are indicated as stars and crosses upon branches, respectively. The polyploidization events inferred by the results of ChromEvol are indicated as diamonds on branches. The Pli and Ple indicate the geological periods of Pliocene and Pleistocene, respectively. The arrowheads indicate seven highly supported clades in the *Deparia* phylogeny.

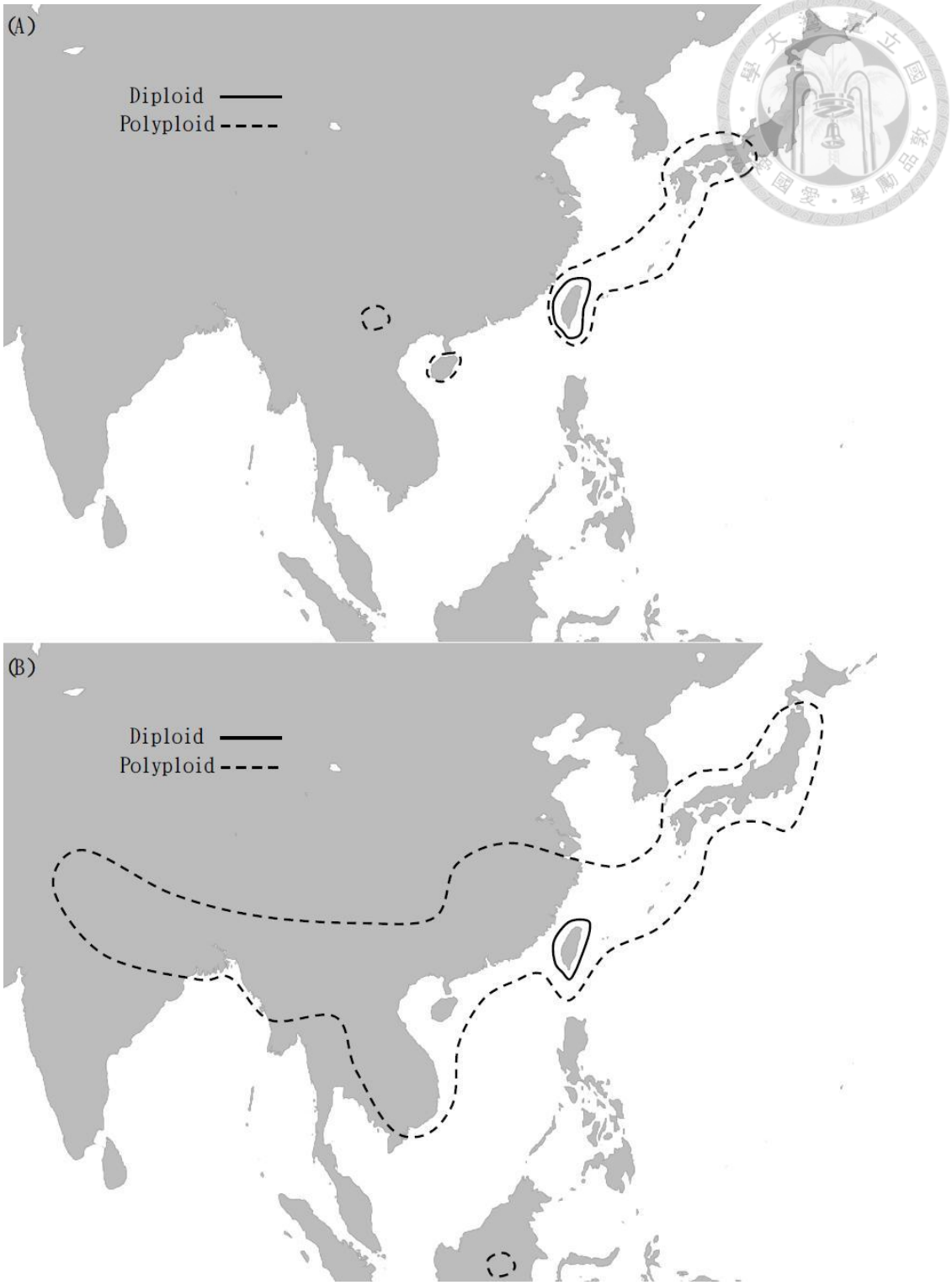

Fig. 2.3. The cytogeography of *Deparia petersenii* subsp. *petersenii* (A) and *Deparia lancea* (B). The distribution of diploids and polyploids (including tetraploids and hexaploids) are indicated as solid and dashed lines, respectively. The cytotype distributions of *Deparia petersenii* subsp. *petersenii* and *Deparia lancea* are modified from Shinohara *et al.* (2006) and Kuo *et al.* (2008), respectively.

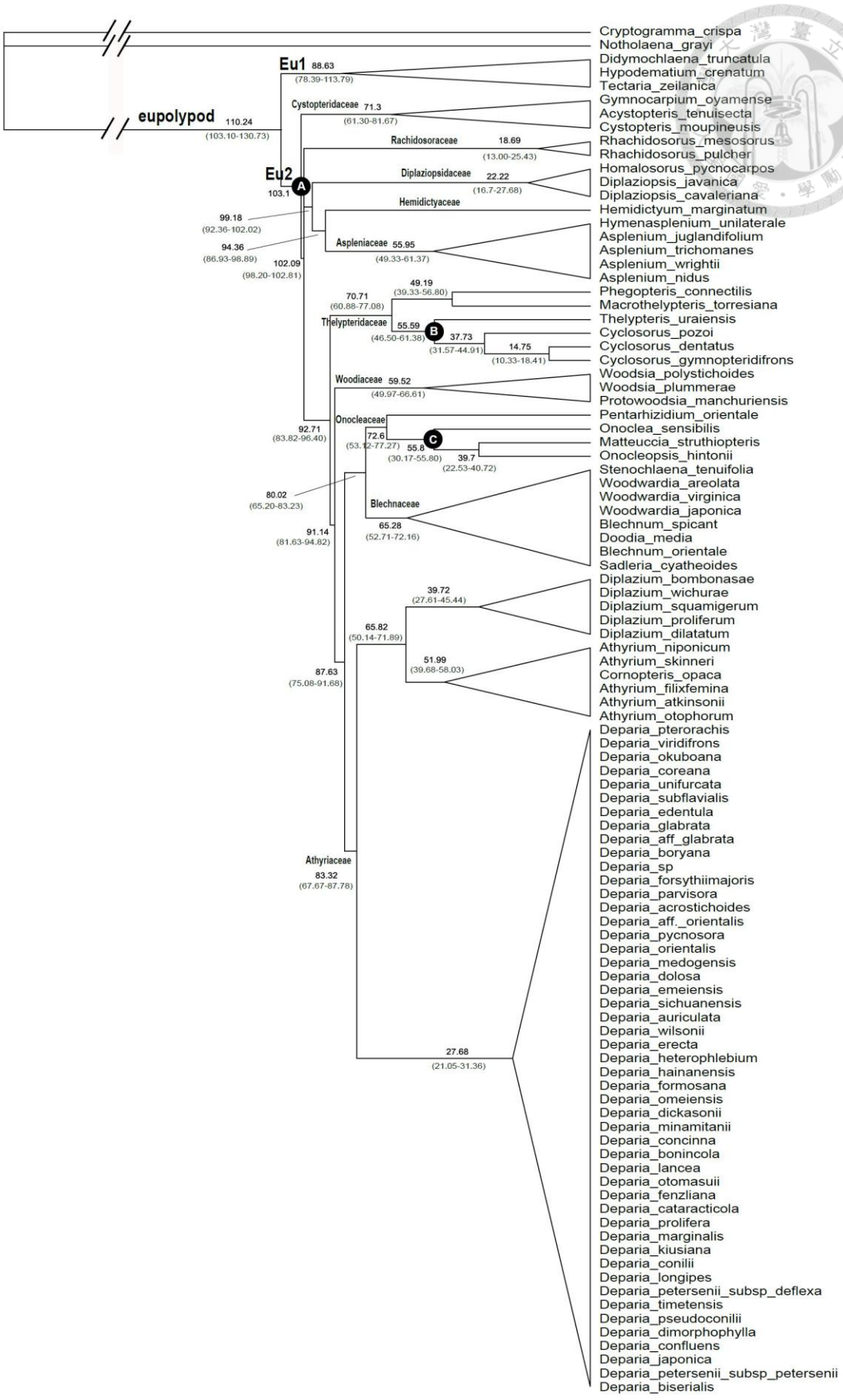
Cryptogramma_crispa
Notholaena_grayi
Eu1 88.63
(78.39-113.79)
Didymochlaena_truncatula
Hypodematium_crenatum
Tectaria_zeilanica
eupolypod 110.24
(103.10-130.73)
Cystopteridaceae 71.3
(61.30-81.67)
Gymnocarpium_oyamense
Acystopteris_tenuisecta
Cystopteris_moupineusis
Rachidosoraceae 18.69
(13.00-25.43)
Rhachidosorus_mesosorus
Rhachidosorus_pulcher
Eu2
A
103.1
Diplaziopsidaceae 22.22
(16.7-27.68)
Homalosorus_pycnocarpos
Diplaziopsis_javanica
Diplaziopsis_cavaleriana
Hemidictyaceae
Hemidictyum_marginatum
99.18
(92.36-102.02)
Hymenasplenium_unilaterale
94.36
(86.93-98.89)
Aspleniaceae 55.95
(49.33-61.37)
Asplenium_juglandifolium
Asplenium_trichomanes
Asplenium_wrightii
102.09
(98.20-102.81)
Asplenium_nidus
49.19
(39.33-56.80)
Phegopteris_connectilis
70.71
(60.88-77.08)
Macrothelypteris_torresiana
Thelypteridaceae
55.59
(46.50-61.38)
B
Thelypteris_uraiensis
37.73
(31.57-44.91)
Cyclosorus_pozoi
14.75
(10.33-18.41)
Cyclosorus_dentatus
Cyclosorus_gymnopteridifrons
Woodsiaceae 59.52
(49.97-66.61)
Woodsia_polystichoides
Woodsia_plummerae
Protowoodsia_manchuriensis
Onocleaceae
Pentarhizidium_orientale
92.71
(83.82-96.40)
Onoclea_sensibilis
72.6
(53.12-77.27)
C
Matteuccia_struthiopteris
55.8
(30.17-55.80)
Onocleopsis_hintonii
39.7
(22.53-40.72)
Stenochlaena_tenuifolia
80.02
(65.20-83.23)
Blechnaceae
Woodwardia_areolata
Woodwardia_virginica
Woodwardia_japonica
65.28
(52.71-72.16)
Blechnum_spicant
91.14
(81.63-94.82)
Doodia_media
Blechnum_orientale
Sadleria_cyatheoides
Diplazium_bombonasae
39.72
(27.61-45.44)
Diplazium_wichurae
Diplazium_squamigerum
Diplazium_proliferum
65.82
(50.14-71.89)
Diplazium_dilatatum
Athyrium_niponicum
51.99
(39.68-58.03)
Athyrium_skinneri
87.63
(75.08-91.68)
Cornopteris_opaca
Athyrium_filixfemina
Athyrium_atkinsonii
Athyrium_otophorum
Deparia_pterorachis
Deparia_viridifrons
Deparia_okuboana
Deparia_coreana
Deparia_unifurcata
Deparia_subflavialis
Deparia_edentula
Deparia_glabrata
Deparia_aff_glabrata
Deparia_boryana
Deparia_sp
Athyriaceae
83.32
(67.67-87.78)
Deparia_forsythiimajoris
Deparia_parvisora
Deparia_acrostichoides
Deparia_aff._orientalis
Deparia_pycnosora
Deparia_orientalis
Deparia_medogensis
Deparia_dolosa
Deparia_emeiensis
Deparia_sichuanensis
Deparia_auriculata
Deparia_wilsonii
Deparia_erecta
27.68
(21.05-31.36)
Deparia_heterophlebium
Deparia_hainanensis
Deparia_formosana
Deparia_omeiensis
Deparia_dickasonii
Deparia_minamitanii
Deparia_concinna
Deparia_bonincola
Deparia_lancea
Deparia_otomasuii
Deparia_fenzliana
Deparia_cataracticola
Deparia_prolifera
Deparia_marginalis
Deparia_kiusiana
Deparia_conilii
Deparia_longipes
Deparia_petersenii_subsp_deflexa
Deparia_timetensis
Deparia_pseudoconilii
Deparia_dimorphophylla
Deparia_confluens
Deparia_japonica
Deparia_petersenii_subsp_petersenii
Deparia_biserialis

Fig. S2.1. The chronogram of Eupolyplod II and *Deparia* of the most likely ML tree based on *rbcL* + *matK* only dataset, which is inferred by the penalize rate smoothing. The values on the branches are their estimated mean divergence time (95% HPD inferred from 250 bootstrap chronograms) in unit of Ma. Eupolypod I and II are indicated as Eu1 and Eu2 on the chronogram, respectively. For its penalize rate smoothing, node A as is applied the fix age constrain for Eupolypod II (=103.2 Ma). The node B and C are the minimum age constrains applied for *Cyclosorus* (≥ 33.9 Ma) and *Onoclea* (≥ 55.8 Ma) divergence, respectively. The details of the setting of penalize rate smoothing can be checked in the main text.

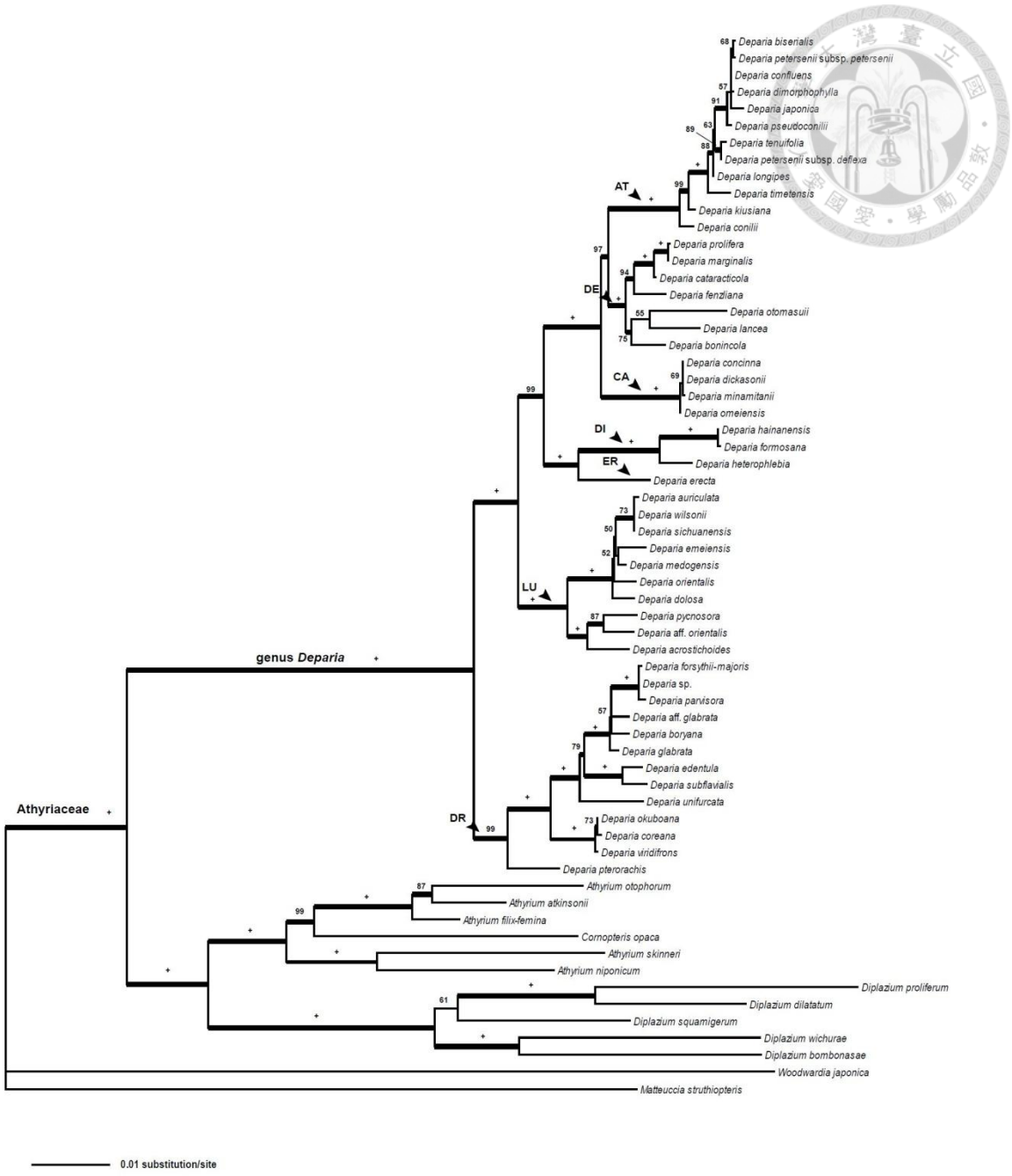

Fig. S2.2. The maximum likelihood (ML) phylogram of *Deparia* based on *rps16-matK* IGS + *matK* + *rbcL* + *trnL-L-F* dataset. The values on the branches of phylogram are the ML bootstrap (MLBS) values, and only the values larger than 50 are shown. The plus (+) signs represent MLBS = 100. The thickened branches indicate MLBS ≥ 70. The arrowheads indicate the seven highly supported clades in the *Deparia* phylogeny.

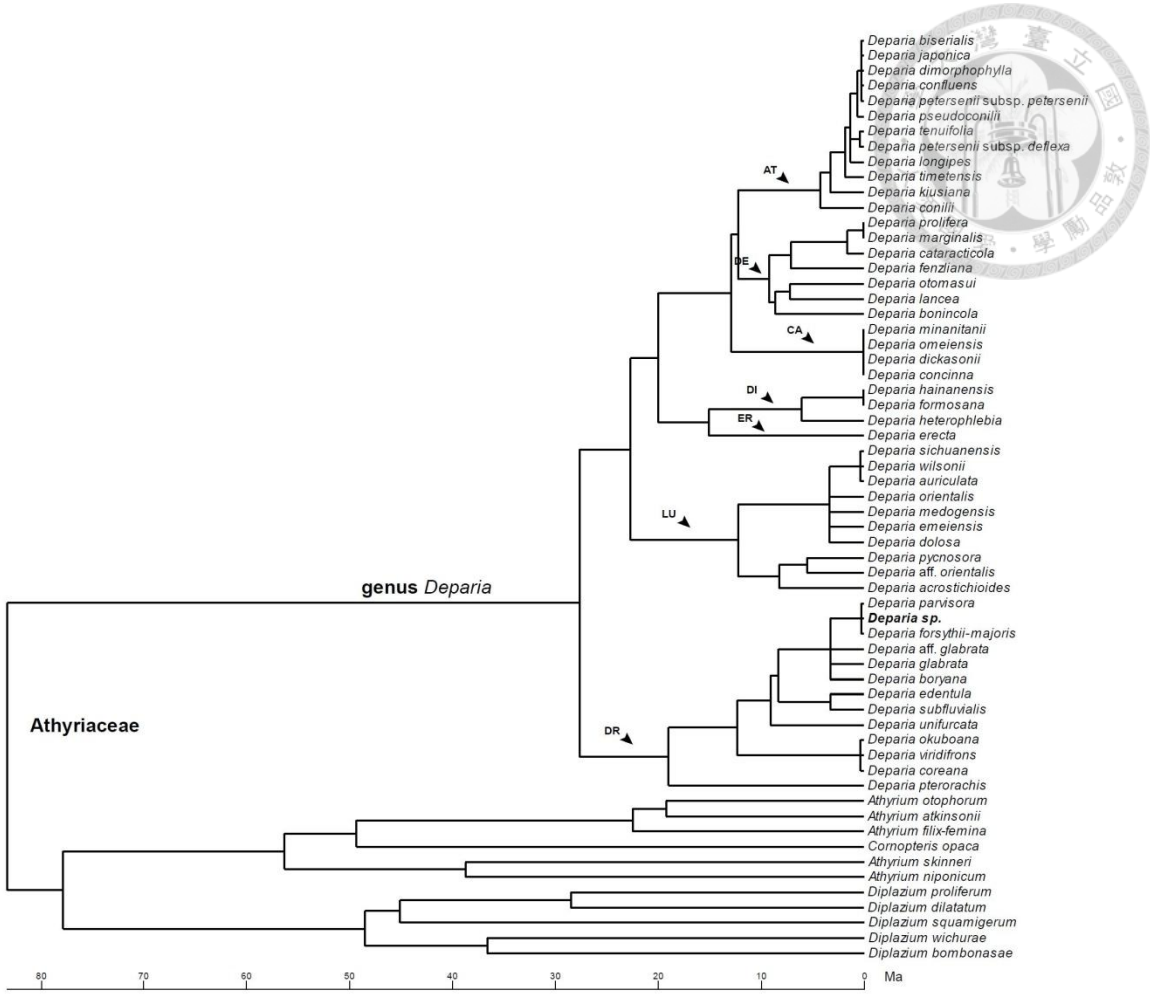

Fig. S2.3. The chronogram of *Deparia* based on *rps16-matK* IGS + *matK* + *rbcL* + *trnL-L-F* dataset. The arrowheads indicate the seven highly supported clades in the *Deparia* phylogeny.

Table 2.1. The estimated divergent time of certain nodes in *Deparia* phylogeny.

Nodes no.[a]	Node	R8S[b]	R8S[c]	R8S/ mean (95% HPD)[d]	BEAST/ mean (95% HPD)[e]
0	*Deparia* crown group	27.68 Ma	27.68 Ma	28.70 (27.68-33.99) Ma	40.39 (26.71-54.70) Ma
a	Continental Asia / Africa + Madagascan	6.74 Ma	8.34 Ma	9.23 (6.41-15.54) Ma	10.89 (6.09-16.38) Ma
b	African + Madagascan crown group	3.60 Ma	3.25 Ma	4.54 (1.99-10.18) Ma	5.18 (2.45-8.30) Ma
c	Madagascan crown group	0.50 Ma	0.26Ma	1.35 (0.00-6.85) Ma	0.89 (0.17-1.84) Ma
d	Continental Asia / northeast North America	8.06 Ma	8.24 Ma	9.38 (5.78-16.17) Ma	10.92 (7.36-18.06) Ma
e	Continental Asia / Hawaiian Islands	8.52 Ma	9.24 Ma	10.58 (7.02-17.35) Ma	12.40 (6.22-17.42) Ma
f	Hawaiian crown group	7.02 Ma	7.13 Ma	7.56 (3.95-14.42) Ma	8.83 (4.02-14.11) Ma
g	Continental Asia /South Pacific islands	-	1.86 Ma	3.05 (0.64-8.49) Ma	4.43 (2.34-6.95) Ma
h	Continental Asia / Australia + New Zealand	-	0.44Ma	1.49 (0.00-6.54) Ma	1.07 (0.01-2.42) Ma
i	Continental Asia /Southeast Asia	1.50 Ma	0.28Ma	1.40 (0.00-6.97) Ma	1.81 (0.48-2.11) Ma

[a]The nodes correspond to those in Fig. 2.1.

[b]The results inferred by the first molecular dating analysis.

[c]The results of the most likely tree inferred by the second molecular dating analysis.

[d]The results of 500 bootstrap trees inferred by the second molecular dating analysis.

[e]The results inferred by the third molecular dating analysis.

Table 2.2. The summary of dispersal and polyploidization events in *Deparia.*

	Retaining diploidy	Coupled with polyploidization	After polyploidization
Total tree lengths of phylogenetic branches (Ma)	308.19	-	42.97
Number of phylogenetic branch with dispersal	7	1	0
Number of phylogenetic branch without dispersa	69	9	11
Number of range expansion within species*	0	5	0
Number of no range expansion within species*	30	8	8

*Only including the terminal branches and species' current statuses.

Table S2.1. The distribution and cytotype records of *Deparia* species and the Athyriaceae outgroup used in this study. (The "-" indicates the species don't distribute in that biogeographical region. The "?" indicates the species distribute in that biogeographical region but without availible cytological information. The cytotype with the seual and apomictic reproduction mode are indicated in simple and double under lines, respectively.)

Biogeographical regions*	**A**	**B**	**C**	**D**	**E**	**F**	**G**	**H**
Ingroup								
Deparia acrostichioides	-	$2X^{a, b}$	-	-	-	-	-	-
Deparia aff. *glabrata*	-	-	-	-	-	?	-	-
Deparia auriculata	?	-	-	-	-	-	-	-
Deparia biserialis	-	-	?	-	-	-	-	-
Deparia bonincola	$\underline{2X}^{c}$	-	-	-	-	-	-	-
Deparia boryana	-	-	-	-	-	?	-	-
Deparia cataracticola	-	-	-	-	-	-	?	-
Deparia concinna	$4X^{d}$	-	-	-	-	-	-	-
Deparia confluens	-	-	?	-	-	-	-	-
Deparia conilii	$\underline{6X}^{c}$	-	-	-	-	-	-	-
Deparia coreana	$4X^{d}$, $6X^{d}$	-	-	-	-	-	-	-
Deparia dickasonii	?	-	-	-	-	-	-	-
Deparia dimorphophylla	$\underline{6X}^{d}$	-	-	-	-	-	-	-
Deparia dolosa	$\underline{2X}^{e}$	-	-	-	-	-	-	-
Deparia edentula (incl. *D. boryana* subsp. *austroindica*)	$\underline{2X}^{f}$, $\underline{\underline{3X}}^{g}$	-	?	-	-	-	-	-
Deparia emeiensis	2X	-	-	-	-	-	-	-
Deparia erecta	$\underline{2X}^{d}$	-	-	-	-	-	-	-
Deparia fenzliana	-	-	-	-	-	-	-	$\underline{4X}^{l}$
Deparia formosana	$\underline{2X}^{c, h}$	-	-	-	-	-	-	-
Deparia forsythii-majoris	-	-	-	-	-	?	-	-
Deparia glabrata	-	-	-	-	-	$\underline{2X}^{l}$	-	-
Deparia hainanensis	?	-	-	-	-	-	-	-
Deparia henryi	$6X^{d}$	-	-	-	-	-	-	-
Deparia heterophlebia	?	-	-	-	-	-	-	-
Deparia japonica	$\underline{6X}^{c}$	-	-	-	-	-	-	-
Deparia kiusiana	$6X^{o}$	-	-	-	-	-	-	-
Deparia lancea	$\underline{2X}^{i}$, $\underline{4X}^{c, e, i}$, $\underline{6X}^{c, i}$	-	$\underline{4X}^{i}$, $\underline{6X}^{i}$	-	-	-	-	-
Deparia longipes	?	-	-	-	-	-	-	-
Deparia marginalis	-	-	-	-	-	-	-	?
Deparia medogensis	?	-	-	-	-	-	-	-
Deparia minanitanii	$6X^{o}$	-	-	-	-	-	-	-
Deparia mucilagina[p]	$\underline{2X}^{c}$	-	-	-	-	-	-	-
Deparia okuboana	$\underline{\underline{3X}}^{c, e, f}$, $\underline{6X}^{c}$	-	-	-	-	-	-	-
Deparia omeiensis	?	-	-	-	-	-	-	-
Deparia orientalis	$\underline{2X}^{f}$	-	-	-	-	-	-	-
Deparia otomasui	$\underline{2X}^{c}$	-	-	-	-	-	-	-
Deparia parvisora	-	-	-	-	-	$\underline{2X}^{l}$	-	-
Deparia petersenii subsp. *deflexa* (incl. subsp. *congrua*)	?	-	?	?	-	-	$\underline{2X}^{j}$, $\underline{4X}^{j}$	-
Deparia petersenii subsp. *petersenii*	2X, $\underline{4X}^{k}$, $\underline{6X}$	-	?	-	-	?	-	-

(Table S2.1 cont.)

Deparia prolifera	-	-	-	-	-	-	-	4X[l]
Deparia pseudoconilii	?	-	-	-	-	-	-	-
Deparia pterorachis	2X[c]	-	-	-	-	-	-	-
Deparia pycnosora	2X[c]	-	-	-	-	-	-	-
Deparia sichuanensis	?	-	-	-	-	-	-	-
Deparia sp.	-	-	-	-	-	?	-	-
Deparia subfluvialis	3X[f]	-	?	?	-	-	-	-
Deparia tenuifolia	-	-	-	-	-	-	?	-
Deparia timetensis	-	-	-	?	-	-	-	-
Deparia unifurcata	2X[e], 3X[c, e, f]	-	-	-	-	-	-	-
Deparia vegetius	4X[d]	-	-	-	-	-	-	-
Deparia viridifrons	2X[c]	-	-	-	-	-	-	-
Deparia wilsonii	2X[e]	-	-	-	-	-	-	-
Estimated number of species/subspecies	50-55	1	8	4	0	6-7	2	5
Percentage of missing data	48-52%	0%	88%	100%	0%	67-71%	50%	60%
Percentage of diploid species	29-32%	100%	N. A.	N. A.	0%	22-28%	50%	0%
Percentage of polyploid species	25-28%	0%	N. A.	N. A.	0%	0%	50%	100%
Outgroup								
Athyrium atkinsonii	2X[d]	-	-	-	-	-	-	-
Athyrium otophorum	4X[c]	-	-	-	-	-	-	-
Athyrium filix-femina	2X[f]	2X[b]	-	-	-	-	-	-
Cornopteris opaca	2X[c], 4X[c]	-	4X[m]	-	-	-	-	-
Athyrium niponicum	2X[c, e]	-	-	-	-	-	-	-
Athyrium skinneri	-	-	-	-	?	-	-	-
Diplazium wichurae	2X[c, e]	-	-	-	-	-	-	-
Diplazium proliferum (incl. *D. accedens*)	?	-	2X[m]	-	-	?	-	-
Diplazium squamigerum	4X[c]	-	-	-	-	-	-	-
Diplazium bombonasae	-	-	-	-	?	-	-	-
Diplazium dilatatum	2X[c, n], 3X[c, n]	-	3X[m], 4X[m]	?	-	-	2X[j], 3X[j]	-

*A = continental Asia, B = northeast North America, C = Southeast Asia, D = south Pacific islands, E = Central and South America, F = Africa + Madagascar + neighbouring islands, G = Australia + New Zealand, and H = Hawaiian Islands.

[a]Britton (1964); [b]Love & Love (1976); [c]Takamiya (1996);[d]Wang *et al.* (2013); [e]Cheng & Zhang (2010); [f]Kato *et al.* (1992); [g]Frasser-Jinkin (2008); [h]Sano *et al.* (2000); [i]Kuo *et al.* (unpublished); [j]Tindale & Roy (2002); [k]Shinohara *et al.* (2006); [l]this study; [m]Praptosuwiryu & Darnaedi (1994); [n]Takamiya *et al.* (1999); [o]Nakato, personal communication; [p]misidentified as *D. pycnosora* var. *vegetius* in Takamiya (1996).

Table S2.2. PCR primers used in this study.

Region	Name	Sequence 5' - 3'	Reference
For outgroup taxa			
IGS	FERN rps16 fSRQE*	CCCGRMRAGAAGGGARAG	Kuo *et al.* (2011)
	De rps16 fSTE*	GAAGAAGGGGCGCAATCAACGGAAAC	Rothfels *et al.* (2012)
	BLE matK rDVP*	AATAGATGTRRAAATGGCACATC	Rothfels *et al.* (2012)
	ASP matK rLVV*	TTCGTGTCCRTAAAACAACCAA	Rothfels *et al.* (2012)
	Athy matK rHTY*	CACACRAAGTTTYGTAYGTGTGAA	Rothfels *et al.* (2012)
	Di matK rTYK*	CCACACRAAGTTTTGTACGTGT	Rothfels *et al.* (2012)
	FERmatK fEDR*	ATTCATTCRATRTTTTTATTTHTGGARGAYAGATT	Kuo *et al.* (2011)
	FERmatK rAGK	CGTRTTGTACTYYTRTGTTTRCVAGC	Kuo *et al.* (2011)
trnL-L-F	f*	ATTTGAACTGGTGACACGAG	Taberlet *et al.* (1991)
	FernLr1*	GGCAGCCCCCAGATTCAGGGGAACC	Li *et al.* (2011)
For *Deparia* species			
rbcL	F1F*	ATGTCACCACAAACAGAAACTAAAGCAAGT	Wolf *et al* . (1994)
	1379R*	TCACAAGCAGCAGCTAGTTCAGGACTC	Pryer *et al* . (2001)
	De rbcL fAGV	GTTGGATTCAAAGCTGGTGTC	This study
	De rbcL rVFA*	GCACCCAATTCTCTAGCARAAACA	This study
	De rbcL fFKS*	GTAGCAGAAGCTCTTTTCAAATCCC	This study
	De rbcL rEII	CACTTACTAGCTTCACGAATAATTTC	This study
IGS	De rps16 fSTE*	GAAGAAGGGGCGCAATCAACGGAAAC	Li *et al.* (2011)
	De rmf1	CTTGGGAGTTACTGCGATGA	This study
	De matK rANR	GATATGGGAAACAATCTCGATTAGCG	This study
	De matK fHVL*	GATTGCCAAAATCTAGCCACGTTTTAGA	Li *et al.* (2011)
	De matK rHTY*	ACGAAGTTTTGTACGTGTGAA	Rothfels *et al.* (2012)
	De matK fFHG*	ATCTCTCATAGGTTTTCATGGAAC	This study
	De matK rSCV	GTAACCCAAGAATAAAACACAGCTG	This study
	FERmatK rAGK	CGTRTTGTACTYYTRTGTTTRCVAGC	Kuo *et al.* (2011)
trnL-L-F	f*	ATTTGAACTGGTGACACGAG	Taberlet *et al.* (1991)
	FernLr1*	GGCAGCCCCCAGATTCAGGGGAACC	Li *et al.* (2011)
	De trnL 1Ir1*	GTGAATGGAGGTAGAGTCCC	This study
	De trnL 3'Ef1*	CTCATTGGGGATAGAGGGA	This study

*The primer for sequencing.

Table S2.3. The voucher information of *Deparia* and their GenBank secession number of DNA regions applied in this study (XXXXXXXX indicate the sequences generated in this study)**.**

Taxa	Voucher	Collection locality	*matK*	*rbcL*	*trnL-L-F*	*rps16-matK* IGS
Deparia acrostichoides (Sw.) M. Kato	*Kuo120* (TAIF)	Massachusetts, USA	JN673820	JN673929	JN673904	XXXXXXXX
Deparia aff. *glabrata*	*MO6262952* (MO)	Kakamega, Kenya	XXXXXXXX	XXXXXXXX	XXXXXXXX	XXXXXXXX
Deparia aff. *orientalis*	*TNS763886* (TNS)	Saitama Pref., Japan	JN673855	AB574957	AB575595	XXXXXXXX
Deparia auriculata (W. M. Chu & Z. R. Wang) Z. R. Wang	*Kuo1300* (TAIF)	Yunnan, China	XXXXXXXX	XXXXXXXX	XXXXXXXX	XXXXXXXX
Deparia biserialis (Baker) M. Kato	*Shinohara0810501* (KYO)	Kinabalu, Indonesia	JN673822	JN673931	JN673906	XXXXXXXX
Deparia bonincola (Nakai) M. Kato	*TNS774841* (TNS)	BoninIs., Japan	JN673823	AB574940	AB575578	XXXXXXXX
Deparia boryana (Willd.) M. Kato	*P02432539* (P)	Saint-Louis, La Ré union	XXXXXXXX	XXXXXXXX	XXXXXXXX	XXXXXXXX
Deparia cataracticola M. Kato	*Wood12767* (PTBG)	Hawaii, USA	XXXXXXXX	AB046982*	XXXXXXXX	XXXXXXXX
Deparia concinna (Z.R.Wang) M. Kato	*Kuo2268* (TAIF)	Sichuan, China	XXXXXXXX	XXXXXXXX	XXXXXXXX	XXXXXXXX
Deparia confluens (Kunze) M. Kato	Cultivated in Koshikawa Botanical Garden	Surnbawa, Indonesia	JN673824	JN673932	JN673907	XXXXXXXX
Deparia conilii (Fr. & Sav.) M. Kato	*TNS768165* (TNS)	Hachijo Is., Japan	JN673825	AB574941	AB575579	XXXXXXXX
Deparia coreana (H. Christ) M. Kato	*TNS776382* (TNS)	Aomori Pref., Japan	JN673826	AB574942	AB575580	XXXXXXXX
Deparia dickasonii M. Kato	*Liu9433* (TAIF)	Yunnan, China	JN673827	JN673933	JN673908	XXXXXXXX
Deparia dimorphophylla (Koidz.) M. Kato	*TNS764256* (TNS)	Kagoshima Pref., Japan	JN673828	AB574943	AB575581	XXXXXXXX
Deparia dolosa (Christ) M. Kato	Kuo1315 (TAIF)	Yunnan, China	JN673829	JN673934	JN673909	XXXXXXXX
Deparia edentula (Kunze) X. C. Zhang	*TNS1112754* (TNS)	Java, Indonesia	XXXXXXXX	XXXXXXXX	XXXXXXXX	XXXXXXXX
Deparia emeiensis (Z. R. Wang) Z. R. Wang	*Liu9703* (TAIF)	Sichuan, China	XXXXXXXX	XXXXXXXX	XXXXXXXX	XXXXXXXX
Deparia erecta (Z. R. Wang) M. Kato	*Kuo2219* (TAIF)	Sichuan, China	XXXXXXXX	XXXXXXXX	XXXXXXXX	XXXXXXXX
Deparia fenzliana (Luers.) M. Kato	*OppenheimerH20920* (TAIF)	Hawaii, USA	XXXXXXXX	D43900*	XXXXXXXX	XXXXXXXX
Deparia formosana (Rosenst.) R. Sano	*Kuo2306* (TAIF)	Yilan, Taiwan	XXXXXXXX	XXXXXXXX	XXXXXXXX	XXXXXXXX
Deparia forsythii-majoris (C. Chr.) M. Kato	*P02432852* (P)	Anjanaharibe Sud, Madagascar	XXXXXXXX	XXXXXXXX	XXXXXXXX	XXXXXXXX
Deparia glabrata (Mett. *ex* Kuhn) M. Kato	*P01515373* (P)	Oloitia, Equatorial Guinea	XXXXXXXX	XXXXXXXX	XXXXXXXX	XXXXXXXX
Deparia hainanensis (Ching) R. Sano	*PE01385619* (PE)	Hainan, China	XXXXXXXX	XXXXXXXX	XXXXXXXX	XXXXXXXX
Deparia heterophlebia (Mett.) R. Sano	*Liu9426* (TAIF)	Yunnan, China	XXXXXXXX	XXXXXXXX	XXXXXXXX	XXXXXXXX
Deparia japonica (Thunb. *ex* Murray) M. Kato	*TNS763869* (TNS)	Ibaraki Pref., Japan	JN673831	AB574945	AB575583	XXXXXXXX
Deparia kiusiana (Koidz.) M. Kato	*TNS764364* (TNS)	Nara Pref., Japan	JN673832	AB574946	AB575584	XXXXXXXX
Deparia lancea (Thunb. *ex* Murray) Fras.- Jenk.	*Kuo1914* (TAIF)	Taipei, Taiwan	JN673839	JN673941	JN673916	XXXXXXXX
Deparia marginalis (Hilleb.) M. Kato	*OppenheimerH20917* (TAIF)	Hawaii, USA	XXXXXXXX	AB046981*	XXXXXXXX	XXXXXXXX
Deparia medogensis (Ching & S. K. Wu) Z. R. Wang	*Liu9453* (TAIF)	Yunnan, China	XXXXXXXX	XXXXXXXX	XXXXXXXX	XXXXXXXX
Deparia minamitanii S. Serizawa	*TNS774852* (TNS)	Miyazaki Pref., Japan	JN673847	AB574948	AB575586	XXXXXXXX
Deparia okuboana (Makino) M. Kato	*TNS764345* (TNS)	Shizuoka Pref., Japan	JN673848	AB574949	AB575587	XXXXXXXX
Deparia omeiensis (Z. R. Wang) M. Kato	*Liu9671* (TAIF)	Sichuan, China	JN673849	JN673949	JN673924	XXXXXXXX
Deparia orientalis (Z. R. Wang & J. J. Chien) T. Nakaike	*TNS763932* (TNS)	Tokyo Metropolis, Japan	JN673850	AB574956	AB575594	XXXXXXXX
Deparia otomasui (Kurata) S. Serizawa	*TNS764339* (TNS)	Kumamoto Pref., Japan	JN673851	AB574950	AB575588	XXXXXXXX
Deparia parvisora (C. Chr.) M.Kato	*P00243925* (P)	Marojejy, Madagascar	XXXXXXXX	XXXXXXXX	XXXXXXXX	XXXXXXXX
Deparia petersenii subsp. *deflexa* (Kunze) M. Kato	*Wade1096* (TAIF)	Java, Indonesia	JN673846	JN673948	JN673923	XXXXXXXX
Deparia petersenii subsp. *petersenii* (Kuntze) M. Kato	*Kuo1922* (TAIF)	Taipei, Taiwan	JN673852	JN673950	JN673925	XXXXXXXX
Deparia prolifera (Kaulf.) Hook. & Grev.	*Wood13449* (PTBG)	Hawaii, USA	XXXXXXXX	D43906*	XXXXXXXX	XXXXXXXX
Deparia pseudo-conilii (S. Serizawa) S. Serizawa	*TNS764016* (TNS)	Okinawa Pref., Japan	JN673853	AB574952	AB575590	XXXXXXXX
Deparia pterorachis (H. Christ) M. Kato	*TNS766637* (TNS)	Nagano Pref., Japan	JN673854	AB574954	AB575592	XXXXXXXX
Deparia pycnosora (Christ) M. Kato	*Lu14388* (TAIF)	Changbai Mt., China	XXXXXXXX	XXXXXXXX	XXXXXXXX	XXXXXXXX
Deparia sichuanensis (Z. R. Wang) Z. R. Wang	*Kuo2243* (TAIF)	Sichuan, China	XXXXXXXX	XXXXXXXX	XXXXXXXX	XXXXXXXX

(Table S2.3 cont.)

Deparia sp.	*MO6173394* (MO)	Sava region, Madagascar	XXXXXXXX	XXXXXXXX	XXXXXXXX	XXXXXXXX
Deparia subfluvialis (Hayata) M. Kato	*Kuo168* (TAIF)	Nantu, Taiwan	JN673857	JN673951	JN673926	XXXXXXXX
Deparia tenuifolia (Kirk) M.Kato	*Perrie6488* (WELT)	North Island, New Zealand	-	KJ400018	KJ400019	-
Deparia timetensis (E. Brown) M. Kato	*Wood10048* (PTBG)	Tahiti, French Polynesia	XXXXXXXX	XXXXXXXX	XXXXXXXX	XXXXXXXX
Deparia unifurcata (Baker) M. Kato	*Kuo2197* (TAIF)	Sichuan, China	XXXXXXXX	XXXXXXXX	XXXXXXXX	XXXXXXXX
Deparia viridifrons (Makino) M. Kato	*TNS766472* (TNS)	Nara Pref., Japan	JN673861	AB574959	AB575597	XXXXXXXX
Deparia wilsonii (Christ) X. C. Zhang	*Kuo2087* (TAIF)	Sichuan, China	XXXXXXXX	XXXXXXXX	XXXXXXXX	XXXXXXXX

* From Kato (2001).

Table S2.4. The GenBank secession number of DNA regions of the outgroup taxa applied in this study. **The sequences generated in this study are with their own footnotes informed with their voucher/living collection information. KBCC = Dr Cecilia Koo Botanic Conservation Center (XXXXXXXX indicate the sequences generated in this study).**

Taxa	*matK*	*rbcL*	*trnL-L-F*	*rps16-matK* IGS
Pteroids				
Cryptogramma crispa (L.) Bernh.	JF832265	EF452148	-	-
Notholaena grayi Davenp.	JF832280	EU268794	-	-
Eupolypod Ⅰ				
Didymochlaena truncatula (Sw.) J. Sm.	JF303942	JF303975	-	-
Decken	JF303944	EF463205	-	-
Tectaria zeilanica (Houtt.) Sledge	JF303951	EF463275	-	-
Eupolypod Ⅱ				
Cystopteridaceae				
Acystopteris tenuisecta (Blume) Tagawa	JF832251	JF832053	-	-
Gymnocarpium oyamense Ching	JF832278	JF832069	-	-
Cystopteris moupinensis Franch.	JF832268	JF832064	-	-
Hemidictyaceae				
Hemidictyum marginatum (L.) C. Presl	JF303927	EF463318	-	-
Diplaziopsidaceae				
Chr.	JF832272	D43909	-	-
Diplaziopsis javanica (Blume) C. Chr.	JF303928	JF303970	-	-
Homalosorus pycnocarpos (Spreng.) Pic. Serm.	JF303929	AB021722	-	-
Rhachidosoraceae				
Rhachidosorus pulcher (Tagawa) Ching	JF303962	JF303971	-	-
Ching	JF832287	AB574996	-	-
Aspleniaceae				
Hymenasplenium unilaterale (Lam.) Hayata	JF303924	EF452140	-	-
Asplenium juglandifolium Lam.	JF832252	EF463151	-	-
Asplenium trichomanes L.	JF832256	EF463157	-	-
Asplenium nidus L.	XXXXXXXX[c]	AF525270	-	-
Hook.	XXXXXXXX[b]	AY549730	-	-
Thelypteridaceae				
Macrothelypteris torresiana (Gaudich.) Ching	JF303931	EF463277	-	-
Phegopteris connectilis (Michx.) Watt	JF303932	AF425111	-	-
Thelypteris uraiensis (Rosenst.) Ching	JF303933	JF303972	-	-
Cyclosorus gymnopteridifrons (Hayata) C. M. Kuo	JF303961	JF303973	-	-
Cyclosorus pozoi (Lag.) C. M. Kuo	JF303934	AB013340	-	-
Cyclosorus dentatus (Forssk.) Ching	JF832290	EF463284	-	-
Woodsiaceae				
Woodsia polystichoides D. C. Eaton	JF303930	U05657	-	-
Woodsia plummerae Lemmon	JF832295	JF832088	-	-

(Table S2.4 cont.)

Protowoodsia manchuriensis (Hook.) Ching	JF832284	AB575001	-	-
Onocleaceae				
Hayata	JF832282	JF832079	-	-
Onoclea sensibilis L.	JF303935	U62036	-	-
Matteuccia struthiopteris (L.) Tod.	JF303936	AB232415	XXXXXXXX[c]	XXXXXXXX[c]
Onocleopsis hintonii F. Ballard	JF832281	U62033	-	-
Blechnaceae				
Moore	JF832289	EF463163	-	-
Woodwardia areolata (L.) T. Moore	JF832296	AF425102	-	-
Woodwardia virginica (L.) Sm.	XXXXXXXX[c]	AB040606	-	-
Woodwardia japonica (L. f.) Sm.	JF303937	AB040600	DQ683432	XXXXXXXX[e]
Blechnum spicant (L.) Roth	JF832262	JF832059	-	-
Blechnum orientale L.	JF303938	AB040568	-	-
Doodia media R. Br.	JF832276	U05922	-	-
Sadleria cyatheoides Kaulf.	JF832288	EF463161	-	-
Athyriaceae				
Athyrium skinneri T. Moore	JF832259	JF832058	XXXXXXXX[f]	XXXXXXXX[f]
Athyrium niponicum (Mett.) Hance	JF832257	JF832057	AF515256	XXXXXXXX[g]
Athyrium filix-femina (L.) Roth	JF303941	HQ676497	HQ676519	XXXXXXXX[h]
Cornopteris opaca (D. Don) Tagawa	XXXXXXXX[j]	AB574937	XXXXXXXX[i]	XXXXXXXX[i]
Athyrium otophorum (Miq.) Koidz.	JF832258	EF463305	AF515236	XXXXXXXX[j]
Athyrium atkinsonii Bedd.	JF832285	JF832083	EU329070	XXXXXXXX[k]
Diplazium wichurae (Mett.) Diels	JF832275	D43915	AF515245	XXXXXXXX[l]
Diplazium bombonasae Rosenst.	JF832273	EF463308	XXXXXXXX[m]	XXXXXXXX[m]
Diplazium dilatatum Blume	JF832274	EF463311	XXXXXXXX[n]	XXXXXXXX[n]
Diplazium proliferum (Lam.) Thouars	JF303939	JF303974	XXXXXXXX[o]	XXXXXXXX[o]
Diplazium squamigerum (Mett.) Christ	XXXXXXXX[l]	AB574984	XXXXXXXX[p]	XXXXXXXX[p]

[a]Taipei, Taiwan, K012666 (KBCC); [b]Orchid Is., Taiwan, K013016 (KBCC); [c]cultivated, K019687 (KBCC); [d]North Carolina, USA, Rothfels2458 (DUKE); [e]Pingtong, Taiwan, K017010 (KBCC); [f]Nayarit, Mexico, Rothfels 3155 (DUKE); [g]cultivated, K016544 (KBCC); [h]Massachusetts, USA, Kuo117(TAIF); [i]Ilan, Taiwain, Kuo2323 (TAIF); [j]Shizuoka, Japan, Ebihara et al. 07021002 (TNS); [k]Nantou, Taiwan, Kuo477 (TAIF); [l]Taiwan, Kuo986 (TAIF); [m]Pastaza, Ecuador, Moran7493 (NY); [n]Taipei, Taiwan, Kuo987 (TAIF); [o]cultivated, K014215 (KBCC); [p]Hualien, Taiwan, Kuo158(TAIF).

Table S2.5. The spore size information of *Deparia* samples measured in this study.

Phylogenetic clade[a]	Taxa	Voucher	Spore number per sporangium	Spore size (μm^2)[c]	Ploidy	Estimated cytotype
DR	*Deparia unifurcata*	PE01385680 (PE)[b]	64	652.818123 ± 143.067176	diploid	
DR	*Deparia glabrata*	MO6262952 (MO)	64	754.558656 ± 186.539721		diploid
DR	*Deparia viridifrons*	TNS766472 (TNS)	64	779.320652 ± 124.479706	diploid	
DR	*Deparia parvisora*	MO5604016 (MO)	64	785.107669 ± 121.900507		diploid
DR	*pterorachis*	TNS935289 (TNS)	64	929.640313 ± 178.420035	diploid	
DE	*Deparia otomasui*	TNS01135994 (TNS)	64	741.284105 ± 168.621674	diploid	
DE	*Deparia lancea*	Kuo1914 (TAIF)[b]	64	785.008645 ± 121.696125	diploid	
DE	*Deparia bonincola*	TNS290718 (TNS)[b]	64	1295.22276 ± 257.543432	diploid	
DE	*Deparia fenzliana*	OppenheimerH20920 (TAIF)	64	1471.10972 ± 236.040795		polyploid
DE	*Deparia prolifera*	TNS01153706 (TNS)	64	1672.51192 ± 228.430152		polyploid

[a]The phylogenetic clade corresponding to Fig. 1 and 2 in the main text.

[b]The voucher specimen of diploid records.

[c]The length X width from 100 spores representing in the mean ± standard deviation.

Chapter 3.

The rapid geographical range expansions and oversea dispersals of polyploid lineages in *Deparia lancea* (Athyriaceae)

Abstract

This chapter focused on cytogeography and the inferred dispersal rates of both diploids and polyploids in *Deparia lancea*. Based on a comprehensive sampling throughout its species geological range, a restricted and a wide distribution pattern for diploids and polyploids (sexual tetraploids and sexual hexaploids) were revealed, respectively. Diploids were found only in Taiwan while both sexual tetraploids and hexaploids were not only found in Taiwan but also in other regions. The tetraploids were also found in Japan, China, Korea, Himalaya region, and Borneo. The hexaploids were also found in Japan and the Philippines (Batan Is.). The cpDNA and nDNA phylogenies further identified the multiple origins in these autopolyploids during Pleistocene. In comparison with the diploids, these descendent polyploid lineages were demonstrated with higher inferred dispersal rates and higher abilities in oversea dispersals. These suggested the rapid range expansions of the *D. lancea* polyploid lineages can been achieved by their increased colonization ability, but not be limited by their young evolutionary ages and sea barrier formations seperating East Asia island chain during the Early Pleistocene.

Introduction

This chapter targeted on a single *Deparia* species, *Deparia lancea* (Thunb. ex Murray) Fraser-Jenk. (Athyriaceae), which comprises both diploids and polyploids. Widely distributed *D. lancea* polyploids have been discovered: tetraploids - Taiwan (Tsai & Shieh 1984), Japan (Honshu and Kyushu; Nakato & Mitui 1979), China (Fukien; Weng 1990) and Nepal (Matsumoto & Nakaike 1990); hexaploids - Japan (Honshu and Ryukyu Islands; Nakato & Mitui 1979). By contrast, diploids have been reported only in Taiwan (Tsai & Shieh 1984). In addition, both of

the close relatives of *D. lancea*, *Deparia otomasui* (Kurata) Seriz. and *Deparia bonincola* (Nakai) M. Kato, are known with diploids only and are also restrictedly distributed (i.e. Kyushu endemic and Bonin Island endemic, respectively; Takamiya 1996; Kato & Ebihara 2011; also see in Chapter 2). These cytological records and distribution imply that the infra-specific range expansion of *D. lancea* is associated with polyploidization, which has also been suggested by the historical biogeography in genus *Deparia* (see Chapter 2). However, this idea still needs to be confirmed from advanced survey with much more compressive sampling in phylogeographical analyses. Most importantly, further molecular dating analyses (i.e. to infer the evolutionary ages of diploids and polyploids) are indispensable to ascertain if any of certain historical factors is likely to shape natural distribution of polyploids and/or of diploids.

In this chapter, first, the cytogeography of *Deparia lancea* was revealed by confirming the ploidy level of individuals throughout its entire range. Second, the cpDNA and nDNA molecular phylogenies based on these individuals were reconstructed to clarify the relationships between cytotypes. Next, the dated phylogenies were applied to reveal the timing of polyploidization events and divergence times within polyploid lineages. Finally, with the distribution data of these sampling and results from molecular dating, a novel approach was adopted, which was resulted from continuous phylogeographic analyses, to infer and compare the dispersal rates between diploids and polyploid lineages. These should allowed me to examine if the historical factors, including evolutionary age and geographic process in East Asia during Pleistocene, are possible to affect their distribution range.

Materials and methods

Materials

A total of 73 individuals of *Deparia lancea* from all different locations were included in this study. These individuals were collected from all different locations across Taiwan, Japan, China, Korea (Jeju Island), the Philippines (Batan Islands), Indonesia (Borneo), Vietnam, Thailand, Myanmar, Nepal, Bangladesh, and north India. Except for Sri Lanka and Laos, this sampling included the all distributed countries of *D. lancea*. Samples of 9 individuals were from only herbarium specimens while the others were collected with both living materials and herbarium

specimens. For the phylogenetic analyses, additional 12 *Deparia* species were selected as outgroups, which represent the all phylogenetic clades inferred in Chapter 2. The details of these locations and voucher specimen are provided in Table 3.1.

Ploidy and reproductive mode inference

To count somatic chromosomes, root tips were collected between 8-12 AM and pretreated with 70 ppm cycloheximide and 250 ppm 8-hydroxyquinoline (1:1) at 18-20℃ for 24 hours. They were fixed sequentially in 100% acetic acid and absolute ethanol (1:3) overnight and preserved in 70% ethanol at 4℃. Then they were macerated in 1 N HCl at 60℃ for 1 minute, and digested with 4% pectinase (SIGMA, St. Louis, Missouri) for 3 hours. Finally, mitotic chromosomes were stained by modified carbol fuchsin stain and examined under a microscope (Sharma 1982; Huang *et al.* 2006). Based on $X = 40$ of genus *Deparia* (Rothfels *et al.* 2012b), somatic chromosome numbers of a selected diploid, a selected tetraploid, and a selected hexaploid individual of *Deparia lancea* were confirmed. These individuals were further applied as the standards for the flow cytometry analyses, and used to determine the ploidy level of other samples. The protocol of flow cytometry analyses was modified from Ebihara *et al.* (2005) and detailed in Protocol 3. The BD FACSCan system (BD Biosciences, Franklin Lake, New Jersey) was used.

For the samples unavailable with living collection, their ploidies were determined by spore size and guard cell length measured from specimen materials, and such way of ploidy estimation had been successfully applied to many studies of ferns (e.g. Shinohara *et al.* 2006). For each sample, sizes of 100 spores and 100 guard cells from the adaxial sides of sporophyll lamina were measured. These sizes were further compared with the ranges of values measured from the samples with known ploidies, which were previously confirmed by either the somatic chromosome numbers or c flow ytometry analyses.

Reproductive mode was assessed by counting their spore number per sporangium based on five sporangia per individual. In *Deparia*, 64 and 32 spores per sporangium suggest sexual and apomixis, respectively (Kato *et al.* 1992).

Chloroplast and nuclear dataset

DNA was extracted using a modified CTAB procedure, and were

detailed in Protocol 1 and 2. Sequences of five chloroplast DNA (cpDNA) regions, including the *rps16-matK* intergenic spacer (IGS), *ndhF-trnN* IGS, *trnL-L-F* (including *trnL* intron and *trnL-F* IGS), *matK* gene, and *ndhF* gene, were obtained for phylogenies. For *ndhF* gene, a universal primer set [i.e. "FernN2245" (Chen *et al.* 2013) + "Poly ndhF fYMV"] was applied, and then designed specific primers for *Deparia* (i.e. "De ndhF fPTQ" and "De ndhF rPSL"). The PCR reactions were performed in 15 μL volume solution, including 20 ng genomic DNA, 1×PCR buffer, 200 μM dNTP, 15 pmol of each primer, and 0.5 U polymerase (GENETBIO ExPrime Taq DNA Polymerase, Korea). PCR conditions and PCR primer sets of the other regions followed Li *et al.* (2011), Rothfels *et al.* (2012a), Kuo *et al.* (2011), and same as in Chapter 2. The detailed information of these primers can be found in Table S3.1.

A low-copy nuclear gene, the first intron of the cryptochrome gene 2 (*CRY2*), was applied for nuclear DNA (nDNA) phylogeny reconstructions. Based on the published *CRY2* sequence of *Adiantum capillus-veneris* (GenBank accession no.: AB012630) and an unpublished *CRY2* 1st exon partial sequence of *Humata repens*, one degenerate primer (i.e. "POLY CRY2 fVMR") accompanied with "And CRY rDLL" (Zhang *et al.* 2014) to target the 1st intron. After Iobtained partial *CRY2* 1st exon and 2nd exon sequences from outgroup *Deparia* species and few selected *D. lancea* individuals, a *Deparia*-specific primer set was designed: "De CRY2 fEAT" and "De CRY2 rVSL". The PCR reactions were performed in 15 μL volume reactions, including 100 ~ 200 ng genomic DNA, 1×PCR buffer, 200 μM dNTP, 15 pmol of each primer, and 1 U polymerase (GENETBIO ExPrime Taq DNA Polymerase, Korea). To isolate PCR products with different sequence types (i.e. alleles or homoeologs), single-strand conformation polymorphism (SSCP) was used. The protocols of SSCP electrophoresis and silver staining were modified from Ebihara *et al.* (2005) and were detailed in Protocol 4. Before SSCP electrophoresis, the PCR products were purified using a Gel/PCR purification kit (Geneaid, Taipei, Taiwan) and eluted with ddH_2O. For electrophoresis, either acrylamide gel contained MDE solution (Mutation Detection Enhancement; LONZA, Rockland, USA) or 30% acrylamide/bis-acrylamide solution (29:1) was used. The electrophoreses were performed in a dual slab PAGE gel electrophoresis system (AE-6290, ATTO, Tokyo, Japan) with 0.5×TBE buffer at 350V for 24 hours under either a gradient temperature from 20 to 2℃ or a fixed

temperature at 20℃. After SSCP electrophoresis, all gel slices containing the separated single-strand DNA products were purified by the same purification kit above, and were re-amplified and sequenced by another nested primer set, "De CRY2 fATQ" and "De CRY2 rDVP". The detailed information of these primers can be found in Table S3.1. When sequencing of SSCP products failed, these products were cloned into pGEM-T Easy vectors (Promega, Madison, USA) to isolate the mixed sequence types. Ligation, transformation, plating and selection of clones followed manufacturer's protocol.

Phylogenetic analyses

DNA sequences, *rps16-matK* IGS + *ndhF-trnN* IGS + *trnL-L-F* + *matK* + *ndhF* and *CRY2* 1st intron, were first aligned using ClustalW implemented in BioEdit (Hall 1999). The alignments were further edited manually, and the ambiguous alignment regions were removed. Garli 2.0 (Zwickl 2006) was used to reconstruct the maximum likelihood (ML) phylogeny. The proportion of invariant sites and state frequencies were estimated by the program. The GTR + I + Γ model was applied, and "genthreshfortopoterm" option was set to 20,000. To calculate ML bootstrap support (MLBS) values, 500 replicates were run under the same criteria. Bayesian phylogenetic inference posterior probability (BIPP) was performed by MrBayes v.3.1.2 (Huelsenbeck & Ronquist 2001; Ronquist & Huelsenbeck 2003). Two simultaneous runs were carried out with four chains (10^6 generations each), in which each chain was sampled every 1,000 generations. The first 25% of the sample was discarded as burn-in, and the rest were used to calculate the 50% majority-rule consensus tree.

Divergence time estimates

Coalescent model implemented in BEAST 1.7.1 (Drummond *et al.* 2012) was used for divergence time estimates within *Deparia lancea*. The alignment with either cpDNA or nDNA matrix including the sequences from all individuals (i.e. the same as used in ML phylogeny reconstruction) was applied under the optimization of GTR + I + Γ model, an uncorrelated lognormal clock model, and a coalescent constant population model. Each of polyploidy lineages, which were inferred by ML phylogenies and assumed single origin, was constrained as a monophyletic group in order to access to its stem and crown age. The clade DE [i.e. *Deparia lancea* + *D. otomasui* + *D. bonincola* + Hawaiian

Deparia species (i.e. either *D. marginalis* or *D. fenziliana*); also see in Chapter 2] was constrained with a mean age of 8.52 Ma and a standard deviation of 2 Ma under a normal distribution according to the results of divergence time range in Chapter 2. The MCMC chain was set to 50 million with 10% burnin, and saving the tree and log file every 1000 generations. To confirm the accuracy on infraspecies divergence time of *D. lancea*, the alignments included only two most diverged sequences of *D. lancea* with the same outgroups taxa while removing redundant allele-like sequences (i.e. one sequence per species/locus for outgroup) were applied under the optimization of speciation Yule model implemented BEAST 1.7.1. In addition to age constrain on the DE clade, the root age was constrained with a mean age of 27.68 Ma and a normal distribution of 2 Ma standard deviation, which were accorded to the divergence time range based on the previous results (see in Chapter 2). Other prior setting and MCMC chain length followed as those in coalescent model. The Tracer v1.5 (Rambaut & Drummond 2007) was used to examine the ESS values of each BEAST replicate. TreeAnnotator (Drummond *et al.* 2012) was used to summarize the results of molecular dating analysis.

Dispersal rate inference

Gathering the latitude/longitude data and the results of molecular dating inferred from coalescent model (see in *Divergence time estimates*), a continuous phylogeography using relaxed random walk model [implemented in BEAST 2.1.2 (Lemey *et al.* 2010; Bouchaert *et al.* 2014)] was reconstructed for the diploids and for each polyploid lineage in *Deparia lancea*. In these analyses, only *D. lancea* was included, either containing diploids or one of non-endemic polyploid lineages (i.e. those appear in more than one location). These continuous phylogeographic analyses in this study solely aimed on the application of a relaxed random walk model to infer the possible geographic distances moving through evolutionary time among all MCMC trees. Because sequences under each polyploid lineage was invariant, thereby being unable for me to infer robust infra-lineage phylogenies (see the phylograms in Figs 3.4 and 3.5), this study were not going to present their reconstructed dispersal routes from continuous phylogeographies. The setting of priors was under the optimization of a GTR + I + Γ model, a coalescent constant population model, a relaxed clock log normal model for location data, a strict clock

rate for sequence alignment, and a root age with a normal distribution. The initial values of the last two priors were according to the molecular dating results (see in *divergence time estimates* and Table S3.2). In addition, based on distribution range of analyzed individuals, I set the "root-location prior" as the point with the middle of their latitude range and the middle of their longitude range, and set "randomizelower" and "randomizeupper" according to their minimum and maximum values of latitude/longitude. The details of these prior setting were provided in Table S3.2. The MCMC chain was set to 50 million with 10% burnin, and saving the tree and log file every 1000 generations. The Tracer v1.5 (Rambaut & Drummond 2007) was used to examine if the MCMC runs of a BEAST replicate were into convergence. TreeAnnotator (Drummond *et al.* 2012) was used to summarize the results of continuous phylogeography analyses, and MATLAB 8.0 (D'Errico 2005) was used to calculate the geographical distances along the phylogenetic branches according to the latitude/longitude of reconstructed ancestral states and tip states. Finally, the dispersal rates of the diploids and each polyploid lineage were individually inferred by a total of geographical distances dividing a total of evolutionary ages within a reconstructed continuous phylogeography.

Results

Cytotypes, reproductive mode, and distributions

A diploid, a tertaploid, and hexaploid were first determined by their somatic chromosome numbers (Fig. 3.1 and Table 3.1). Additional 18 diploids, 23 tetraploids, 2 pentaploids, and 18 hexaploids were further identified based on the flow cytometry analyses (Fig. 3.1 and Table 3.1). With the ranges of guard cell length and spore size (length × width) inferred from these individuals (Fig. 3.2), 6 tetraploids and 3 hexaploids were identified from specimen materials (Table 3.1). Within diploids and tetraploids, and hexaploids, only sexual reproductive mode (i.e. producing only 64-spored sporangia) was found with one exception of sterile hexaploid (Table 3.1). All pentaploids were regarded as sterile individuals, which produce spores in abnormal shapes or debris forms. In current study, diploids were found only in Taiwan, while polyploids were revealed with a broad distribution covering species distribution range (Fig. 3.3). Tetraploids were found in Taiwan, Japan (Honshu and Shikoku), Korea (Jeju Island), China, Indonesia (Borneo), Vietnam, Thailand,

Burma, Nepal, Bangladesh, and north of India. Hexaploids were found in Taiwan, Japan (Kyushu, Honshu, and Ryukyu), and the Philippines (Batan Islands). Pentaploid were found in Japan (Kyushu and Honshu), where belongs to the overlapped distribution range of tetraploid and hexaploid (Fig. 3.3), and are the presumed sterile hybrids between these two cytotypes (Nakato & Mitui 1979).

Phylogenies and divergence time

The cpDNA matrix and nDNA matrix contained 4,561 and 1,145 characters, repectively. The log-likelihood score for the most likely ML tree based on the cpDNA matrix and nDNA matrix was -10,746.028439 and -3,491.701513, respectively. In the cpDNA phylogeny, *Deparia lancea* formed a highly supported monophyletic group (MLBS = 100 and BIPP = 1.00) nested in the clade DE (Fig. 3.4). Within *D. lancea*, one tetraploid (i.e. Ta) and three hexaploids (i.e. Ha-c) sequence groups were identified. Only sequence group Ha has the identical sequences with that in diploids.

In the nDNA phylogeny, *D. lancea* also formed a highly supported monophyletic group (MLBS = 100 and BIPP = 1.00) nested in clade DE (Fig. 3.5). Within *D. lancea*, four tetraploid (i.e. T1-4) and nine hexaploid (i.e. H1-7, H12, H14) sequence groups were identified. In H1, H2, and T1, the identical sequences were also found in the diploids. The sequence groups of polyploids in the nDNA phylogeny are all nested in the diploids' sequences, and the earliest diverging lineage in *D. lancea* is a diploid sequence sharing a 10-bp indel with sequences in other outgraoup species (Fig. 3.5). However, in the cpDNA phylogeny, diploids' sequences are nested in the polyploids' sequence groups (Fig. 3.4).

In these phylogenies, no relationship between sampled tetraploids and hexaploids was found, except for the close relationships of Ta/Hc and of T2/H4. Under assumption that each of these sequence groups in polyploids is composed by a single origin (i.e. originated from the diploids only once), the dated phylogenies inferred from the coalescent model were shown in Fig. 3.6. The divergence times of diploids and polyploid lineages using the coalescent model were summarized in Table 3.2. The crown ages (i.e. the age of the first divergence) of *D. lancea* revealed by molecular dating using the speciation Yule model are 1.85 and 3.80 Ma for cpDNA and nDNA phylogeny, respectively, which are mostly consistent with those revealed by the coalescent model (Table 3.2)

suggesting the accuracy of estimated infra-species divergences. However, the stem ages of *D. lancea* (i.e. the divergence age between *D. lancea* and sister group) are quite different among analyses (Table 3.2; 5.17 for cpDNA and 8.82 Ma for nDNA phylogeny using the Yule speciation model), which are likely attributed to the topological uncertainty/difference on inter-species relationships under DE clade (Figs 3.4 and 3.5) and the different molecular dating models. In all analyses, the crown ages of *D. lancea* and its diploids are consistently younger in cpDNA dated phylogenies than in nDNA dated phylogenies (Fig. 3.6 and Table 3.2). For polyploids, their estimated divergence times show no obvious difference between cpDNA and nDNA dated phylogenies (Fig. 3.6 and Table 3.2). In tetraploids, polyploidization(s) was estimated in between 1.33 - 0.66 Ma (i.e. between the oldest stem age and the youngest crown or stem age; Table 3.2). In hexaploids, polyploidization(s) was estimated in between 2.80 - 0.28 Ma (Table 3.2).

Inferred dispersal rates in the diploids and polyploid lineages

In both results from cpDNA and nDNA continuous phylogenies, the inferred dispersal rates of polyploid lineages are higher than that of diploids (Table 3.2). The highest inferred dispersal rate is in tetraploid cpDNA lineage, Ta, and the lowest one is in diploids nDNA lineage (Table 3.2). The range of the diploids is 232 – 623 km Ma^{-1} while those in tetraploids and hexaploids are 3,129 – 10,021 and 350 – 5,569 km Ma^{-1}, respectively (Table 3.2).

Discussion

Conflict relationship and divergence time between cpDNA and nDNA phylogenies

In the nDNA phylogeny, all polyploid lineages of *Deparia lancea* were revealed nested in the diploids (Fig. 3.5). In contrast, the diploids were as a group embedded in the polyploid lineages in the cpDNA phylogeny (Fig. 3.4). The most plausible explanation is the early extinction in ancestral cpDNA haplotypes in the diploids, which are no longer exist or too rare to be represented by current sampling. This possibility was also reflected by that younger divergence times of both diploids and *D. lancea* inferred from cpDNA sequences comparing with those inferred from nDNA sequences (Table 3.2). Such phenomenon is usually referred to cytoplasmic bottleneck, in which the cytoplasmic

effective population size (i.e. effective population size of female and/or bisexual progeny in most plants) has decreased (e.g. Mayer & Soltis 1994; Provan *et al.* 1999). The causes of a strong reduction of cytoplasmic effective population size can be attributed to organelle-adaptive or male-sterile mating system (e.g. sex ratio biased to male) or continuously population decline (Laporte *et al.* 2000; Wade & Goodnight 2006). The continuously population decline in *D. lancea* diploids is also implied by a reconstruction of past species distribution and demographical change after the last interglacial maximum (see Chapter 4 and 6), and might result in the higher fixation rate in uniparentally inherited cpDNA comparing with biparentally inherited nDNA. In addition, because gynodioecy and androdioecy can be maintained and determined in the gametophyte generation of homosporous ferns, sex ratio dynamic in gametophyte population could possibly act as another important role resulting in cytoplasmic bottleneck.

Multiple origins of polyploids

Both cpDNA and nDNA phylogenies supported that the origins of the polyploids in *Deparia lancea* is not resulted from interspecies hybridization (Figs 3.4 and 3.5). In nDNA phylogeny, all polyploids' sequences are nested in diploids' (Fig. 3.5). Further, no sterile-like individual was found among diploids (Table 3.1), and this indicated that cryptic species unlikely exist in diploids. Based on above, tetraploids and hexaploids in *D. lancea* should be regarded as autopolyploids instead of allopolyploids resulted from genome doubling after interspecies hybridization. In tetraploids, although cpDNA phylogeny might not resolve their multiple origins due to the possible extinction of ancient haplotype in diploids and uniparental inheritance of plastid genome, the nDNA phylogeny suggests that tetraploid genomes were arisen from at least four different haploid genomes through independent polyploidization events (Fig. 3.5). In addition, the nDNA genotyping results suggest that diverse genome combinations among tetraploids are not only resulted from multiple origins also possibly from recombination between duplicated homoeologous genomes after polyploidization(s). The majority of tetraploids are composed by either the genotype T1T3 and T2T3 (Fig. 3.3 and Table 3.1), which suggest that T3 is on one of a pair of homoeologous chromosomes and T1 and T2 occupy on the another one, whereas the existence of rare genotype T1T2 seems to be a

consequence of occasionally homoeologous chromosomes recombination between two duplicated *CRY2* loci. In hexaploids, at least three independent origins could be inferred from the cpDNA and nDNA phylogenies, but these origins are not associated with these tetraploids (Figs 3.4 and 3.5). If these tetraploids generated "diploid" gametes to contribute their nuclear genomes to hexaploids, the origins of two homoeologs should share between these two cytotypes and might be revealed in the nDNA phylogeny. However, except for H4, no *CRY2* sequence in hexaploids was found to be related with those in tetraploids (Fig. 3.5).

Among hexaploids, one independent and isolated lineage was revealed with unique sequences types in both cpDNA and nDNA, Hc and H12 and H14, and such hexaploid individual was found only in a single location in Taiwan (Fig. 3.3). For the other hexaploids, either with Ha or Hb in their cpDNA haplotypes, and either H6, H3, or both present in their nDNA genotypes (Fig. 3.3). In addition, these hexaploids are also diverse in composition with different origins of cpDNA and/or nDNA sequences. In cpDNA phylogeny, they can be found with two independent origin - Ha and Hb (Fig. 3.4). Similar situation is also found in their nDNA phylogeny (Fig 3.5). Most of them contain H3 + H6 sequence groups combined with either H1, H2, or H5, which might be different independent origins (Fig s 2.3 and 3.5). Even though revealed with multiple origins, these different lineages in hexaploids are likely to interbreed with each other. For example, the reciprocal combinations between two cpDNA origins, Ha and Hc, and two presumed nDNA origins, H5 and H2, can be all found; and all individuals with these different haplotype/genotype combinations are sexual in reproduction but not sterile [except Ha/H2H3H7]. For pentaploids, because of their sterility and distribution overlapped with the both ranges of tetraploids and hexaploids, they can be regarded as the intercytotype hybrids, which have also been reported in the previous study (Nakato & Mitui 1979).

Polyploidization events

Since both tetraploids and hexaploids in *D. lancea* are multiple origins, it could also mean that multiple polyploidization events exist in both cytotypes. For tetraploids, the formation in every single origin requires at least one polyploidization event generating from diploids, and this process could be involved with or without an intermediate triploid. In

addition to one polyploidization event, the formation in every single origin in the hexaploids requires another one demipolyploidization event, which might be involved in the process of either a diploid to an intermediate triploid or an intermediate tetraploid to hexaploid. However, no such intermediate individual was found based on current samplings and phylogenies (Figs 3.4 and 3.5 and Table 3.1). Although polyploidization events could not be simply identified by tracking the formation of these polyploids, different polyploidization events can be indicated by their differences in estimated divergence times. In tetraploids, at least one polyploidization event is likely in the time period between 1.3 to 0.66 Ma corresponding to the ages of Ta and T1-T3 while another one seems much recent within 0.3 Ma (i.e. corresponding to the stem age of T4) (Fig. 3.6 and Table 3.2). In the isolate hexaploid lineage, Hc/H12H14, one polyploidization and one demipolyploidization event are suggested to be less than 2.4 Ma, when were after its diverge from ancestral diploids, but the estimated divergence times of Hc, H12, and H14 show no consistence (Fig. 3.6 and Table 3.2). Among the other hexaploids, there seems an earlier (demi)polyploidization event(s) during 2.80 - 0.8 Ma corresponding to the divergence times of Hb, H6, and H7, and late polyploidization events during 1.84 - 0.28 Ma corresponding to divergence times of the other sequence groups (Fig. 3.6 and Table 3.2). The formations of these hexaploids are suggested within 0.82 Ma since their polyploidy genomes are all composed by the same sequence group (i.e. H3) derived from the late (demi)polyploidization event(s) (Tables 3.1 and 3.2).

Historical effects and rapid range expansion of polyploids

Because all polyploids' lineages in nDNA phylogeny are nested in diploids and diploids are found only in Taiwan (Figs 3.3 and 3.5), it can speculate that the polyploids in *Deparia lancea* were originated from Taiwan. However, current samplings may be inadequate (i.e. one individual per location) to exclude the posiblilty that diploid occur outside of Taiwan. Particularly, diploids did possibly disperse from Taiwan without crossing sea barriers to the other flanking area via the land bridge during the Pleistocene (Osozawa *et al.* 2012). In addition, the estimated divergence time suggests the formation of tetraploids and non-Taiwan endemic hexaploids (i.e. excluding the Hc/H12H14 hexaploid) can be traced up to 1.3 and 0.82 Ma, respectively. In this time

period, sea barriers had first established and blocked connection of Taiwan Main Island with continental East Asia and Southern Ryukyu (Osozawa *et al.* 2012), where are now dominant by tetraploids and hexaploids, respectively (Fig. 3.3). However, the Taiwan Sea Strait might shallow enough to allow land connection between Taiwan Main Island and continental East Asia when sea level decreased during glaciation (Kimura 2000; Huang 2011; Osozawa *et al.* 2012). These indicate that the polyploids, especially for the tetraploids, were possible to be originated from ancient dispersed diploids without limitation of sea barriers. Based on above, current evidences cannot exclude the possibility that the polyploidizations of these polyploids occurred outside of Taiwan.

On the other hand, based on the estimated crown ages of non-endemic sequence groups, expansions of tetraploids and hexaploids are suggested within 1.1 Ma (Table 3.2). For hexaploids, all crown ages of non-endemic sequence groups implied that the expansions of hexaploids started from 1.06 – 0.28 Ma (Table 3.2). During the same time, the Taiwan Main Is., Ryukyu Is., and Japan main Is. were isolated with each other by deep sea gaps (i.e. Younaguni and Tokara gaps; Osozawa *et al.* 2012). Therefore, the expansion of hexaploids is considered to be involved with dispersals crossing sea barriers to spread throughout East Asia Archipelago. In addition, a very similar cytogeographical distribution had also revealed in another *Deparia* species – *D. petersenii* subsp. *petersenii*, in which diploids were only found in Taiwan but polyploids were found distributed throughout Ryukyu Is. to Kyushu (Shinohara *et al.* 2006). Although molecular dating is not available in this *D. petersenii* subsp. *petersenii* study, the shared cpDNA haploptypes between diploids and polyploids suggest that at least some polyploid lineages were recently originated from diploids and further oversea-dispersed outside out Taiwan.

Even *Deparia lancea* diploids are assumed to be distributed in the places outside of Taiwan, they are currently not abundant in these places, and the whole distribution is considered to be very restricted. By contrast, a broad geographical range of the descendant polyploids is revealed not only to be distributed in Taiwan but also across the continental Asia and East Asia and in the Philippines (Batan Islands) and Indonesia (Borneo). These suggest an infraspecific and rapid range expansion associated with polyploidization, which are also reflected by the results of inferred dispersal rates. The inferred dispersal rates of tetraploids and hexaploids

are higher than those of diploids in 7 – 38 and 1.5 – 24 times, respectively (Table 3.2). Aside from the higher inferred dispersal rates, the polyploids in *D. lancea* are also indicated with conducting oversea long-distance dispersals to the Philippines (Batan Islands) and Indonesia (Borneo). In contrast, such dispersal crossing sea barriers is not found in the diploids based on current distribution. Comparing with hexaploids, tetraploids higher inferred dispersal rates (Table 3.2). One plausible explanation is that these tetraploids mostly formed and diverged/expanded earlier than hexaploids (Table 3.2), and, therefore, they first occupied the open habitats and blocked the further colonization by hexaploids.

The higher dispersal/colonization abilities in polyploids always have strong relevance to (1) an increased reproductive success to tolerant inbreeding depression or to be apomictic and/or (2) a broaden ecological niche (te Beest *et al.* 2011; Ramsey & Ramsey 2014). In ferns, the first factor has been suggested in several cases of polyploidy range expansion (Trewick *et al.* 2002; Flinn 2006; Korall & Pryer 2014; also see in Chapter 2), and, under comparisons with conspecific diploids, the higher rates being intragemetophytic selfing (i.e. the selfing of an egg and a sperm from the same gametophyte) have been also revealed in several sexual polyploid species, including *D. lancea* (Masuyama & Watano 1990; Ranker & Geiger 2008; also see in Chapter 5). These gains of inbreeding ability are due to the mask of deleterious alleles by an increased heterozygosity among homoeologs in polyploidy gametophyte genome (Ranker & Geiger 2008). Such genomic heterostasis in autopolyploid population can further be attributed from (1) merging multiple-originated lineages and (2) homoeologous recombination between duplicated genomes (Parisod *et al.* 2010; te Beest *et al.* 2011; Ramsey & Ramsey 2014). These two phenomena are also suggested in the polyploids in *D. lancea*, and multiple origins seen not rare in the formation of fern polyploid species (Trewick *et al.* 2002; Shinohara *et al.* 2006; Adjie *et al.* 2007; Nitta *at al.* 2011; Chen *et al.* 2014; Sigel *et al.* 2014), and seem to be a major rule in naturally established polyploid taxa (Soltis *et al.* 2014). However, in order to disentangle the effects of niche broadening on their dispersal/colonization abilities, advanced study is necessary to focus on the comparisons of ecological niche breadths in both diploids and polyploids of *D. lancea* (also see in Chapter 6).

References

Adjie B, Masuyama S, Ishikawa H, Watano Y (2007) Independent origins of tetraploid cryptic species in the fern *Ceratopteris thalictroides*. *Journal of Plant Research*, **120**, 129–138.

Bouckaert R, Heled J, Kühnert D *et al.* (2014) BEAST 2: a software platform for Bayesian evolutionary analysis. *PLoS Ccomputational Biology*, **10**, e1003537.

Chen CW, Ngan LT, Hidayat A *et al.* (2014) First insights into the evolutionary history of the *Davallia repens* complex. *Blumea*, **59**, 49–58.

Drummond AJ, Suchard MA, Xie D, Rambaut A (2012) Bayesian phylogenetics with BEAUti and the BEAST 1.7. *Molecular Biology and Evolution*, **29**, 1969–1973.

D'Errico J (2005) Surface Fitting using gridfit (http://www.mathworks.com/matlabcentral/fileexchange/8998), MATLAB Central File Exchange. Retrieved May 18, 2006.

Ebihara A, Ishikawa H, Matsumoto S *et al.* (2005) Nuclear DNA, chloroplast DNA, and ploidy analysis clarified biological complexity of the *Vandenboschia radicans* complex (Hymenophyllaceae) in Japan and adjacent areas. *American Journal of Botany*, **92**, 1535–1547.

Flinn K (2006) Reproductive biology of three fern species may contribute to differential colonization success in post-agricultural forests. *American Journal of Botany*, **93**, 1289–1294.

Hall T (1999) BioEdit: a user-friendly biological sequence alignment editor and analysis program for Windows 95/98/NT. *Nucleic Acids Symposium Series*, **41**, 95–98.

Huang SF (2011) Historical biogeography of the flora of Taiwan. *Journal of the National Taiwan Museum*, **64**, 33–63.

Huang YM, Chou HM, Hsieh TC, Wang JC, Chiou WL (2006) Cryptic characteristics distinguish diploid and triploid varieties of *Pteris fauriei* (Pteridaceae). *Canadian Journal of Botany*, **84**, 261–268.

Huelsenbeck JP, Ronquis F (2001) MRBAYES: Bayesian inference of phylogenetic trees. *Bioinformatics*, **3**, 754–755.

Kato M, Ebihara A (2011) *A book series from the National Museum of Nature and Science No. 11 Endemic plants of Japan.* Takai University Press, Kanagawa.

Kato M, Nakato N, Cheng X, Iwatsuki K (1992) Cytotaxonomic study of ferns of Yunnan, southwestern China. *The Botanical Magazine*, **105**, 105–124.

Kimura M (2000) Paleogeography of the Ryukyu Islands. *Tropics*, **10**, 5–24.

Korall P, Pryer KM (2014) Global biogeography of scaly tree ferns (Cyatheaceae): evidence for Gondwanan vicariance and limited transoceanic dispersal. *Journal of Biogeography*, **41**, 402–413.

Kuo LY, Li FW, Chiou WL, Wang CN (2011) First insights into fern matK phylogeny. *Molecular Phylogenetics and Evolution*, **59**, 556–566.

Laporte V, Cuguen J, Couvet D (2000) Effective population sizes for cytoplasmic and nuclear genes in a gynodioecious species: the role of the sex determination system. *Genetics*, **154**, 447–458.

Lemey P, Rambaut A, Welch JJ, Suchard M a (2010) Phylogeography takes a relaxed random walk in continuous space and time. *Molecular Biology and Evolution*, **27**, 1877–1885.

Li FW, Kuo LY, Rothfels CJ *et al.* (2011) *RbcL* and *matK* earn two thumbs up as the core DNA barcode for ferns. *PLoS one*, **6**, e26597.

Masuyama S, Watano Y (1990) Trends for inbreeding in polyploid pteridophytes. *Plant Species Biology*, **5**, 13–17.

Matsumoto S, Nakaike T (1990) Cytological observations of some ferns in Nepal (1). On the related taxa in Japan. *Cryptogams of the Himalayas*, **2**, 163–178

Mayer M, Soltis P (1994) Chloroplast DNA phylogeny of *Lens* (Leguminosae): origin and diversity of the cultivated lentil. *Theoretical and Applied Genetics*, **87**, 773–781.

Nakato N, Mitui K (1979) lntraspecific polyploidy in *Diplazium subsinuatum* (Wall.) Tagawa. *Journal of Japanese Botany*, **54**, 129–140.

Nitta JH, Ebihara A, Ito M (2011) Reticulate evolution in the *Crepidomanes minutum* species complex (Hymenophyllaceae). *American Journal of Botany*, **98**, 1782–1800.

Osozawa S, Shinjo R, Armid A *et al.* (2012) Palaeogeographic reconstruction of the 1.55 Ma synchronous isolation of the Ryukyu Islands, Japan, and Taiwan and inflow of the Kuroshio warm current. *International Geology Review*, **54**, 1369–1388.

Parisod C, Holderegger R, Brochmann C (2010) Evolutionary consequences of autopolyploidy. *New phytologist*, **186**, 5–17.

Provan J, Powell W, Dewar H *et al.* (1999) An extreme cytoplasmic bottleneck in the modern European cultivated potato (*Solanum tuberosum*) is not reflected in decreased levels of nuclear diversity. *Proceedings of the Royal Society B: Biological Sciences*, **266**, 633–639.

Ranker TA, Geiger JMO (2008) Population genetics. In: *Biology and Evolution of ferns and Lycophytes* (eds. Ranker TA, Haufler CH), pp. 107–133. Cambridge University Press, New York.

Ramsey J, Ramsey T (2014) Ecological studies of polyploidy in the 100 years following its discovery. *Proceedings of the Royal Society B: Biological Sciences*, in press.

Ree RH, Smith SA (2008) Maximum likelihood inference of geographic range evolution by dispersal, local extinction, and cladogenesis. *Systematic Biology*, **57**, 4–14.

Ronquist F, Huelsenbeck JP (2003) MrBayes 3: Bayesian phylogenetic inference under mixed models. *Bioinformatics*, **19**, 1572–1574.

Rothfels CJ, Sundue MA, Kuo L-Y *et al.* (2012) A revised family-level classification for eupolypod II ferns (Polypodiidae: Polypodiales). *Taxon*, **61**, 515–533.

Sharma HC (1982) A technique for somatic counts from root tips of cereal seedlings raised by embryo culture. *Current Science*, **51**, 143–144.

Shinohara W, Hsu TW, Moore SJ, Murakami N (2006) Genetic analysis of the newly found diploid cytotype of Deparia petersenii (Woodsiaceae: Pteridophyta): evidence for multiple origins of the tetraploid. *International Journal of Plant Sciences*, **167**, 299–309.

Sigel EM, Windham MD, Pryer KM (2014) Evidence for reciprocal origins in *Polypodium hesperium* (Polypodiaceae): a natural fern model system for investigating how multiple origins shape allopolyploid genomes. *American Journal of Botany*, **101**, 1476–1485.

Soltis DE, Visger CJ, Soltis PS (2014) The polyploidy revolution then...and now: Stebbins revisited. *American Journal of Botany*, **101**, 1057–1078.

Takamiya M (1996) *Index to chromosomes of Japanese Pteridophyta (1910-1996).* Japan Pteridological Society, Tokyo.

te Beest M, Le Roux JJ, Richardson DM *et al.* (2012) The more the better? The role of polyploidy in facilitating plant invasions. *Annals of Botany*, **109**, 19–45.

Trewick S, Morgan-Richards M, Russell SJ *et al.* (2002) Polyploidy, phylogeography and Pleistocene refugia of the rockfern Asplenium

ceterach: evidence from chloroplast DNA. *Molecular Ecology*, **11**, 2003–2012.

Tsai JL, Shieh WC (1984) A cytotaxonomic survey of the pteridophytes in Taiwan (2).Chromosome and spore characteristics. *Journal of Science and Engineering*, **21**, 47–69.

Wade M, Goodnight C (2006) Cyto-nuclear epistasis: two-locus random genetic drift in hermaphroditic and dioecious species. *Evolution*, **60**, 643–659.

Weng RF (1990) Cytological observations on some Chinese ferns. *Acta Phytotaxonomica Sinica*, **28**, 27–33.

Zhang WY, Kuo LY, Li FW, Wang CN, Chiou WL (2014) The hybrid origin of Adiantum meishanianum (Pteridaceae): a rare and endemic species in Taiwan. *Systematic Botany*, **39**, 1034–1041.

Zwickl DJ (2006) Genetic algorithm approaches for the phylogenetic analysis of large biological sequence datasets under the maximum likelihood criterion. Ph. D thesis, The University of Texas, Austin.

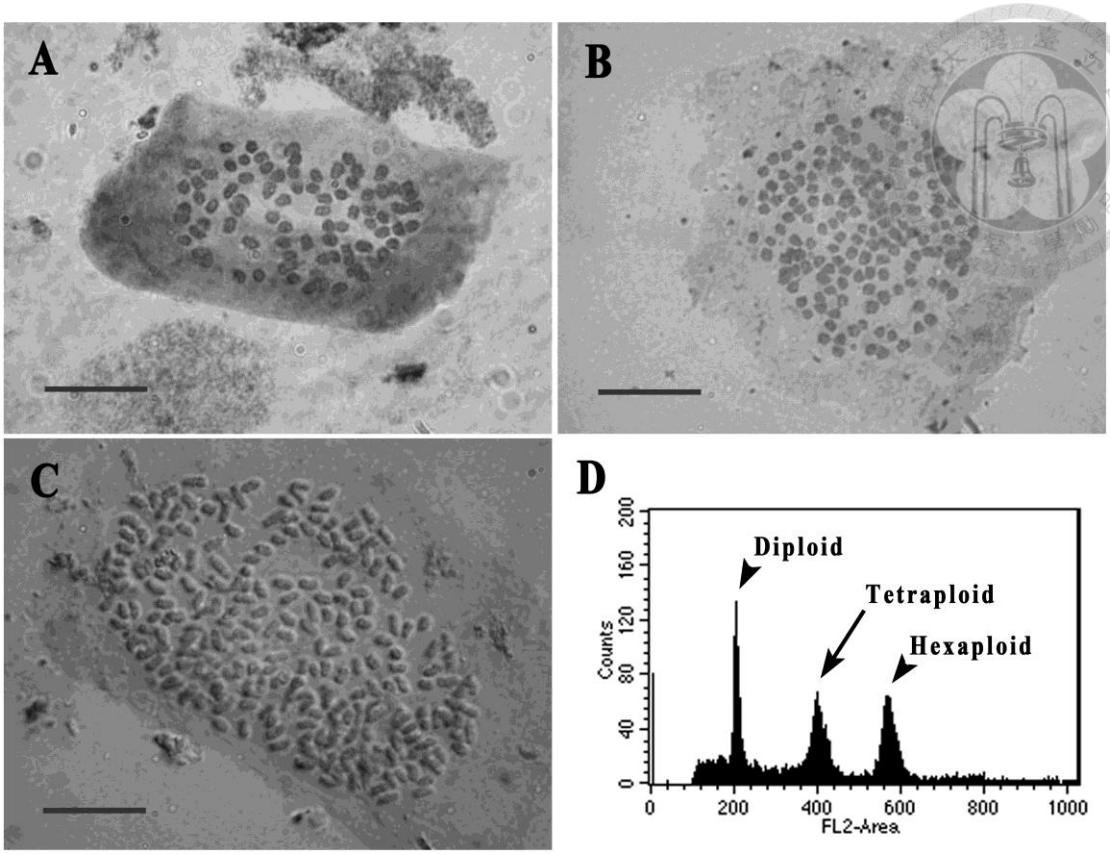

Fig. 3.1. Somatic chromosome photograph of *Deparia lancea* (A) diploid (*2n* = 80), (B) tetraploid (*2n* = ca. 160), and (C) hexaploid (*2n* = ca. 240); scale bars = 20 μm. (D) Flow cytometry results of diploid, tetraploid, and hexaploid.

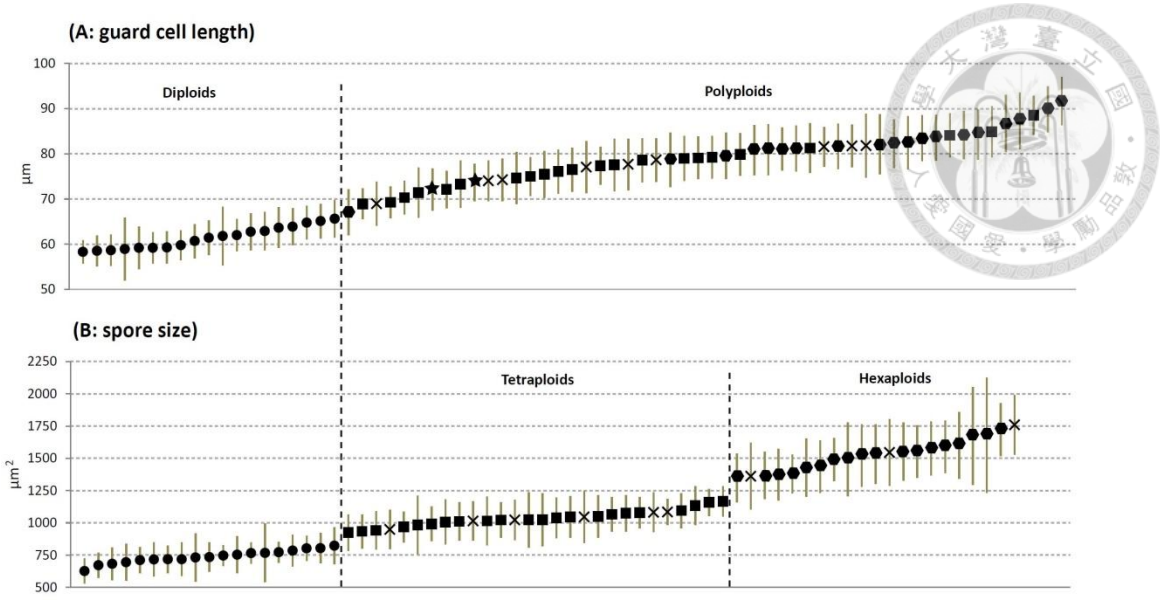

Fig. 3.2. Range of (A) guard cell lengths and (B) spore sizes (length X width) in different cytotypes of *Deparia lancea*. For each individual, the mean value of 100 cells is presented with error bars indicating one standard deviation. The circles, squares, stars, and hexagons represent diploids, tetraploids, pentaploids, and hexaploids, respectively, for which their ploidies are confirmed by either somatic chromosome number or flow cytometry analyses. The crosses present the individuals from specimen materials.

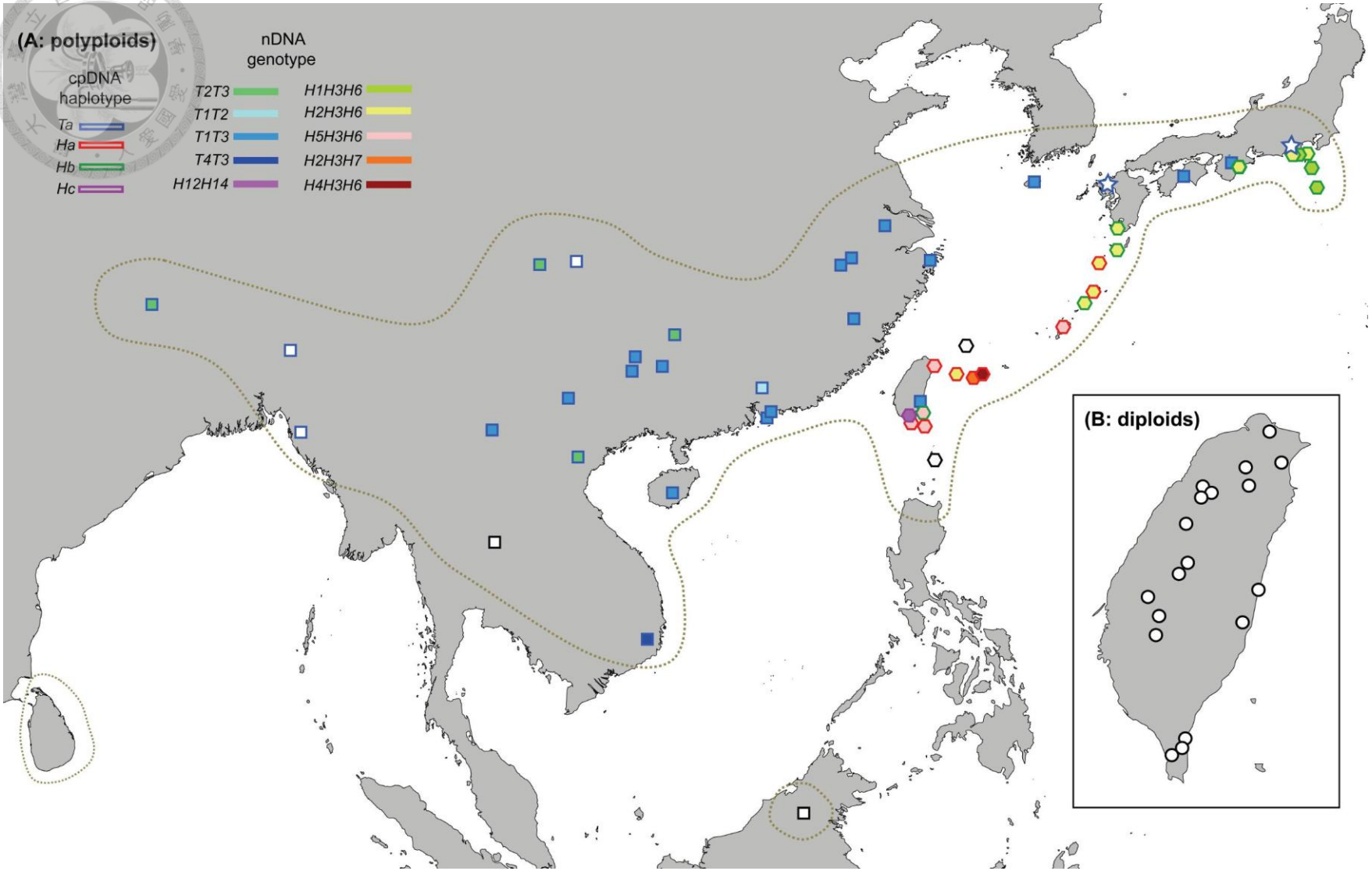
(A: polyploids)
cpDNA haplotype
Ta
Ha
Hb
Hc
nDNA genotype
T2T3
T1T2
T1T3
T4T3
H12H14
H1H3H6
H2H3H6
H5H3H6
H2H3H7
H4H3H6
(B: diploids)

Fig. 3.3. The distribution map of cytotypes, cpDNA haplotypes, and nDNA genotypes in *Deparia lancea*. The cytotypes are presented in different shapes: circles (2X), squares (4X), stars (5X), and hexagons (6X). (A) The cpDNA haplotypes (*rps16-matK* IGS + *ndhF-trnN* IGS + *trnL-L-F* + *matK* + *ndhF*) and nDNA genotypes (*CRY2* 1st intron) of polyploids are indicated by circumference and internal colors, respectively, which are based on the sequence groups indicated by the phylogenies (see in Figs 3.4 and 3.5). The dash lines indicate the current distribution of *D. lancea*. (B) Distribution of the diploids.

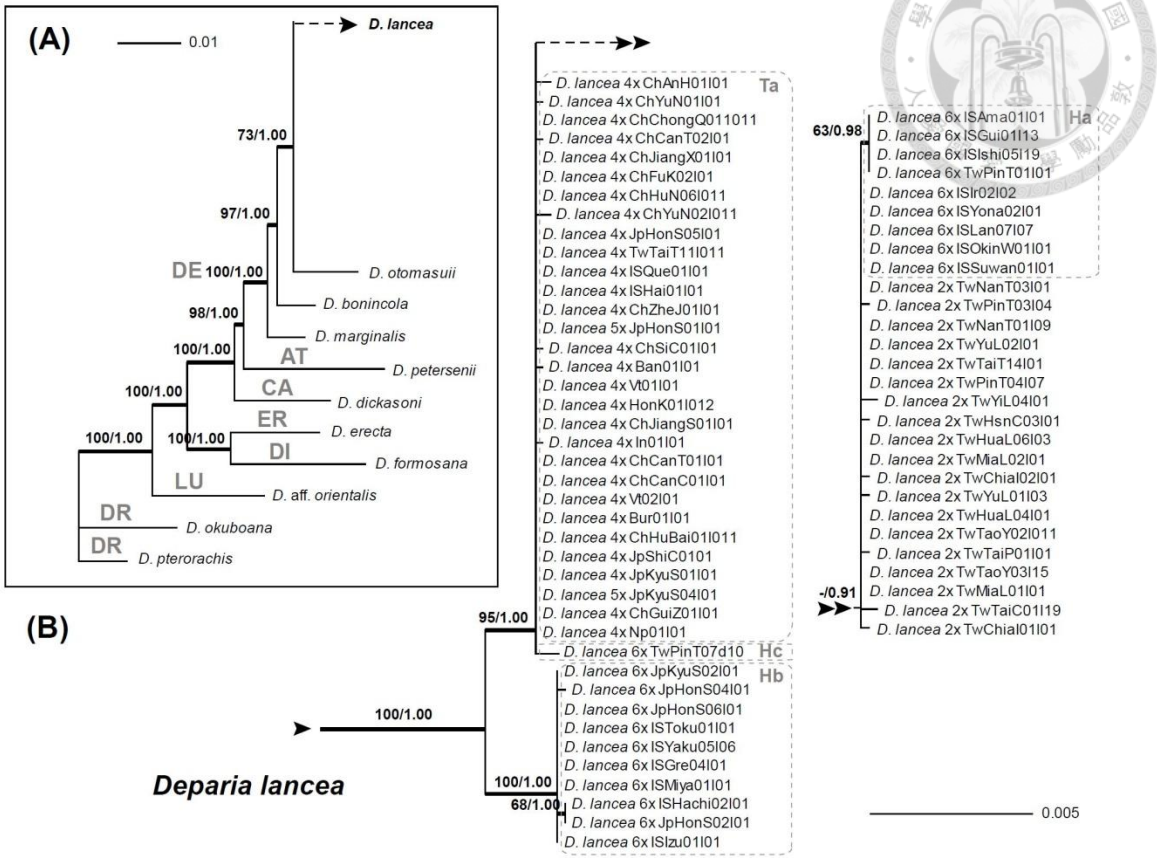

Fig. 3.4. The cpDNA phylogeny of *Deparia lancea* with 10 selected outgroup taxa in *Deparia* based on *rps16-matK* IGS + *ndhF-trnN* IGS + *trnL-L-F* + *matK* + *ndhF*. ML bootstrap support (MLBS) values and Bayesian inference posterior probabilities (BIPP) are indicated on branches as MLBS/BIPP. The thickened branch indicates BIPP ≥ 0.95. (A) The species relationships of *D. lancea* and outgroups. The different infrageneric clades inferred in Chapter 2 are indicated in gray on the branches. (B) The infraspecies relationships within *D. lancea*. The dashed boxes indclude the different sequence groups of haplotypes in polyploids.

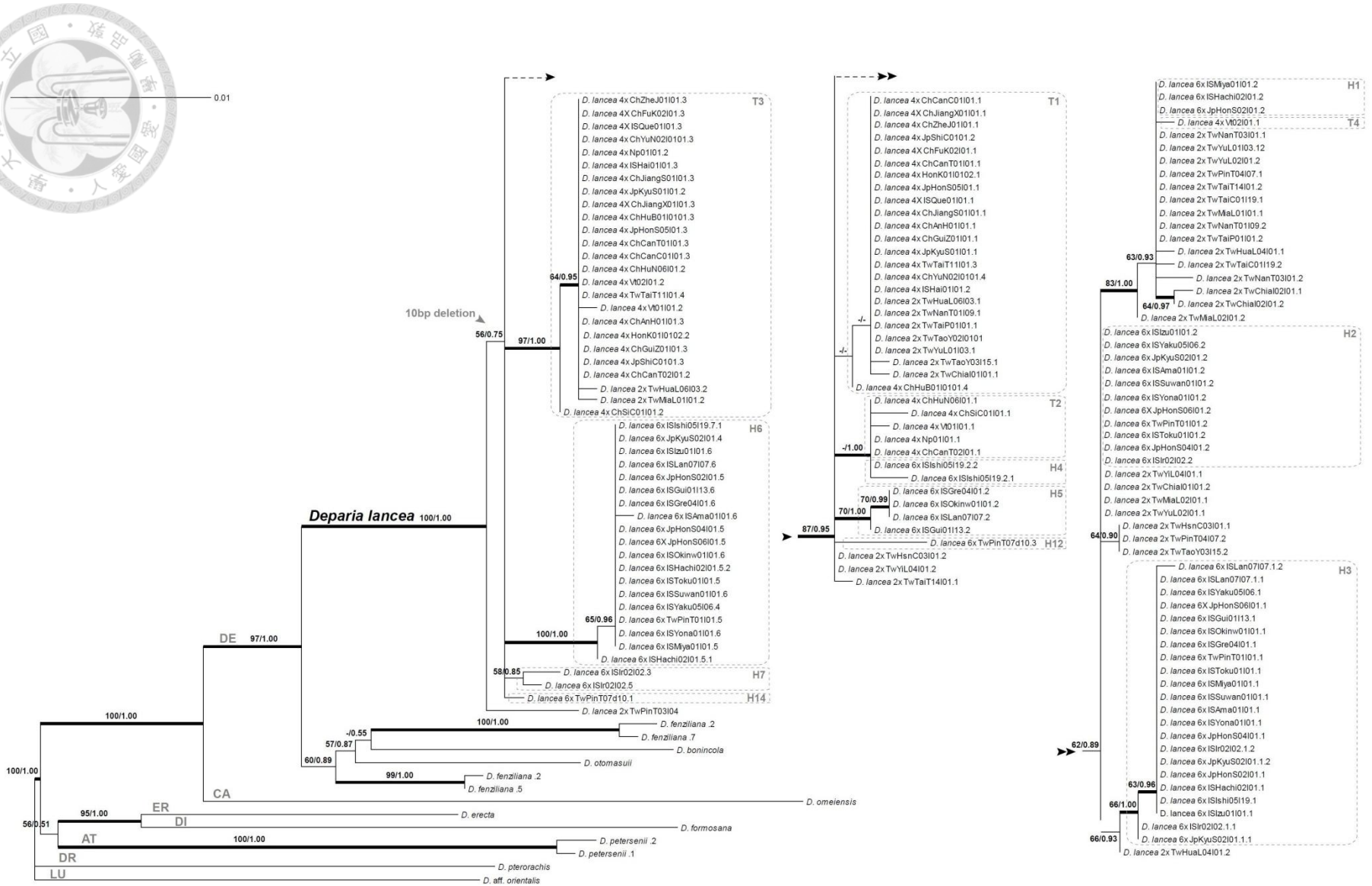
0.01
10bp deletion
Deparia lancea 100/1.00
DE 97/1.00
CA
ER
DI
AT
DR
LU
T3
T1
T2
T4
H1
H2
H3
H4
H5
H6
H7
H12
H14
D. omeiensis
D. erecta
D. formosana
D. petersenii .2
D. petersenii .1
D. pterorachis
D. aff. orientalis
D. otomasuii
D. bonincola
D. fenziliana .2
D. fenziliana .7
D. fenziliana .5

Fig. 3.5. The nDNA phylogeny of *Deparia lancea* and 9 selected outgroup taxa in *Deparia* based on *CRY2* 1st intron. ML bootstrap support (MLBS) values and Bayesian phylogenetic inference posterior probabilities (BIPP) are indicated on branches as MLBS/BIPP. The thickened branch indicates BIPP ≥ 0.95. The different infrageneric clades inferred in Chapter 2 are indicated in gray on the branches. The dashed boxes include the different sequence groups in polyploids.

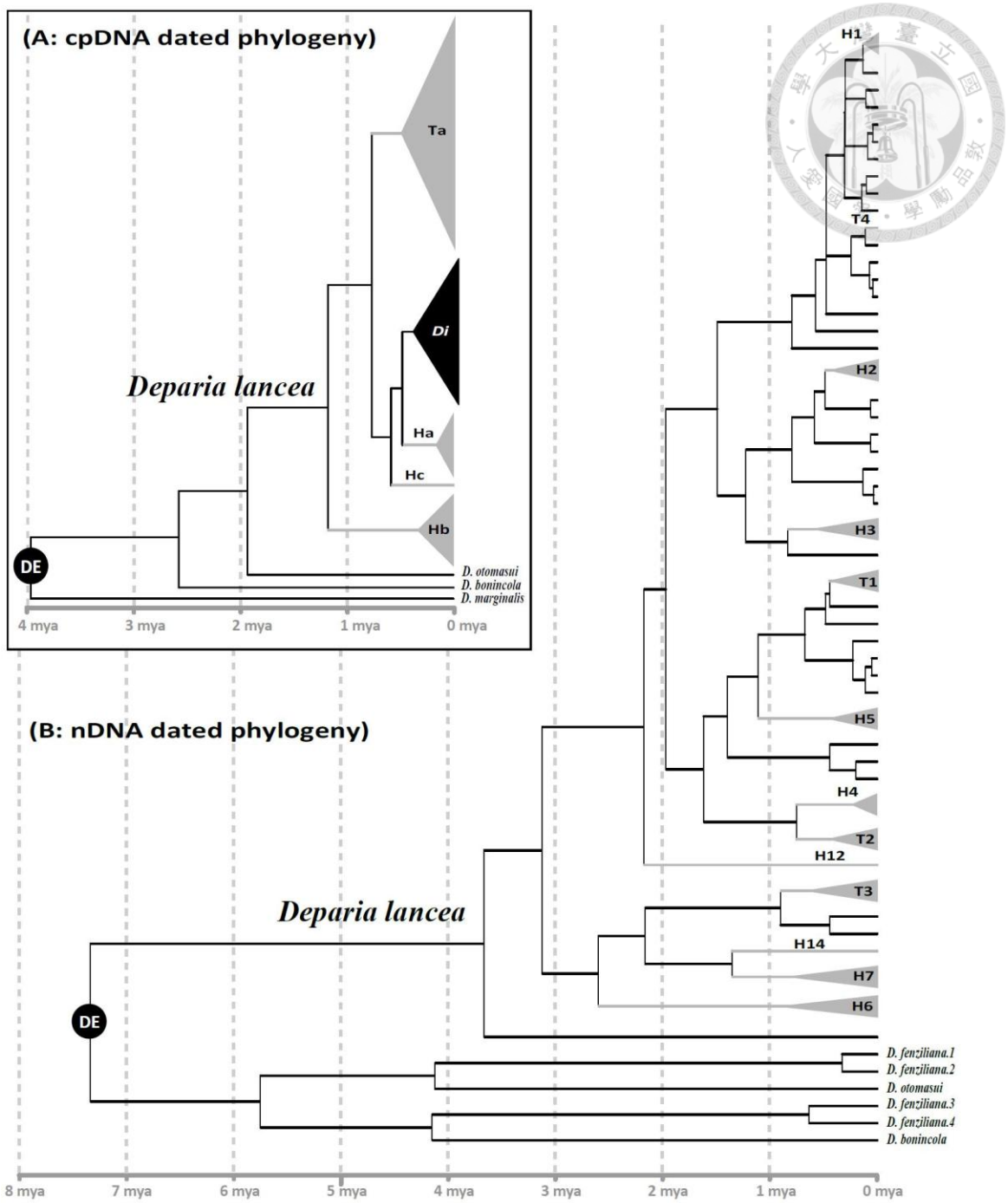

Fig. 3.6. The dated phylogenies inferred from (A) cpDNA and (B) nDNA based on a coalescent model including all *Deparia lancea* individuals. This figure shows only the part of chronogram including DE clade members. The gray on the phylogenies indicate the polyploid lineages in *D. lancea*. "*Di*" = diploids.

Table 3.1. The information *Deparia lancea* individuals included in this study.

Sample name	GPS (N E)	Location	In Chinese or Japanese	Ploidies	Reproduction[e]	Guard cell length (mean ± SDμm)	Spore size (mean ± SD μm^2)	Polyploids cpDNA haplotype	Polyploids nDNA genotype	Voucher
Tw-ChiaI-01-l01	23.27182 120.58389	Tsengwen reservoir, Chiayi County, Taiwan	台灣 嘉義縣 曾文水庫	2X[b]	Sexual	62.74 ± 4.09	711.44 ± 99.09	-	-	*Kuo4035* (TAIF)
Tw-ChiaI-02-l01	23.43624 120.61078	Chukou, Chiayi County, Taiwan	台灣 嘉義縣 觸口	2X[b]	Sexual	61.98 ± 3.55	735.07 ± 114.86	-	-	*Kuo4036* (TAIF)
Tw-HsnC-03-l01	24.57622 121.10840	Taoshan Primary School, Hsinchu County, Taiwan	台灣 新竹縣 桃山國小	2X[b]	Sexual	63.86 ± 4.08	718.65 ± 130.82	-	-	*Kuo4037* (TAIF)
Tw-HuaL-04-l01	23.38662 121.37350	Mt. Chihke, Hualien County, Taiwan	台灣 花蓮縣 赤柯山	2X[b]	Sexual	59.27 ± 3.53	672.10 ± 97.54	-	-	*Kuo4038* (TAIF)
Tw-HuaL-06-l03	23.67425 121.52039	Mt. Taibalang, Hualien County, Taiwan	台灣 花蓮縣 太巴塱山	2X[b]	Sexual	61.79 ± 6.46	731.76 ± 185.40	-	-	*Kuo4039* (TAIF)
Tw-MiaL-01-l01	24.62774 121.02280	Nanchuang, Miaoli County, Taiwan	台灣 苗栗縣 南庄	2X[b]	Sexual	63.65 ± 4.49	626.87 ± 96.47	-	-	*Kuo4040* (TAIF)
Tw-MiaL-02-l01	24.52434 121.00670	Mt. Chiali, Miaoli County, Taiwan	台灣 苗栗縣 加里山	2X[b]	Sexual	60.69 ± 3.76	682.17 ± 124.84	-	-	*Kuo4041* (TAIF)
Tw-NanT-01-l09	23.92204 120.88192	Lienhuachih, Nantou County, Taiwan	台灣 南投縣 蓮華池	2X[b]	Sexual	59.21 ± 3.44	717.41 ± 106.81	-	-	*Kuo4042* (TAIF)
Tw-NanT-03-l01	23.82262 120.79073	Chilu Bridge, Nantou County, Taiwan	台灣 南投縣 集鹿大橋	2X[b]	Sexual	58.30 ± 2.59	802.35 ± 96.08	-	-	*Kuo4043* (TAIF)
Tw-PinT-03-l04	22.23193 120.83682	Shouka logging trail, Pingtung County, Taiwan	台灣 屏東縣 壽卡林道	2X[b]	Sexual	62.89 ± 4.25	804.41 ± 117.03	-	-	*Kuo4044* (TAIF)
Tw-PinT-04-l07	22.15952 120.72589	Mt. Lilung, Pingtung County, Taiwan	台灣 屏東縣 里龍山	2X[b]	Sexual	58.65 ± 3.48	767.67 ± 226.81	-	-	*Kuo4045* (TAIF)
Tw-TaiC-01-l19	24.28095 120.86977	Tungshihlinchang, Taichung City, Taiwan	台灣 台中市 東勢林場	2X[b]	Sexual	65.64 ± 4.11	765.81 ± 81.10	-	-	*Kuo4046* (TAIF)
Tw-TaiP-01-l01	25.13168 121.59285	Tienhsiyuan, Taipei City, Taiwan	台灣 台北市 天溪園	2X (*2n* = 80)	Sexual	59.78 ± 3.26	785.01 ± 121.70	-	-	*Kuo1914* (TAIF)
Tw-TaiT-14-l01	22.32001 120.86147	Tawu, Taitung County, Taiwan	台灣 台東縣 大武	2X[b]	Sexual	58.91 ± 6.96	753.70 ± 142.90	-	-	*Lu21665* (TAIF)
Tw-TaoY-02-l01	24.64108 121.43641	Ssuling, Taoyuan County, Taiwan	台灣 桃園縣 四稜	2X[b]	Sexual	64.78 ± 3.67	694.40 ± 143.41	-	-	*Kuo4047* (TAIF)
Tw-TaoY-03-l15	24.79777 121.42064	Mt. Peichatien, Taoyuan County, Taiwan	台灣 桃園縣 北插天山	2X[b]	Sexual	61.43 ± 3.77	772.31 ± 80.73	-	-	*Kuo4048* (TAIF)
Tw-YiL-04-l01	24.83086 121.73535	Linmei trail, Chiaohsi , Ilan County, Taiwan	台灣 宜蘭縣 礁溪 林美步道	2X[b]	Sexual	58.51 ± 3.42	716.98 ± 131.52	-	-	*Kuo4049* (TAIF)
Tw-YuL-01-l03	23.68459 120.61985	Hushan reservoir, Yunlin County, Taiwan	台灣 雲林縣 湖山水庫	2X[b]	Sexual	65.10 ± 3.83	746.71 ± 79.14	-	-	*Kuo4050* (TAIF)
Tw-YuL-02-l01	23.61066 120.50198	Shihpi, Yunlin County, Taiwan	台灣 雲林縣 石壁	2X[b]	Sexual	59.18 ± 4.72	823.66 ± 142.08	-	-	*Lu22421* (TAIF)
Ch-AnH-01-l01	29.82550 118.05986	Zhenye village, Mt. Qiyun, Huangshan City, Anhui Province, China	中國 安徽省 黃山市 齊雲山 鎮葉村	4X[b]	Sexual	84.08 ± 4.90	1022.30 ± 139.22	Ta	T1T3	*Kuo4051* (TAIF)
Ch-CanC-01-l01	24.68750 107.82111	Hechi town, Hechi City, Guangxi Province, China	中國 廣西省 壯族自治區 河池市 河池鎮	4X[b]	Sexual	76.49 ± 4.86	967.14 ± 119.80	Ta	T1T3	*Leong4068* (HAST)
Ch-CanT-01-l01	22.57856 114.18260[a]	Wutongshan trail, Shenzhen City, Guangdong, China	中國 廣東省 深圳市 梧桐山步道	4X[b]	Sexual	79.08 ± 4.69	941.24 ± 149.14	Ta	T1T3	*Kuo4052* (TAIF)
Ch-FuK-02-l01	27.04494 118.13918[a]	Wanmulin nature reserve, Jianou City, Fujian Province, China	中國 福建省 建甌市 萬木林自然保護區	4X[b]	Sexual	74.98 ± 4.28	1158.24 ± 103.43	Ta	T1T3	*Chao1315* (TAIF)
Ch-GuiZ-01-l01	25.32229 107.93578[a]	Maolan nature reserve, Libo County, Guizhou Province, China	中國 貴州省 荔波縣 茂蘭保護區	4X[b]	-	-	-	Ta	T1T3	*Kuo4054* (TAIF)
Ch-HuB-01-l01	24.71642 109.18393[a]	Qinglingshan forest park, Xianfeng County, Hubei Province, China	中國 湖北省 咸豐縣 青靈山森林公園	4X[b]	Sexual	77.55 ± 5.79	991.52 ± 132.54	Ta	T1T3	*Kuo4055* (TAIF)
Ch-JiangS-01-l01	31.22055 119.69854[a]	Longchi Mountain, Yixing County, Jiangsu Province, China	中國 江蘇省 宜興縣 龍池山	4X[b]	Sexual	70.31 ± 3.68	1011.10 ± 148.66	Ta	T1T3	*Kuo4056* (TAIF)
Ch-JiangX-01-l01	29.53920 117.57745[a]	Yaoli Village, Jingde Town, Fuliang County, Jiangxi Province, China	中國 江西省 浮梁縣 景德鎮 瑤里	4X[b]	Sexual	78.58 ± 4.83	1038.62 ± 156.80	Ta	T1T3	*Kuo4057* (TAIF)
Ch-YuN-02-l01	23.37447 104.77298	Fadou town, Xichou County, Yunnan Province, China	中國 雲南省 西疇縣 法斗鄉	4X[b]	Sexual	77.36 ± 4.20	1045.58 ± 160.92	Ta	T1T3	*Kuo3025* (TAIF)
Ch-ZheJ-01-l01	29.80531 121.79427[a]	Tiantongshan national forest park, Ningbo City, Zhejiang Province, China	中國 浙江省 寧波市 天童山國家森林公園	4X[b]	Sexual	79.22 ± 4.67	1079.65 ± 119.24	Ta	T1T3	*Kuo1916* (TAIF)
HonK-01-l01-2	22.42722 114.11848[a]	Mt. Guanyin, Taipo district, Hong Kong	香港 大浦區 觀音山	4X[b]	Sexual	78.94 ± 4.97	1166.56 ± 117.79	Ta	T1T3	*Kuo4058* (TAIF)
IS-Hai-01-l01	18.98167 109.88250	Wuzhishan national natural reserve, Hainan Provinve, China	中國 海南島省 五指山國家級自然保護區	4X[b]	Sexual	75.46 ± 5.16	1094.59 ± 134.79	Ta	T1T3	*Chao1198* (TAIF)
IS-Que-01-l01	33.32449 126.60859[a]	Donneko valley, Jeju Isand, Korea		4X[b]	Sexual	74.62 ± 5.72	1006.50 ± 173.79	Ta	T1T3	*Kr42* (TNS)
Jp-HonS-05-l01	34.42972 135.80694	Shimizutani, Takatori-cho, Takaichi-gun, Nara Pref., Japan	日本 奈良県 高市郡 高取町清水谷	4X[b]	Sexual	73.28 ± 5.22	1134.15 ± 149.95	Ta	T1T3	*AE sn. 2909* (TAIF)
Jp-KyuS-01-l01	32.73032 129.84337	Kibachi, Kosedo-machi, Nagasaki-shi, Nagasaki Pref, Japan	日本 長崎市 小瀬戸町	4X[b]	Sexual	79.86 ± 4.73	1014.42 ± 188.74	Ta	T1T3	*Kuo4053* (TAIF)
Jp-ShiC-01-01	33.54265 133.63962	Nojiri, Satokaida, Nankoku-shi, Kochi Pref., Japan	日本 高知県 南国市 里改田野尻	4X[b]	Sexual	81.26 ± 5.50	924.37 ± 140.46	Ta	T1T3	*AE sn. 2910* (TAIF)
Tw-TaiT-11-l01	22.89356 121.19131	Mt. Tulan, Taitung County, Taiwan	台灣 台東縣 都蘭山	4X (*2n* = ca	Sexual	84.84 ± 5.64	1065.71 ± 133.63	Ta	T1T3	*Kuo4059* (TAIF)
Ch-CanT-02-l01	23.63514 113.89416[a]	Mt. Nankun, Longmen County, Huizhou City, Guangdong Province, China	中國 廣東省 惠州市 龍門縣 南崑山	4X[b]	Sexual	76.06 ± 4.84	1049.34 ± 164.77	Ta	T1T2	*Kuo4060* (TAIF)
Ch-HuN-06-l01	26.36028 109.83667	Mujiaolongdi, Tongdao County, Hunan Province, China	中國 湖南省 通道縣 木腳龍底	4X[b]	Sexual	88.54 ± 4.25	984.11 ± 225.87	Ta	T2T3	*Kuo4061* (TAIF)
Ch-SiC-01-l01	29.56518 103.44324[a]	Baoguo temple, Mt. Emei, Sichuang Province, China	中國 四川省 峨嵋山市 報國寺	4X[b]	Sexual	-	-	Ta	T2T3	*Kuo4062* (TAIF)
Np-01-l01	27.70831 85.35126[a]	Kathmandu, Pashupatinath, Nepal		4X[b] (*2n* = 160)[d]	Sexual	69.26 ± 3.46	1023.34 ± 204.49	Ta	T2T3	*Kuo1915* (TAIF)
Vt-01-l01	20.54778 105.19639	Hoa Binh, Vietnam		4X[b]	Sexual	71.40 ± 5.57	1074.64 ± 139.77	Ta	T2T3	*WP-244* (MO)
Vt-02-l01	12.03798 108.62985[a]	Đa Lat, Vietnam		4X[b]	Sexual	72.11 ± 4.11	933.62 ± 132.48	Ta	T4T3	*Wade1604* (TAIF)
Ch-ChongQ-01-l01	29.69016 105.25905[a]	Mt. Simian, Chongqing City, China.	中國 重慶市 四面山	4X[b]	Sexual	68.90 ± 3.37	1023.12 ± 213.73	Ta	-	*Kuo1917* (TAIF)
Ch-YuN-01-l01	21.92019 101.27665[a]	Menglun tropical botanical garden, Xishuangbanna Daizu Zizhizhou, Yunnan Province, China	中國 雲南省 西雙版納傣族自治州 猛輪熱帶植物園	4X[c]	Sexual	74.22 ± 4.75	948.35 ± 150.44	Ta	-	*Lu19805* (TAIF)
Ban-01-l01	21.79871 92.43096[a]	Chittagong division, Bandarban district, Bangladesh		4X[c]	Sexual	77.03 ± 5.70	1083.90 ± 100.29	Ta	-	*TAIFS302253* (TAIF)
Bur-01-l01				4X[c]	Sexual	68.96 ± 4.86	1080.96 ± 153.63	Ta	-	*Deng3149* (IBSC)
In-01-l01	25.63623 91.90399[a]	Meghalaya, East khasi hills district, Shillong, India		4X[c]	Sexual	74.00 ± 4.50	1022.84 ± 154.96	Ta	-	*TAIF319555* (TAIF)
Bo-01-l01	4.05000 115.78333	Kalimantan Timur, Borneo, Indonesia		4X[c]	Sexual	77.65 ± 5.71	1045.93 ± 202.72	-	-	*Kato et al. 10727* (TI)
Th-01-l01	16.70443 101.52108[a]	Nam Nao national park, Thailand		4X[c]	Sexual	81.72 ± 4.74	1014.26 ± 150.34	-	-	*TNS461979* (TNS)
Jp-HonS-01-l01	34.80132 138.85115	Shirakawa, Nishi-izu-cho, Shizuoka Pref., Japan	日本 静岡県 西伊豆町白川	5X[b]	Sterile	72.08 ± 4.69	-	Ta	-	*Kuo4063* (TAIF)
Jp-KyuS-04-l01	33.31001 130.06881[a]	Makise, Kyuragi-cho, Karatsu-shi, Saga Pref., Japan	日本 佐賀県 唐津市 厳木町牧瀬	5X[b]	Sterile	73.67 ± 4.09	-	Ta	-	*AE sn. 2945* (TAIF)
IS-Ama-01-l01	28.28689 129.38733	Sumiyo River, Kamiya, Amami-shi, Amami Isand, Kagoshima Pref., Japan	日本 鹿児島県 奄美市 住用町 神屋住用川	6X[b]	Sexual	84.26 ± 5.56	1600.08 ± 258.42	Ha	H2H3H6	*Goro12286* (TNS)
IS-Suwan-01-l01	29.61397 129.70147	Yahata-Jinja, Suwanose Isand, Toshima-mura, Kagoshima-gun, Kagoshima., Japan	日本 鹿児島県 鹿児島郡 十島村 諏訪瀬島 八幡神社	6X[b]	Sexual	83.57 ± 5.06	1722.25 ± 205.32	Ha	H2H3H6	*Goro11383* (TNS)

(Table 3.1 cont.)

Tw-PinT-01-l01	22.08879 120.84813	Nanjenshan, Pingtung County, Taiwan	台灣 屏東縣 南仁山	6X (*2n* = ca	Sexual	81.07 ± 4.73	1436.29 ± 202.64	Ha	H2H3H6	*Kuo4064* (TAIF)
IS-Yona-02-l01	24.44761 122.96967	Mt. Ubura-dake, Yonaguni-cho, Yonaguni Island, Japan	日本 沖縄県 八重山郡 與那國町 宇部良嶽	6X[c]	Sexual	81.79 ± 7.08	1361.20 ± 258.51	Ha	H2H3H6	*Goro14122* (TNS)
IS-Ishi-05-l19	24.42583 124.18453	Mt. Omoto, Ishigaki Island, Japan	日本 石垣島 於茂登山	6X[b]	Sexual	78.67 ± 6.00	1533.65 ± 230.87	Ha	H4H3H6	*Kuo4065* (TAIF)
IS-Gui-01-l13	24.84184 121.95060	Guishan Island, Ilan County, Taiwan	台灣 宜蘭縣 龜山島	6X[b]	Sexual	82.48 ± 5.86	1374.78 ± 199.11	Ha	H5H3H6	*Kuo4066* (TAIF)
IS-Lan-07-l07	22.01380 121.57271	Orchid Island, Taitung County, Taiwan	台灣 台東縣 蘭嶼	6X[b]	Sexual	89.83 ± 5.11	1491.58 ± 286.05	Ha	H5H3H6	*Kuo4067* (TAIF)
IS-Okinw-01-l01	26.62723 127.93681	Yaeyama-gun, Okinawa Pref., Japan	日本 沖縄県 八重山郡	6X[b]	Sexual	86.68 ± 6.28	1674.48 ± 377.92	Ha	H5H3H6	*Kuo4068* (TAIF)
IS-Ir-02-l02	24.36667 123.88333	Yutsun river, Iriomote Island, Japan	日本 西表島	6X[b]	Sterile	80.89 ± 5.64	-	Ha	H2H3H7	*Kuo4069* (TAIF)
IS-Hachi-02-l01	33.06264 139.81669	Nakanogo, Hachijo Island, Tokyo Pref., Japan	日本 八丈島 中之郷	6X[b]	Sexual	87.24 ± 6.27	1349.22 ± 187.80	Hb	H1H3H6	*Kuo4070* (TAIF)
IS-Miya-01-l01	34.05111 139.52890	Tairo-ike, Miyake-jima Island, Tokyo Pref., Japan	日本 東京都 三宅支庁 三宅島大路池	6X[b]	Sexual	82.10 ± 6.63	1366.62 ± 183.55	Hb	H1H3H6	*Kuo4071* (TAIF)
Jp-HonS-02-l01	34.65335 138.98986	Tsumeki-zaki, Suzaki Peninsula, Shimoda-shi, Shizuoka Pref., Japan	日本 静岡県 下田市 須騎半島 爪木崎	6X[b]	Sexual	82.21 ± 5.36	1427.61 ± 225.50	Hb	H1H3H6	*Kuo1920* (TAIF)
IS-Izu-01-l01	34.76122 139.38465[a]	Izu-Oshima Island, Tokyo Pref., Japan	日本 東京都 伊豆大島	6X[b]	Sexual	81.61 ± 5.04	1588.36 ± 202.98	Hb	H2H3H6	*Kuo4072* (TAIF)
IS-Toku-01-l01	27.76000 128.97600	Yama, Tokunoschima-cho, Tokunoshima Island, Kagoshima Pref., Japan	日本 德之島 大島郡 德之島町山	6X[b]	Sexual	84.13 ± 5.33	1379.53 ± 150.49	Hb	H2H3H6	*Goro12585* (TNS)
IS-Yaku-05-l06	30.24923 130.54040	Yakushima Island, Japan	日本 屋久島	6X[b]	Sexual	91.65 ± 5.35	1489.53 ± 165.76	Hb	H2H3H6	*Kuo4073* (TAIF)
Jp-HonS-04-l01	34.66612 138.95246	Shiroyama, Shimoda-Shi, Shizuoka Pref., Japan	日本 静岡県 下田市 城山公園	6X[b]	Sexual	81.16 ± 5.03	1553.59 ± 202.17	Hb	H2H3H6	*Kuo4074* (TAIF)
Jp-HonS-06-l01	34.06722 136.17639	Obarano, Owase-shi, Mie Pref., Japan	日本 三重県 尾鷲市 小原野	6X[b]	Sexual	83.46 ± 5.08	1521.62 ± 239.76	Hb	H2H3H6	*AE sn. 2913* (TAIF)
Jp-KyuS-02-l01	31.17659 130.53064	Mt. Kaimon, Kagoshima Pref., Japan	日本 鹿兒島県 開聞嶽	6X[b]	Sexual	79.50 ± 5.11	1679.17 ± 447.26	Hb	H2H3H6	*Kuo4075* (TAIF)
IS-Gre-04-l01	22.65929 121.50578	Green Island, Taitung County, Taiwan	台灣 台東縣 綠島	6X[b]	Sexual	80.83 ± 5.55	1551.70 ± 226.11	Hb	H5H3H6	*Kuo1919* (TAIF)
Tw-PinT-07-d10	22.40390 120.77592	Mt. Kutzulun, Pingtung County, Taiwan	台灣 屏東縣 姑子崙山	6X[b]	Sexual	67.07 ± 5.03	1577.16 ± 208.34	Hc	H12H14	*Kuo4076* (TAIF)
IS-Batan-01-l01	20.45835 122.00981	Dujtak site, Batanes, the Philippines		6X[c]	Sexual	81.58 ± 4.40	1544.45 ± 258.50	-	-	*Barcelona991* (RNU)
IS-Senk-01-l01	25.74142 123.47581[a]	Diaoyu Island (Senkaku Island)	釣魚台	6X[c]	Sexual	78.63 ± 4.81	1759.08 ± 231.92	-	-	*RYU33619* (RYU)

[a]GPS of a reference point; [b]confirmed by cytometry flow analyses; [c]inferred by spore size and guard cell length; [d]Matsumoto & Nakaike 1990; [e]sexual = 64-spored sporangia, sterile = mostly with abornal spores

Table 3.2. The distribution, divergence time, and inferred dispersal rate of diploids and polyploid lineages in *Deparia lancea* .

Lineages	Ploidies	Endemic or not	Medium of stem age (95%HPD)*	Medium of crown age (95%HPD)*	Inferred dispersal rate (km/Ma)
cpDNA phylogeny					
Deparia lancea	Mixed	non-endemic	2.39 (0.60 - 6.25)	1.64 (0.23 - 2.44)	-
Diploids	Diploids	non-endemic	0.93 (0.14 - 1.48)	0.84 (0.10 - 1.15)	623
Ta	Tetraploids	non-endemic	1.28 (0.15 - 1.72)	0.95 (0.09 - 1.18)	10021
Ha	Hexaploids	non-endemic	0.93 (0.14 - 1.48)	0.63 (0.02 - 0.50)	4439
Hb	Hexaploids	non-endemic	1.64 (0.23 - 2.44)	0.80 (0.04 - 0.97)	2247
Hc	Hexaploids	endemic (Taiwan)	1.05 (0.14 - 1.48)	-	-
nDNA phylogeny					
Deparia lancea	Mixed	non-endemic	7.53 (4.22 - 10.38)	3.88 (1.90 - 5.55)	-
Diploids	Diploids	non-endemic	7.53 (4.22 - 10.38)	3.88 (1.90 - 5.55)	232
T1	Tetraploids	non-endemic	0.67 (0.16 - 0.78)	0.66 (0.14 - 0.84)	6883
T2	Tetraploids	non-endemic	1.33 (0.76 - 2.54)	0.68 (0.09 - 0.96)	3129
T3	Tetraploids	non-endemic	1.13 (0.30 - 1.68)	0.85 (0.21 - 1.14)	8902
T4	Tetraploids	endemic (Veitnam)	0.32 (0.00 - 0.35)	-	-
H1	Hexaploids	non-endemic	0.33 (0.01 - 0.27)	0.28 (0.00 - 0.29)	350
H2	Hexaploids	non-endemic	0.71 (0.12 - 1.02)	0.65 (0.09 - 0.93)	3615
H3	Hexaploids	non-endemic	0.82 (0.31 - 1.48)	0.62 (0.21 - 1.08)	5569
H4	Hexaploids	endemic (Ishigaki Is.)	1.84 (0.76 - 2.54)	0.44 (0.00 - 0.60)	-
H5	Hexaploids	non-endemic	1.33 (0.44 - 1.96)	0.63 (0.04 - 0.94)	1010
H6	Hexaploids	non-endemic	2.80 (1.33 - 4.01)	1.06 (0.24 - 1.62)	4376
H7	Hexaploids	endemic (Iriomote Is.)	2.38 (1.00 - 3.47)	0.98 (0.07 - 1.77)	-
H12	Hexaploids	endemic (Taiwan)	2.39 (1.13 - 3.38)	-	-
H14	Hexaploids	endemic (Taiwan)	1.60 (0.29 - 2.67)	-	-

*inferred from a coalencent constant population model

Table S3.1. PCR primers used in this study.

Region	Name	Sequence 5' - 3'	Reference
matK + rps16-matK IGS	De rps16 fSTE*	GAAGAAGGGGCGCAATCAACGGAAA	Li *et al.* (2011)
	De rmf1	CTTGGGAGTTACTGCGATGA	This study
	De matK rANR	GATATGGGAAACAATCTCGATTAGCC	This study
	De matK fHVL*	GATTGCCAAAATCTAGCCACGTTTTA	Li *et al.* (2011)
	De matK rHTY*	ACGAAGTTTTGTACGTGTGAA	Rothfels *et al.* (2012)
	De matK fFHG*	ATCTCTCATAGGTTTTCATGGAAC	This study
	De matK rSCV	GTAACCCAAGAATAAAACACAGCTG	This study
	FERmatK rAGK	CGTRTTGTACTYYTRTGTTTRCVAGC	Kuo *et al.* (2011)
trnL-L-F	f*	ATTTGAACTGGTGACACGAG	Taberlet *et al.* (1991)
	FernLr1*	GGCAGCCCCCAGATTCAGGGGAACC	Li *et al.* (2011)
	De trnL 1Ir1*	GTGAATGGAGGTAGAGTCCC	This study
	De trnL 3'Ef1*	CTCATTGGGGATAGAGGGA	This study
ndhF + ndhF-trnN IGS	Poly ndhF fYMV*	ACHATGTCYCARTTRGGATATATGGT	This study
	De ndhF fPTQ*	GGAGTTGTCGACCCAACYCAAAA	This study
	De ndhF rPSL*	CAATAAGGGATAAACTAAGCGAAGG	This study
	FernN2245	CTACGACCMATCGGTTAACAGCCG	Chen *et al.* (2013)
CRY2 1st intron	POLY CRY2 fVMR*	CCTTGGAGCTCCYCTTGTHATGCG	This study
	And CRY rDLL*	GGCTCATACAGVARRTCKSCATTRAA	Zhang *et al.* (2014)
	De CRY2 fEAT*	CCTCTTGGAAATTGTTGAAGCCACAG	This study
	De CRY2 fATQ*	CCACAGGAGCCACTCAAG	This study
	De CRY2 rVSL*	TCACSCACAAGGGATACRGG	This study
	De CRY2 rDVP*	CACAAGGGATACRGGATC	This study

*The primer for sequencing.

Table S3.2. The prior setting for continuous phylogeographic analyses.

Lineage	Mean of root age (SD =	Subsituition rate	Randomizelower*	Randomizeupper*	Root-location prior*
cpDNA					
Ta	0.9543	0.000832	12.03 85.35	34.81 138.86	23.42 112.105
Ha	0.6275	0.001128	22.01 120.84	29.62 129.71	25.815 125.275
Hb	0.8015	0.003903	22.65 121.5	34.77 139.82	28.71 130.66
Diploids	0.8381	0.001059	21.89 120.02	25.30 122.01	23.875 121.0
nDNA					
H6	1.0629	0.001320	22.01 120.84	34.77 139.82	28.39 130.32
H5	0.6338	0.001188	22.01 121.50	26.63 127.94	24.27 124.72
H3	0.6175	0.001421	22.01 120.84	34.77 139.82	28.39 130.33
H2	0.6465	0.001055	22.09 120.85	34.77 139.39	28.43 130.12
H1	0.2825	0.001107	33.06 139.52	34.66 139.82	33.86 139.67
T3	0.8478	0.001067	12.03 85.35	34.66 135.81	23.345 110.58
T2	0.6820	0.001129	20.54 85.35	29.57 113.9	25.055 99.625
T1	0.6623	0.001088	18.98 104.77	34.66 135.81	26.82 120.29
Diploids	3.8759	0.002173	21.89 120.02	25.30 122.01	23.875 121.0

*presented in "latitude longitude"

Chapter 4.

The phylogeography and population genetics of the *Deparia lancea* hexaploids

Abstract

In this chapter, genetic diversities of 9 diploid populations and 17 hexaploid *Deparia lancea* populations across their distribution range were surveyed. Among hexaploids, there are three genetically different lines with different independent origins, and including two local endemic lines and one widespread line. In two local hexaploid lines, H12-14-6.4 and H7-10-15 were found only in Taiwan Main Is. and Southern Ryukyu (Ireomote and Ishigaki Is.), respectively. In the widespread line hexaploids, the distribution of their populations was revealed ranging from Taiwan to Japan (Ryukyu, Kyushu, and Honshu), and the nDNA phylogenies further revealed that it is composed by at least eight origins arisen from diploids' haploid genomes. Among populations of the widespread line hexaploids, the marginal distributed populations were with the simplest genetic composition. Comparing to diploids, the significant higher F_{IS} in the widespread line hexaploid populations implied their increased colonization ability by inbreeding. By contrast, diploid populations had been revealed lower F_{IS} values and distributed in Taiwan Main Is. only. Based on the results from Bayesian skyline plot, this widespread line was suggested to be formed during 0.06-0.004 Ma, and, thus, had expanded their population expansion after 0.06 Ma. Regarding to these findings and the hypothesized formation mechanism of these hexaploids, I proposed the most probably scenario for the origins and expansions in these widespread line hexaploid. They were likely formed in Taiwan Main Is., and had subsequent oversea dispersals for their population establishment. Recent continuous range expansions in these hexaploids might start from the region of northern Taiwan – Central Ryukyu toward Honshu of Japan and southern Taiwan.

Introduction

This chapter repsented the phylogeography and population genetics of both diploids and conspecific autohexaploids in *Deparia lancea*

(Thunb.) Fraser-Jenk. (Athyriaceae). These successfully established hexaploids are revealed with a sexual reproduction mode, multiple origins, a rapid range expansion in the East Asia Archipelagos, throughout Taiwan, the Philippines (Batan Islands), and Japan (Ryukyu, Honshu, and Kyushu) (also see in Chapter 3). Current study aimed on (1) inferring their colonization/dispersal ability by *F*-stastics, and (2) inferring the origins and expansions of these hexaploids at time and spatial scales based on the confirmation of cytotype distribution and phylogeographical analyses.

Materials and methods

Sampling and cytotype confirmation

A total of 739 individuals were collected from 51 locations across Taiwan and Japan (Ryukyu, Kyushu, and Honshu). Due to the possibilities of vegetative ropagation via long-creeping rhizome, a different individual in one location was defined with a distance more than 10 meters from the others in the same location. The detailed sampling information was shown in Table 4.1. To confirm ploidy level of every individual, the flow cytometry analyses were used, and the protocol and standards followed those in Chapter 2. After ploidies of all sampling individuals were determined, only the diploid and hexaploid individuals were included for the following molecular experiments and analyses (see below).

Low-copy nDNA marker

In this study, a low-copy nuclear DNA (nDNA) marker, *CRY2* 1st intron (the first intron of cryptochrome gene 2), was applied to assess the genetic diversity. The PCR primer sets and PCR conditions, and single-strand conformation polymorphism (SSCP) protocol for *CRY2* 1st intron followed description in Chapter 3. The SSCP electrophoreses were under a gradient temperature from 20 to 2℃. In the situation when SSCP products did not resolve the mixed sequence types or sequencing of SSCP products failed, the SSCP products cloned into pGEM-T Easy Vectors System (Promega, Madison, USA) to isolate the mixed sequence types, or, if there is If only a base calling with two overlapping peaks, I just directly resolved them as two sequence types.

Genotyping for low-copy nDNA region CRY2 *1st intron*

In the beginning, the individuals were sorted belonging to different

banding patterns revealed by SSCP gels. Each of different banding patterns on one SSCP gel was sequenced by one represented individual. After these, the genotypes of analyzed individuals were first coded based on the sequence types inferred from SSCP banding patterns. In other words, the individuals revealed with the same banding pattern on one SSCP gel were regarded with the same composition of sequence types. In addition, the sequence types not resolved by SSCP (see above in *low-copy nDNA marker*; i.e. two sequencing types exist in one SSCP band) were regarded as the same one. For every diploid individual, the genotype was further identified as either homozygotes or heterozygotes according to their inferred sequence type(s).

Because the (neo-)polyploids have recent whole genome duplication resulting additional sets of homoeologs, a certain genetic region in polyploids should have multiple alleles with very similar sequences. These alleles are composited by different homoeologs with different inheritances. Therefore, identification and assumption of the inheritances for alleles from a genetic region are the major difficulties for population genetic study of polyploidy taxa (Dufresne *et al.* 2014). For the hexaploids in *Deparia lancea*, most individuals are likely composed by three origins of sequence types representing three sets of duplicated genomes, which are assumed to be resulted from one polyploidization and one demipolyploidization event (see Chapter 3) but are on the different homoeologous chromosomes probably behaving disomic inherence (i.e. no homoeologous recombination; see Chapter 3). To further confirm the inheritance of these sequence types with different homoeologous origins, doubled haploid lines (DHL; the sporophyte line resulted from fertilization of an egg and a sperm from the same gametophyte; Fig 4.1) were generated from the spores of a hexaploid individual with H5-11-3-6 genotype (see below for genotyping). After comparing the genotypes of these F1 DHL offspring with those of their parents, these sequence types could be identified and sorted to different hypothetic homoeologous loci by understanding the meiosis paring (Fig. 4.1). Therefore, either homozygotic or heterozygotic genotype for each hypothetic homoeologous locus can be further recognized.

Phylogeny and divergence time estimates

The sequences types of *CRY2* 1st intron were aligned using ClustalW implemented in BioEdit (Hall 1999). Garli 2.0 (Zwickl 2006) was used to

reconstruct the maximum likelihood (ML) phylogeny. The proportion of invariant sites and state frequencies were estimated by the program. The GTR + I + Γ model was applied, and "genthreshfortopoterm" option was set to 20,000. To calculate ML bootstrap support (MLBS) values, 500 replicates were run under the same criteria. Bayesian phylogenetic inference posterior probability (BIPP) was performed by MrBayes v.3.1.2 (Huelsenbeck & Ronquist 2001; Ronquist & Huelsenbeck 2003). Two simultaneous runs were carried out with four chains (10^6 generations each), in which each chain was sampled every 1,000 generations. The first 25% of the sample was discarded as burn-in, and the rest were used to calculate the 50% majority-rule consensus tree.

BEAST 2.1.2 (Bouchaert *et al.* 2014) was applied to estimate divergent times under *Deparia lancea*. In this analysis, only the unique sequence types from each cytotype of *Deparia lancea* and the sequences from outgroup members belonging DE clade were included (see Chapter 2 and 3). The setting of priors was under the optimization of a GTR + I + Γ model, a coalescent constant population model, and an uncorrelated lognormal relaxed clock model. Each polyploidy lineages inferred by ML phylogenies was constrained as a monophyletic group. The root age (i.e. the age of clade DE) and the age of *D. lancea* were set under a normal distribution with a mean age of 7.53 Ma and 2 Ma standard deviation and with a mean age of 3.88 Ma and 1.5 Ma standard deviation, respectively, which are accorded to the mediums and ranges inferred in Chapter 2; and this calibration on the age of *D. lancea* should avoid to underestimate the divergent time due to exclusive of all other identical sequences. The MCMC chain was set to 100 million with 10% burnin, and saving the tree and log file every 1000 generations. The Tracer v1.5 (Rambaut & Drummond 2007) was used to examine the ESS values of each BEAST replicate. TreeAnnotator (Drummond *et al.* 2012) was used to summarize the results of molecular dating analysis.

Examine genetic diversity shrinkage in hexaploid and past demographic dynamics of diploid population

To examine genetic diversity shrinkage in hexaploid, the analyses of Bayesian skyline plot (implemented in BEAST 1.7.1; Drummond *et al.* 2012) and mismatch distribution (implemented in ARLEQUIN version 3.5.1.2; Excoffier & Lischer 2010) were applied. In both analyses, *CRY2* 1st intron sequences from current study and and additional 8 hexaploids

from the previous chapter (see Chapter 3) were used. These *CRY2* 1st intron sequences were generated based on genotype identification (Table S4.1 and S4.2); but, for those sequence types unable to be recognized by SSCP banding patterns, the consensus sequences were used to replace those inferred sequence types without sequencing results. For example, due to that SSCP banding pattern could not separate these two sequence types, H4.1 and H4.2, the consensus sequence of these two sequence types were applied to replace those H4.1 and H4.2 recognized by only SSCP banding pattern. In Bayesian skyline plot analyses, I applied the strick clock model with the rate of 2.174×10^{-3} substitution/site/Ma inferred from previous cahpter (see Table S3.2 in Chapter 3), and the MCMC chain was set to 300 million with 10% burnin, and saving the tree and log file every 1000 generations. Finally, the Bayesian skyline plot results were summarized in Tracer v1.5 (Rambaut & Drummond 2007). In mismatch distribution analyses, both pure demographic expansion and spatial expansion models were used to examine if there is any possible past population expansion in diploids or hexaploids, and the number of bootstrap was set to 100.

To examine past demographic dynamics of diploid population, *CRY2* 1st intron sequences from current study and and additional 8 diploids from the previous chapter (see Chapter 3) were used. The approach to deal with their sequence and setting for Bayesian skyline plot and mismatch distribution were same as those for hexaploids.

F_{ST} and F_{IS}

For the *F*-statistics of diploid and hexaploid populations, the genotype data were used and followed by the coding approaches as descripted above (see *Genotyping for low-copy nDNA region* CRY2 *1st intron*). Because some sequence types could not be separated by SSCP, them were translated into a same one before analyses. For instance, D13, D16, and D49 were unable to be separated by SSCP, these three sequence types were translated into a same one using D13 as a selected representative.

Pairwise F_{ST} values between populations were estimated using ARLEQUIN version 3.5.1.2 (Excoffier & Lischer 2010). The point-to-point geographical distances between populations were calculated by MATLAB 8.0 (D'Errico 2005). In addition to point-to-point distances, stepping stone distances were also inferred for hexaploids. This

stepping stone was based on the hypothesized dispersal route along East Asia Archipelago., and the hypothesized steps of stepping stone were defined in Fig. 4.2. For population pairs within one step difference, their geographical distances were calculated by their point-to-point geographical distances. To detect whether gene flow between populations were correlected with geographical distances, the isolation-by-distance analyses were applied using Mantel tests on website serve of IBDWS (http://ibdws.sdsu.edu/~ibdws/). For these analyses, F_{ST} values were applied as genetic distances, and "number of randomizations' were set to 1,000.

The F_{IS} values for each diploid and hexaploid population were calculated following the formula: $1-(H_{ex}-H_{ob})/H_{ex}$, in which the H_{ex} and H_{ob} represented the expected and observed heterozygosity, respectively.

Results

Cytotype and genetic variations in locations/populations

Ploidies of 739 individuals from 51 locations across Taiwan and Japan were confirmed via flow cytometry analyses (Table 4.1). Among these locations, diploids were found only in Taiwan and restricted in Taiwan Main Is., while hexaploids were found in the eastern Taiwan (including the flanking islands) and Japan. Although the ranges of diploids and of hexaploids were revealed to be overlapped in the eastern Taiwan, these two cytotypes were never found in a same location (Table 4.1). However, there are some putative tetraploid hybrids cross between diploid and hexaploid (i.e. the abnormal spores indicating their hybrid origins) in Taiwan Main Is. and its flanking islands, which are considered reachable by both parental cytotypes' spores (see the locations under population code 202, 203, 604, 606, and 608 in Table 4.1). Such tetraploid hybrids are most abundant (20 out of 31 individuals) in Guishan Is., where is occupied by hexaploid, the only sexual cytotype on the island, but less than 22 km distant from a known diploid population (i.e. the location with population code 209 in Table 4.1 and Fig. 4.1). Combined results of 8 diploid and 8 hexaploid individuals revealed previously, a total of 171 individuals from 9 defined populations and 330 individuals from 17 defined populations were applied to infer genetic diversity for diploid and hexaploid populations in this study, respectively (Table 4.1). Including other individuals applied in the previous chapter (see Chapter 3), a total of 49 and 25 sequence types of *CRY2* 1st intron

were revealed among the diploids and the hexaploids, respectively (Fig. 4.2 and Table 4.1). The genetic composition for each location and population was also summarized in Table 4.1.

Phylogeny, diversity, inheritance, genotype coding of CRY2 *1st intron sequence types*

The log-likelihood score for the most likely ML tree based on the *CRY2* 1st intron matrix was -2,859.480053. The ML phylogeny revealed that all sequence of *Deparia lancea* formed a highly supported monophyletic group (MLBS = 100 and BIPP ≥ 0.95), and that *D. lancea* polyploid were nested in the diploids' (Fig. 4.3). Among the hexaploid sequence types, there are several monophyletic groups, which is assumed with a single origin from the diploids, including, H6 (6.1-6.4), H3 (3.1-3.4), H7 (7.1-7.2), and H15 (15.1-15.3). For H4 in hexaploids, they have one same sequence type shared with tetraploids – T2.2 but these tetraploids are unlikely to direct involve the formation of hexaploids (see Chapter 3). Therefore, H4 (4.1-4.2) in the hexaploids was also regarded as a single origin. In addition, there are several hexaploid sequence types are same as those in diploids: H1 (=D02), H2 (=D13), H3.1 (=D19), H5 (=D31), H8 (D15), H9 (=D24), and H11 (=D48).

On the other hands, the genotyping results of DHL individuals from spores of the hexaploid with H5-11-3-6 genotype revealed that (1) H5 and H11 cannot both inherent, and (2) either H5 or H11 co-inherent with H3.3 and H6.1. Since hexaploids might have three sets of genomes, these implied that H3 and H6 are on two of three duplicated homoeologous while independent loci; and H5 and H11 are on another homoeologous locus but two different chromosomes because they could not cosegregate. Based on these information, H5 and H11 were hypothesized on one homoeologous locus - the *CRY2* hypothetic homoeologous locus one (*L* I). H3 and H6 group were hypothesized on another two homoeologous loci - *CRY2* hypothetic homoeologous locus two (*L* II) and three (*L* III), respectively. These three duplicated *CRY2* loci should represent the three duplicated sets of hexaploidy genome. Generally, the majority of hexaploids are composed by the sequence types of both H3 and H6. Based on assumption that none allele/homoeologs do not exist in the inferred genotypes and the three duplicated sets of hexaploidy genomes in are all represented by different sequence types, ed other sequence types were further identified to presumablely located on *L* I: H1, H2, H4 group,

H8, H9, and H16. For these, these hexaploids could be defined with *L* I sequence types + H3 + H6 (referred as the widespread line hexaploids in below) and all of H1-3-6, H2-3-6, H4-3-6, H5-3-6, H8-3-6, H9-3-6, and H11-3-6 genotypes could be found (Table S4.2). Based on the defined homoeologous relationships, genotype of each hypothetic homoeologous locus of these hexaploids could be found with only one or two sequence types. There is no conflict result that reveals more than two alleles occupy on a single homoeologous locus.

However, based on the current evidences, there are some sequence types, including H12, H14, H6.4, H7, H10, or H15, unable to be recognized with their exact hypothetic homoeologous locus. It seems that the hexaploids with such sequence type are related to another two independent lines. The distributions of these hexaploids were relatively local comparing with that of widespread line hexaploid. Regarding to these, two local line of hexaploid were identified: H12-14-6.4 and H7-10-15, which, in this study, were found only in Taiwan Taitung 2 population (code 603; Table 4.1) and in Iriomote Is. and Ishigaki Is. populations (code 607 and 608; Table 4.1), respectively. In addition, there are some hybrids between the local lines with the widespread line in these populations (Table 4.1). For H7-10-15 local line, it seems to have introgressions with the widespread line, which result diverse combinations of genotypes found in Iriomote Is. and Ishigaki Is. populations. For H12-14-6.4 hexaploid line, only F1 hybrid-like individuals were found, which cross with widespread line in the same population. In order to clarify if there is any introgression, further deep sampling is necessary.

Based the sequencing results of SSCP product and compared to their SSCP banding pattern, the following sequence types within each group were found to be indistinguishable in their SSCP banding patterns: (D13, D16, D49), (D34, D36, D38), (D02, D03, D04, D05, D14), (D26, D27), (H3.3, H3.2), and (H4.1, H4.2). The Table 4.1 summarized the original sequence types' amount (i.e. without translation) for each locus in each location and population.

The overall phylogeogrphical pattern

In addition to the two genetically different and local lines in hexaploids as (i.e. H12-14-6.4 and H7-10-15 line), the genetic diversity of *L* I in the widespread line hexaploid also shows difference among

populations. The Fig. 4.2 summarized the composition of *L* I for each population of widespread line hexaploid. Generally, the populations in the marginal distribution are low in genetic diversity (i.e. population code 601 and 617; Table 4.1 and Fig. 4.2), and the lowest one is the most distant population (i.e. Hachijo Is.; population code 617), which is composed with only one genotype (Fig. 4.2 and Table 4.1). In construct, the populations from the northern Taiwan to Okinawa display a higher genetic diversity. In addition, H9, the only population endemic sequence type, was found in this region and in riomote Is. only.

On the other hand, the diploid populations mostly exhibit high sequence type diversity (Figs. 4.1 and 4.2; Table 4.1), and the highest one is in the Taiwan Taoyuan population (population code 208; Table 4.1 and Fig. 4.2), which has 16 sequence types among 18 individuals. In view of sequence types identical to the hexaploids, Ilan population in eastern Taiwan (code 209; Table 4.1 and Fig. 4.2) has the highest proportion, which is over 80%. The proportion of sequence types identical to the hexaploids is slightly higher in that adding up eastern Taiwan populations (71/118; including code 202, 205, and 209; Table 4.1) than in that adding up the western Taiwan populations (105/224; including code 201, 203, 204, 206, 207, and 208; Table 4.1).

Genetic diversity shrinkage in hexaploid and past demographic dynamics of diploid population

The observed and model simulated mismatch distributions are shown in Fig. 4.4, and the values for sum of square deviations (SSD) and raggedness index (RAG) were listed in Table 4.2. The *p*-values for these results suggested both diploid and widespread line hexaploid populations are not significantly deviated from the unimodel expectations under either pure demographic expansion or spatial expansion (Table 4.2). However, there is an obvious peak of 4bp-difference mismatch in widespread line hexaploid population, which implies a genetic diversity shrinkage like event. A population decline relevant to this diversity shrinkage like event is also suggested in the Bayesian skyline plot results during 0.06-0.004 Ma although it seems not very obvious (Fig. 4.4). In the Bayesian skyline plot result of diploid population, it did not suggest a unimodel population expansion but implied an expansion first (0.04-0.36 Ma) with a subsequent decline (Fig. 4.4).

F_{ST} and F_{IS}

F_{ST} values of hexaploid population have significant positive correlation with both the point-to-point and stepping stone geographical distance (p values for $r \geq 0$ larger than 0.95; Fig 4.5). No positive correlation between F_{ST} values and geographical distance in diploid population (p value for $r > 0$ larger is 0.31; Fig 4.5). F_{ST} values from hexaploids populations are significantly larger than those from diploid populations (Table 4.3), but are less significant in those data with stepping stone geographical distance < 335 km (i.e. the maxmum pairwise geographical distance for diploids populations; F_{ST}^{b} in Table 4.3). For F_{IS} values, the hexaploid populations were significantly higher than the diploid populations (Table 4.3).

Discussion

Colonization and dispersal ability

The significant higher F_{IS} value of hexaploids indicates an increased *in situ* inbreeding ability for their populations than those in the diploid populations (Table 4.3). These differences in F_{IS} values between *D. lancea* diploids and hexaploids are corresponded to other ferns (other F_{IS} values reviewed in Ranker & Geiger 2008). A higher inbreeding ability in *D. lancea* hexaploids is also supported by the "*ex situ*" experiments underlying their inbreeding tending gender expression and higher inbreeding tolerance (i.e. higher DHL formation rate) in laboratory gametophyte populations (see in Chapter 5). This inbreeding capacity has been considered to be a general phenomenon in fern polyploids (Masuyama & Watano 1990; Verma 2003; Ranker & Geiger 2008). These increased inbreeding abilities postulated hexaploids have an increased colonization ability for their oversea population establishment. On the other hand, diploid population exhibit very low F_{IS} values suggesting that the diploids have low tolerance to inbreeding and are less able to establish oversea population, which should be initiated by limited inbreeding founders.

Current study revealed that extant diploid population is unlikely distributed in Japan and the islands flanking Taiwan Main Is. (Table 4.1 and Fig. 4.2; also see Chapter 6). However, this does not mean that their haploid spores are unable to disperse across sea barriers. Instead, abundant putative tetraploid hybrids (i.e. cross between gametophytes of diploid and hexaploid) were found in Guishan Is., which is less than 22

km distant from a nearby diploid population in Taiwan Main Is. (i.e. the diploid population of Taiwan Ilan; Table 4.1), and a few of such hybrid individuals are also found in Orchid Is. and Ishigaki Is (Table 4.2). Therefore, the colonization ability of diploids is unlikely limited by their spore dispersability, but is limited by their low tolerance to inbreeding. The inbreeding depression in the diploids is also supported by their significantly lower *ex situ* inbreeding tolerances (intragametophytic selfing rates are 0.01 - 0.10; see in Chapter 5).

The origins of hexaploids

Overall, at least ten origins are inferred to comprise the hexaploids in *Depraia lancea*. The two formations of H12-14-6.4 and H7-10-15 hexaploid lines can be traced up to 1.28 Ma and to 1.92 Ma, respectively (Fig. 4.3). In widespread line hexaploid, the *L* I was formed by at least eight origins from the haploid genomes contributioned by diploid progenitors (Fig. 4.3). These multiple origins but with limited genetic diversity from the ancestral diploid population should cause a genetic diversity shrinkage in evolutionary history of these hexaploi populations. In other words, by identifying and timing this diversity shrinkage event in *L* I, the formation time of the widespread line hexaploid could be inferred. Based on Bayesian skyline plot results, the formation time of widespread line hexaploid was suggested during 0.06 - 0.004 Ma, when a genetic diversity shrinkage like event appeared (Fig. 4.4). Meanwhile, the dated nDNA phylogey implied their origin can be traced up to 1.1.Ma (Fig. 4.3).

Regarding to their formation mechanism, every independent hexaploid line needed at least two polyploidization events (including demipolyploidization), which are mediated by either tetraploids or triploids (Fig. 4.6). Among diploid populations, there are several triploid individuals found in this study but most of them are with sterile-like spores excepting for one individual has well-formed and presumed genome unreduced spores from 32-spored sporangia (Table 4.1). However, none of these triploids is phylogenetically related to these hexaploids (data not shown). Besides, those tetraploids found with well-formed and sexual spores are not involved in the formations of hexaploids (Fig. 4.3; also see in Chapter 3). Nonetheless, the putative tetraploid hybrids between the diploids and hexaploids, which were most abundant within or nearby diploid populations (Table 4.1) suggesting the

possibility of recurrent formations for the widespread line hexaploid (as the tetraploid intermediate mechanism in Fig 4.6A). Although no such intermediate was found, based on above, it is reasonable to speculate that such triploid and tetraploid intermediates occurred geographically close to diploid populations because their formations were also relied on diploid population.

For H12-14-6.4 hexaploid line, its populations were found only in Taiwan Main Is. (Table 4.1 and see Chapter 3), where their diploid parentals should also exist. Therefore, the Taiwan Main Is origin in this hexaploid line should be less doubted. Whereas, the H7-10-15 line hexaploids are not distributed in Taiwan Main Is., and the highest genetic diversity of *L* I in the widespread hexaploid line is revealed from northern Taiwan to Central Ryukyu suggesting these areas can be origins of these two hexaploid lines. Since the formation of hexaploids, as well as their triploid and tetraploid intermediates, should relay on the diploid populations, it is important to understand the past distribution of diploid populations for deciphering where these hexaploids originated. Although the diploids might have limited oversea colonization ability, the possibility of a broad past distribution of diploids from Taiwan Main Is. to Ryukyu is implied by the past land connection before 2.0 Ma (Osozawa *et al.* 2012). Assuming diploids were originally widely distributed throught East Asia Archipelago, the scenario for the origin(s) of hexaploid would be that, (1) broad diploid distribution were fragmented into many island populations as a result of sea barrier establishment (i.e. since 2.0-1.5 Ma; Osozawa *et al.* 2012), (2) the hexaploids were formed indipandently from these island populations, and (3) excepting those in Taiwan Main Is., all island populations of diploids were finally extinct while their decendent hexaploids were survive. However, this scenario is considered to be less possible because many independent extinction events of diploid island populations are required. In addition, according to minority cytotype exclusion rule, the likehood should be very low for that these diploid populations on different islands were outcompeted and completely wiped out by descendent hexaploid. Alternatively, the more probably scenario should be that (1) sea barriers were well established since 2.0-1.55 Ma and diploids were distributed only in Taiwan Main Is., (2) hexaploids were formed in Taiwan Main Is., and (3) then dispersed to East Asia Archipelago. This scenario is especially possible for the widespread line hexaploids since they were

revealed with an increased colonization ability for their oversea population establishments, which seem lacking in diploids (see discussion in *Colonization and dispersal ability*). The divergence time result also supports that the widespread line hexaploids lines formed after this geographical barrier established. Most importantly, such scenario stands for that the ancestral diploid population generating these hexaploids had not expanded outside of Taiwan Main Is.

The expansion of hexaploids

For H12-14-6.4 and H7-10-15 hexaploid lines, they are distributed only in Taiwan Main Is. and Southern Ryukyu, respectively (Table 4.1), and, therefore, their expansions are considered to be locally. Meanwhile, the widespread line hexaploids are distributed across southern Taiwan to Honshu of Japan. These hexaploids expansions are suggested to be within 0.06 Ma (Fig. 4.4), when is well after the establishments of geographical barriers in Ryukyu Islands. The current geological evidences imply that terrestrial boundaries within Ryukyu were formed since 1.55 Ma when the sea barriers first appeared in between continental East Asia and Ryukyu and in Yonguni, Kerama, and Tokara gaps (Fig. 4.2) (Osozawa *et al.* 2012). Subsequently, Taiwan Main Is., continental East Asia, and the island groups in Kyushu and Ryukyu separated by these three gaps were inconnected to each other. Only when glaciation periods were the land bridges possible to emerge from shallow submarine straits as results of sea level decrease, which connected Taiwan Main Is. and Kyushu to continental East Asia resulted (Osozawa *et al.* 2012). In addition, the islands flanking Taiwan, including Guishan Is., Green Is., and Orchid Is., are formed by volcanism and revealed still being active until 0.02 Ma (Yang 1992; Chen *et al.* 2001), suggesting their floras were established by recent oversea dispersals. As implied by significant isolation-by-distance pattern in the widespread line hexaploids (Fig. 4.5), their range expansions were likely continuous and mediated by island-by-island dispersals. These hexaploids might have expansion within 0.06 Ma from the region from northern Taiwan to Central Ryukyu, in where populations tend to have higher genetic diversity (i.e. with higher number of sequence types), toward Honshu and southern Taiwan, in where marginal populations exhibit the simplest population genetic structure (Fig. 4.2).

References

Bouckaert R, Heled J, Kühnert D *et al.* (2014) BEAST 2: a software platform for Bayesian evolutionary analysis. *PLoS Ccomputational Biology*, **10**, e1003537.

Chen YG, Wu WS, Chen CH, Liu TK (2001) A date for volcanic eruption inferred from a siltstone xenolith. *Quaternary Science Reviews*, **20**, 869–873.

D'Errico J (2005) Surface Fitting using gridfit (http://www.mathworks.com/matlabcentral/fileexchange/8998), MATLAB Central File Exchange. Retrieved May 18, 2006.

Dufresne F, Stift M, Vergilino R, Mable BK (2014) Recent progress and challenges in population genetics of polyploid organisms: an overview of current state-of-the-art molecular and statistical tools. *Molecular Ecology*, **23**, 40–69.

Drummond AJ, Suchard MA, Xie D, Rambaut A (2012) Bayesian phylogenetics with BEAUti and the BEAST 1.7. *Molecular Biology and Evolution*, **29**, 1969–1973.

Excoffier L, Lischer HEL (2010) Arlequin suite ver 3.5: a new series of programs to perform population genetics analyses under Linux and Windows. *Molecular Ecology Resources*, **10**, 564–567.

Hall T (1999) BioEdit: a user-friendly biological sequence alignment editor and analysis program for Windows 95/98/NT. *Nucleic Acids Symposium Series*, **41**, 95–98.

Huelsenbeck JP, Ronquis F (2001) MRBAYES: Bayesian inference of phylogenetic trees. *Bioinformatics*, **3**, 754–755.

Osozawa S, Shinjo R, Armid A *et al.* (2012) Palaeogeographic reconstruction of the 1.55 Ma synchronous isolation of the Ryukyu Islands, Japan, and Taiwan and inflow of the Kuroshio warm current. *International Geology Review*, **54**, 1369–1388.

Rambaut A, Drummond AJ (2007) Tracer v1.5. http://beast.bio.ed.ac.uk/Tracer

Ranker TA, Geiger JMO (2008) Population genetics. In: *Biology and Evolution of ferns and Lycophytes* (eds. Ranker TA, Haufler CH), pp. 107–133. Cambridge University Press, New York.

Ronquist F, Huelsenbeck JP (2003) MrBayes 3: Bayesian phylogenetic inference under mixed models. *Bioinformatics*, **19**, 1572–1574.

Yang CY (1992) Magma evolution of north Luzon Arc and the tectonic implication. Master thesis, National Taiwan University.

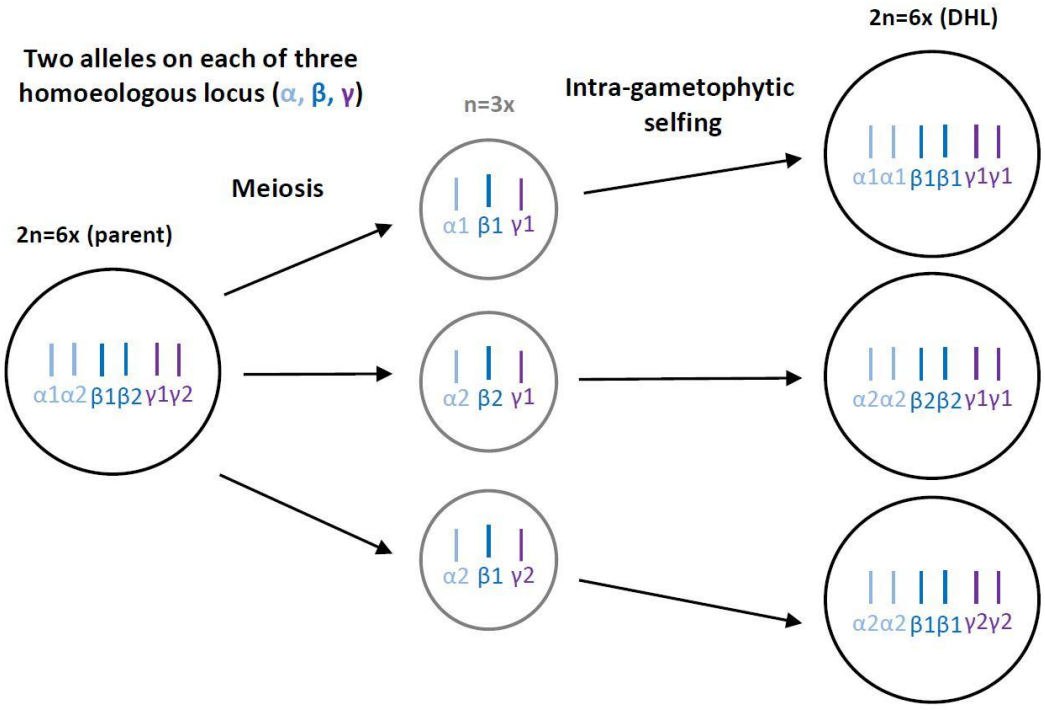

Fig. 4.1. Diagram of formation of doubled haploid lines (DHL) for *Deparia lancea* hexaploids. In a certain genetic region of hexaploidy genome, α, β, and γ represent the three different homoeologous loci.

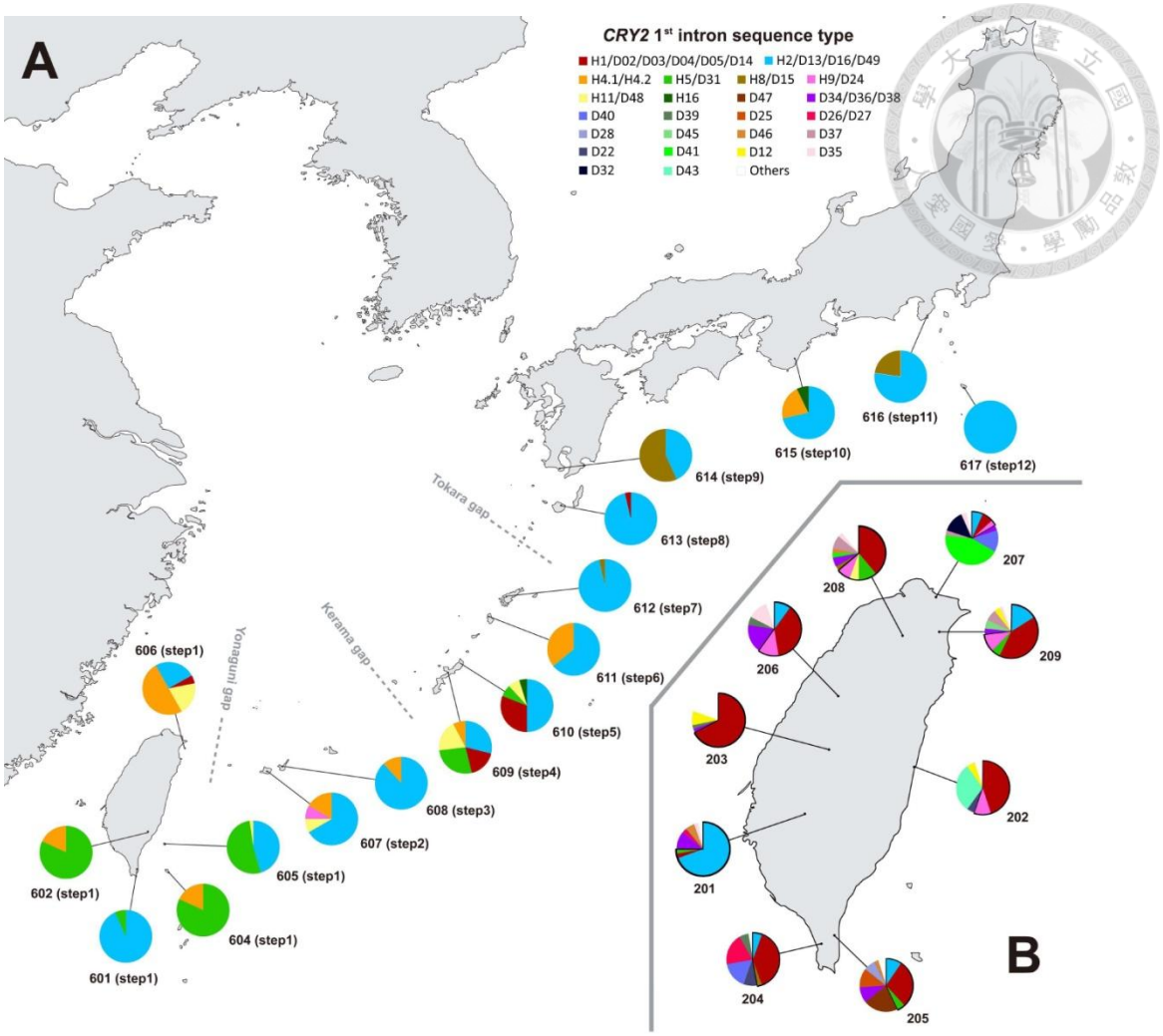

Fig. 4.2. The genetic composition of *CRY2* 1st intron of *Deparia lancea*. (A) The hypothetic homoeologous locus one of widespread line hexaploid populations and (B) the diploid populations. The population code (same as in Table 4.1) and the steps in a hypothesized stepping stone rout are indicated behind the pie charts. In diploid populations, the sequence types in pie charts with back circumference are those shared with same sequence types in the widespread line hexaploids.

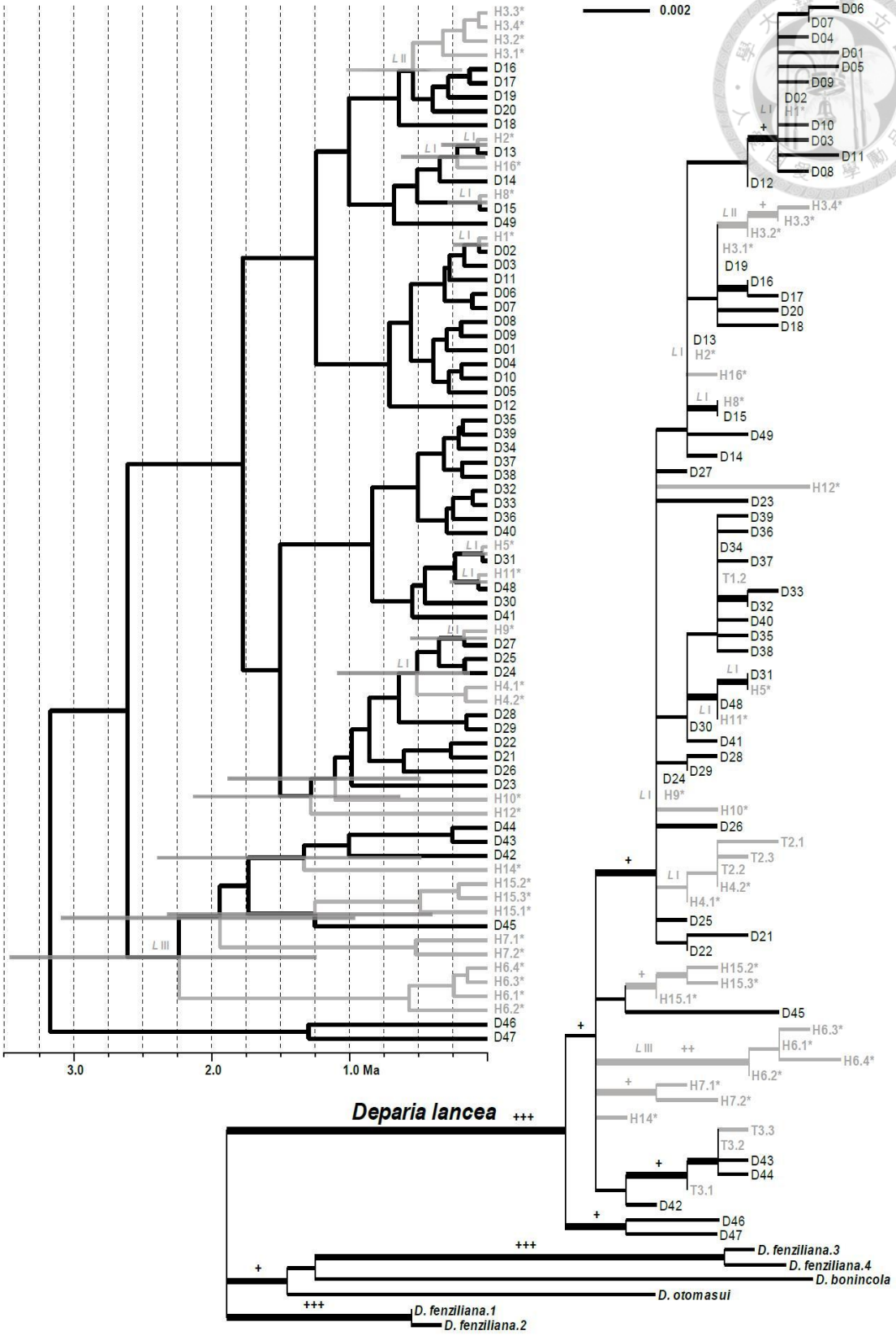
0.002
3.0
2.0
1.0 Ma
Deparia lancea
D. fenziliana.3
D. fenziliana.4
D. bonincola
D. otomasui
D. fenziliana.1
D. fenziliana.2

Fig. 4.3. The phylogram (right) and chronogram (left) *CRY2* 1st intron sequence types of different cytotypes of *Deparia lancea*. The polyploids and diploids are indicated in gray and black color, respectively, and the hexaploid sequence types are indicated with "*". The *L* I, *L* II, and *L* III on the branches represents the *CRY2* hypothetic homoeologous locus one, two, and three in the widespread line hexaploid, respectively. In the phylogram, the thickened branch indicates BIPP ≥ 0.95; and "+", "++", "+++" represents MLBS ≥ 70, ≥85, =100, respectively. In the chronogram, the bars on the branches indicate the 95% HPD of those divergence times of hexaploid lineages.

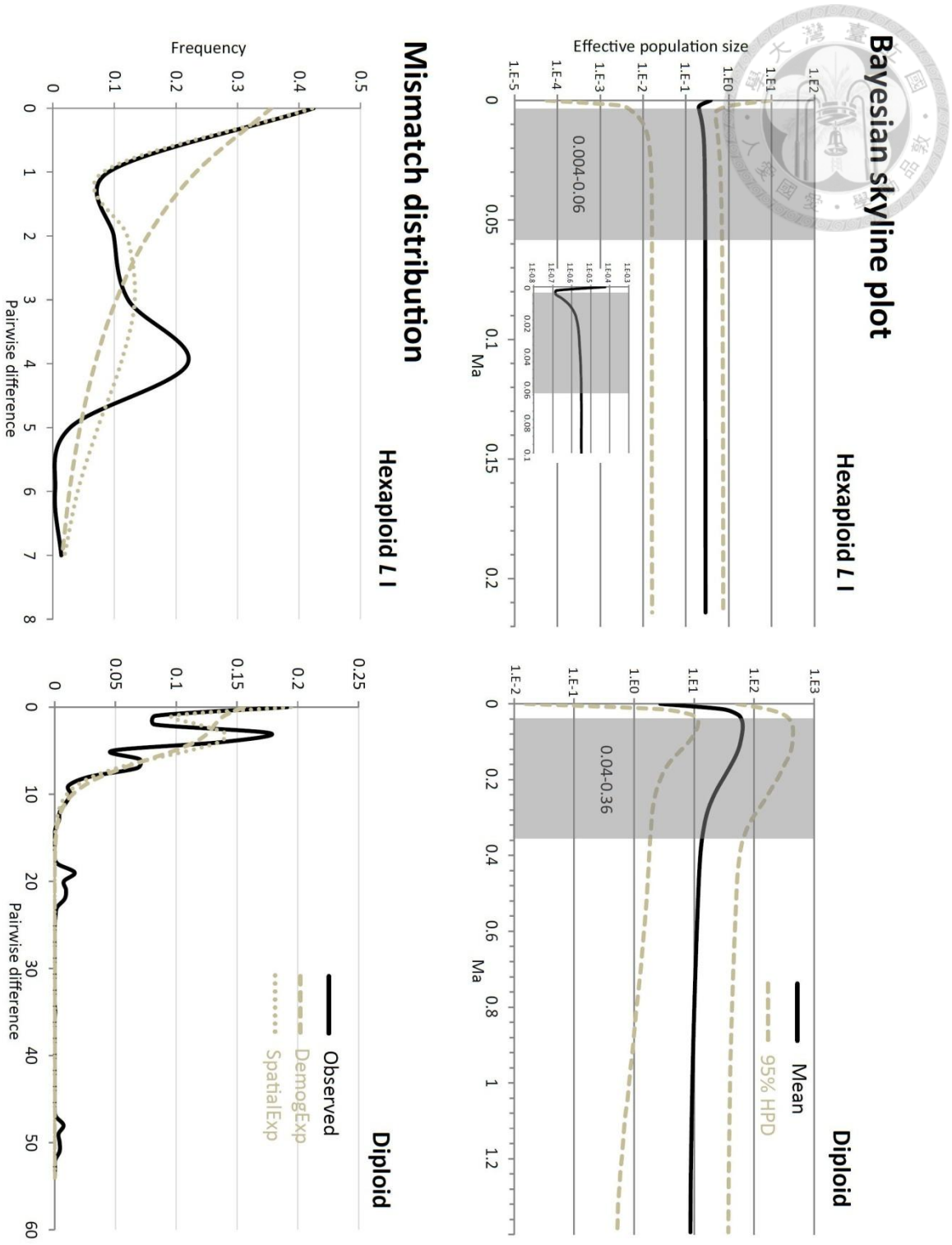

Fig. 4.4. The examination of genetic diversity shrinkage in the widespread line hexaploids and past demographic reconstruction of diploids of *Deparia lancea* using Bayesian skyline plot method (upper) and mismatch distribution (lower) analyses using *CRY2* 1st intron sequences. In mismatch distribution, the "DemogExp" and "SpatialExp"

represent the simulated null distribution under a demographic sudden expansion model and spatial expansion model, respectively.

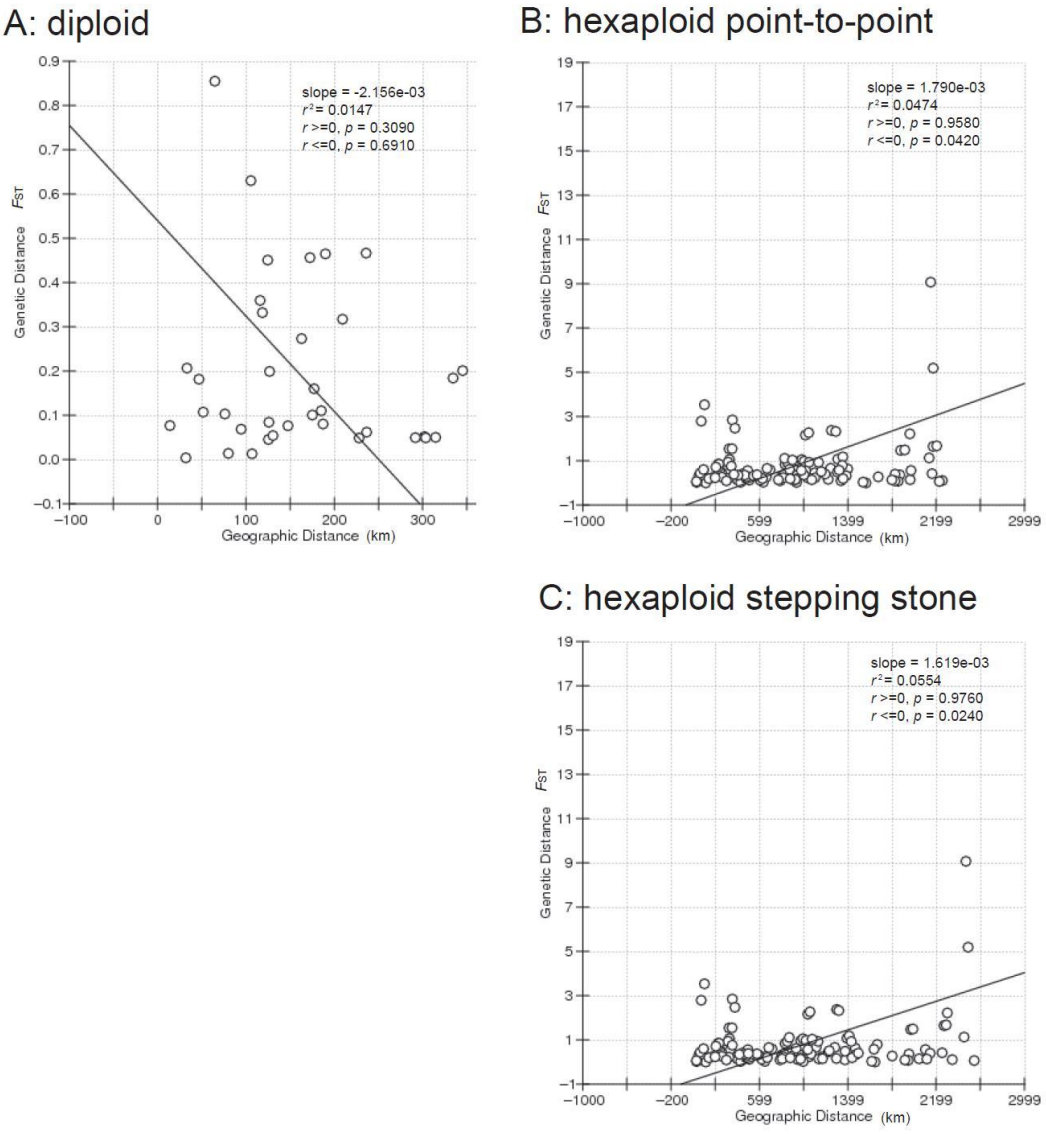

Fig. 4.5. The Mantel tests of isolation-by-distance for diploid (A) and hexaploid (B, C) populations in *Deparia lancea*. The results using the point-to-point and steepping stone geographical distances of hexaploids are shown in (B) and (C), respectively.

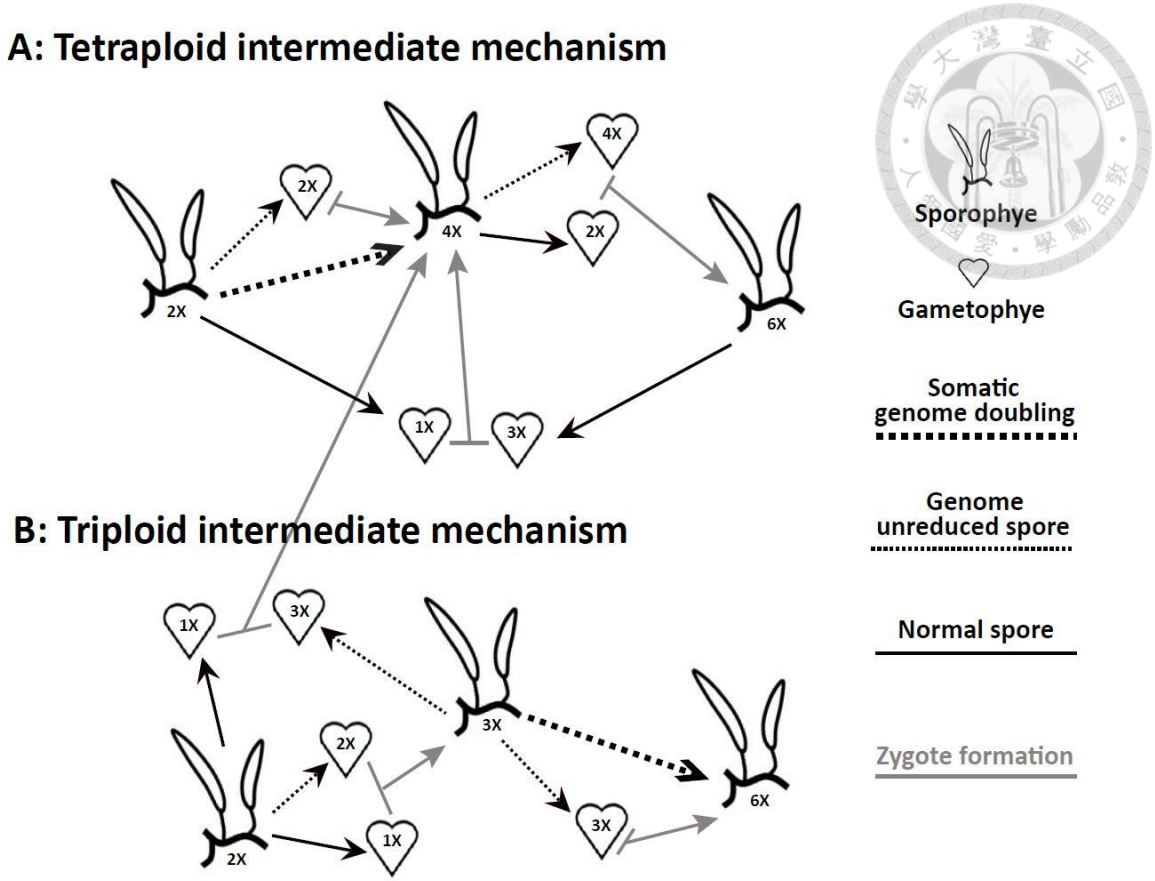

Fig. 4.6. The hypothetic formation mechanisms of *Deparia lancea* hexaploids.

Table 4.1. The sequence type, cytotype, location information of *Deparia lance* individuals used in this study. (The underlined sequence type are those shared with diploid and hexaploid.)

Defined population	Population code	Location	Longitude	Latitude	Cytotypes (individual number)	For population genetics (individual	Sequence type (allele nunmber in population) [other unrecognized genotypes (individual number)]
Taiwan Chiayi	201	Tsengwen reservoir, Chiayi County, Taiwan	120.5839	23.2718	2X (20)	2X (18)	D13 (25) D34 (2) D36 (2) D46 (2) D02 (1) D27 (1) D31 (1)
Taiwan Hualien	202	Mt. Taibalang, Hualien County, Taiwan	121.5204	23.6742	2X (19) 4X (2)[a]	2X (10)	D02 (9) D43 (6) D24 (2) D42 (1) D22 (1) D12 (1)
Taiwan Nantou	203	Chilu Bridge, Nantou County, Taiwan	120.7907	23.8226	2X (23)	2X (23)	D02 (31) D12 (4) D09 (2) D23 (2) D21 (2) D18 (2) D01 (2) D39 (1) D34 (1)
Taiwan Pingtung 1	204	Mt. Lilung, Pingtung County, Taiwan	120.7259	22.1595	2X (19)	2X (18)	D02 (13) D40 (6) D26 (5) D22 (3) D14 (3) D39 (2) D27 (2) D13 (2) D15 (1) D11 (1)
Taiwan Pingtung 2	205	Shouka logging trail, Pingtung County, Taiwan	120.8368	22.2319	2X (23) 3X (1)	2X (21)	D02 (11) D47 (9) D25 (5) D34 (4) D28 (3) D16 (3) D31 (2) D17 (2) D46 (1) D14 (1) D13 (1)
Taiwan Taichung	206	Tungshihlinchang, Taichung City, Taiwan	120.8698	24.2809	2X (21)	2X (20)	D34 (7) D02 (7) D04 (5) D35 (5) D24 (5) D49 (2) D39 (2) D30 (2) D13 (2) D03 (1)
Taiwan Taipei	207	Hsinshan-menghu, New Taipei City, Taiwan	121.7069	25.1285	2X (16) 4X (2)[a]	2X (15)	D41 (13) D40 (4) D32 (4) D02 (2) D38 (1) D37 (1) D35 (1) D33 (1) D24 (1) D13 (1)
Taiwan Taoyuan	208	Mt. Peichatien, Taoyuan County, Taiwan	121.4206	24.7978	2X (18) 3X (1)[b]	2X (18)	D03 (5) D02 (5) D05 (4) D31 (4) D37 (3) D24 (3) D48 (2) D20 (2) D08 (1) D46 (1) D41 (1) D38 (1)
Taiwan Ilan	209	Linmei trail, Chiaohsi, Ilan County, Taiwan	121.7353	24.8309	2X (37)	2X (28)	D02 (23) D13 (9) D24 (6) D37 (4) D45 (3) D31 (3) D34 (2) D12 (2) D10 (2) D35 (1) D29 (1)
Taiwan Pingtung 3	601	Nanjenshan, Pingtung County, Taiwan	120.8481	22.0888	6X (7)	6X (7)	H02 (14); H3.3 (14); H6.1 (14)
		Luliaochsi, Pingtung County, Taiwan	120.8675	22.0500	6X (5)	6X (5)	H02 (8) H05 (2); H3.3 (10); H6.1 (10)
		Mt. Teraso, Pingtung County, Taiwan	120.8688	22.0119	6X (1) 3X (1)[a]	6X (1)	H02 (2); H3.3 (2); H6.1 (2)
		Mt. Wanlite, Pingtung County, Taiwan	120.8462	22.0698	6X (2) 3X (5)[a]	6X (2)	H02 (4); H3.3 (4); H6.1 (4)
Taiwan Taitung 1	602	Luye Gaotai, Taitung County, Taiwan	121.1017	22.9463	6X (11)	6X (11)	H05 (18) H4.2 (4); H3.3 (20) H3.2 (2); H6.1 (22)
Taiwan Taitung 2	603	Mt. Hsinkang, Taitung County, Taiwan	121.2981	23.1448	6X (8)	6X (5)	[H12-13-14 (3) H3.3-6.1-11-12-13 (1) H3.3-6.1-12-13-14 (1)]
Orchid Island	604	Ssulaokou, Orchid Island, Taitung County, Taiwan	121.5737	22.0093	6X (1)	6X (1)	H05 (2); H3.3 (2); H6.1 (2)
		Tienchih, Orchid Island, Taitung County, Taiwan	121.5727	22.0138	6X (16)	6X (12)	H05 (24); H3.3 (23) H3.4 (1); H6.1 (24)
		Tungching stream, Orchid Island, Taitung County, Taiwan	121.5540	22.0635	6X (11) 4X (1)[a]	6X (9)	H05 (10) H4.2 (8); H3.3 (14) H3.2 (4); H6.1 (18)
Green Island	605	Kuanyintung to Haishenping, Green Island, Taitung County, Taiwan	121.4943	22.6602	6X (11)	6X (8)	H02 (10) H05 (5) H11 (1); H3.3 (16); H6.1 (16)
		Kuoshan trail site 1, Green Island, Taitung County, Taiwan	121.4840	22.6578	6X (12)	6X (11)	H05 (16) H02 (6); H3.3 (22); H6.1 (22)
		Kuoshan trail site 2, Green Island, Taitung County, Taiwan	121.4831	22.6543	6X (3)	6X (2)	H02 (4); H3.3 (4); H6.1 (4)
		Haishenping, Green Island, Taitung County, Taiwan	121.5058	22.6593	6X (3)	6X (1)	H05 (2); H3.3 (2); H6.1 (2)
Guishan Island	606	401 high land, Guishan Island, Ilan County, Taiwan	121.9506	24.8418	6X (10) 5X (1) 4X (20)[a]	6X (10)	H4.2 (10) H2 (5) H11 (4) H1 (1); H3.3 (13) H3.2 (8); H6.1 (20)
Iriomote Island	607	Yutsun river, Iriomote Isand, Okinawa Prefecture, Japan	123.8833	24.3667	6X (9)	6X (8)	H02 (4); H3.3 (4); H6.1 (4) [H6.1-7.2-10-15.2-15.3 (3) H3.2-7.2-11 (1) H7.2-10-15.3 (1) H2-3.2-3.3-7.1-
		Nakama River, Iriomote Island, Okinawa Prefecture, Japan	123.8333	24.3167	6X (17)	6X (11)	H02 (12) H11 (2) H09 (2) H4.1 (2) H4.2 (2); H3.3 (19) H3.2 (1); H6.1 (20) [H2-6.1-10-15 (1)]
Ishigaki Island	608	Nagura, Ishigaki Island, Okinawa Prefecture, Japan	124.1798	24.4051	6X (3)	6X (2)	H02 (4); H3.3 (4); H6.1 (4)
		Omoto, Ishigaki Island, Okinawa Prefecture, Japan	124.1833	24.4167	6X (2)	6X (2)	H02 (2); H3.3 (2); H6.1 (2) [H2-9-3.2-3.3-6.1-7.2 (1)]
		Mt. Omoto, Ishigaki Island, Okinawa Prefecture, Japan	124.1845	24.4258	6X (16) 4X (1)[a]	6X (15)	H02 (24) H4.2 (3) H4.1 (1); H3.3 (28); H6.1 (28) [H7.2-10-15.3 (1)]
		Arakawa, Ishigaki Island, Okinawa Prefecture, Japan	124.1822	24.4430	6X (4)	6X (2)	[H7.2-10-15.3 (2)]
Middle Okinawa	609	Sukuta, Nago-shi, Okinawa Prefecture, Japan	127.9877	26.5630	6X (30)	6X (16)	H02 (15) H05 (14) H11 (10) H01 (9) H4.2 (4); H3.3 (32); H6.1 (32)
Northern Okinawa	610	Mt. Yonaha-dake, Kunigami-son, Okinawa Prefecture, Japan	128.2111	26.7308	6X (23)	6X (21)	H02 (21) H01 (13) H05 (3) H11 (3) H16 (2); H3.3 (42); H6.1 (42)
Tokunoshima Island	611	Inutabu, Isen-cho, Tokunoshima Island, Kagoshima Prefecture, Japan	128.9121	27.7181	6X (6)	6X (3)	H02 (6); H3.3 (3) H3.2 (3); H6.1 (6)
		Todoroki, Tokunoshima-cho, Tokunoshima Island, Kagoshima	128.9207	27.8424	6X (21)	6X (11)	H4.2 (14) H02 (8); H3.2 (9) H3.3 (9) H3.1 (4); H6.1 (22)
		Kametsu, Tokunoshima-cho, Tokunoshima Island, Kagoshima	128.9763	27.7586	6X (21)	6X (11)	H02 (18) H4.2 (4); H3.3 (12) H3.2 (8) H3.1 (2); H6.1 (22)
Amami Isand	612	Mt. Yuwan-dake, Yamato-son, Amami-oshima Island, Kagoshima	129.3213	28.2978	6X (28)	6X (16)	H02 (31) H08 (1); H3.1 (22) H3.3 (10); H6.1 (32)
		Naon, Yamato-son, Amami-oshima Island, Kagoshima Prefecture, Japan	129.3374	28.3268	6X (25)	6X (16)	H02 (23) H08 (1); H3.3 (16) H3.1 (8); H6.1 (24)
Yakushima Island	613	Onoaida, Yakushima-cho, Yakushima Island, Kagoshima Prefecture, Japan	130.5481	30.2412	6X (4)	6X (3)	H02 (6); H3.3 (6); H6.1 (6)
		Shirataniunsuikyo, Yakushima-cho, Yakushima Island, Kagoshima Prefecture, Japan	130.5746	30.3800	6X (9)	6X (8)	H02 (16); H3.3 (12) H3.1 (4); H6.1 (16)
		Hirauchi, Yakushima-cho, Yakushima Island, Kagoshima Prefecture, Japan	130.4855	30.2560	6X (5)	6X (5)	H02 (10); H3.3 (6) H3.1 (4); H6.1 (10)
		Nagata, Yakushima-cho, Yakushima Island, Kagoshima Prefecture, Japan	130.3948	30.3847	6X (3)	6X (3)	H02 (4) H1 (2); H3.3 (6); H6.1 (6)

(Table 4.1 cont.)

		Onoaida, Yakushima-cho, Yakushima Island, Kagoshima Prefecture, Japan	130.5404	30.2492	6X (13)	6X (9)	H02 (18); H3.3 (16) H3.1 (2); H6.1 (18)
Kyuhsu	614	Mt. Kaimon, Kagoshima Prefecture, Japan	130.5347	31.1925	6X (7) 4X (2)[c]	6X (4)	H02 (4) H08 (4); H3.3 (4) H3.1 (4); H6.1 (8)
		Tosenkyo Park, Ibusuki-shi, Kagoshima Prefecture, Japan	130.5423	31.2201	6X (15) 5X (3)	6X (10)	H08 (17) H02 (3) ; H3.3 (20); H6.1 (20)
		Eboshi-dake Tunnel, Minamikyushu-shi, Kagoshima Prefecture, Japan	130.5340	31.2441	6X (12) 4X (4)[c] 5X (5)	6X (8)	H02 (12) H08 (4); H3.3 (16); H6.1 (16)
Middle Honshu	615	Kuwanoki Valley, Ohga, Shungu-shi, Wakayama Prefecture, Japan	135.9321	33.7285	6X (8) 5X (11)	6X (8)	H02 (8) H4.2 (6) H16 (2); H3.3 (13) H3.2 (3); H6.1 (16)
		UchiganoValley, Takata, Shungu-shi, Wakayama Prefecture, Japan	135.9321	33.7285	6X (3)	6X (3)	H02 (6); H3.3 (6); H6.1 (6)
		Tashiro, Kiho-cho, Mie Prefecture, Japan	135.9020	33.7323	6X (3) 4X (1)[c]	6X (3)	H02 (6); H3.3 (6); H6.1 (6)
Northern Honshu	616	Shimoda, Shizuoka Prefecture, Japan	138.9732	34.7118	6X (35)	6X (22)	H02 (34) H08 (10); H3.3 (42) H3.1 (2); H6.1 (44)
Hachijo Island	617	Nakanogo, Hachijo Island, Tokyo Metropolis, Japan	139.8166	33.0639	6X (36) 5X (3)	6X (18)	H02 (36); H3.3 (36); H6.1 (36)
		Mt. Mihara, Hachijo Island, Tokyo Metropolis, Japan	139.8194	33.0891	6X (8) 5X (17)	6X (4)	H02 (8); H3.3 (8); H6.1 (8)
		Mt. Hachijo-fuji, Hachijo Island, Tokyo Metropolis, Japan	139.7653	33.1384	6X (7)	6X (3)	H02 (6); H3.3 (6); H6.1 (6)

[a]with only abnormal spores; [b]with well-formed spores in 32-spored sporangia; [c]with well-formed spores in 64-spored sporangia

Table 4.2. Results of mismatch distribution of *Deparia lancea.*

	Pure demographic expansion		Spatial expansion	
	SSD (*p* -value)	RAG (*p* -value)	SSD (*p* -value)	RAG (*p* -value)
Diploid	0.01 (0.59)	0.03 (0.54)	0.01 (0.75)	0.03 (0.81)
Hexaploid*	0.05 (0.33)	0.16 (0.28)	0.02 (0.71)	0.16 (0.74)

*including only the hypothetic homoeologous locus one of widespread lin

SSD = sum of square deviations; RAG = raggedness index.

Table 4.3. The summary of *F* -statistics between the diploid and the widespread line hexaploid populations in *Deparia lancea* . (All values are presented with mean ± one

	Diploid	Hexaploid	*p* -value of *t* -test
F_{IS}	0.032±0.200	0.763±0.420	**0.001**>
F_{ST}[a]	0.194±0.196	0.746±1.104	**0.001**>
F_{ST}[b]	0.194±0.196	0.680±0.822	0.006

[a]for hexaploid population, all population pairs are included.

[b]for hexaploid population, only population pairs with stepping stone geographical distance < 335 km are included.

Table S4.1. The diploid *CRY2* 1st intron genotype reults.
(The original sequence type before translation.)

Population code	Genotype		Identification
201	D13	D13	Sequencing
201	D13	D13	Sequencing
201	D13	D13	SSCP banding
201	D13	D13	SSCP banding
201	D13	D13	SSCP banding
201	D13	D13	SSCP banding
201	D13	D13	SSCP banding
201	D13	D13	SSCP banding
201	D13	D13	SSCP banding
201	D13	D13	SSCP banding
201	D02	D26 (D27)	Sequencing
201	D13	D31	Sequencing
201	D13	D34	Sequencing
201	D13	D34 (D36)	Sequencing
201	D34	D34 (D36)	Sequencing
201	D13	D46	Sequencing
201	D13	D46	SSCP banding
202	D02	D22	Sequencing
202	D02	D24	Sequencing
202	D02	D24	SSCP banding
202	D12	D42	Sequencing
202	D02	D43	Sequencing
202	D02	D43	Sequencing
202	D02	D43	Sequencing
202	D02	D43	Sequencing
202	D02	D43	SSCP banding
202	D02	D43	SSCP banding
203	D01	D02	Sequencing
203	D02	D12	Sequencing
203	D02	D12	SSCP banding
203	D02	D12	SSCP banding
203	D01	D18	Sequencing
203	D02	D02	Sequencing
203	D02	D02	Sequencing
203	D02	D02	SSCP banding
203	D02	D02	SSCP banding
203	D02	D02	SSCP banding
203	D02	D02	SSCP banding
203	D02	D02	SSCP banding
203	D02	D02	SSCP banding
203	D02	D02	SSCP banding
203	D02	D02	SSCP banding
203	D02	D02	SSCP banding

(Table S4.1 cont.1)

203	D02	D23	SSCP banding
203	D12	D34	Sequencing
203	D02	D39	Sequencing
203	D02	D09	Sequencing
203	D02	D09	Sequencing
204	D02	D15	Sequencing
204	D02	D02	Sequencing
204	D02	D02	SSCP banding
204	D02 (D14)	D22	Sequencing
204	D02 (D14)	D22	SSCP banding
204	D02 (D14)	D22	SSCP banding
204	D11	D26	Sequencing
204	D02	D26	Sequencing
204	D02	D26	SSCP banding
204	D26	D26 (D27)	Sequencing
204	D26	D26 (D27)	Sequencing
204	D13	D39	Sequencing
204	D13	D39	Sequencing
204	D02	D40	Sequencing
204	D02	D40	SSCP banding
204	D02	D40	SSCP banding
204	D02	D40	SSCP banding
204	D02	D40	SSCP banding
204	D02	D40	SSCP banding
205	D02	D02 (D14)	Sequencing
205	D13	D13 (D16)	Sequencing
205	D02	D02	Sequencing
205	D02	D25	Sequencing
205	D02	D25	Sequencing
205	D02	D25	Sequencing
205	D02	D25	SSCP banding
205	D02	D25	SSCP banding
205	D13 (D16)	D31	Sequencing
205	D13 (D16)	D31	Sequencing
205	D02	D34	Sequencing
205	D28	D34	Sequencing
205	D28	D34	Sequencing
205	D28	D34	SSCP banding
205	D17	D47	Sequencing
205	D17	D47	SSCP banding
205	D02	D47	Sequencing
205	D02	D47	SSCP banding
205	D46	D47	Sequencing
205	D47	D47	Sequencing

(Table S4.1 cont.2)

205	D47	D47	Sequencing
206	D02 (D03)	D02	Sequencing
206	D02 (D04)	D30	Sequencing
206	D02 (D04)	D30	SSCP banding
206	D02	D34	Sequencing
206	D02	D34	SSCP banding
206	D02	D34	SSCP banding
206	D02	D34	SSCP banding
206	D02	D34	SSCP banding
206	D24	D35	Sequencing
206	D24	D35	Sequencing
206	D24	D35	SSCP banding
206	D24	D35	SSCP banding
206	D24	D35	SSCP banding
206	D34	D39	Sequencing
206	D34	D39	Sequencing
206	D02	D02 (D04)	Sequencing
206	D02	D02 (D04)	SSCP banding
206	D02	D02 (D04)	SSCP banding
206	D13	D13 (D49)	Sequencing
206	D13	D13 (D49)	SSCP banding
207	D02	D32	Sequencing
207	D32	D32	Sequencing
207	D02	D33	Sequencing
207	D13	D35	Sequencing
207	D32	D34 (D38)	Sequencing
207	D13	D41	Sequencing
207	D24	D41	Sequencing
207	D37	D41	Sequencing
207	D40	D41	Sequencing
207	D40	D41	SSCP banding
207	D40	D41	SSCP banding
207	D40	D41	SSCP banding
207	D41	D41	Sequencing
207	D41	D41	Sequencing
207	D41	D41	Sequencing
208	D08	D02 (D03)	Sequencing
208	D02 (D03)	D31	Sequencing
208	D02 (D03)	D31	SSCP banding
208	D02 (D03)	D31	SSCP banding
208	D02 (D03)	D31	SSCP banding
208	D15	D35	Sequencing
208	D20	D37	Sequencing
208	D20	D37	SSCP banding

(Table S4.1 cont.3)

208	D34	D34 (D38)	Sequencing
208	D02	D41	Sequencing
208	D29	D46	Sequencing
208	D24	D48	Sequencing
208	D24	D48	SSCP banding
208	D02	D02 (D05)	Sequencing
208	D02	D02 (D05)	Sequencing
208	D02	D02 (D05)	SSCP banding
208	D02	D02 (D05)	SSCP banding
209	D02	D10	Sequencing
209	D13	D13	Sequencing
209	D02	D02	Sequencing
209	D02	D02	Sequencing
209	D02	D02	Sequencing
209	D02	D02	SSCP banding
209	D02	D02	SSCP banding
209	D02	D02	SSCP banding
209	D02	D02	SSCP banding
209	D02	D02	SSCP banding
209	D13	D24	Sequencing
209	D13	D24	Sequencing
209	D13	D24	Sequencing
209	D13	D24	SSCP banding
209	D13	D24	SSCP banding
209	D13	D24	SSCP banding
209	D02	D29	Sequencing
209	D02	D31	Sequencing
209	D31	D31	Sequencing
209	D02	D34	Sequencing
209	D02	D34	Sequencing
209	D12	D37	Sequencing
209	D12	D37	SSCP banding
209	D13	D37	Sequencing
209	D02	D37	Sequencing
209	D10	D45	Sequencing
209	D02	D45	Sequencing

Table S4.2. The widespread line hexaploid *CRY2* 1st intron genotype reults. (The original sequence type before translation.)

Population code	Genotype *L* I		Genotype *L* II		Genotype *L* III		Identification
601	H02	H02	H3.3	H3.3	H6.1	H6.1	Sequencing
601	H02	H02	H3.3	H3.3	H6.1	H6.1	Sequencing
601	H05	H05	H3.3	H3.3	H6.1	H6.1	Sequencing
601	H02	H02	H3.3	H3.3	H6.1	H6.1	SSCP banding
601	H02	H02	H3.3	H3.3	H6.1	H6.1	SSCP banding
601	H02	H02	H3.3	H3.3	H6.1	H6.1	SSCP banding
601	H02	H02	H3.3	H3.3	H6.1	H6.1	SSCP banding
601	H02	H02	H3.3	H3.3	H6.1	H6.1	SSCP banding
601	H02	H02	H3.3	H3.3	H6.1	H6.1	SSCP banding
601	H02	H02	H3.3	H3.3	H6.1	H6.1	SSCP banding
601	H02	H02	H3.3	H3.3	H6.1	H6.1	SSCP banding
601	H02	H02	H3.3	H3.3	H6.1	H6.1	SSCP banding
601	H02	H02	H3.3	H3.3	H6.1	H6.1	SSCP banding
601	H02	H02	H3.3	H3.3	H6.1	H6.1	SSCP banding
601	H02	H02	H3.3	H3.3	H6.1	H6.1	SSCP banding
602	H4.1 (H4.2)	H4.1 (H4.2)	H3.3	H3.3 (H3.2)	H6.1	H6.1	SSCP banding
602	H4.1 (H4.2)	H4.1 (H4.2)	H3.3	H3.3 (H3.2)	H6.1	H6.1	SSCP banding
602	H05	H05	H3.3	H3.3	H6.1	H6.1	SSCP banding
602	H05	H05	H3.3	H3.3	H6.1	H6.1	SSCP banding
602	H05	H05	H3.3	H3.3	H6.1	H6.1	SSCP banding
602	H05	H05	H3.3	H3.3	H6.1	H6.1	SSCP banding
602	H05	H05	H3.3	H3.3	H6.1	H6.1	SSCP banding
602	H05	H05	H3.3	H3.3	H6.1	H6.1	SSCP banding
602	H05	H05	H3.3	H3.3	H6.1	H6.1	SSCP banding
602	H05	H05	H3.3	H3.3	H6.1	H6.1	SSCP banding
602	H05	H05	H3.3	H3.3	H6.1	H6.1	SSCP banding
604	H05	H05	H3.3	H3.3	H6.1	H6.1	Sequencing
604	H05	H05	H3.3	H3.3	H6.1	H6.1	Sequencing
604	H05	H05	H3.3	H3.3	H6.1	H6.1	SSCP banding
604	H05	H05	H3.3	H3.3	H6.1	H6.1	SSCP banding
604	H05	H05	H3.3	H3.3	H6.1	H6.1	SSCP banding
604	H05	H05	H3.3	H3.3	H6.1	H6.1	SSCP banding
604	H05	H05	H3.3	H3.3	H6.1	H6.1	SSCP banding
604	H05	H05	H3.3	H3.4	H6.1	H6.1	SSCP banding
604	H05	H05	H3.3	H3.3	H6.1	H6.1	SSCP banding
604	H05	H05	H3.3	H3.3	H6.1	H6.1	SSCP banding
604	H05	H05	H3.3	H3.3	H6.1	H6.1	SSCP banding
604	H05	H05	H3.3	H3.3	H6.1	H6.1	SSCP banding
604	H05	H05	H3.3	H3.3	H6.1	H6.1	SSCP banding
604	H05	H05	H3.3	H3.3	H6.1	H6.1	SSCP banding
604	H05	H05	H3.3	H3.3	H6.1	H6.1	SSCP banding
604	H05	H05	H3.3	H3.3	H6.1	H6.1	SSCP banding
604	H4.1 (H4.2)	H4.1 (H4.2)	H3.3 (H3.2)	H3.3	H6.1	H6.1	SSCP banding
604	H4.1 (H4.2)	H4.1 (H4.2)	H3.3 (H3.2)	H3.3	H6.1	H6.1	SSCP banding
604	H4.1 (H4.2)	H4.1 (H4.2)	H3.3 (H3.2)	H3.3	H6.1	H6.1	SSCP banding
604	H05	H05	H3.3	H3.3	H6.1	H6.1	SSCP banding
604	H05	H05	H3.3	H3.3	H6.1	H6.1	SSCP banding
604	H4.1 (H4.2)	H4.1 (H4.2)	H3.3 (H3.2)	H3.3	H6.1	H6.1	SSCP banding

(Table S4.2 cont.)

605	H11	H05	H3.3	H3.3	H6.1	H6.1	Sequencing
605	H02	H02	H3.3	H3.3	H6.1	H6.1	Sequencing
605	H05	H05	H3.3	H3.3	H6.1	H6.1	Sequencing
605	H05	H05	H3.3	H3.3	H6.1	H6.1	SSCP banding
605	H05	H05	H3.3	H3.3	H6.1	H6.1	SSCP banding
605	H02	H02	H3.3	H3.3	H6.1	H6.1	SSCP banding
605	H02	H02	H3.3	H3.3	H6.1	H6.1	SSCP banding
605	H02	H02	H3.3	H3.3	H6.1	H6.1	SSCP banding
605	H02	H02	H3.3	H3.3	H6.1	H6.1	SSCP banding
605	H02	H02	H3.3	H3.3	H6.1	H6.1	SSCP banding
605	H02	H02	H3.3	H3.3	H6.1	H6.1	SSCP banding
605	H02	H02	H3.3	H3.3	H6.1	H6.1	SSCP banding
605	H05	H05	H3.3	H3.3	H6.1	H6.1	SSCP banding
605	H05	H05	H3.3	H3.3	H6.1	H6.1	SSCP banding
605	H05	H05	H3.3	H3.3	H6.1	H6.1	SSCP banding
605	H05	H05	H3.3	H3.3	H6.1	H6.1	SSCP banding
605	H05	H05	H3.3	H3.3	H6.1	H6.1	SSCP banding
605	H05	H05	H3.3	H3.3	H6.1	H6.1	SSCP banding
605	H05	H05	H3.3	H3.3	H6.1	H6.1	SSCP banding
605	H02	H02	H3.3	H3.3	H6.1	H6.1	SSCP banding
605	H02	H02	H3.3	H3.3	H6.1	H6.1	SSCP banding
605	H05	H05	H3.3	H3.3	H6.1	H6.1	SSCP banding
606	H01	H11	H3.3 (H3.2)	H3.3	H6.1	H6.1	Sequencing
606	H02	H11	H3.3 (H3.2)	H3.3	H6.1	H6.1	Sequencing
606	H11	H11	H3.3	H3.3	H6.1	H6.1	SSCP banding
606	H02	H02	H3.3	H3.3	H6.1	H6.1	SSCP banding
606	H02	H02	H3.3	H3.3	H6.1	H6.1	SSCP banding
606	H4.1 (H4.2)	H4.1 (H4.2)	H3.3 (H3.2)	H3.3	H6.1	H6.1	SSCP banding
606	H4.1 (H4.2)	H4.1 (H4.2)	H3.3 (H3.2)	H3.3	H6.1	H6.1	SSCP banding
606	H4.1 (H4.2)	H4.1 (H4.2)	H3.3 (H3.2)	H3.3	H6.1	H6.1	SSCP banding
606	H4.1 (H4.2)	H4.1 (H4.2)	H3.3 (H3.2)	H3.3	H6.1	H6.1	SSCP banding
606	H4.1 (H4.2)	H4.1 (H4.2)	H3.3 (H3.2)	H3.3	H6.1	H6.1	SSCP banding
607	H4.1 (H4.2)	H4.1	H3.3	H3.3	H6.1	H6.1	Sequencing
607	H4.1 (H4.2)	H4.1	H3.3	H3.3	H6.1	H6.1	Sequencing
607	H02	H02	H3.3	H3.3	H6.1	H6.1	SSCP banding
607	H02	H02	H3.3	H3.3	H6.1	H6.1	SSCP banding
607	H02	H02	H3.3	H3.3	H6.1	H6.1	SSCP banding
607	H02	H02	H3.3	H3.3 (H3.2)	H6.1	H6.1	SSCP banding
607	H11	H11	H3.3	H3.3	H6.1	H6.1	SSCP banding
607	H02	H02	H3.3	H3.3	H6.1	H6.1	SSCP banding
607	H09	H09	H3.3	H3.3	H6.1	H6.1	SSCP banding
607	H02	H02	H3.3	H3.3	H6.1	H6.1	SSCP banding
607	H02	H02	H3.3	H3.3	H6.1	H6.1	SSCP banding
607	H02	H02	H3.3	H3.3	H6.1	H6.1	SSCP banding
608	H4.1 (H4.2)	H4.1 (H4.2)	H3.3	H3.3	H6.1	H6.1	Sequencing
608	H02	H02	H3.3	H3.3	H6.1	H6.1	Sequencing
608	H4.1 (H4.2)	H4.1	H3.3	H3.3	H6.1	H6.1	Sequencing
608	H02	H02	H3.3	H3.3	H6.1	H6.1	SSCP banding
608	H02	H02	H3.3	H3.3	H6.1	H6.1	SSCP banding
608	H02	H02	H3.3	H3.3	H6.1	H6.1	SSCP banding
608	H02	H02	H3.3	H3.3	H6.1	H6.1	SSCP banding

(Table S4.2 cont.2)

608	H02	H02	H3.3	H3.3	H6.1	H6.1	SSCP banding
608	H02	H02	H3.3	H3.3	H6.1	H6.1	SSCP banding
608	H02	H02	H3.3	H3.3	H6.1	H6.1	SSCP banding
608	H02	H02	H3.3	H3.3	H6.1	H6.1	SSCP banding
608	H02	H02	H3.3	H3.3	H6.1	H6.1	SSCP banding
608	H02	H02	H3.3	H3.3	H6.1	H6.1	SSCP banding
608	H02	H02	H3.3	H3.3	H6.1	H6.1	SSCP banding
608	H02	H02	H3.3	H3.3	H6.1	H6.1	SSCP banding
608	H02	H02	H3.3	H3.3	H6.1	H6.1	SSCP banding
608	H02	H02	H3.3	H3.3	H6.1	H6.1	SSCP banding
609	H11	H11	H3.3	H3.3	H6.1	H6.1	Sequencing
609	H02	H02	H3.3	H3.3	H6.1	H6.1	Sequencing
609	H02	H02	H3.3	H3.3	H6.1	H6.1	Sequencing
609	H4.1 (H4.2)	H4.1 (H4.2)	H3.3	H3.3	H6.1	H6.1	Sequencing
609	H05	H05	H3.3	H3.3	H6.1	H6.1	Sequencing
609	H01	H02	H3.3	H3.3	H6.1	H6.1	SSCP banding
609	H01	H02	H3.3	H3.3	H6.1	H6.1	SSCP banding
609	H01	H02	H3.3	H3.3	H6.1	H6.1	SSCP banding
609	H01	H02	H3.3	H3.3	H6.1	H6.1	SSCP banding
609	H01	H02	H3.3	H3.3	H6.1	H6.1	SSCP banding
609	H01	H02	H3.3	H3.3	H6.1	H6.1	SSCP banding
609	H01	H02	H3.3	H3.3	H6.1	H6.1	SSCP banding
609	H01	H02	H3.3	H3.3	H6.1	H6.1	SSCP banding
609	H01	H02	H3.3	H3.3	H6.1	H6.1	SSCP banding
609	H11	H05	H3.3	H3.3	H6.1	H6.1	SSCP banding
609	H11	H05	H3.3	H3.3	H6.1	H6.1	SSCP banding
609	H11	H05	H3.3	H3.3	H6.1	H6.1	SSCP banding
609	H11	H05	H3.3	H3.3	H6.1	H6.1	SSCP banding
609	H11	H05	H3.3	H3.3	H6.1	H6.1	SSCP banding
609	H11	H05	H3.3	H3.3	H6.1	H6.1	SSCP banding
609	H11	H05	H3.3	H3.3	H6.1	H6.1	SSCP banding
609	H11	H05	H3.3	H3.3	H6.1	H6.1	SSCP banding
609	H02	H02	H3.3	H3.3	H6.1	H6.1	SSCP banding
609	H4.1 (H4.2)	H4.1 (H4.2)	H3.3	H3.3	H6.1	H6.1	SSCP banding
609	H05	H05	H3.3	H3.3	H6.1	H6.1	SSCP banding
609	H05	H05	H3.3	H3.3	H6.1	H6.1	SSCP banding
610	H01	H02	H3.3	H3.3	H6.1	H6.1	Sequencing
610	H11	H05	H3.3	H3.3	H6.1	H6.1	Sequencing
610	H02	H02	H3.3	H3.3	H6.1	H6.1	Sequencing
610	H01	H02	H3.3	H3.3	H6.1	H6.1	SSCP banding
610	H01	H02	H3.3	H3.3	H6.1	H6.1	SSCP banding
610	H01	H02	H3.3	H3.3	H6.1	H6.1	SSCP banding
610	H01	H02	H3.3	H3.3	H6.1	H6.1	SSCP banding
610	H01	H02	H3.3	H3.3	H6.1	H6.1	SSCP banding
610	H01	H02	H3.3	H3.3	H6.1	H6.1	SSCP banding
610	H01	H02	H3.3	H3.3	H6.1	H6.1	SSCP banding
610	H01	H02	H3.3	H3.3	H6.1	H6.1	SSCP banding
610	H01	H02	H3.3	H3.3	H6.1	H6.1	SSCP banding
610	H01	H02	H3.3	H3.3	H6.1	H6.1	SSCP banding
610	H01	H02	H3.3	H3.3	H6.1	H6.1	SSCP banding
610	H01	H02	H3.3	H3.3	H6.1	H6.1	SSCP banding

(Table S4.2 cont.3)

610	H11	H05	H3.3	H3.3	H6.1	H6.1	SSCP banding
610	H11	H05	H3.3	H3.3	H6.1	H6.1	SSCP banding
610	H16	H16	H3.3	H3.3	H6.1	H6.1	SSCP banding
610	H02	H02	H3.3	H3.3	H6.1	H6.1	SSCP banding
610	H02	H02	H3.3	H3.3	H6.1	H6.1	SSCP banding
610	H02	H02	H3.3	H3.3	H6.1	H6.1	SSCP banding
611	H02	H02	H3.3 (H3.2)	H3.3	H6.1	H6.1	Sequencing
611	H02	H02	H3.1	H3.1	H6.1	H6.1	Sequencing
611	H4.1 (H4.2)	H4.1 (H4.2)	H3.3 (H3.2)	H3.3	H6.1	H6.1	Sequencing
611	H02	H02	H3.3 (H3.2)	H3.3	H6.1	H6.1	Sequencing
611	H02	H02	H3.3 (H3.2)	H3.3	H6.1	H6.1	SSCP banding
611	H02	H02	H3.3 (H3.2)	H3.3	H6.1	H6.1	SSCP banding
611	H4.1 (H4.2)	H4.1 (H4.2)	H3.3 (H3.2)	H3.3	H6.1	H6.1	SSCP banding
611	H4.1 (H4.2)	H4.1 (H4.2)	H3.3 (H3.2)	H3.3	H6.1	H6.1	SSCP banding
611	H4.1 (H4.2)	H4.1 (H4.2)	H3.3 (H3.2)	H3.3	H6.1	H6.1	SSCP banding
611	H4.1 (H4.2)	H4.1 (H4.2)	H3.3 (H3.2)	H3.3	H6.1	H6.1	SSCP banding
611	H02	H02	H3.1	H3.1	H6.1	H6.1	SSCP banding
611	H4.1 (H4.2)	H4.1 (H4.2)	H3.3 (H3.2)	H3.3	H6.1	H6.1	SSCP banding
611	H02	H02	H3.3 (H3.2)	H3.3	H6.1	H6.1	SSCP banding
611	H02	H02	H3.3 (H3.2)	H3.3	H6.1	H6.1	SSCP banding
611	H4.1 (H4.2)	H4.1 (H4.2)	H3.3 (H3.2)	H3.3	H6.1	H6.1	SSCP banding
611	H4.1 (H4.2)	H4.1 (H4.2)	H3.3 (H3.2)	H3.3	H6.1	H6.1	SSCP banding
611	H02	H02	H3.3 (H3.2)	H3.3	H6.1	H6.1	SSCP banding
611	H02	H02	H3.3 (H3.2)	H3.3	H6.1	H6.1	SSCP banding
611	H02	H02	H3.3 (H3.2)	H3.3	H6.1	H6.1	SSCP banding
611	H02	H02	H3.1	H3.1	H6.1	H6.1	SSCP banding
611	H02	H02	H3.3 (H3.2)	H3.3	H6.1	H6.1	SSCP banding
611	H02	H02	H3.3 (H3.2)	H3.3	H6.1	H6.1	SSCP banding
611	H4.1 (H4.2)	H4.1 (H4.2)	H3.3 (H3.2)	H3.3	H6.1	H6.1	SSCP banding
611	H02	H02	H3.3	H3.3	H6.1	H6.1	SSCP banding
611	H02	H02	H3.3	H3.3	H6.1	H6.1	SSCP banding
612	H02	H02	H3.3	H3.3	H6.1	H6.1	Sequencing
612	H02	H8	H3.3	H3.3	H6.1	H6.1	Sequencing
612	H02	H02	H3.1	H3.1	H6.1	H6.1	Sequencing
612	H02	H02	H3.1	H3.1	H6.1	H6.1	SSCP banding
612	H02	H02	H3.1	H3.1	H6.1	H6.1	SSCP banding
612	H02	H8	H3.3	H3.3	H6.1	H6.1	SSCP banding
612	H02	H02	H3.3	H3.3	H6.1	H6.1	SSCP banding
612	H02	H02	H3.1	H3.1	H6.1	H6.1	SSCP banding
612	H02	H02	H3.3	H3.3	H6.1	H6.1	SSCP banding
612	H02	H02	H3.1	H3.1	H6.1	H6.1	SSCP banding
612	H02	H02	H3.1	H3.1	H6.1	H6.1	SSCP banding
612	H02	H02	H3.3	H3.3	H6.1	H6.1	SSCP banding
612	H02	H02	H3.1	H3.1	H6.1	H6.1	SSCP banding
612	H02	H02	H3.1	H3.1	H6.1	H6.1	SSCP banding
612	H02	H02	H3.1	H3.1	H6.1	H6.1	SSCP banding
612	H02	H02	H3.1	H3.1	H6.1	H6.1	SSCP banding
612	H02	H02	H3.1	H3.1	H6.1	H6.1	SSCP banding
612	H02	H02	H3.1	H3.1	H6.1	H6.1	SSCP banding
612	H02	H02	H3.3	H3.3	H6.1	H6.1	SSCP banding

(Table S4.2 cont.4)

612	H02	H02	H3.1	H3.1	H6.1	H6.1	SSCP banding
612	H02	H02	H3.1	H3.1	H6.1	H6.1	SSCP banding
612	H02	H02	H3.3	H3.3	H6.1	H6.1	SSCP banding
612	H02	H02	H3.3	H3.3	H6.1	H6.1	SSCP banding
612	H02	H02	H3.1	H3.1	H6.1	H6.1	SSCP banding
612	H02	H02	H3.3	H3.3	H6.1	H6.1	SSCP banding
612	H02	H02	H3.3	H3.3	H6.1	H6.1	SSCP banding
612	H02	H02	H3.3	H3.3	H6.1	H6.1	SSCP banding
612	H02	H02	H3.3	H3.3	H6.1	H6.1	SSCP banding
613	H02	H02	H3.3	H3.3	H6.1	H6.1	Sequencing
613	H02	H02	H3.3	H3.3	H6.1	H6.1	Sequencing
613	H02	H02	H3.3	H3.3	H6.1	H6.1	Sequencing
613	H02	H02	H3.1	H3.1	H6.1	H6.1	Sequencing
613	H01	H1	H3.3	H3.3	H6.1	H6.1	Sequencing
613	H02	H02	H3.3	H3.3	H6.1	H6.1	Sequencing
613	H02	H02	H3.3	H3.3	H6.1	H6.1	Sequencing
613	H02	H02	H3.1	H3.1	H6.1	H6.1	Sequencing
613	H02	H02	H3.3	H3.3	H6.1	H6.1	SSCP banding
613	H02	H02	H3.3	H3.3	H6.1	H6.1	SSCP banding
613	H02	H02	H3.1	H3.1	H6.1	H6.1	SSCP banding
613	H02	H02	H3.3	H3.3	H6.1	H6.1	SSCP banding
613	H02	H02	H3.1	H3.1	H6.1	H6.1	SSCP banding
613	H02	H02	H3.3	H3.3	H6.1	H6.1	SSCP banding
613	H02	H02	H3.3	H3.3	H6.1	H6.1	SSCP banding
613	H02	H02	H3.3	H3.3	H6.1	H6.1	SSCP banding
613	H02	H02	H3.3	H3.3	H6.1	H6.1	SSCP banding
613	H02	H02	H3.3	H3.3	H6.1	H6.1	SSCP banding
613	H02	H02	H3.1	H3.1	H6.1	H6.1	SSCP banding
613	H02	H02	H3.3	H3.3	H6.1	H6.1	SSCP banding
613	H02	H02	H3.3	H3.3	H6.1	H6.1	SSCP banding
613	H02	H02	H3.3	H3.3	H6.1	H6.1	SSCP banding
613	H02	H02	H3.3	H3.3	H6.1	H6.1	SSCP banding
613	H02	H02	H3.3	H3.3	H6.1	H6.1	SSCP banding
613	H02	H02	H3.3	H3.3	H6.1	H6.1	SSCP banding
613	H02	H02	H3.3	H3.3	H6.1	H6.1	SSCP banding
613	H02	H02	H3.3	H3.3	H6.1	H6.1	SSCP banding
613	H02	H02	H3.3	H3.3	H6.1	H6.1	SSCP banding
614	H02	H02	H3.1	H3.1	H6.1	H6.1	Sequencing
614	H02	H8	H3.3	H3.3	H6.1	H6.1	Sequencing
614	H02	H02	H3.3	H3.3	H6.1	H6.1	Sequencing
614	H8	H8	H3.3	H3.3	H6.1	H6.1	Sequencing
614	H8	H8	H3.3	H3.3	H6.1	H6.1	SSCP banding
614	H02	H02	H3.1	H3.1	H6.1	H6.1	SSCP banding
614	H8	H8	H3.3	H3.3	H6.1	H6.1	SSCP banding
614	H8	H8	H3.3	H3.3	H6.1	H6.1	SSCP banding
614	H02	H02	H3.3	H3.3	H6.1	H6.1	SSCP banding
614	H8	H8	H3.3	H3.3	H6.1	H6.1	SSCP banding
614	H8	H8	H3.3	H3.3	H6.1	H6.1	SSCP banding
614	H8	H8	H3.3	H3.3	H6.1	H6.1	SSCP banding
614	H8	H8	H3.3	H3.3	H6.1	H6.1	SSCP banding
614	H8	H8	H3.3	H3.3	H6.1	H6.1	SSCP banding

(Table S4.2 cont.5)

614	H8	H8	H3.3	H3.3	H6.1	H6.1	SSCP banding
614	H8	H8	H3.3	H3.3	H6.1	H6.1	SSCP banding
614	H02	H02	H3.3	H3.3	H6.1	H6.1	SSCP banding
614	H02	H02	H3.3	H3.3	H6.1	H6.1	SSCP banding
614	H02	H02	H3.3	H3.3	H6.1	H6.1	SSCP banding
614	H8	H8	H3.3	H3.3	H6.1	H6.1	SSCP banding
614	H02	H02	H3.3	H3.3	H6.1	H6.1	SSCP banding
614	H02	H02	H3.3	H3.3	H6.1	H6.1	SSCP banding
615	H16	H16	H3.3	H3.3	H6.1	H6.1	Sequencing
615	H02	H02	H3.3	H3.3	H6.1	H6.1	Sequencing
615	H02	H02	H3.3	H3.3	H6.1	H6.1	Sequencing
615	H02	H02	H3.3	H3.3	H6.1	H6.1	SSCP banding
615	H4.1 (H4.2)	H4.1 (H4.2)	H3.3	H3.3 (H3.2)	H6.1	H6.1	SSCP banding
615	H4.1 (H4.2)	H4.1 (H4.2)	H3.3	H3.3 (H3.2)	H6.1	H6.1	SSCP banding
615	H4.1 (H4.2)	H4.1 (H4.2)	H3.3	H3.3 (H3.2)	H6.1	H6.1	SSCP banding
615	H02	H02	H3.3	H3.3	H6.1	H6.1	SSCP banding
615	H02	H02	H3.3	H3.3	H6.1	H6.1	SSCP banding
615	H02	H02	H3.3	H3.3	H6.1	H6.1	SSCP banding
615	H02	H02	H3.3	H3.3	H6.1	H6.1	SSCP banding
615	H02	H02	H3.3	H3.3	H6.1	H6.1	SSCP banding
615	H02	H02	H3.3	H3.3	H6.1	H6.1	SSCP banding
615	H02	H02	H3.3	H3.3	H6.1	H6.1	SSCP banding
616	H02	H02	H3.3	H3.3	H6.1	H6.1	SSCP banding
616	H02	H02	H3.3	H3.3	H6.1	H6.1	SSCP banding
616	H02	H02	H3.3	H3.3	H6.1	H6.1	SSCP banding
616	H02	H02	H3.3	H3.3	H6.1	H6.1	SSCP banding
616	H02	H02	H3.3	H3.3	H6.1	H6.1	SSCP banding
616	H02	H02	H3.3	H3.3	H6.1	H6.1	SSCP banding
616	H02	H02	H3.3	H3.3	H6.1	H6.1	SSCP banding
616	H02	H02	H3.3	H3.3	H6.1	H6.1	SSCP banding
616	H02	H02	H3.3	H3.3	H6.1	H6.1	SSCP banding
616	H02	H02	H3.3	H3.3	H6.1	H6.1	SSCP banding
616	H02	H02	H3.3	H3.3	H6.1	H6.1	SSCP banding
616	H02	H02	H3.3	H3.3	H6.1	H6.1	SSCP banding
616	H02	H02	H3.3	H3.3	H6.1	H6.1	SSCP banding
616	H02	H02	H3.3	H3.3	H6.1	H6.1	SSCP banding
616	H02	H02	H3.3	H3.3	H6.1	H6.1	SSCP banding
616	H02	H02	H3.3	H3.3	H6.1	H6.1	SSCP banding
616	H02	H02	H3.1	H3.1	H6.1	H6.1	SSCP banding
616	H8	H8	H3.3	H3.3	H6.1	H6.1	SSCP banding
616	H8	H8	H3.3	H3.3	H6.1	H6.1	SSCP banding
616	H8	H8	H3.3	H3.3	H6.1	H6.1	SSCP banding
616	H8	H8	H3.3	H3.3	H6.1	H6.1	SSCP banding
616	H8	H8	H3.3	H3.3	H6.1	H6.1	SSCP banding
617	H02	H02	H3.3	H3.3	H6.1	H6.1	Sequencing
617	H02	H02	H3.3	H3.3	H6.1	H6.1	SSCP banding
617	H02	H02	H3.3	H3.3	H6.1	H6.1	SSCP banding
617	H02	H02	H3.3	H3.3	H6.1	H6.1	SSCP banding
617	H02	H02	H3.3	H3.3	H6.1	H6.1	SSCP banding
617	H02	H02	H3.3	H3.3	H6.1	H6.1	SSCP banding

(Table S4.2 cont.6)

617	H02	H02	H3.3	H3.3	H6.1	H6.1	SSCP banding
617	H02	H02	H3.3	H3.3	H6.1	H6.1	SSCP banding
617	H02	H02	H3.3	H3.3	H6.1	H6.1	SSCP banding
617	H02	H02	H3.3	H3.3	H6.1	H6.1	SSCP banding
617	H02	H02	H3.3	H3.3	H6.1	H6.1	SSCP banding
617	H02	H02	H3.3	H3.3	H6.1	H6.1	SSCP banding
617	H02	H02	H3.3	H3.3	H6.1	H6.1	SSCP banding
617	H02	H02	H3.3	H3.3	H6.1	H6.1	SSCP banding
617	H02	H02	H3.3	H3.3	H6.1	H6.1	SSCP banding
617	H02	H02	H3.3	H3.3	H6.1	H6.1	SSCP banding
617	H02	H02	H3.3	H3.3	H6.1	H6.1	SSCP banding
617	H02	H02	H3.3	H3.3	H6.1	H6.1	SSCP banding
617	H02	H02	H3.3	H3.3	H6.1	H6.1	SSCP banding
617	H02	H02	H3.3	H3.3	H6.1	H6.1	SSCP banding
617	H02	H02	H3.3	H3.3	H6.1	H6.1	SSCP banding
617	H02	H02	H3.3	H3.3	H6.1	H6.1	SSCP banding
617	H02	H02	H3.3	H3.3	H6.1	H6.1	SSCP banding
617	H02	H02	H3.3	H3.3	H6.1	H6.1	SSCP banding
617	H02	H02	H3.3	H3.3	H6.1	H6.1	SSCP banding

Chapter 5.

Inbreeding reproductive biology associaing with autopolyploidization in the *Deparia lancea* hexaploid

Abstract

In this chapter, the gametophyte developmental process and inbreeding tolerances in both diploid and hexaploid *Deparia lancea* were examined. Diploids were revealed with a typical outcrossing reproduction, for which gametophytes maintained a significant unisexuality expression (i.e. male or female) in population and behaved with significant increase in sporophyte generating rates when the outcrossing opportunity increased. Different from diploids, the gametophytes of hexaploid biased to bisexual in population, and exhibited an ability to simultaneously express both antheridium and archegonium. This inbreeding tending gender expression was hypothesized to associate with a delay/prolong antheridiogen sensitivity, which can result in antheridium formation in the late development stages or even after archegonium is formed. Such relating phenomena of gender expression can be also found in other polyploidy fern species but seems more obvious in autopolyploids than allopolyploids. In addition to inbreeding tending gender expression, the higher inbreeding ability in *D. lancea* hexaploids was also assessed by their significant increase in inbreeding tolerance comparing to diploids. This increased inbreeding ability in hexaploid can, therefore, assist the assortative mating in hexaploids and avoid to be outcompeted by the gametes from diploids during initial polyploidy establishment. Regarding to evolution of gametophyte development process, a peramorphosis for archegonium formation and a paedomorphsis for offerspring sporophyte generating were implied for hexaploids.

Introduction

The inbreeding tolerance of sexual polyploid ferns has been reported in many previous studies, measuring the inbreeding tolerance from lab cultures and the genetic diversity in field populations (Masuyama & Watano 1990; Ranker & Geiger 2008). In addition, their increased ability to promote inbreeding is also indicated by differentiation in gametangium

development at temporal and spatial scales (Masuyama & Watano 1990; Verma 2003). For example, bisexual gametophytes in tetraploid *Phegopteris decursive-pinnata* Fée (Thelypteridaceae, Polypodiales) are mainly generated under a rapid sequential from female to bisexual whereas those in conspecific diploids are mostly formed by a slow sequential from male to bisexual (Masuyama 1979). In addition, the antheridia in bisexual gametophytes of these tetraploids develop at positions surrounding the notch meristem, where is nearby or mixed with archegonia, while those in diploids are at the basal positions of the gametophyte and relatively distant to archegonia (Masuyama 1979). These imply that developmental changes in fern gametophyte are coupled with polyploidization to increase their inbreeding opportunity. From the evolutionary view, it is also critical for gametophytes of sexual polyploids evolve an assortative mating mechanism during their initial establishment. Assortative mating mechanism in polyploids, such as a bisexual tendency in gametophytes, can provide a prezygotic reproductive isolation with their diploid progenitors, and, thus, avoid the extinction due to outcompeting by the dominate gametes from diploid progenitors (i.e. minority cytotype exclusion; Ramsey & Ramsey, 2014). However, there are still limited studies underlying how polyploidy fern gametophytes differ their breeding strategies from those of their diploid progenitors.

In this chapter, gametophyte development of both sexual hexaploids and diploids in *Deparia lancea* (Thunb.) Fraser-Jenk. (Athyridaceae, Polypodiales) was investigated. These hexaploids have been revealed as successfully established autopolyploids with a pronounced geographical range expansion, which indicates an increased colonization ability (Chapter 3 and 4). In order to identify if this increase in colonization ability is attributed by their inbreeding ability, this study focused on the gender expression during their gametophyte stage and their inbreeding tolerances inferred from isolated gametophytes cultures. To quantify their bisexualities in gametophyte population, a novel index was applied to evaluate their dioecy degree. Finally, gametophytes developmental processes of hexaploid *D. lancea* were characterized by their gender expression and gametophyte size increase through time, and, comparing with the diploid, the gametophyte developmental changes in these hexaploids associated with polyploidy evolution were summarized.

Materials and methods

Plant materials

The ploidy levels of all sporophyte individuals included in this study were first confirmed by flow cytometry analyses followed the approaches described in Chapter 3. Spores from two diploid populations and two hexaploid populations in Taiwan were used in this study. A total of 7 different diploid sporophyte individuals from the populations in Taoyuan County and Taichung City were selected, and 8 different hexaploid sporophyte individuals from the populations Green Is. and Luye Gaotai (both in Taitung County) were selected (Table 5.1). These hexaploids belong to the widespread line regarded previously (i.e. in Chapter 3 and 4). In this study, different sporophyte individuals in the same population were sampled with > 10 m distance from each another. Among these sporophyte individuals, 5 from diploid Taoyuan population and 7 from hexaploid Green Is. population were selected for a diploid and a hexaploid multi-individual multispore culture, respectively (see below for the definition of multi-individual multispore culture). Another two diploid individuals from the Taoyuan and Taichung populations were selected for one two-individual multispore cultures, two single-individual multispore cultures, and two single-individual isolated gametophyte cultures (see below for the definition of these cultures); another two hexaploid individuals from the Green Is. and Taitung populations were selected for spore cultures using the same manner as for diploid individuals.

Confirmation of sexual reproduction mode

Before sowing the spores, the reproductive mode of each individuals applied in this study was confirmed by their spore numbers per sporangium (S/S) from five sporangia. In *Deparia*, 64 and 32 S/S are refered to be sexual and apomixis, respectively (Kato *et al.* 1992). After the formation rate of sporophytes offspring from spore cultures were stable, 20 gametophyte individuals without juvenile sporophyte (in size around 0.5 cm^2) and juvenile leave tissue from offspring sporophytes for each cytotype were used for flow cytometry analyses. By comparing to the parental and offspring sporophytes, the sexual reproduction mode for these gametophytes could be accertained if their nuclear DNA contains were estimated as a half of those measured from the sporophytes. The method of flow cytometry analyses followed that described in Chapter 3.

Cultures and cultivation condition

In multi-individual multispore (MM) cultures, spores from 5-7 sporophyte individuals were mixed and sowed in four boxes with a density estimated to 320-350 spores cm^{-2}, and these cultures were used for the observation of gender expression (see below). The two-individual multispore (TM) and single-individual multispore (SM) cultures contained the spores from two individuals of different populations and from a single individual, respectively. In all multispore cultures, they were cultivated in 7.5 cm ^{x} 9 cm size plastic boxes (PHYTATRAY II^{TM} No. P5929, Sigma, USA). For the single-individual isolated gametophyte (SI) cultures, each of the asexual (or called presexual) gametophytes from SM cultures was transferred to a cell in 3.7 cm^2. These asexual gametophytes were selected within three weeks after sowing (WAS). The medium contained a mixture of vermiculite:peat:perlite in 2:2:1. Gametophytes of terrestrial ferns grown on such soil-like medium are considered to development much similar as that in their natural habitat (Farrar *et al.* 2008). The culture condition was under LED white fluorescent illumination of 6.3 ± 0.3 μmole m^{-2} s^{-1} for 10 h d^{-1} (LI-250A, light meter, LI-COR) and the daily temperature ranged from 20–28℃. Humidity was monitored to avoid desiccation of the cultures.

Gender expression and gametophyte size

Randomly sampled gametophyte individuals were removed (and not returned) from MM cultures to record their sexuality, age, and size in profile area every two weeks from gametangium appearing to juvenile sporophyte generating. The program Image-Pro 5.0 was applied to calculate the profile area of gametophytes. During 4-12 WAS, for each cytotype, a total of 100 gametophytes from four boxes (25 per box) were observed. After 12 weeks, the observation numbers of total gametophytes were reduced to 80 or 50 (20 or 12-13 per box) due to samples availability. To quantify their bisexuality in gametophyte populations of these MM cultures, a novel index, “dioecy index” was applied and calculated by the formula of $B_E - B_O$. The B_E and B_O represented the expected and observed proportion of bisexual gametophytes, respectively, and B_E was equal to multiplying the observed proportion of individuals with antheridium by that with archegonium in the same gametophyte population. Given that there is a half of individuals in one gametophyte

population with antheridium and a half with archegonium, in one extreme situation, if they produce only one kind of gametangia (i.e. 50% male and 50% female; $B_E = 0.5 \times 0.5$, $B_O = 0$) a high dioecy index of 0.25 will be revealed in this population. In another extreme situation, if they produce both kinds of gametangia (i.e. 50% bisexual and 50% asexual) a low of −0.25 will be revealed. The *chi*-square tests (df = 3 as for a total of four sexualities) were applied to infer the significance of the observed values against to their expected ones (i.e. significant positive and negative values indicate significant dioecy and bisexual tendancy, respectively). The ratios of different sexualities [i.e. asexual, male, female, bisexual, bearing antheridium (male + bisexual), and bearing archegonium (female + bisexual)] and values of dioecy index were presented by means counted from the four box culctures, and Tukey's Studentized Range HSD Test (SAS software V. 9.1) was applied to reveal the significant difference among ages and between cytotypes. To detect significances in size differentiations among ages and cytotypes, *t*-Tests LSD (SAS software V. 9.1) were used.

Inbreeding tolerance comparison

All of the cultures, including those of MM, TM, SM, and SI, were applied for the inbreeding tolerance comparison. These cultures were designed with a gradient outcrossing opportunity: MM & TM > SM > SI. To evaluate inbreeding tolerance of SI cultures, the offspring sporophyte formation rates from the bisexual gametophytes were calculated when numbers of these appeared juveniles were stable through observation time. These formation rates were compared with those measured from other multispore cultures using the same manner as in the SI cultures but only selecting 50 archegonium bearing gametophytes. Fisher's exact tests were used to identify if the increase of outcrossing opportunity or ploidy was accompanied with significant increase of offspring sporophyte formation rates.

Results

Reproduction mode confirmation

All diploid and hexaploid individuals applied in this study were 64 S/S. In both diploid and hexaploid, the genome size values of gametophytes from MM cultures were half as the ones of parental (data not shown) and offspring sporophytes (Fig. 5.1). These implied that

gametophytes in both diploids and hexaploids reproduce sexually and are monoploidy and triploidy, respectively.

Gender expression and dioecy index

The gametophytes of diploid and hexaploid initiated their gender expression from 4 WAS, and generated juvenile sporophytes at 14 and 16 WAS, respectively. During 16 WAS, five 2.27 cm^2 circle patches were randomly selected from four MM culture boxes for each cytotype, which revealed that gametophyte population densities of diploid and hexaploid ranged 7.05 – 9.70 and 4.00 – 10.58 individuals cm^{-2}, respectively. However, this density difference between cytotypes is not significant (data not shown). The proportions of different gametophyte sexualities and their ages (presented in WAS) were summarized in Table 5.2 and Figs. 5.2 and 5.3A. In gametophytes of diploid, the first appearing sexualities were female and male, and the bisexuals were found 2 weeks after (i.e. 6 WAS). In hexaploid, males were first revealed in 4 WAS, and females and bisexuals appeared in 6 WAS. The overall trends of decrease of asexual proportion and increase of male proportion were same in diploid and hexaploid, and these trends became siginicant during 6-8 WAS (Fig. 5.2). The proportions of female were different between theses two cytotypes since 6 WAS, and these differences became significant since 8 WAS (Fig. 5.2). For bisexual proportion, hexaploid were averagely higher than the diploid but not significant. Regarding to their antheridium and archegonium bearing gametophyte proportions, these two cytotypes showed no significant difference although hexaploid tended to produce antheridium and tended not to produce archegonium (Fig. 5.3A).

Regarding to dioecy index, hexaploid and diploid expressed very different through ages (Table 5.2 and Fig. 5.3B). Gametophyte population of diploid displayed significantly positive dioecy index since 8 WAS whereas hexaploid displayed a significant negative value during 6 WAS and insignificant positive values after 6 WAS (Table 5.2). Between two cytotypes, these dioecy index values were significant differently since 6 WAS (Fig. 5.3B). Across density gradient (same as randomly selected five 2.27 cm^2 circle patches mentioned above), the lower values in the hexaploid were observed, and these values were non-overlapped with those in diploid (data not shown).

Gametophyte sizes and ages

The sizes of gametophytes with different sexualities from 3 WAS through their development ages were summarized in Table 5.3 and Fig. 5.4. In diploid gametophytes, the sizes were significantly different among sexualities since 8 WAS, and showed a trend of female > bisexual > male (Fig. 5.4B). The females significantly increased in size and were significant larger than bisexuals since 8 WAS. The males grew slowly, and did not become significant larger than initiate asexuals (i.e. those in 3 WAS) until 14 WAS (Figs. 5.4B and C). Above trends can be also found in hexaploid gametophytes but their size differences between females and bisexuals are not significantly different, and their males have larger size variations, which can even overlap with the ranges of females or bisexuals after 8 WAS (Fig. 5.4A).

In the comparisons between the gametophytes of two cytotypes, the males in hexaploid were averagely and significantly larger than those in the diploid after 6 WAS (Fig. 5.4C). The developmental trace from asexual, archgonium formation, to sporophyte generating revealed the growth rate (i.e. the slope in Fig. 5.4C) differences between two cytotypes. In diploid, archgonium bearing gametophytes were appeared to exhibit a dual growth, in which had an obvious acceleration of growth rate starting from 6 WAS (Fig. 5.4D). In comparison, the hexaploid showed a constant growth rate throughout their archgonium formation stage, which was slower than the elevated growth rate in diploid and resulted significantly smaller sizes than diploid during 14 and 16 WAS.

Inbreeding tolerances comparison

The numbers and proportions of gametophyte with/without sporophyte offspring and their sexuality are summarized in Table 5.4 and Fig. 5.5. In the SI cultures, all formation rates of offspring sporophyte became stable around 10 months after spores were sowed. Both diploid and hexaploid gametophytes in these SI cultures were found all with archegonium. For multispore cultures, all their formation rates were stable around 8 months after spores were sowed. The inbreeding tolerances were found lower in diploids, and their sporophyte formation rates via intragametophyte selfing (i.e. the offspring formation rates in SI cultures) were significantly lower than the hexaploid, except for one comparison showed *p*-value 0.095 (Fig. 5.5 and Table 5.5). In addition, the sporophyte formation rates in diploid were found higher accompanied

with the increased outcrossing opportunity (i.e. MM & TM > SM > SI), and some of these increase were significant. There was neither such trend nor such significance in the hexaploid. Instead, in hexaploid, significantly higher sporophyte formation rates in SI cultures were found comparing to those in some multispore cultures (Fig. 5.5 and Table 5.5).

Discussion

Higher inbreeding tolerance in hexaploid

In the case of *Deparia lancea*, both diploids and hexaploids were confirmed with sexual reproduction (Fig. 5.1) and able to inbreed via inter- and intragametophyte selfing (Fig. 5.5 and Table 5.4). Comparing to hexaploids, diploids have lower inbreeding tolerances revealed by the significant lower formation rate of sporophyte offspring via intragametophyte selfing (Table 5.5). In other words, diploids can only lessen inbreeding depression through their outcrossing. This is suggested by the significant higher sporophyte offspring formation rates in multiple-individual cultures and the increased formation rates after taking female gametophyte into account in those multispore cultures (Table 5.5 and Fig. 5.5); while these situations are not in hexaploids. High inbreeding tolerance in other fern polyploids comparing to their conspecific diploids has been documented previously (Masuyama & Watano 1990). In the natural habitat, the tendency of inbreeding of fern polyploid species has also been indicated by the population genetic studies (i.e. higher F_{IS}; reviewed in Ranker & Geiger 2008). These, together, strongly suggest the general rule for the increase of genomic heterosis after polyploidization results the breakdown for inbreeding depression in ferns as in other vascular plants (reviewed in Haulfer 2014).

Interestingly, the significant higher sporophyte offspring formation rates in SI cultures were found in hexaploids comparing to some of their multispore cultures (Table 5.5). One plausible explanation is that, regardless of outcrossing opportunity, there is a negative density dependent effect on sporophyte generating, in which polyploidy nuclear/cell/tissue is assumed to require more nutrients as hypothesized in some studies (e.g. Neiman *et al.* 2013 and Šmarda *et al.* 2013). Based on such assumption, the polyploid juvenile is expected to be, in a certain degree, more possibly generated in low density population such as those in the SI cultures (0.07 individual cm^{-2}) than in higher destiny population, such as those multispore cultures found with 4.00 – 10.58 individual cm^{-2}.

In order to clarify the density effect on sporophyte offspring formation, the further experiments need to examine the degree of resource competition by gametophyte cultures with a density gradient.

Gender expression relating to antheridiogen effects

The antheridiogen is a kind of pheromones promoting outcrossing in gametophyte population of letposprangiate ferns (Polypodiales), the most dominate lineage in the extant ferns, and its chemical structures are revealed relating to gibberellins compound. The typical functions of antheridiogen include: (1) induction of spore germination in dark condition, (2) induction of gametophytes to produce antheridium, (3) retarding growth of initial ameristic gametophytes (i.e. those without notch meristem) to develop into meristic gametophyte, and directly or indirectly slowdown the production of archegonium (reviewed in Näf 1979, Raghavan 1989, Yamane 1998, and Scheneller 2008; Tanaka *et al.* 2014). In addition, higher sensitivity to and lower secretion of antheridiogen is usually found in ameristic gametophytes but the invert situation is in meristic gametophytes, which are able to produce archegonium (Näf 1979; Yamane 1998; Wen *et al.* 1999; Tanaka *et al.* 2014). In other words, well-developed (i.e. meristic in the later developmental stages) and usually bearing archegounium gametophytes secret antheridiogen to induce only the initial individuals to produce antheridia but not the others in later developmental stages. Therefore, the outcrossing can be promoted by maintaining dioecy in a gametophyte population at a temporal scale because of the maleness in initial individuals and the femaleness in the well-developed ones under this sensitivity-secretion antheridiogen mechanism.

Although no previous study demonstrated the presence of antheridiogen in *Deparia*, the antheridiogen system is revealed in its sister genus, *Athyrium* (Schneller 1979; Greer & Curry 2004), and the following phenomena also suggest the antheridiogen reacts in *Deparia lancea* gametophytes: (1) significant lower number of individuals with antheridium in SI cultures comparing to multispore cultures (i.e. without vs. with antheridiogen effect from other individuals) (Table 5.6), (2) male gametophytes are significantly smaller in size than those bearing archegonium (Fig. 5.4), and (3) the dioecy tendency through developmental stages (Table 5.2 and Fig. 5.3B). The first two phenomena were revealed in both diploid and hexaploid (Fig. 5.4 and Table 5.6), and

the last one was not found in hexaploid (Table 5.3 and Fig. 5.3B). The antheridiogen effects are already determined in several polyploid fern species but they are all presumed to be allopolyploids (Pangua *et al.* 2003; Jiménez *et al.* 2008; Testo *et al.* 2015; and others reviewed in Schneller 2008). Currently, there is no research to detail how antheridiogen system reacts in autopolyploid sexual fern gametophytes, which are presumed to have an inbreeding trend in gender expression (see below).

The inbreeding tending gender expression in hexaploid

In the overall sexuality trends, only the proportion of female gametophyte has significant differences between diploid and hexaploid (Figs. 5.2 and 5.3A). In both cytotypes, formation of antheridium and archegonium are mostly concentrated during 4-8 WAS. However, these two cytotypes behave very different in their gender expression among individuals within gametophyte population. In that, diploid gametophytes tend to express two kinds of unisexuality (i.e. male and female) rather than bisexual, and maintain dioecy tendency at the population level (Table 5.2). This is supported by the significant increase of dioecy index from 6 to 8 WAS (Fig. 5.3B), and the significant dioecy tendency (i.e. significant positive value of dioecy index) detected after 6 WAS (Table 5.2). In addition, since 8 WAS, the smaller and significantly smaller size of bisexual gametophytes comparing to females indicates that the predominant bisexuals were transferred from males, which were under a retarded growth with much smaller size. This exclusive antheridium/archegonium formation via an ontogenetic way can facilitat outcrossing in diploid, and is seemly resulted from a typical sensitivity-secretion antheridiogen mechanism as mentioned above.

On the other hand, the gametophyte populations of hexaploid behave a significant bisexual tendency (i.e. significant negative value of dioecy index) during 6 WAS and insignificant dioecy tendency (i.e. insignificant positive value of dioecy index) from 8 to 16 WAS. These suggest the gametophyte gender expression in hexaploid tend to be inbreeding. These insignificant significant dioecy tendencies, in other words, indicate the independence between antheridium and archegonium formation, or indirectly imply that archegonium production and the sensitivity of antheridiogen can both occur on majority of individuals in a gametophyte population. Therefore, it can be expected that the larger individual, even already generating archegonium, can also respond to antheridiogen and

produce antheridium. Indeed, when antheridium and archegonium first coexisted in the gametophyte population, size overlap between males and archegonium bearing individuals was relatively higher in hexaploid comparing with diploid, which were not overlapped during 4 WAS and slightly overlapped during 6 WAS, (Fig. 5.6 and Table 5.3). In addition, during their first appearance of male (i.e. both are 4 WAS; Table 5.3), the maximum size of diploid and hexaploid gametophyte individual were similar (2.88 vs. 2.45 mm^2), suggesting their developmental stages starting to secretion of antheridiogen are similar. These findings further point out the possibility that antheridia produced in those larger gametophytes were resulted from a prolonged or delayed antheridiogen sensitivity instead of a delay of antheridiogen secretion. Based on these, a gametophyte of hexaploid, even becoming meristic and female, is able to produce antheridium in the later developmental stages via the antheridiogen secreting by other gametophytes or itself, and, to access to bisexual, there is a rapid developmental process by transition from the female. In the hexaploid, this idea can be implied by other evidences: (1) maintaining high proportions of bisexual sexuality in isolated gametophytes (Table 5.4), (2) there is still 10% increase of antheridium bearing gametophytes during 10-16 WAS (Fig. 5.3A), and (3) a constant growth rate of archegonium-bearing gametophyte formation (see below). In summary, gametophytes in hexaploid *Deparia lancea* gain an increased ability to simultaneously produce both gametangia in comparison with diploid, and, thus, promote inbreeding. Such association between gender expression and ploidy is also supported by previous studies (Masuyama & Watano 1990; Verma 2003). The hypothesized extension of antheridiogen sensitivity in late developmental stage of polyploids requires further evidences from experiments with antheridiogen treatments.

Gametophyte development in auto- and allo-polyploids

As mentioned above, the hexaploid of *Deparia lancea* as well as many other fern polyploids has an inbreeding tending gender expression, which is generally different from the outcrossing tending ones in diploids (Masuyama & Watano 1990; Verma 2003). However, most previous cases less concerned about evolutionary history of these polyploids, which might be formed with or without a prior interspecies hybridization before polyploidization, and, respectively, referred to either allopolyploids or

autopolyploids. In addition, limited empirical studies had ever compared gender expression between polyploid taxa with their diploid closely relatives. The examples of two allotetraploid species, *Dryopteris corleyi* Fraser-Jenk. and *Polystichum aculeatum* (L.) Roth (Dryopteridaceae, Polypodiales), show that their gender expression and gametophyte growth behave somewhat intermediacy of their parental diploid species (Pangua *et al.* 2003; Jiménez *et al.* 2008). These indicated the developmental switch in allopolyploid fern gametophytes can be attributed to the hybridization effects rather than to a solely consequence of polyploidy evolution.

Similar to *Deparia lancea* hexaploid presented in this study, another case of sexual tetraploids in *Phegopteris decursive-pinnata* (Thelypteridaceae, Polypodiales), with a presumed autopolyploidization origin, was demonstrated by Masuyama (1979). The gametophytes of tetraploid *P. decursive-pinnata*, comparing to that of conspecific diploid, are able to simultaneously produce both gametengia via a rapidly growing process transiting from female to bisexual. Based on Masuyama's data, *P. decursive-pinnata* was found with significant dioecy tendency in the diploids and with insignificant dioecy tendency and significant bisexual tendency in the tetraploids (Table S5.1). This comes to the same conclusion from current study that diploids maintained a higher and significant dioecy tendencies in their gametophyte population via individuals' gender expressions, which is assumed resulted from sensitivity-secretion antheridiogen mechanism. In addition, these phenomena found in these two autopolyploid cases seem to be inconspicuous or absent in current allopolyploids cases (i.e. those allopolyploid ferns worked by Pangua *et al.* 2003, Jiménez *et al.* 2008, and Testo *et al.* 2015).

Evolution of inbreeding reproduction in hexaploid

In this study, ther inbreeding ability in *Deparia lancea* hexaploids was demonstrated not only resulting from their high inbreeding tolerances but also from an inbreeding tending gender expression in their gametophyte population (see above). Regarding to this, this inbreeding tending gender expression is hypothesized as the resulted of a prolonged/delayed antheridiogen sensitivity, which extends to the late developmental stages. If this hypothesis is true, it can be expected that the prolonged/delayed antheridiogen sensitivity is selected as a pre-adaptive

trait during the evolutionary establishment of a polyploidy taxon to enhance its prezygotic isolation with diploid progenitors. Indeed, infraspecific variation of antheridiogen sensitivity had been reported (Näf 1979). Such variable trait possibly exist the parental diploids of *D. lancea* hexaploids as revealed by varied antheridium formation rates in diploid SI cultures (Table 5.4). Consequently, after the trait of prolonged/delayed antheridiogen sensitivity is fixed, a sexual but recently formed fern polyploid taxon can mate assortatively by the maintenance of co-expression of antheridium and archegonium.

Heterochrony of hexaploid gametophyte

Based on developmental trace from asexual to sporophyte offspring generating, two phases can be defined (1) from asexual to archegonium formation and (2) from archegonium formation to sporophyte generating (Fig. 5.4D). In the phase one, the archegonium formation has a two-week delayed in hexaploids comparing to diploids (Fig. 5.4D). Indicated by insigficant chages in sizes of both cytotypes during 3-4 WAS (Fig. 5.4D), the insignificantly different between growth rate was found. This, gathering the phenomenon of late archegonium occurrence, implies a hypomorphsis, a kind of peramorphosis, extending development of decedent hexaploid. However, developmental process seems to involve more factors through the phase two. A dual growth rate found in diploid gametophytes had a switch point at 6 WAS, after when the growth rate is elevated, whereas the gametophyte growth rate in hexaploid was constant during this phase (Fig. 5.4D). The gametophyte growth rate change from 6 to 8 WAS in diploid could be associated with their antheridiogen sensitivity. I proposed that gametophyte growth rate elevation in diploid is attributed to the reduction of antheridiogen sensitivity, for which one of its function is to retard growth. As mentioned above, gametophytes of diploid maintain the dioecy tendency at population level and are assumed to be insensitive to antheridiogen during the late developmental stages. On the other hand, the relatively constant growth rate without any elevation in gametophyte of hexaploid can also support the hypothesis of prolonged/delayed antheridiogen sensitivity as mentioned previously. In addition to the constant growth rate due to the presumed effects of late antheridiogen sensitivity, gametophytes of hexaploid exhabited a two-week delay in their sporophyte generating, and finally stopped to growth at the size as the immature developmental stage (i.e. without

sporophyte) in diploids (Fig. 5.4D). Taking these phenomena together, a paedomorphsis in gametophyte development of hexaploid is implied for its sporophyte generating, and this paedomorphsis is combined with a neoteny of gametophyte growth rate deceleration and a hypomorphsis of delayed sporophyte generating.

However, it is necessary to note that current conclusions for heterochronic development in hexaploid gametophyte are based on the results from multispore cultures with a stage criteria defined by individual area size. The gametophyte developments can be different when effects of antheridiogen pheromone are weak as in the condition in those single-individual or lower density cultures (e.g. DeSoto *et al.* 2008). In addition, there are some accompanied biophysical effects on polyploidized cells influencing the total growth rate: enlarged cell size and decelerate cell division rate (Comai 2005; Ramsey & Ramsey 2014); at least, the enlarged cell size in polyploidy fern gametophyte has been documented (Ebihara *et al.* 2009). In order to disentangle the pheromone effects and such cellular physical effects regulating on polyploidy gametophyte development, new approaches to efficiently and accurately estimate cell number/size are needed to be explored, and cultures of isolated single gametophyte can be applied to understand the developmental process in lack of atheridiogen.

References

Comai L (2005) The advantages and disadvantages of being polyploid. *Nature Reviews Genetics*, **6**, 836–846.

DeSoto L, Quintanilla LG, Méndez M (2008) Environmental sex determination in ferns: effects of nutrient availability and individual density in *Woodwardia radicans*. *Journal of Ecology*, **96**, 1319–1327.

Ebihara A, Matsumoto S, Ito M (2009) Hybridization involving independent gametophytes in the *Vandenboschia radicans* complex (Hymenophyllaceae): a new perspective on the distribution of fern hybrids. *Molecular Ecology*, **18**, 4904–4911.

Farrar D, Dassler C, Watkins Jr JE, Skelton C (2008) Gametophyte ecology. In: *Biology and Evolution of ferns and Lycophytes* (eds.

Ranker TA, Haufler CH), pp. 222–256. Cambridge University Press, New York.

Greer G, Curry D (2004) Pheromonal interactions among cordate gametophytes of the lady fern, *Athyrium filix-femina*. *American Fern Journal*, **94**, 1–8.

Haufler CH (2014) Ever since Klekowski: testing a set of radical hypotheses revives the genetics of ferns and lycophytes. *American Journal of Botany*, **101**, 2036–2042.

Jiménez A, Quintanilla LG, Pajarón S, Pangua E (2008) Reproductive and competitive interactions among gametophytes of the allotetraploid fern *Dryopteris corleyi* and its two diploid parents. *Annals of Botany*, **102**, 353–359.

Kato M, Nakato N, Cheng X, Iwatsuki K (1992) Cytotaxonomic study of ferns of Yunnan, southwestern China. *The Botanical Magazine*, **105**, 105–124.

Masuyama S (1979) Reproductive biology of the fern *Phegopteris decursive-pinnata* I. The dissimilar mating systems of diploids and tetraploids. *The Botanical Magazine, Tokyo*, **92**, 275–289.

Masuyama S, Watano Y (1990) Trends for inbreeding in polyploid pteridophytes. *Plant Species Biology*, **5**, 13–17.

Näf U (1979) Atheridiogens and antheridial development. In: *The Experimental Biology of Ferns* (eds. Dyer AF), pp. 436–456. Academic Press, New York.

Neiman M, Kay A, Krist A (2013) Can resource costs of polyploidy provide an advantage to sex? *Heredity*, **110**, 152–159.

Pangua E, Quintanilla LG., Sancho A, Pajarón S (2003) A comparative study of the gametophytic generation in the *Polystichum aculeatum* group. *International Journal of Plant Sciences*, **164**, 295–303.

Raghavan V (1989) *Developmental biology of fern gametophytes*. Cambridge University Press, New York.

Ramsey J, Ramsey TS (2014) Ecological studies of polyploidy in the 100 years following its discovery. *Proceedings of the Royal Society of London: Biological Sciences*, **369**, 20130352. http://dx.doi.org/10.1098/rstb.2013.0352.

Schneller JJ (2008) Atheridiogens. In: *Biology and Evolution of ferns and Lycophytes* (eds. Ranker TA, Haufler CH), pp. 134–151. Cambridge University Press, New York.

Schneller J (1979) Biosystematic investigations on the lady fern (*Athyrium filix-femina*). *Plant Systematics and Evolution*, **277**, 255–277.

Šmarda P, Hejcman M, Březinová A *et al.* (2013) Effect of phosphorus availability on the selection of species with different ploidy levels and genome sizes in a long-term grassland fertilization experiment. *New Phytologist*, **200**, 911–921.

Tanaka J, Yano K, Aya K *et al.* (2014) Antheridiogen determines sex in ferns via a spatiotemporally split gibberellin synthesis pathway. *Science*, **346**, 469–473.

Verma SC (2003) Some aspects of reproductive biology of the gametophyte generation of homosporous ferns. In: *Pteridophyte in the New Millennium* (eds. Chandra S, Srivastava M), pp. 455–484. Kluwer Academic Publishers, the Netherlands.

Testo W, Watkins Jr J, Barrington D (2015) Dynamics of asymmetrical hybridization in North American wood ferns: reconciling patterns of inheritance with gametophyte reproductive biology. *New Phytologist*, *New Phytologist*, **206**, 785–795.

Wen CK, Smith R, Banks J (1999) *ANI1*: a sex pheromone–induced gene in *Ceratopteris* gametophytes and its possible role in sex determination. *The Plant Cell*, **11**, 1307–1317.

Yamane H (1998) Fern antheridiogens. *International Review of Cyrology*, **184**, 1–32.

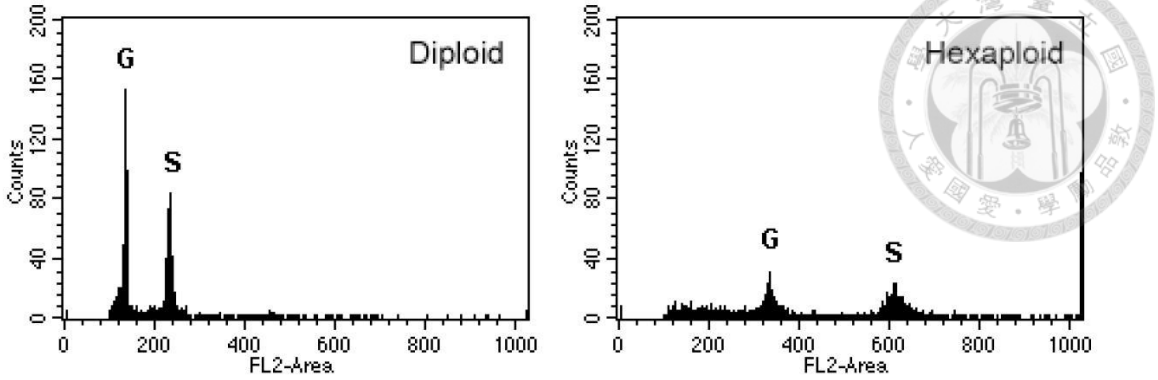

Fig. 5.1. The flow cytometry results of gametophytes (G) and their offspring sporophytes (S) of diploid and hexaploid.

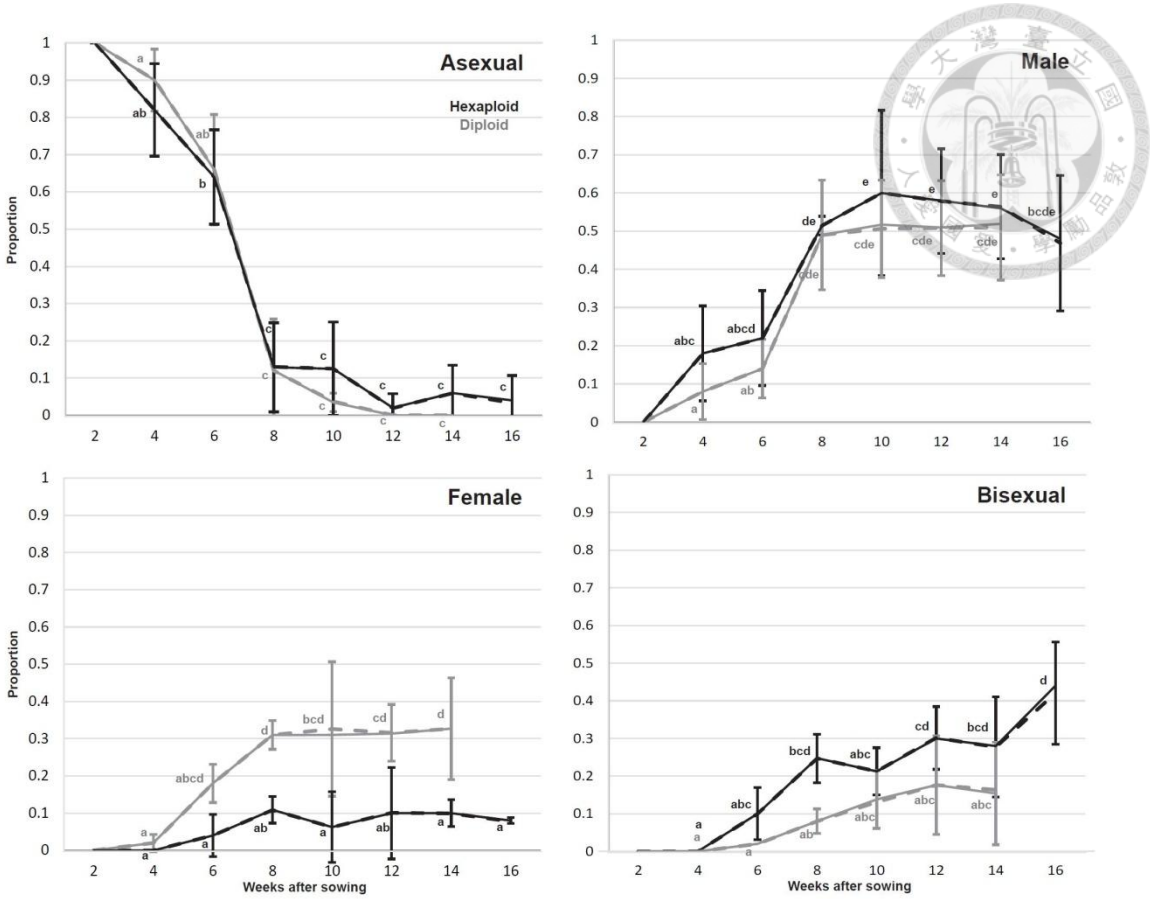

Fig. 5.2. The proportions of different sexualities of gametophytes of diploid and hexaploid through ages. The black and grey lines indicate diploid and hexaploid, respectively. The dash lines indicate that the mean proportion of each sexuality of different boxes. The solid lines indicate that overall proportion inferred by pooling all individuals from different boxes. The bars on the dash lines indicate one standard deviation of the proportions of different boxes. The different alphabets on the dash lines indicate the statistic grouping inferred by Tukey's Studentized Range HSD Test with $p < 0.0001$.

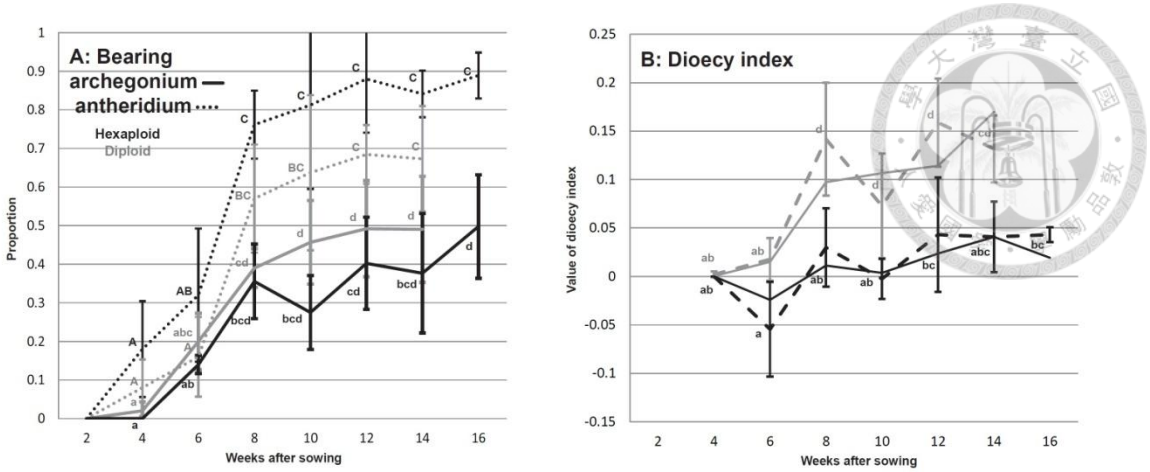

Fig. 5.3. The proportions of archegonium and antheridium bearing gametophytes (A) and dioecy index (B) of gametophytes of diploid and hexaploid through ages. The black and grey lines indicate diploid and hexaploid, respectively. In (A), the dash lines indicate that the mean proportion of each sexuality of different boxes. The solid lines indicate that overall proportion inferred by pooling all individuals from different boxes. In (B), the dash lines indicate that the mean value of each sexuality of different boxes. The solid lines indicate that the value calculated by pooling all individuals from different boxes. The bars on the dash lines indicate one standard deviation of the proportions/values of different boxes. The different alphabets on the dash lines indicate the statistic grouping inferred by Tukey's Studentized Range HSD Test with $p < 0.0001$.

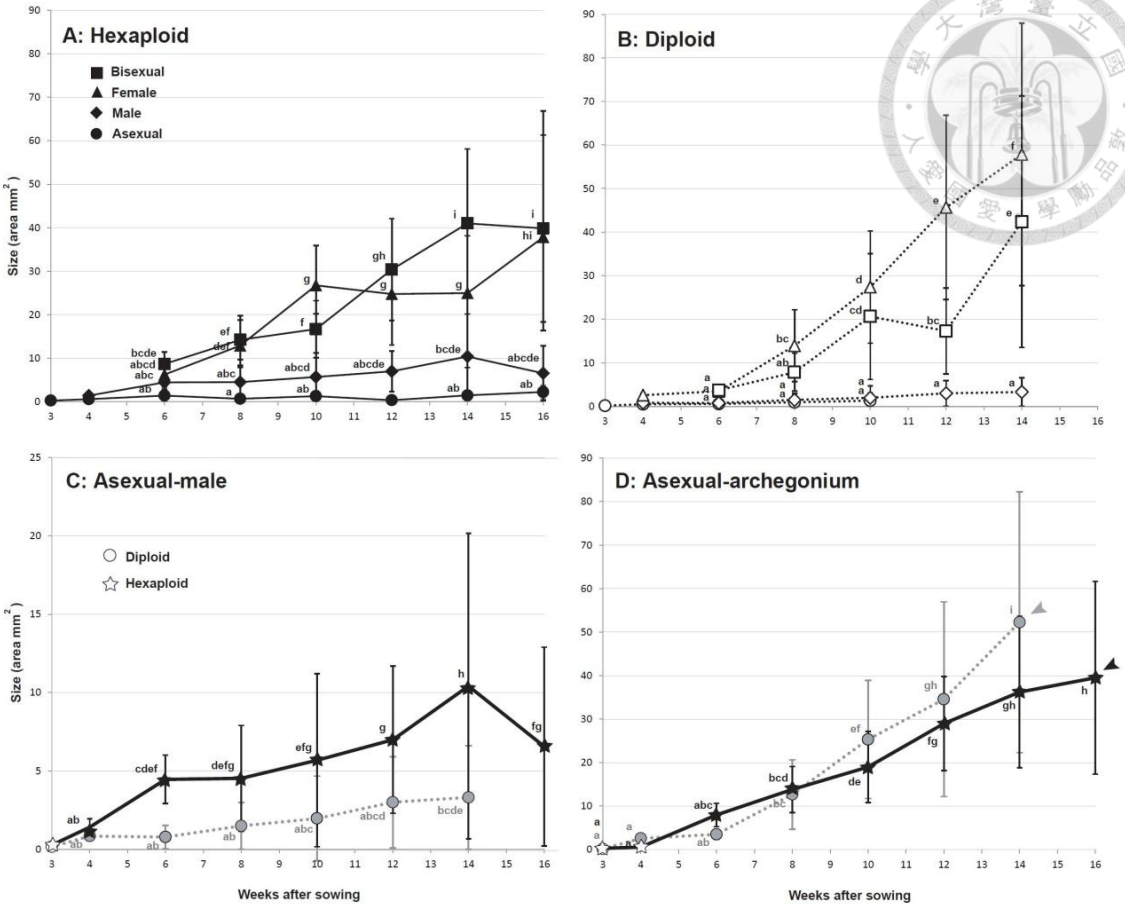

Fig. 5.4. The gametophyte profile area size of diploid and hexaploid through ages. In (A: hexaploid) and (B: diploid), the gametophytes sizes of different sexualities through ages ages are shown. In (C), the open and filled symbols indicate asexual and male gametophyte, respectively. In (D), the open and filled symbols indicate asexual and archegonium bearing gametophyte, respectively. The arrowheads indicate the ages when offerspring sporophyte start to form. The bars on the symbols indicate the one standard deviation of size variation for a particular sexuality. The different alphabets on the symbols indicate the statistic grouping inferred by *t*-Tests LSD with $p < 0.0001$.

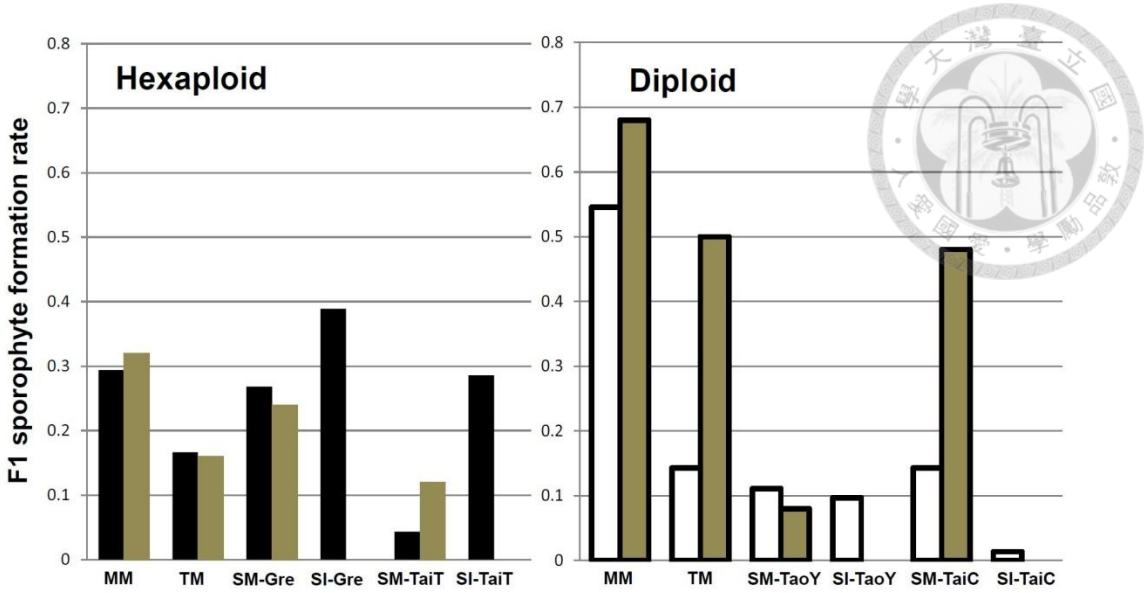

Fig. 5.5. The offering sporophyte formation rates from the different designed cultures in diploids and hexaploids. The black/white and gray bars represent the formation rates from bisexual gametophytes and from archegonium bearing gametophytes (i.e. female + bisexual), respectively.

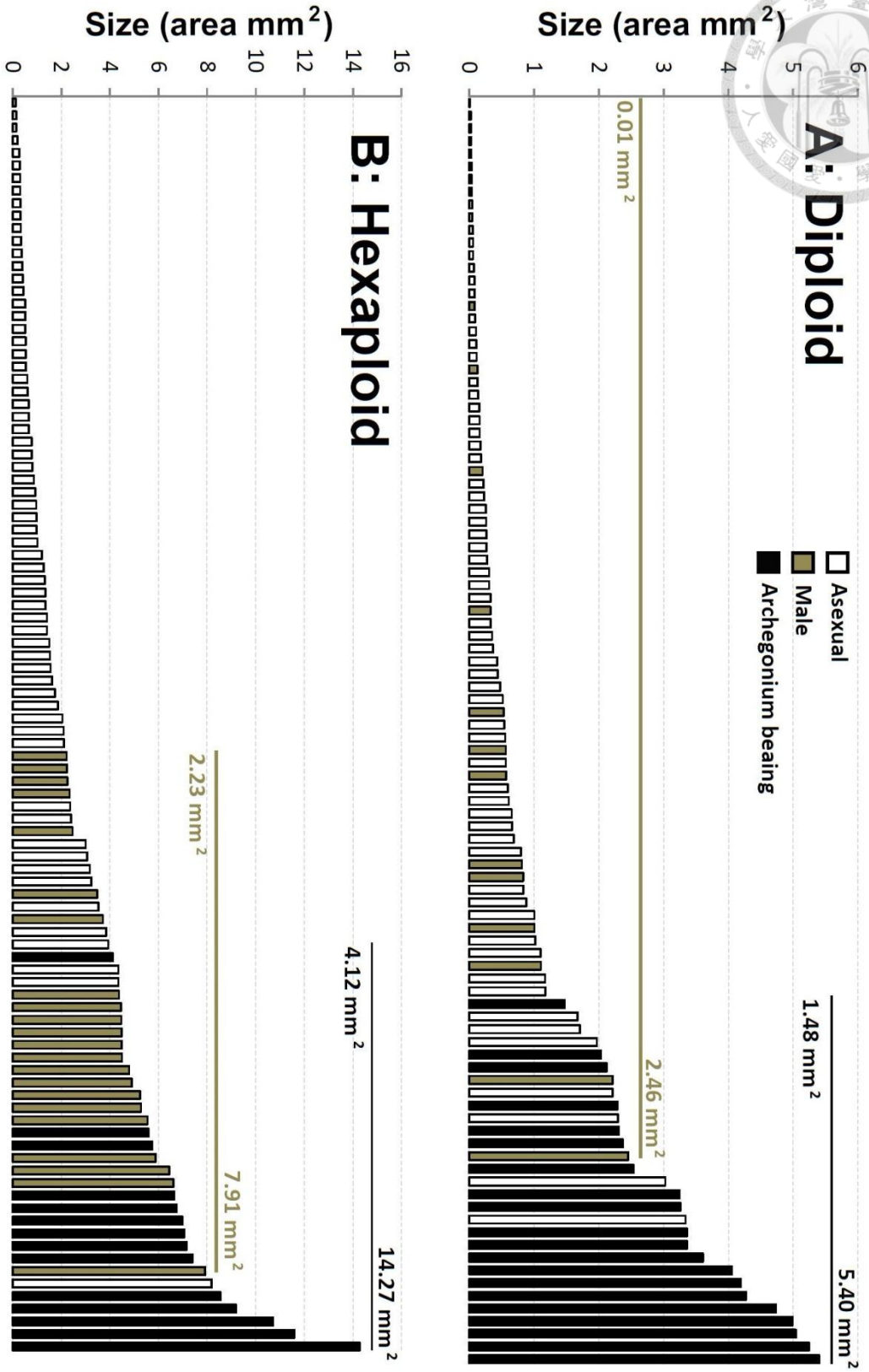

Fig. 5.6. The area size ranks in gametophyte individuals of (A) diploid and (B) hexaploid with different sexualities during 6 weeks after sowing.

Table 5.1. The cultures and samples applied in this study.

Ploidies	Culture	ndividual for spore source (total number of individual
2X	Multiple-individual multiple spore (MM)	Tw-TaoY-03-l04, 08, 12, 14, 19 (5)[a]
2X	Two-individual multi-spore (TM)	Tw-TaoY-03-l09[a], Tw-TaiC-01-l19[b] (2)
2X	Single-individual multi-spore (SM)-TaoY	Tw-TaoY-03-l09[a] (1)
2X	Single-individual multi-spore (SM)-TaiC	Tw-TaiC-01-l19[b] (1)
2X	ingle-individual isolated gametophyte (SI)-Tao	Tw-TaoY-03-l09[a] (1)
2X	Single-individual isolated gametophyte (SI)-Tai	Tw-TaiC-01-l19[b] (1)
6X	Multiple-individual multiple spore (MM)	IS-Gre-01-l01, 02, 05, 08, 10, 12, 13 (7)[c]
6X	Two-individual multi-spore (TM)	IS-Gre-01-l09[c], Tw-TaiT-13-l05[d] (2)
6X	Single-individual multi-spore (SM)-Gre	IS-Gre-01-l09[c] (1)
6X	Single-individual multi-spore (SM)-TaiT	Tw-TaiT-13-l05[d] (1)
6X	Single-individual isolated gametophyte (SI)-Gre	IS-Gre-01-l09[c] (1)
6X	Single-individual isolated gametophyte (SI)-Tai	Tw-TaiT-13-l05[d] (1)

[a]Mt. Peichatien, Taoyuan County, Taiwan (GPS: 121.4206, 24.7978)

[b]Tungshihlinchang, Taichung City, Taiwan (GPS: 120.8698, 24.2809)

[c]Kuanyintung to Haishenping, Green Island, Taitung County, Taiwan (GPS: 121.4943, 22.6602)

[d]Luye Gaotai, Taitung County, Taiwan (GPS: 121.1017, 22.9463)

Table 5.2. The proportion of different sexualities and dioecy index values of gametophyte of diploid and hexaploid through ages.

Sexuality[a]\Weeks after sowing	4	6	8	10	12	14	16
2X							
Asexual	0.90 (0.90±0.08)	0.66 (0.66±0.15)	0.12 (0.12±0.14)	0.03 (0.04±0.02)	0.00 (0.00±0.00)	0.00 (0.00±0.00)	-
Male	0.08 (0.08±0.07)	0.14 (0.14±0.08)	0.49 (0.49±0.14)	0.52 (0.51±0.13)	0.51 (0.51±0.12)	0.52 (0.51±0.14)	-
Female	0.02 (0.02±0.02)	0.18 (0.18±0.05)	0.31 (0.31±0.04)	0.31 (0.33±0.18)	0.31 (0.32±0.08)	0.33 (0.33±0.14)	-
Bisexual	0.00 (0.00±0.00)	0.02 (0.02±0.04)	0.08 (0.08±0.03)	0.14 (0.13±0.08)	0.18 (0.18±0.13)	0.15 (0.16±0.14)	-
Bearing antheridium	0.08 (0.08±0.07)	0.16 (0.16±0.10)	0.57 (0.57±0.14)	0.66 (0.64±0.20)	0.69 (0.68±0.08)	0.67 (0.67±0.14)	-
Bearing archegonium	0.02 (0.02±0.02)	0.20 (0.20±0.07)	0.39 (0.39±0.05)	0.45 (0.46±0.11)	0.49 (0.49±0.12)	0.48 (0.49±0.14)	-
Dioecy index	0.0004 (0.0020±0.0030)	0.0150 (0.0176±0.0221)	0.0974** (0.1416±0.0583)	0.1066** (0.0728±0.0540)	0.1142** (0.1588±0.0454)	0.1697** (0.1316±0.0346)	-
6X							
Asexual	0.82 (0.82±0.12)	0.64 (0.64±0.13)	0.13 (0.13±0.12)	0.13 (0.13±0.13)	0.02 (0.02±0.04)	0.06 (0.06±0.07)	0.04 (0.03±0.07)
Male	0.18 (0.18±0.12)	0.22 (0.22±0.12)	0.51 (0.51±0.02)	0.60 (0.60±0.22)	0.58 (0.58±0.14)	0.56 (0.56±0.14)	0.48 (0.47±0.18)
Female	0.00 (0.00±0.00)	0.04 (0.04±0.06)	0.11 (0.11±0.04)	0.06 (0.06±0.09)	0.10 (0.10±0.12)	0.10 (0.10±0.04)	0.08 (0.08±0.01)
Bisexual	0.00 (0.00±0.00)	0.10 (0.10±0.07)	0.25 (0.25±0.06)	0.21 (0.21±0.06)	0.30 (0.30±0.08)	0.28 (0.28±0.13)	0.44 (0.42±0.14
Bearing antheridium	0.18 (0.18±0.12)	0.32 (0.32±0.17)	0.76 (0.76±0.09)	0.81 (0.81±0.22)	0.88 (0.88±0.14)	0.84 (0.84±0.06)	0.92 (0.89±0.06)
Bearing archegonium	0.00 (0.00±0.00)	0.14 (0.14±0.02)	0.36 (0.36±0.10)	0.28 (0.28±0.10)	0.40 (0.40±0.12)	0.38 (0.38±0.15)	0.52 (0.50±0.13)
Dioecy index	0.0000 (0.0000±0.0000)	-0.0242* (-0.0544±0.0487)	0.0113 (0.0299±0.04056)	0.0037 (-0.0025±0.0206)	0.0236 (0.0431±0.0590)	0.0408 (0.0408±0.0363)	0.0192 (0.0431±0.0077)

[a]indicated by "propotion/values inferred by pooling four boxes individuals (the mean propotion of four boxes ± one standard deviation)"; *chi* -square test (df=3) * 0.01>*p* >0.001 **0.001>*p*

Table 5.3. The aree size[a] of different sexualities of diploid and hexaploid gametophyte through ages.

Sexuality\Weeks afte	3	4	6	8	10	12	14	16
2X								
Asexual	0.15±0.08	0.50±0.51	0.56±0.71	0.95±1.09	1.31±1.89	-	-	-
Male	-	0.84±0.28	0.78±0.74	1.48±1.50	1.96±2.70	2.99±2.92	3.30±3.31	-
Female	-	2.58±0.43	3.47±1.26	13.92±8.26	27.39±12.87	45.67±21.18	57.85±30.09	-
Bisexual	-	-	3.73±0.66	7.83±4.38	20.64±14.45	17.30±9.87	42.36±28.82	-
Bearing archegonium	-	2.58±0.43	3.50±1.20	12.67±7.98	25.31±13.55	34.57±22.38	52.27±30.00	-
All	0.15±0.08	0.57±0.58	1.18±1.43	5.78±7.50	12.41±14.90	17.82±22.08	27.31±32.39	-
6X								
Asexual	0.27±0.16	0.58±0.39	1.41±1.41	0.69±0.45	1.29±1.25	0.36	1.45±1.19	2.24±1.54
Male	-	1.41±0.53	4.46±1.54	4.52±3.38	5.68±5.53	6.99±4.70	10.41±9.75	6.55±6.35
Female	-	-	6.23±1.45	12.90±6.83	26.76±9.14	24.77±6.81	24.98±13.18	37.85±29.01
Bisexual	-	-	8.69±2.79	14.22±4.56	16.70±6.55	30.39±11.72	41.02±17.12	39.85±21.48
Bearing archegonium	-	-	7.99±2.68	13.82±5.29	18.98±8.20	28.99±10.83	36.21±17.41	39.52±22.17
All	0.27±0.16	0.73±0.53	3.00±2.89	7.38±6.35	8.79±8.84	15.66±13.41	20.39±18.71	22.20±23.08

[a]the gametophyte size indicated by mean area±one standard deviation (mm^2)

Table 5.4. Number of archegonium bearing gametophytes with/without sporophyte offspring in different cultures. (Abbreviations for these cultures can be seen in Table. 5.2.)

	Bisexual		Female	
Sporophyte offspring	with	without	with	without
2X-SI-TaiC	1	73	0	24
2X-SI-TaoY	3	28	0	106
2X-SM-TaiC	1	6	20	24
2X-SM-TaoY	1	8	3	38
2X-TM	1	6	19	24
2X-MM	6	5	28	11
6X-SI-TaiT	8	20	0	25
6X-SI-Gre	28	44	0	29
6X-SM-TaiT	1	22	22	5
6X-SM-Gre	10	24	10	6
6X-TM	6	30	12	12
6X-MM	10	24	10	6

Table 5.5. Fisher's exact test of sporophyte formation rate for culture pairs. (Abbreviations for these cultures can be seen in Table. 5.2.)

Comparison type	Gametophyte sexuality applied	Comparision cultures[a]	*p* -values
Among ploidy	Bisexual	6X-SI-Gre > 2X-SI-TaiC	**0.001>**
Among ploidy	Bisexual	6X-SI-Gre > 2X-SI-TaoY	**0.003**
Among ploidy	Bisexual	6X-SI-TaiT > 2X-SI-TaiC	**0.001>**
Among ploidy	Bisexual	6X-SI-TaiT > 2X-SI-TaoY	0.095
Among cultures (2X)	Bisexual	2X-SM-TaoY > 2X-SI-TaoY	1.000
Among cultures (2X)	Bisexual	2X-SM-TaiC > 2X-SI-TaiC	0.166
Among cultures (2X)	Bisexual	2X-TM > 2X-SI-TaoY	1.000
Among cultures (2X)	Bisexual	2X-TM > 2X-SI-TaiC	0.166
Among cultures (2X)	Bisexual	2X-TM > 2X-SM-TaiC	0.395
Among cultures (2X)	Bisexual	2X-TM > 2X-SM-TaoY	1.000
Among cultures (2X)	Bisexual	2X-MM > 2X-SI-TaoY	**0.005**
Among cultures (2X)	Bisexual	2X-MM > 2X-SM-TaoY	0.070
Among cultures (2X)	Bearing archegonium	2X-TM > 2X-SM-TaoY	**0.001>**
Among cultures (2X)	Bearing archegonium	2X-TM > 2X-SM-TaiC	1.000
Among cultures (2X)	Bearing archegonium	2X-MM > 2X-SM-TaoY	**0.001>**
Among cultures (6X)	Bisexual	6X-SM-Gre < 6X-SI-Gre	0.222
Among cultures (6X)	Bisexual	6X-SM-TaiT < 6X-SI-TaiT	**0.031**
Among cultures (6X)	Bisexual	6X-TM < 6X-SI-Gre	**0.027**
Among cultures (6X)	Bisexual	6X-TM < 6X-SI-TaiT	**0.001**
Among cultures (6X)	Bisexual	6X-TM < 6X-SM-Gre	0.410
Among cultures (6X)	Bisexual	6X-TM > 6X-SM-TaiT	0.229
Among cultures (6X)	Bisexual	6X-MM < 6X-SI-Gre	0.175
Among cultures (6X)	Bisexual	6X-MM > 6X-SM-Gre	1.000
Among cultures (6X)	Bearing archegonium	6XTM < 6X-SM-Gre	0.454
Among cultures (6X)	Bearing archegonium	6X-TM > 6X-SM-TaiT	0.774
Among cultures (6X)	Bearing archegonium	6X-MM > 6X-SM-Gre	0.505

[a]in among culture comparsions, each of underline culture is higher outcrossing opertunities one

Table 5.6. Number of gametophytes with/without antheridium and Fisher's exact test between MM and SI cultures. (Abbreviations for these cultures can be seen

	Antheridium		
Culture	With	Without	*p* -values
2X-SI-TaoY	31	106	0.001>
2X-MM (14 WAS)	35	17	
6X-SI-Gre	72	29	0.024
6X-MM (16 WAS)	46	6	

Table S5.1. The dioecy index of *Phegopteris decursive-pinnata* diploid and tetraploid gametophyte cultures based on he sexual proportion reported by Masuyama (1979). (* 0.05>*p* >0.01, ** 0.01>*p* >0.001, ***0.001>*p*)

Ploidy	2x	2x	2x	2x	2x	4x	4x	4x	4x	4x
Medium (individual No.)	Agar (2)	Agar (16)	Agar (35)	Agar (98)	Soil	Agar (53)	Agar (66)	Agar (71)	Agar (97)	Soil
swoing										
40	0.1462***	0.1104***	0.0589*	0.0812**	0.0348*	0.0194	-0.0250	-0.0165	0.0016	0.0152
50	0.0640***	0.0408**	0.1224***	0.1058***	-	0.0000	0.0000	0.0000	-0.0097***	-
60	0.0517*	0.0488**	0.0318	0.0396	0.0164*	0.0000	0.0000	0.0000	0.0000	0.0048
80	-	-	-	-	0.0184	-	-	-	-	0.0000
90	-	-	-	-	0.0040	-	-	-	-	0.0000

Chapter 6.

Do climatic niche shifts facilitate geographical range expansions in the *Deparia lancea* hexaploids?

Abstract

As previously revealed, the hexaploids in *Deparia lancea* were found with increased colonization ability and range expansion but ecological factors attributing on these are still unclear. This chapter is going to examine whether ecological niche evolution in these hexaploids is likely to contribute their range expansion and oversea dispersals to outside of Taiwan Main Is. By inferring niche inside and outside of Taiwan Main Is., these climatic niche breathes and preferences from the hexaploids with that in diploids were compared. Regarding to climatic niche, I found that, although overall significant niche dissimilarities were found between two cytotypes, these climatic niche shifts in the hexaploids in Taiwan Main Is. were unlikely primary cause for their subsequent range expansion. On the other hand, the conserved climatic niche breadths between hexaploids in Taiwan Main Is. and diploids were revealed by their reveal occurrences. The reconstructed past potential distribution of hexaploid revealed a complete overlap with the diploids, and this further implied that the niche evolution in the hexaploid might be processed from niche expasion rather than spontaneous niche differentiation. Based on these findings, this study concluded that the ecophysiological pre-adaptation might less contribute for oversea colonization and subsequent range expansion in the Instead of the ecological adaptation, the inbreeding reproduction of hexaploids should be the most possible primary force exploring their potential distribution as well as their geographical distribution.

Introduction

Although some cases certainly identify that polyploidization in plant "pre-adaptively" contribute to the ecological niche shift (e.g. Ramsey 2011), recently, accumulated data inferred from niche modeling show absences of prevalent and significant ecological niche shift in natural established polyploids in comparison with their diploids close relatives (Godsoe *et al.* 2013; Glennon *et al.* 2014; Harbert *et al.* 2014; Visser &

Molofsk 2015). Instead of ecological factors, those studies implied reproductive traits, such as dispersal mechanism, might generally play a relative important role in the potential distribution evolution of polyploids (Glennon *et al.* 2014; Harbert *et al.* 2014). The plant taxa with long-distance dispersal ability tend to exhibit niche expansion (Glennon *et al.* 2014). This indication also recalled that the effects relating to dispersal mechanism should be carefully considered when evaluating the ecological niche shift in polyploidy evolution.

No previous biogeographical study had discussed whether natural establishment in fern polyploids involves any ecological niche shift. Current study presented the first case in fern polyploids, in which on climatic niche evolution in the autohexaploids in *Deparia lancea* Fraser-Jenk. (Athyriaceae) was revealed. These hexaploids are thought to be originated from Taiwan Main Is. with oversea dispersals resulting in subsequent range expansions throughout East Asia Archipelagos (see Fig 6.1A for their distribution range). Meanwhile, their conspecific diploids seem to be Taiwan Main Is. endemic and are revealed withiout oversea established population (see in Chapter 3 and 4). These imply an increased colonization ability in *D. lancea* hexaploids, which is also generally found in other fern polyploid taxa (reviewed in Masuyama & Watano 1990 and Ranker & Geiger 2008).

By inferring potential distributions of both inside aand oustside of Taiwan Main Is., this study aimed on examining whether a climatic niche shift as a sign of ecophysiological pre-adaption associating with range expansion and increased colonization ability for the hexaploids. In other words, under the comparison with the diploid progenitors, if the same climatic niche shift is consistently revealed in the hexaploids of both inside and outside of Taiwan Main Is., this should imply these hexaploids have adapted to new climatic niches enabling their range expansion and oversea colonization. Particularly, polyploids must overcome "minority disadvantage" to outcompete their diploid parents in the same locality. Alternatively, if a niche conservatism is revealed, the increased colonization ability of hexaploids might relate to other mechanism rather than climatic niche shift. To test above predications, the current climatic niches of diploids, hexaploids in Taiwan Main Is., and hexaploids out of in Taiwan Main Is. were inferred by niche modeling based on their occurrences. Based on the modeling results, their climatic niche preference and breadth were further evaluated for statistical analyses

underlying their climatic niche similarity. Finally, the niche equivalency inferred from current and past climate were applied to identify the possible scenario for the niche influence on the evolution of *D. lancea* hexaploids.

Materials and methods

Sampling and ploidy determination

Diploids of *Deparia lancea* were found only in Taiwan Main Is. While the distribution of hexaploid of *Deparia lancea* range from Taiwan to Honshu in Japan, and also in the Philippines (Batans Is.) (Chapter 3 and 4). In addition to the cytological records identified previously, samplings of *D. lancea* from other locations within their known distribution ranges were added. These additional samples included both living and herbarium collections (Table 6.1). To determine the ploidy of these samples, flow cytometry analyses were applied for the living materials and spore size measurements and were applied for herbarium materials. All methodologies for these ploidy determination followed approaches described in Chapter 3. Among my samplings, I did not include the individual that has Hc/H12H14 (or called H12-14-6.4 local line in Chapter 4) genotype, which belongs an independent autohexaploid lineage endemic to a Taiwan Main Is. endemic and is genetically isolated from the other hexaploids (Chapter 3 and 4). Other details of these collections were in Table 6.1.

Climatic niche modeling

The 19 current climatic variables in 0.5 arcmin grid from Worldclim database (BIO1-19; http://www.worldclim.org/) were applied for this study. The details of these climatic variables were listed in Table 6.2. For analyses of hexaploid, these climatic variables were restricted in a polygon geographic region covering Taiwan Main Is. and its eastern flanking islands, Batan Islands, and Ryukyu, Kyushu, and Honshu in Japan (Fig. 6.1A). For analyses of diploids, a geographical region containing only Taiwan Main Is. was applied (Fig. 6.1B), where diploids' natural distribution known only from there, to avoid the inaccuracy of suitability inferences due to an enlarged background data. The MaxEnt version 3.3.3k (Phillips & Dudík 2008) was used for the climatic niche modeling. For MaxEnt analysis of each cytotype, all modeling were performed with 10 replicates and 5000 iterations, and set to logistic

output. 10% and 90% of occurrences were applied for testing and training the models, respectively (i.e. the default setting using 10 replicates). The average results of 10 replicates were adopted in the following analyses of each cytotype.

Search climatic variable with the potentially highest contribution

Because different climatic variables auto-correlated with each other in a certain geographic region, the analyses of original climatic niche modeling was unable to detect the reveal contribution of each climatic variable. Therefore, auto-correlated climatic variables were removed from further climatic niche modeling. In practice, among the climatic variables inbetween absolute *r* value of pairwise Pearson correlation > 0.75 existing (ENMTools 1.3; Warren *et al*. 2010), only one of them was selected to include in further nich modeling. Except for input climate variable, other settings for these modeling analyses were the same as originally descripted (see in *Climatic niche modeling*). The contributive variable with the possibly highest contribution in niche modeling for each cytotype was identified according to its own MaxEnt results of "analysis of variable contributions".

Climatic niche similarity test

For each cytotype, the criteria of Lowest Presence Threshold (LPT, Pearson *et al.* 2007) were modified to filtrate reliable distributed grids from its own climatic niche modeling results. Thus, for LPT in this study, 95% highest logistic values (i.e. suitability) among all real occurrences were adopted as the threshold (i.e. 5% was discarded). This approach can reduce an overestimation of potential distribution range, and should better represent their potential distributions. For hexaploid, these filtrated grids were further separated into two grid sets: one containing Taiwan Main Is. only (referred as 6xA below) while another one excluding Taiwan Main Is. (referred as 6xB below). Thus, 6xA covered the same geographical region as that in the diploid (referred as 2x grid set below). In other words, 6xA and 6xB grid sets represented the inferred potential distributions of hexaploids in and out of Taiwan Main Is., respectively. Based on these 19 climatic variables, two PCA (Principal Component Analysis) variables were reconstructed based on the largest background region (i.e. the same polygon geographic region described above for hexaploid climatic niche modeling) using ArcGIS 10 (ESRI 2011). These PCA variables were

thought to better present an overall climatic trend(s) in these focal regions.

Based on these inferred potential distributions, the climatic niche similarity tests in this study included two parts: climatic niche preference and niche breadth. To infer their climatic niche preferences, the 10,000 grids with the highest suitability were evaluated from each ploidy-region grid set (i.e. 6xA, 6xB, or 2x), and then, based on these 10,000 grids, extracted their corresponding values of these 21 variables (i.e. 19 climatic and two PCA variables). In each particular variable, the significance of difference ($0.001 > p$) between values from two ploidy-region grid sets was detected using Turkey HSD test. To infer their niche breadth, for each variable, I first removed those grids with values out of the range inferred by real occurrences in that certain region (i.e. either inside of Taiwan Main Is. or outside of Taiwan Main Is.) from these ploidy-region grid sets to avoid overestimation. Next, in each grid set, I inferred the breadth variation of each variable by transforming the values into abs(ni − Median), and the "ni" and "Median" represented the value of a particular grid and the median value in a particular variable, respectively. To infer the significant difference in climatic breadth variation between two ploidy-region grid sets, two tailed *t*-tests were applied.

Inferred potential distribution equivalency and overlap

The previous phylogeographical results suggest the formation of wide spread line hexaploids in *Deparia lancea* can be traced up to 1.1 Ma, and an inferred population expansion is estimated after 0.06 Ma (see Chapter 4). Therefore, in addition to current climatic variables, I also applied those climatic variables with a same resolution (i.e. in 0.5 arcmin grid) from the Last inter-glacial (LIG, 0.14-0.12 Ma; http://www.worldclim.org/), the time period before hexaploids range expansion, for niche equivalency tests. Because these analyses aimed to identify the potential distribution evolution of hexaploid before their range expansion, the occurrences of both cytotypes and the climatic variable were restricted to Taiwan Main Is. These niche equivalency tests were conducted by generating the observed Schoener's D values (Schoener 1968) and then comparing them against null distribution of simulated values. In practice, current and LIG niche modeling of two cytotypes conducted with raw MaxEnt score output. In both analyses of current and LIG, "measuring niche overlap" and "identity tests" function

of ENMTools 1.3 (Warren *et al.* 2010) were used to infer their observed and null distributed Schoener's D values, respectively. For niche equivalency tests of LIG climate, the current climate variables were used as background data and projected to those from LIG. These null distributed Schoener's D values were resulted from 100 replicates of simulation. If the observed value was less than 95% of the simulated ones, there was significant evidence of inter-cytotype niche dissimilarity.

To measure the current potential distribution overlap between cytotypes, the same LPT criteria and climatic niche modeling results as mentioned above (see *Climatic niche similarity test* in Materials and methods) were used to calculate the proportion of overlapping grids of these two cytotypes. To measure their LIG potential distribution overlap, the same manner was adopted using another climatic niche modeling with projecting layer of the LIG climatic variables.

Results

Cytotype occurrences and climatic niche modeling

Additional 40 diploid and 20 hexaploid records were confirmed in this study (Table 6.1). Diploids were found only in Taiwan Main Is. while hexaploids were found in Eastern Taiwan Main Is. and islands from Batan Islands to Japan Honshu (Fig. 6.1). Finally, a total of 60 diploid and 74 hexaploid occurrences were applied to their climatic niche modeling. The AUC (area under the curve) score for diploid and hexaploid climatic niche modeling was 0.853 ± 0.078 and 0.978 ± 0.015 (average ± one standard deviation among 10 replicates), respectively. The suitability score of LPT was 0.128 for diploids and 0.200 for hexaploids. Their occurrences and climatic niche modeling results were also mapped in Fig. 6.1.

Climatic variable with the potentially highest contribution in niche modeling

In diploids distribution range, four groups of climatic variables with Pearson *r* values larger than 0.75 were revealed: group one (BIO 1, 5, 6, 8, 9, 10, and11), group two (BIO 2, 3, 4, and 7), group three (BIO 12, 13, 16, and 18), and group four (BIO 14, 15, 17, and 19). For the hexaploids, there were three groups: group one (BIO 1, 3, 4, 5, 6, 7, 9, 10, and 11), group two (BIO 12, 13, 16, and 18), and group three (BIO 14, 19, and 17); while the BIO 2, 8, and 15 had no such correlation with others. Therefore,

the further climatic niche modeling of diploids included only BIO 1, 4, 12, and 14, which were selected from one of each group; and the most contributive two were BIO 4 and 12 with a contribution of 38.6% and 33.5%, respectively. For climatic variable selection in hexaploids analysis, I applied the same manner as that for diploids, and included BIO 2, 4, 8, 12, 14, and 15 for the further climatic niche modeling; and the most contributive two were BIO 4 and 2 with a contribution of 53.3% and 27.8%, respectively.

Climatic niche similarity

The climatic niche preference in hexaploids out of Taiwan Main Is. (i.e. 6xB) were found to be significantly different to that of hexaploids in Taiwan Main Is. and diploids in all variables, including both climatic and PCA ones (Fig. 6.2). Whereas, the climatic niche preference of hexaploids in Taiwan Main Is. (i.e. 6xA) were revealed to be insignificantly different with diploids for five climatic variables: BIO 5, 6, 19, 12, and 13 (Fig. 6.2). For climatic niche breadth, the hexaploids out of Taiwan Main Is. had significantly narrowed breadthes in precipitation-relating variables (i.e. BIO 12-19; Fig. 6.2), and had significant wider breadthes in the majority of temperature-relating variables, except for BIO 3, 5, 8, and 10 (Fig. 6.2). In comparison with diploids, the hexaploids in Taiwan Main Is. not always had broadened climatic niche breadth, which occurred in eight (i.e. BIO 3, 4, 7, 12, 13, 16, 18, and 19) of 19 climatic and two PCA variables (Fig. 6.2). The Fig. 6.3 shows two dimensional niche ranges of PCA and the climatic variable with the possibly highest contribution

Inferred potential distribution equivalency and overlap

The results of inferred potential distribution equivalency and overlap were summarized in Table 6.3. The distribution of hexaploid inferred potential distribution in Taiwan Main Is. were revealed highly overlapped with those of diploids, and 83% (4235/5066) and 100% (39/39) of grids in hexaploid inferred current and LIG potential distributions were found overlapped with diploids', respectively (Table 6.3). For the potential distribution equivalence in Taiwan Main Is., two cytotypes were significantly different in inferred current and LIG potential distributions (Table 6.3; p values < 0.05 in both) while less significance was revealed in that of their LIG potential distributions (Fig. 6.4).

Discussion

Climatic niche differentiation and geographical expansion in the hexaploids

Overall, the hexaploids in *Deparia lancea* tend to have niche differentiations in preference and breadth comparing with diploids (Fig. 6.2), but these climatic niche shifts in the hexaploids might less contribute to the primary cause of their oversea colonization ability. For those hexaploids outside of Taiwan Main Is., they display differentiate climatic niche preferences but have expanded climatic niche breadths only in temperature-relating variables which is expected due to spatial autocorrelation with their distribution along a greater latitudinal range (Fig. 6.2). However, the hexaploids in Taiwan Main Is.were not revealed with insistent trends of these climatic niche breadth expasions. By contrast, in those hexaploids in Taiwan Main Is., only two (i.e. BIO 4 and 7) out of these seven temperature-relating climatic and PCA 1 variables had statically expanded breadthes, rather than from multiple and independent climatic factors. Moreover, these temperature seasonality variables were also highly correlated with each other (see in *Climatic niche similarity* in Results section). On the other hand, conserved climatic niche ranges between diploids and the hexaploids in Taiwan Main Is. were revealed based on their real occurrences (Fig. 6.2) and based on that in their two-dimension ranges of those climatic variables with the potentially highest contribution (Fig. 6.3). These suggest that climatic niche broadening is not prevalent in the hexaploids in Taiwan Main Is., and has limited contribution on climatic niche breadth of the hexaploids dispered out of Taiwan Main Is. In orther words, this prevalent climatic niche conservatism failed to support that an increased ecophysiological tolerance as major pre-adaptive mechanism assist the range expansion in the hexaploids. The climatic niche differentiation in hexaploids, if occurred, should be mostly resulted by the process during range expansion after dispersing out of Taiwan Main Is. Similarly, the climatic niche differentiation in precipitation-relating variables of the hexaploids out of Taiwan Main Is. was also reflected by their restricted breadths, for which were usually correlated with the niche breadths of their distribution range (Fig. 6.2).

Potential distribution differentiation and polyploidy evolution

In addition to the result of climatic niche dissimilarity, the hexaploids

and diploids in Taiwan Main Is. also have significant differences in niche equivalency tests based on either current or LIG climatic variables. However, this differentiation in potential distribution was less significant than that in LIG period (Fig. 6.4; i.e. less deviated from null distribution), especially hexaploids were revealed completely overlapped with diploids (i.e. 39/39 Table 6.3). This high overlapping further suggests the possibility that hexaploids formation/establishment were evolved from niche expansion without a spontaneous niche diverge. This also indicates that there was a strong habitat competition between these two cytotypes to forced hexaploids to evolve with increased colonization ability. Regarding to the origin of hexaploids (as discussed in Chapter 4), the most probable scenario is likely that hexaploids expanded their geographical range as well as climatic niches accompanied by subsequent dispersals and oversea colonization. As mentioned previously, broaden climatic niche seems not the primary attribution for increased colonization ability in hexaploids but other factors, such as those relating to reproductive biology, might play a relatively important role to initiate their range expansion. This finding corresponds with the indication by Glennon *et al.* (2014), in which the importance of reproductive biology on polyploidy niche exploration is emphasized. Indeed, comparing with diploids, higher inbreeding abilities in both *D. lancea* hexaploids in and outside of Taiwan Main Is had been found (Chapter 4 and 5). Such inbreeding trends in polyploids are a general phenomenon in ferns (Masuyama & Watano 1990; Verma 2003; Ranker & Geiger 2008). In order to further identify if any deterministic ecological factor (e.g. those temperature seasonality reflecting by BIO4 and 7) or ecophysiological adaptation has shaped *Deparia lancea* cytogeography, transplant experiments in their natural habitats and/or common garden experiments should be undertaken for these diploids and hexaploids. The preliminary observation in both Tsukuba (Honshu, Japan) and Taipei (Taiwan) Botanical gardens suggests there is no obvious difference between the successes of sporing and survival of two cytotypes' mature sporophytes (Kuo personal observation).

References

Arrigo N, Barker MS (2012) Rarely successful polyploids and their legacy in plant genomes. *Current Opinion in Plant Biology*, **15**, 140–146.

Buggs RJA, Wendel JF, Doyle JJ *et al.* (2014) The legacy of diploid progenitors in allopolyploid gene expression patterns. *Philosophical Transactions of the Royal Society B: Biological Sciences*, **369**, DOI: 10.1098/rstb.2013.0354.

ESRI (2011) ArcGIS Desktop: Release 10. Redlands, CA: Environmental Systems Research Institute.

Glennon KL, Ritchie ME, Segraves KA (2014) Evidence for shared broad-scale climatic niches of diploid and polyploid plants. *Ecology Letters*, **17**, 574–582.

Godsoe W, Larson M, Glennon KL, Segraves K (2013) Polyploidization in *Heuchera cylindrica* (Saxifragaceae) did not result in a shift in climatic requirements. *American Journal of Botany*, **100**, 496–508.

Harbert RS, Brown AHD, Doyle JJ (2014) Climate niche modeling in the perennial *Glycine* (Leguminosae) allopolyploid complex. *American Journal of Botany*, **101**, 710–721.

Husband BC, Schemske D (2000) Ecological mechanisms of reproductive isolation between diploid and tetraploid *Chamerion angustifolium*. *Journal of Ecology*, **88**, 689–701.

Jiao Y, Paterson A (2014) Polyploidy-associated genome modifications during land plant evolution. *Philosophical Transactions of the Royal Society B: Biological Sciences*, **369**, DOI: 10.1098/rstb.2013.0355.

Jiao Y, Wickett NJ, Ayyampalayam S *et al.* (2011) Ancestral polyploidy in seed plants and angiosperms. *Nature*, **473**, 97–100.

Kreft H, Jetz W, Mutke J, Barthlott W (2010) Contrasting environmental and regional effects on global pteridophyte and seed plant diversity. *Ecography*, **33**, 408–419.

Masuyama S, Watano Y (1990) Trends for inbreeding in polyploid pteridophytes. *Plant Species Biology*, **5**, 13–17.

Patiño J, Carine M, Fernández-Palacios JM *et al.* (2014) The anagenetic world of spore-producing land plants. *New Phytologist*, **201**, 305–311.

Pearson RG, Raxworthy CJ, Nakamura M, Townsend Peterson A (2006) Predicting species distributions from small numbers of occurrence records: a test case using cryptic geckos in Madagascar. *Journal of Biogeography*, **34**, 102–117.

Phillips S, Dudík M (2008) Modeling of species distributions with Maxent: new extensions and a comprehensive evaluation. *Ecography*, **31**, 161–175.

Ramsey J (2011) Polyploidy and ecological adaptation in wild yarrow. *Proceedings of the National Academy of Sciences of the United States of America*, **108**, 7096–7101.

Ramsey J, Ramsey T (2014) Ecological studies of polyploidy in the 100 years following its discovery. *Proceedings of the Royal Society B: Biological Sciences*. DOI: 10.1098/rstb.2013.0352.

Ranker TA, Geiger JMO (2008). Population genetics. In: *Biology and Evolution of ferns and Lycophytes* (eds. Ranker TA, Haufler CH), pp. 107–133. Cambridge University Press, New York.

Schoener T (1968) The Anolis lizards of Bimini: resource partitioning in a complex fauna. *Ecology*, **49**, 704–726.

te Best M, Le Roux JJ, Richardson DM *et al.* (2012) The more the better? The role of polyploidy in facilitating plant invasions. *Annals of Botany*, **109**, 19–45.

Thompson KA, Husband BC, Maherali H (2014) Climatic niche differences between diploid and tetraploid cytotypes of Chamerion angustifolium (Onagraceae). *American Journal of Botany*, **101**, 1868–1875.

Thompson J, Merg K (2008) Evolution of polyploidy and the diversification of plant-pollinator interactions. *Ecology*, **89**, 2197–2206.

Verma SC (2003) Some aspects of reproductive biology of the

gametophyte generation of homosporous ferns. In: *Pteridophyte in the New Millennium* (eds. Chandra S, Srivastava M), pp. 455–484. Kluwer Academic Publishers, the Netherlands.

Visser V, Molofsky J (2015) Ecological niche differentiation of polyploidization is not supported by environmental differences among species in a cosmopolitan grass genus. *American Journal of Botany*, **102**, 36–49.

Warren DL, Glor RE, Turelli M (2010) ENMTools: a toolbox for comparative studies of environmental niche models. *Ecography*, **33**, 607–611.

Wood TE, Takebayashi N, Barker MS *et al.* (2009) The frequency of polyploid speciation in vascular plants. *Proceedings of the National Academy of Sciences of the United States of America*, **106**, 13875–13879.

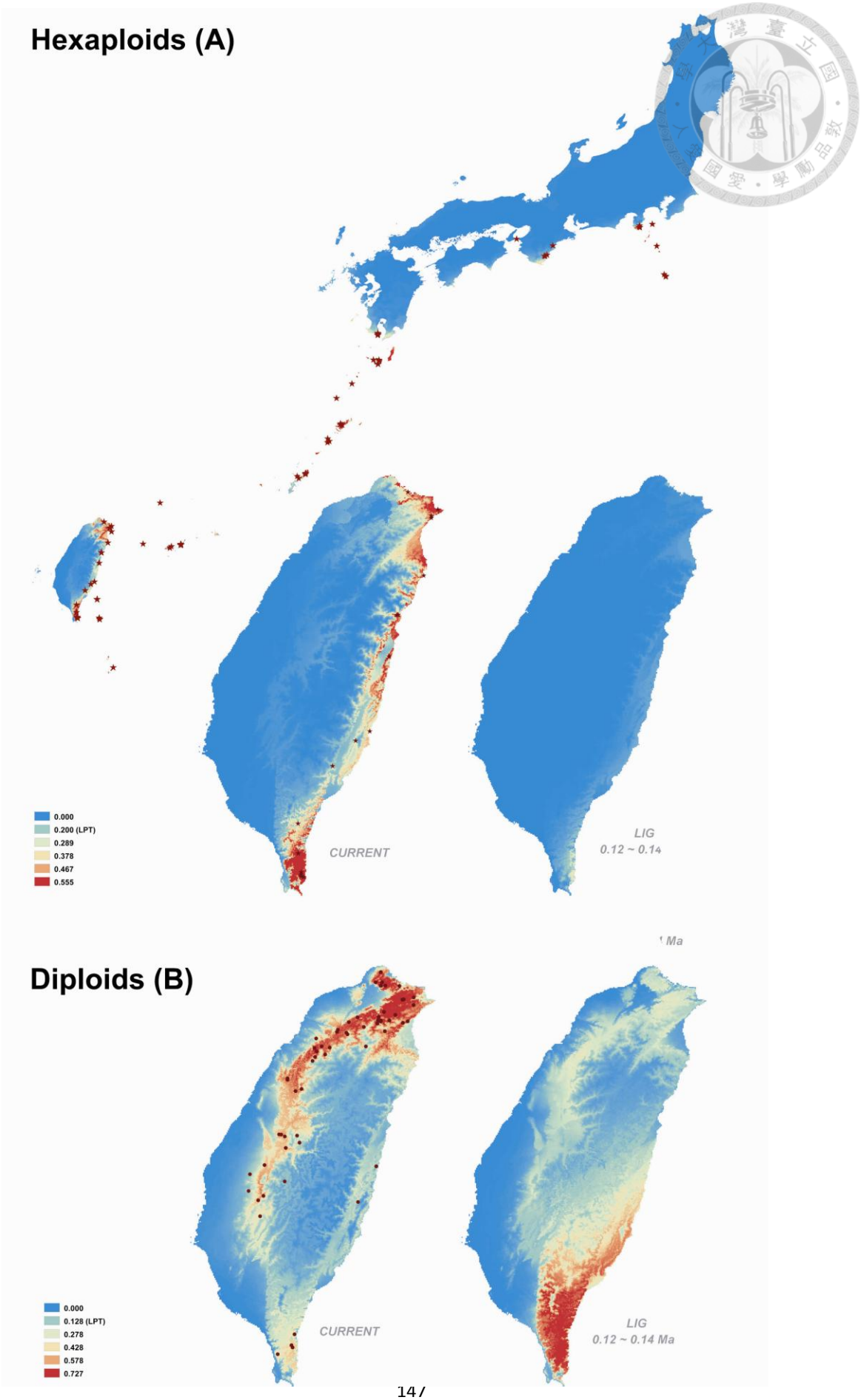
Hexaploids (A)
0.000
0.200 (LPT)
0.289
0.378
0.467
0.555
CURRENT
LIG
0.12 ~ 0.14
Diploids (B)
0.000
0.128 (LPT)
0.278
0.428
0.578
0.727
CURRENT
LIG
0.12 ~ 0.14 Ma

Fig. 6.1. The distributions and potential distributions of hexaploids (A) and diploids (B) *Deparia lancea* inferred from occurrence data. The real occurrences of diploids and hexaploids are indicated by circles and stars on the maps, respectively. In the hexaploids (A), the upper and lower map represents the whole and Taiwan Main Is. only distribution, respectively. The different colors on the maps represent the degrees of suitability inferred by niche modeling. LPT = lowest present threshold; LIG = last inter-glacial.

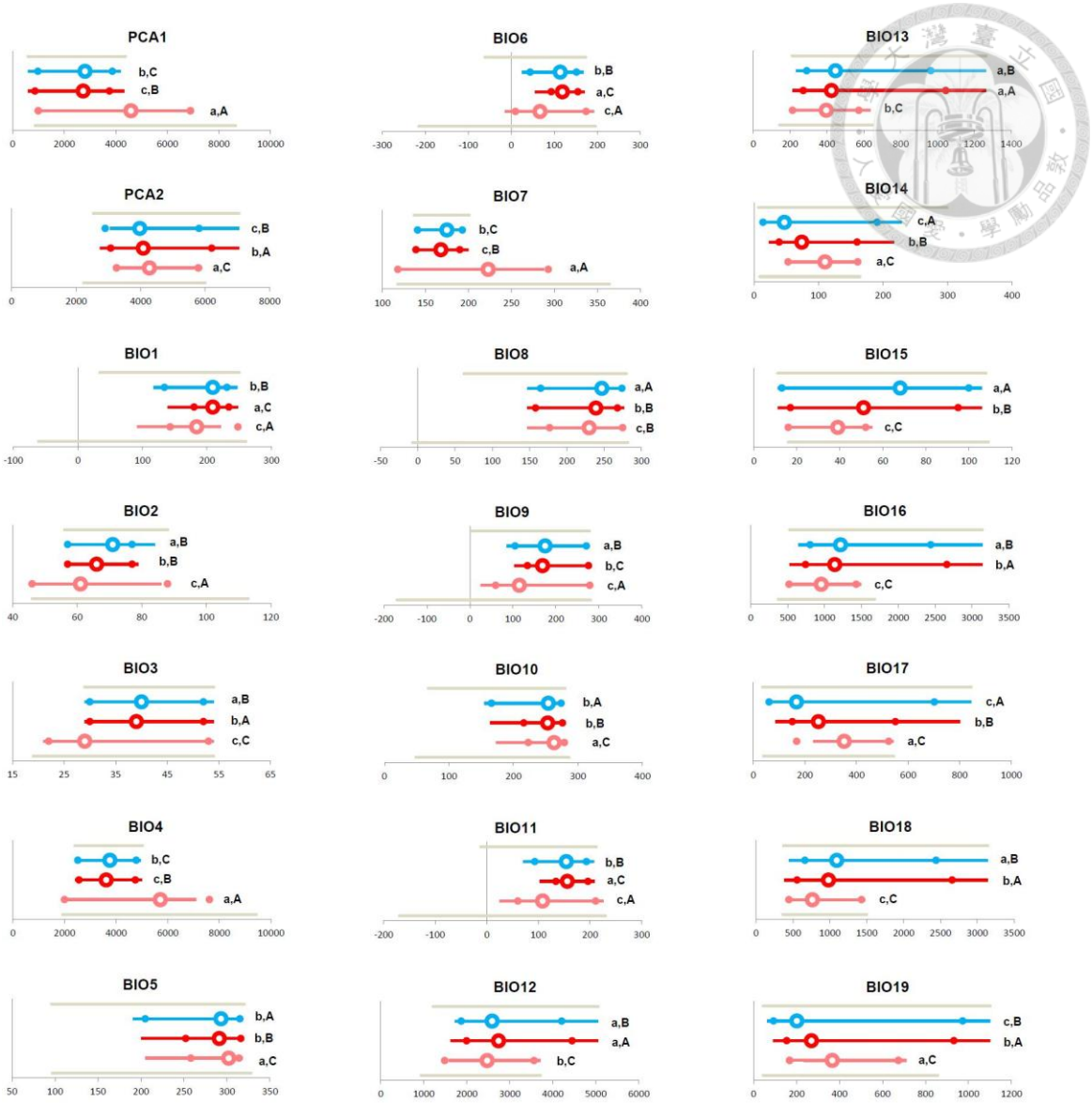

Fig. 6.2. Ranges of climatic variables of diploids and hexaploids in *Deparia lancea*. The diploids, hexaploids in Taiwan Main Is. (i.e. non-dispersed ones), and hexaploids out of Taiwan Main Is. (i.e. dispersed ones) are indicated by blue, red, and pink color, respectively. The solid and open circles indicate the upper/lower limits based on real occurrences and the mediums inferred by niche modeling results. The upper and lower grey lines indicate the ranges of variable (i.e. BIO 1-19 and two PCA variables) of background grids in Taiwan Main Is. and those in other areas out of Taiwan Main Is., respectively. Other lines indicate the ranges of climatic variable in different ploidy-grid sets (i.e. 2x, 6xA, and 6xB; see definitions in Materials and methods). In each variable, the different lowercase letters indicate different groups of niche

preference with $p < 0.0001$; and the different uppercase letters indicate different groups of niche breaths $p < 0.0001$. The definitions of climatic variables BIO 1-19 are shown in Table 6.2.

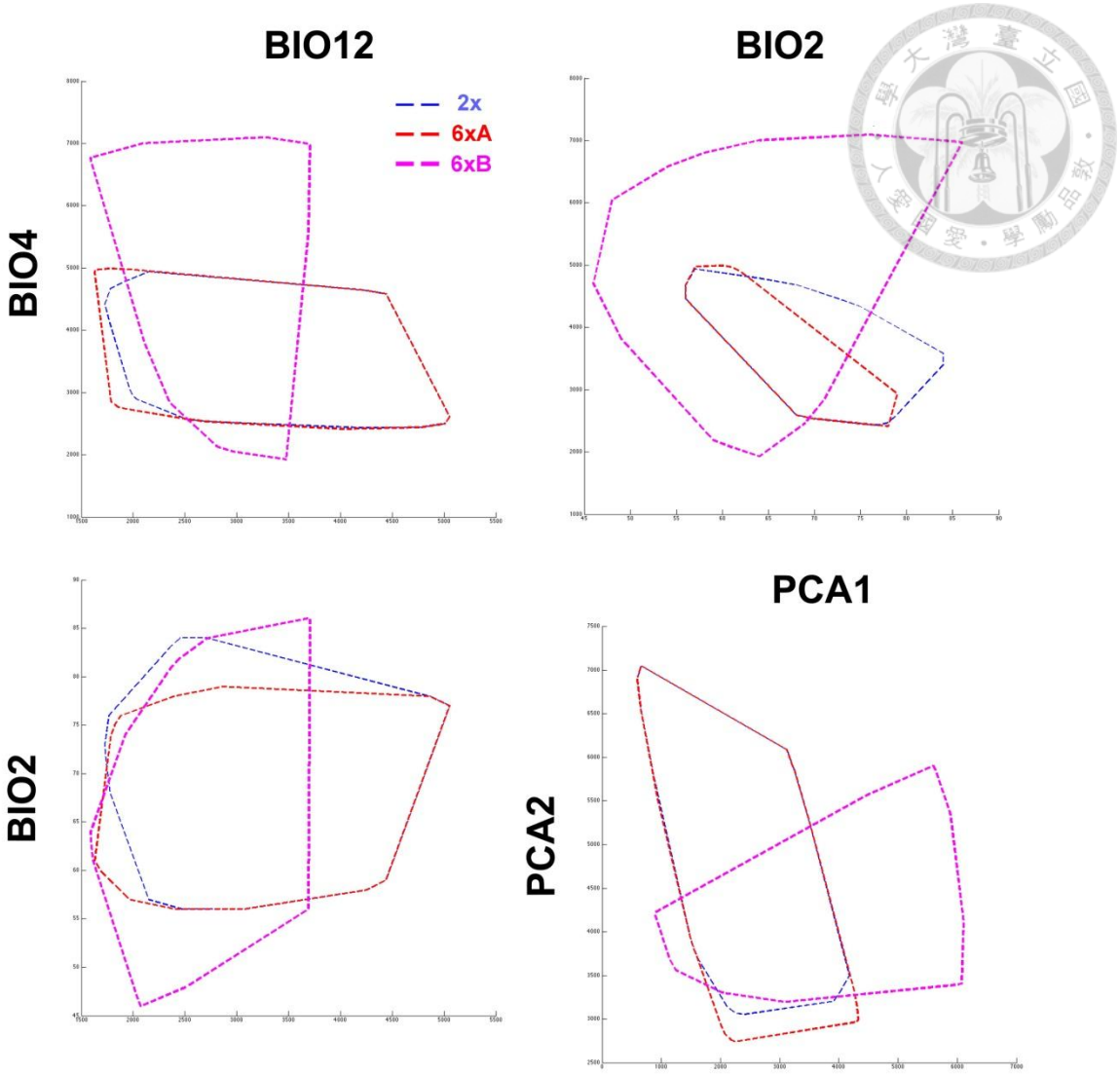

Fig. 6.3. The two-dimensional ranges of climatic variables (BIO2, 4, and 12) (A, B, C) and PCA variables (D) of *Deparia lancea* diploids and hexaploids. The different dash lines indicate the ranges inferred by the minimum hull polygons of different grid sets: 2x (diploids; blue), 6xA (hexaploids in Taiwan Main Is.; red), and 6xB (hexaploids out of Taiwan Main Is.; pink).

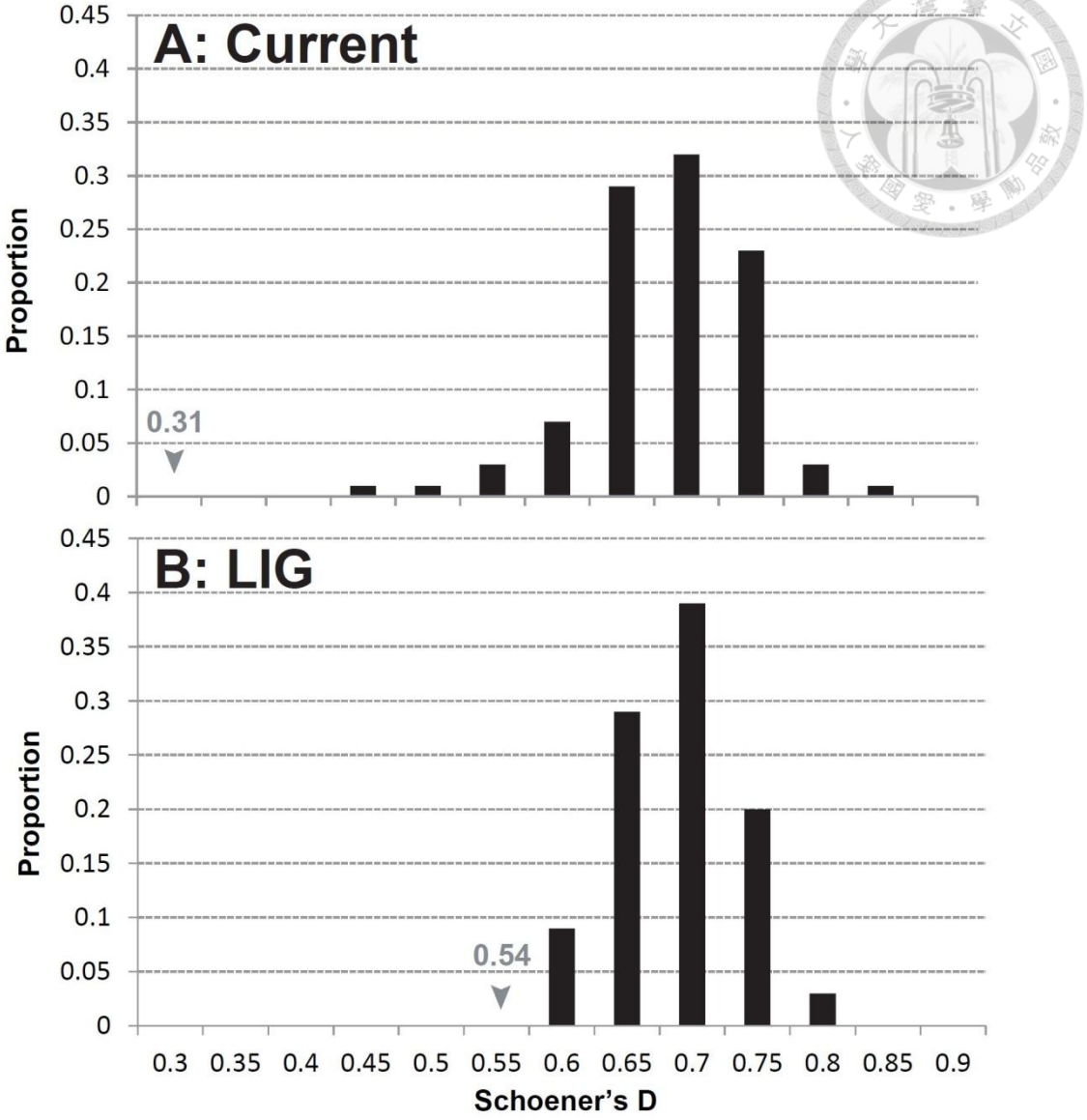

Fig. 6.4. The niche equivalency tests between hexaploid and diploid of *Deparia lancea* based on (A) current and (B; LIG) last inter-glacial climates. The histograms and the arrows indicate the simulated and observed values, respectively.

Table 6.1. The *Deparia lancea* collections used in this study.

Polidy	Locality	Locality Chinese	GPS:E	GPS:N	Vouchers (herbarium)
2X	Neiwen to Shuangliu, Pingtung County, Taiwan	台灣 屏東縣 內文-雙流	120.84557	22.21432	*Kuo4083* (TAIF)
2X	Lantan, Chiayi County, Taiwan	台灣 嘉義市 蘭潭	120.49123	23.47563	*Lu20515* (TAIF)
2X	Shihmeng valley, Fengshan, Chiayi County, Taiwan	台灣 嘉義縣 豐山 石夢谷	120.78234	23.55261	*Lu24437* (TAIF)
2X	Sun Moon Lake, Nantou County, Taiwan	台灣 南投縣 日月潭	120.90161	23.86472	*Kuo4086* (TAIF)
2X	Taiwan	台灣 南投縣 中寮鄉 東勢閣坑	120.78335	23.91525	*Kuo4079* (TAIF)
2X	Taiwan	台灣 南投縣 中寮鄉 樟平溪	120.75469	23.93039	*Kuo4078* (TAIF)
2X	Taiwan	台灣 南投縣 中寮鄉 龍南三號橋	120.73697	23.93160	*Kuo4077* (TAIF)
2X	Mt. Wuchih, Hsinchu County, Taiwan	台灣 新竹縣 五指山	121.08079	24.64124	*Kuo4087* (TAIF)
2X	Beidelaman , Hsinchu County, Taiwan	台灣 新竹縣 北德拉曼	121.28846	24.73895	*Kuo4092* (TAIF)
2X	Yuanyang valley waterfall, Hsinchu County, Taiwan	台灣 新竹縣 鴛鴦谷瀑布	121.27959	24.75070	*Kuo4090* (TAIF)
2X	Mt. Chihke, Kuanhsi, Hsinchu County, Taiwan	台灣 新竹縣 關西 赤柯山	121.20298	24.75850	*Lu24593* (TAIF)
2X	Fushan, Ilan County, Taiwan	台灣 宜蘭縣 福山	121.58961	24.76425	*Kuo2824* (TAIF)
2X	Ssimei bridge, Loma highway, Hsinchu County, Taiwan	台灣 新竹縣 羅馬公路 喜美橋	121.21092	24.77564	*Kuo4089* (TAIF)
2X	Neitung, Wulai, New Taipei City, Taiwan	台灣 新北市 烏來 內洞	121.52906	24.82541	*Kuo4101* (TAIF)
2X	Yunhsien garden, Wulai, New Taipei City, Taiwan	台灣 新北市 烏來 雲仙樂園	121.55683	24.84202	*Kuo4106* (TAIF)
2X	Paoma historic trail , Ilan County, Taiwan	台灣 宜蘭縣 跑馬古道	121.77351	24.84331	*Kuo4122* (TAIF)
2X	Mt. Tatao, New Taipei City, Taiwan	台灣 新北市 大刀山	121.55686	24.84969	*Kuo4107* (TAIF)
2X	Tunghou, Wulai, New Taipei City, Taiwan	台灣 新北市 烏來 桶後	121.62663	24.85077	*Kuo4114* (TAIF)
2X	Mt. Pataoerh, Taipei City, Taiwan	台灣 新北市 拔刀爾山	121.53412	24.85248	*Kuo4102* (TAIF)
2X	Wuliaochien, New Taipei City, Taiwan	台灣 新北市 五寮尖	121.36993	24.87600	*Kuo4093* (TAIF)
2X	Chiachiuliao alley, Wulai, New Taipei City, Taiwan	台灣 新北市 烏來 加九寮步道	121.54017	24.87954	*Kuo4103* (TAIF)
2X	Chinkualiao stream, New Taipei City, Taiwan	台灣 新北市 金瓜寮溪	121.67486	24.89525	*Kuo4116* (TAIF)
2X	Feitsui Reservoir, New Taipei City, Taiwan	台灣 新北市 翡翠水庫	121.58242	24.91911	*Kuo4113* (TAIF)
2X	Pingchi, Taipei City, Taiwan	台灣 台北市 平溪	121.73151	25.01821	*Kuo4119* (TAIF)
2X	Hsiaotzushan, New Taipei City, Taiwan	台灣 新北市 孝子山	121.74143	25.02042	*Kuo4121* (TAIF)
2X	Neishuanghsi, Taipei City, Taiwan	台灣 台北市 內雙溪	121.55763	25.13001	*Kuo4109* (TAIF)
2X	Chuanssu waterfall, Taipei City, Taiwan	台灣 台北市 涓絲瀑布	121.56669	25.15796	*Kuo4110* (TAIF)
2X	Mt. Chungcheng, New Taipei City, Taiwan	台灣 新北市 中正山	121.51561	25.15860	*Kuo4100* (TAIF)
2X	Chingshan waterfall , Shihmen, Keelung City, Taiwan	台灣 基隆市 石門 青山瀑布	121.55714	25.24060	*Kuo4108* (TAIF)
2X*	Taiwan	台灣 嘉義縣 中埔鄉 石弄林場	120.56889	23.40056	*TAIE 017670* (TAIE)
2X*	Wushihkeng, Taichung City, Taiwan	台灣 台中市 烏石坑	120.91814	24.29768	*TAIE 13437* (TAIE)
2X*	Mt. Kuantao, Tahu, Miaoli County, Taiwan	台灣 苗栗縣 大湖 關刀山	120.80490	24.37297	*TAIE 5729* (TAIE)
2X*	Jhihming mine, Sanyi, Miaoli County, Taiwan	台灣 苗栗縣 三義 志銘矽礦	120.80556	24.38333	*HAST 92804* (HAST)
2X*	Shihmen trail, Miaoli County, Taiwan	台灣 苗栗縣 石門古道	121.02739	24.55585	*TAIE 7049* (TAIE)
2X*	Nanchuang, Miaoli County, Taiwan	台灣 苗栗縣 南庄	121.04012	24.60086	*TAIE 1898* (TAIE)
2X*	Huayuan village, Hsinchu County, Taiwan	台灣 新竹縣 花園村	121.14499	24.63126	*Lu14775* (TAIF)
2X*	Paoshan Reservoir, Hsinchu County, Taiwan	台灣 新竹縣 寶山水庫	121.03587	24.70536	*Huang1181* (TAIF)
2X*	Baiji trail, Taoyuan County, Taiwan	台灣 桃園縣 百吉步道	121.29962	24.83659	*TAIE 21360* (TAIE)
2X*	Houliao, New Taipei City, Taiwan	台灣 新北市 後寮	121.82139	24.97500	*TAIF 179249* (TAIF)
2X*	City, Taiwan	台灣 新北市 雙溪鄉 后番子坑溪	121.82232	25.03590	*TAIE 21201* (TAIE)
2X[a]	Mt. Lilung, Pingtung County, Taiwan	台灣 屏東縣 里龍山	120.72589	22.15952	*Kuo4045* (TAIF)
2X[a]	Shouka logging trail, Pingtung County, Taiwan	台灣 屏東縣 壽卡林道	120.83682	22.23193	*Kuo4044* (TAIF)
2X[a]	Tawu, Taitung County, Taiwan	台灣 台東縣 大武	120.86147	22.32001	*Lu21665* (TAIF)
2X[a]	Tsengwen reservoir, Chiayi County, Taiwan	台灣 嘉義縣 曾文水庫	120.58389	23.27182	*Kuo4035* (TAIF)
2X[a]	Mt. Chihke, Hualien County, Taiwan	台灣 花蓮縣 赤柯山	121.37350	23.38662	*Kuo4094* (TAIF)
2X[a]	Chukou, Chiayi County, Taiwan	台灣 嘉義縣 觸口	120.61078	23.43624	*Kuo4036* (TAIF)
2X[a]	Shihpi, Yunlin County, Taiwan	台灣 雲林縣 石壁	120.50198	23.61066	*Lu22421* (TAIF)
2X[a]	Mt. Taibalang, Hualien County, Taiwan	台灣 花蓮縣 太巴塱山	121.52039	23.67425	*Kuo4039* (TAIF)
2X[a]	Hushan reservoir, Yunlin County, Taiwan	台灣 雲林縣 湖山水庫	120.61985	23.68459	*Kuo4050* (TAIF)
2X[a]	Chilu Bridge, Nantou County, Taiwan	台灣 南投縣 集鹿大橋	120.79073	23.82262	*Kuo4043* (TAIF)
2X[a]	Lienhuachih, Nantou County, Taiwan	台灣 南投縣 蓮華池	120.88192	23.92204	*Kuo4042* (TAIF)
2X[a]	Tungshihlinchang, Taichung City, Taiwan	台灣 台中市 東勢林場	120.86977	24.28095	*Kuo4046* (TAIF)
2X[a]	Mt. Chiali, Miaoli County, Taiwan	台灣 苗栗縣 加里山	121.00670	24.52434	*Kuo4041* (TAIF)
2X[a]	Taoshan Primary School, Hsinchu County, Taiwan	台灣 新竹縣 桃山國小	121.10840	24.57622	*Kuo4037* (TAIF)
2X[a]	Nanchuang, Miaoli County, Taiwan	台灣 苗栗縣 南庄	121.02280	24.62774	*Kuo4040* (TAIF)
2X[a]	Ssuling, Taoyuan County, Taiwan	台灣 桃園縣 四稜	121.43641	24.64108	*Kuo4096* (TAIF)
2X[a]	Mt. Peichatien, Taoyuan County, Taiwan	台灣 桃園縣 北插天山	121.42064	24.79777	*Kuo4048* (TAIF)
2X[a]	Linmei trail, Chiaohsi, Ilan County, Taiwan	台灣 宜蘭縣 礁溪 林美步道	121.73535	24.83086	*Kuo4120* (TAIF)
2X[a]	Hsinshan-menghu, New Taipei City, Taiwan	台灣 新北市 新山夢湖	121.70687	25.12847	*Kuo4117* (TAIF)
2X[a]	Tienhsiyuan, Taipei City, Taiwan	台灣 台北市 天溪園	121.59285	25.13168	*Kuo1914* (TAIF)
6X	Mt. Wanlite to Luliaochsi, Pingtung County, Taiwan	台灣 屏東縣 萬里得山-鹿寮溪	120.84477	22.05762	*Kuo4082* (TAIF)
6X	Taiwan	台灣 屏東縣 台9線保線道60	120.82420	22.24140	*Kuo4081* (TAIF)
6X	Mt. Talili, Pingtung County, Taiwan	台灣 屏東縣 大里力山	120.82244	22.48163	*Kuo4080* (TAIF)
6X	Jiciao river, Chengkung Town, Taitung County, Taiwan	台灣 台東縣 成功鎮 堺橋溪	121.40188	23.22671	*Kuo4095* (TAIF)
6X	Mt. Yuehmei , Hualien County, Taiwan	台灣 花蓮縣 月眉山	121.55635	23.82943	*Kuo4105* (TAIF)
6X	Tali village, Hualien County, Taiwan	台灣 花蓮縣 大禮部落	121.63210	24.16728	*Kuo4115* (TAIF)

(Table 6.1 cont. 1)

6X	Mt. Omoto-date, Ishigaki Island, Okinawa Prefecture, Japan		124.18305	24.42068	*Wade3677* (TAIF)
6X	Maeda-gawa, Ishigaki Island, Okinawa Prefecture, Japan		124.20063	24.42577	*Wade3668* (TAIF)
6X	Wushihpi, Nanao, Ilan County, Taiwan	台灣 宜蘭縣 南澳 烏石鼻	121.83650	24.48393	*Kuo4123* (TAIF)
6X	401 high land to island surrouding trail, Guishan Island, Ilan County, Taiwan	台灣 宜蘭縣 龜山島 401高地-環島步道	121.95499	24.84380	*Kuo4127* (TAIF)
6X	Mt. Fanshuliao, Ilan County, Taiwan	台灣 宜蘭縣 蕃薯寮山	121.89844	24.94914	*Kuo4125* (TAIF)
6X	Taoyuan valley, Ilan County, Taiwan	台灣 宜蘭縣 桃源谷	121.89710	24.96810	*Kuo4124* (TAIF)
6X	Kungliao, New Taipei City, Taiwan	台灣 新北市 貢寮	121.95129	25.01842	*Kuo4126* (TAIF)
6X	Dawulun gun emplacement, Keelung City, Taiwan	台灣 基隆市 大武崙砲台	121.70953	25.15870	*Kuo4118* (TAIF)
6X	Mt. Iyu-dake, Okinawa Prefecture, Japan		128.20672	26.69115	*Wade3640* (TAIF)
6X	Hiji river,Kunigami District, Okinawa Prefecture, Japan		128.19658	26.70855	*Wade3663* (TAIF)
6X	near Mt. Imakira-dake, Takara-jima Is., Toshima-mura, Kagoshima-gun, Kagoshima. Japan		129.20461	29.14619	*Goro 11383* (TNS)
6X	AnboMoutain trrail, Yakushima-cho, Yakushima Island, Kagoshima Prefecture, Japan		130.58130	30.35006	*Kuo4146* (TAIF)
6X	Tomogashima, Wakayama Prefecture, Japan		135.01098	34.28159	*Kuo4147* (TAIF)
6X*	Shakatang logging trail , Hualien County, Taiwan	台灣 花蓮縣 砂卡礑林道	121.62000	24.16500	*HAST102493* (HAST)
6X*[a]	Dujtak site, Batanes, the Philippines		122.00981	20.45835	*Barcelona991* (PNH)
6X*[a]	Mt. Ubura-dake, Yonaguni-cho, Yonaguni Island, Japan		122.96967	24.44761	*Goro14157* (TNS)
6X*[a]	Diaoyu Island (Senkaku Island)	釣魚台	123.47581	25.74142	*RYU33619* (RYU)
6X[a]	Ssulaokou, Orchid Island, Taitung County, Taiwan	台灣 台東縣 蘭嶼 四道溝	121.57366	22.00928	*Kuo4112* (TAIF)
6X[a]	Tienchih, Orchid Island, Taitung County, Taiwan	台灣 台東縣 蘭嶼 天池	121.57271	22.01380	*Kuo4067* (TAIF)
6X[a]	Central cross road to Tienchih, Orchid Island, Taitung County, Taiwan	台灣 台東縣 蘭嶼 中橫公路到天池	121.56843	22.03232	*Kuo4111* (TAIF)
6X[a]	Luliaochsi, Pingtung County, Taiwan	台灣 屏東縣 鹿寮溪	120.86755	22.04997	*Kuo4085* (TAIF)
6X[a]	Tungching stream, Orchid Island, Taitung County, Taiwan	台灣 台東縣 蘭嶼 東清溪	121.55402	22.06353	*Kuo4104* (TAIF)
6X[a]	Mt. Wanlite, Pingtung County, Taiwan	台灣 屏東縣 萬里得山	120.84621	22.06982	*Kuo4084* (TAIF)
6X[a]	Nanjenshan, Pingtung County, Taiwan	台灣 屏東縣 南仁山	120.84813	22.08879	*Kuo4064* (TAIF)
6X[a]	Kuoshan trail site 1, Green Island, Taitung County, Taiwan	台灣 台東縣 綠島 過山步道 之一	121.48305	22.65431	*Kuo4097* (TAIF)
6X[a]	Kuoshan trail site 2, Green Island, Taitung County, Taiwan	台灣 台東縣 綠島 過山步道 之二	121.48396	22.65783	*Kuo4098* (TAIF)
6X[a]	Kuanyintung to Haishenping, Green Island, Taitung County, Taiwan	台灣 台東縣 綠島 觀音洞往海參坪	121.49425	22.66017	*Kuo4099* (TAIF)
6X[a]	Haishenping, Green Island, Taitung County, Taiwan	台灣 台東縣 綠島 海參坪	121.49379	22.66362	*Kuo1919* (TAIF)
6X[a]	Luye Gaotai, Taitung County, Taiwan	台灣 台東縣 鹿野高台	121.10169	22.94634	*Kuo4088* (TAIF)
6X[a]	Mt. Hsinkang, Taitung County, Taiwan	台灣 台東縣 新港山	121.28739	23.15065	*Kuo4091* (TAIF)
6X[a]	Nakama River, Iriomote Island, Okinawa Prefecture, Japan		123.83333	24.31667	*Kuo4128* (TAIF)
6X[a]	Yutsun river, Iriomote Isand, Japan		123.88333	24.36667	*Kuo4069* (TAIF)
6X[a]	Nagura, Ishigaki Island, Okinawa Prefecture, Japan		124.17983	24.40512	*Kuo4129* (TAIF)
6X[a]	Omoto, Ishigaki Island, Okinawa Prefecture, Japan		124.18333	24.41667	*Kuo4131* (TAIF)
6X[a]	Mt. Omoto, Ishigaki Island, Okinawa Prefecture, Japan		124.18453	24.42583	*Kuo4065* (TAIF)
6X[a]	Arakawa, Ishigaki Island, Okinawa Prefecture, Japan		124.18222	24.44298	*Kuo4130* (TAIF)
6X[a]	401 high land, Guishan Island, Ilan County, Taiwan	台灣 宜蘭縣 龜山島 401高地	121.95060	24.84184	*Kuo4066* (TAIF)
6X[a]	Sukuta, Nago-shi, Okinawa Prefecture, Japan		127.98767	26.56303	*Kuo4132* (TAIF)
6X[a]	Yaeyama-gun, Okinawa Pref., Japan		127.93681	26.62723	*Kuo4068* (TAIF)
6X[a]	Mt. Yonaha-dake, Kunigami-son, Okinawa Prefecture, Japan		128.21106	26.73083	*Kuo4133* (TAIF)
6X[a]	Inutabu, Isen-cho, Tokunoshima Island, Kagoshima Prefecture, Japan		128.91214	27.71811	*Kuo4134* (TAIF)
6X[a]	Kametsu, Tokunoshima-cho, Tokunoshima Island, Kagoshima Prefecture, Japan		128.97628	27.75864	*Kuo4136* (TAIF)
6X[a]	Todoroki, Tokunoshima-cho, Tokunoshima Island, Kagoshima Prefecture, Japan		128.92069	27.84239	*Kuo4135* (TAIF)
6X[a]	Sumiyo River, Kamiya, Amami-shi, Amami Isand, Kagoshima Pref., Japan		129.38733	28.28689	*Goro12286* (TNS)
6X[a]	Mt. Yuwan-dake, Yamato-son, Amami-oshima Island, Kagoshima Prefecture, Japan		129.32131	28.29775	*Kuo4137* (TAIF)
6X[a]	Naon, Yamato-son, Amami-oshima Island, Kagoshima Prefecture, Japan		129.33742	28.32683	*Kuo4138* (TAIF)
6X[a]	Yahata-Jinja, Suwanose-jima Isand, Toshima-mura, Kagoshima-gun, Kagoshima Prefecture, Japan		129.70147	29.61397	*Goro11383* (TNS)
6X[a]	Onoaida, Yakushima-cho, Yakushima Island, Kagoshima Prefecture, Japan		130.54815	30.24119	*Kuo4143* (TAIF)

(Table 6.1 cont. 2)

6X[a]	Onoaida, Yakushima-cho, Yakushima Island, Kagoshima Prefecture, Japan	130.54040	30.24923	*Kuo4073* (TAIF)
6X[a]	Shirataniunsuikyo, Yakushima-cho, Yakushima Island, Kagoshima Prefecture, Japan	130.57458	30.38003	*Kuo4144* (TAIF)
6X[a]	Hirauchi, Yakushima-cho, Yakushima Island, Kagoshima Prefecture, Japan	130.57458	30.38003	*Kuo4145* (TAIF)
6X[a]	Nagata, Yakushima-cho, Yakushima Island, Kagoshima Prefecture, Japan	130.39477	30.38471	*Kuo4139* (TAIF)
6X[a]	Mt. Kaimon, Kagoshima Pref., Japan	130.53064	31.17659	*Kuo4075* (TAIF)
6X[a]	Mt. Kaimon, Kagoshima Prefecture, Japan	130.53470	31.19254	*Kuo4141* (TAIF)
6X[a]	Tosenkyo Park, Ibusuki-shi, Kagoshima Prefecture, Japan	130.54232	31.22010	*Kuo4142* (TAIF)
6X[a]	Eboshi-dake Tunnel, Minamikyushu-shi, Kagoshima Prefecture, Japan	130.53395	31.24415	*Kuo4140* (TAIF)
6X[a]	Nakanogo, Hachijo Island, Tokyo Metropolis, Japan	139.81657	33.06387	*Kuo4154* (TAIF)
6X[a]	Mt. Mihara, Hachijo Island, Tokyo Metropolis, Japan	139.81940	33.08911	*Kuo4155* (TAIF)
6X[a]	Mt. Hachijo-fuji, Hachijo Island, Tokyo Metropolis, Japan	139.76534	33.13836	*Kuo4153* (TAIF)
6X[a]	Kuwanoki Valley, Ohga, Shungu-shi, Wakayama Prefecture, Japan	135.93206	33.72850	*Kuo4149* (TAIF)
6X[a]	UchiganoValley, Takata, Shungu-shi, Wakayama Prefecture, Japan	135.90200	33.73231	*Kuo4148* (TAIF)
6X[a]	Tashiro, Kiho-cho, Mie Prefecture, Japan	135.99100	33.76384	*Kuo4150* (TAIF)
6X[a]	Tairo-ike, Miyake-jima Island, Tokyo Pref., Japan	139.52890	34.05111	*Kuo4071* (TAIF)
6X[a]	Obarano, Owase-shi, Mie Pref., Japan	136.17639	34.06722	*AE sn. 2913* (TAIF)
6X[a]	Pref., Japan	138.98468	34.65320	*Kuo4152* (TAIF)
6X[a]	Shiroyama, Shimoda-Shi, Shizuoka Pref., Japan	138.95246	34.66612	*Kuo4074* (TAIF)
6X[a]	Shimoda, Shizuoka Prefecture, Japan	138.97318	34.71177	*Kuo4151* (TAIF)
6X[a]	Izu-Oshima Island, Tokyo Pref., Japan	139.38465	34.76122	*Kuo4072* (TAIF)

*The ploidy level determined by spore sizes; [a]the records from previous studies (Chapter 3 and 4).

Table 6.2. Different climatic variables from World Climate database

BIO1	Annual Mean Temperature
BIO2	Mean Diurnal Range (Mean of monthly (max temp - min temp
BIO3	Isothermality (BIO2/BIO7) (* 100)
BIO4	Temperature Seasonality (standard deviation *100)
BIO5	Max Temperature of Warmest Month
BIO6	Min Temperature of Coldest Month
BIO7	
BIO8	Mean Temperature of Wettest Quarter
BIO9	Mean Temperature of Driest Quarter
BIO10	Mean Temperature of Warmest Quarter
BIO11	Mean Temperature of Coldest Quarter
BIO12	Annual Precipitation
BIO13	Precipitation of Wettest Month
BIO14	Precipitation of Driest Month
BIO15	Precipitation Seasonality (Coefficient of Variation)
BIO16	Precipitation of Wettest Quarter
BIO17	Precipitation of Driest Quarter
BIO18	Precipitation of Warmest Quarter
BIO19	Precipitation of Coldest Quarter

equivalency and overlap between two cytotyps of *Deparia lancea.*

	Current	LIG
2X (grids)	18099	23204
6X (grids)	5066	39
Overlap (grids)	4235	39
Schoener's D	0.31	0.54

Chapter 7.

Summary and synthesis

Establishment and range expansion of Deparia *polyploids*

This thesis revealed that the polyploids in the genus *Deparia*, upon species level, might not always involve in the long-distance dispersal, and did not detect a significant difference between the long-distance dispersal rates of diploid and polyploid lineages. However, all *Deparia* species revealed with infra-specific range expansions association with polyploidization. Next, I studied the relationships between infra-specific range expansion and polyploidy evolution in *Deparia lancea*. The widely distributed autopolyploids, including sexual tetraploids and hexaploids distributed crossing East Asia, Himalayas regions, Borneo, and the Philippines (Batan Is.) arised from the conspecific diploids via multiple polyploidization events. The dated phylogenies further suggested the divergences of polyploids are relatively young (1.3 Ma >) comparing to that in the diploids. Nonetheless, the recent range expansions of these polyploid populations had not been restricted by the established sea barriers in East Asia Archipelago, which were first formed during the Early Pleistocene (2.0-1.55 Ma; Osozawa *et al.* 2012). By contrast, the extant diploids were found only in Taiwan Main Is., and there was no evidence for that diploids had established population via oversea dispersal. In addition, even being relative young in evolutionary ages, these sexual polyploids in *D. lancea* can rapidly expand their genetic diversity in populations by merging multiple origins and occasional homeologues recombination, and, thus, enhance their long-term evolutionary success. These, collectively, indicate that the historical factors, including young evolutionary age and recent geographical events, are not limitations for the natural establishment of these nascent polyploids and their subsequent expansion. Instead, as revealed with higher inferred dispersal rates and frequent oversea dispersals, these polyploids are considered to be acquired increased dispersal/colonization ability during their evolutionary process of natural establishment.

In case of *Deparia lancea* widespread line hexaploids, this thesis further demonstrated that reproductive factor should play the most evident role for their success of establishment and subsequent expansions.

Based on the results from inbreeding tolerance and population F_{IS}, these hexaploids were revealed with an increased inbreeding tolerance and less affected by inbreeding depression. Moreover, an inbreeding tending gender expression (i.e. tend to co-express antheridium and archegonium) in the gametophyte population of these hexaploids also suggested that they have been selected to prefer assortative mating and gametophytic selfing. This inbreeding ability, thus, not only assists their evolutionary establishment by avoiding to be outcompeted by the gametes from diploids but also increases their population colonization ability for subsequent range expansion. By contrast, broadening climatic niche in these hexaploids is unlikely primary cause for their range expansions. Although, the overall climatic niche dissimilarity between the diploids and non-dispersed hexaploids (i.e. which is referred for those in Taiwan Main Is. and presumed to characterize the situation before expansion) was resulted from niche modeling, based on the real occurrences, their climatic niches were revealed to be conserved. In addition, based on the model-reconstructed potential distributions (i.e. 0.14-0.12 Ma during the last inter-glacial) before these hexaploids expansion (i.e. as the inferred age after 0.004 Ma), hexaploids distribution range was revealed to be completely overlapped with the diploids. These suggested the potential distribution evolution in establishment of these hexaploids is likely processed from niche expasion without spontaneous niche diverge. Therefore, I concluded that the ecological factors were considered to less contribute to their success of establishment and subsequent range expansions. Instead, the gained inbreeding ability might be the major force for the widespread line hexaploids to explore the niche breathes during their oversea population colonization and range expansion.

Historical factor and formation/establishment of Deparia lancea *polyploids*

The polyploidized taxa, especially for those recently formed polyploids (i.e. neopolyploids), are generally revealed with no elevated diversification rate comparing with their non-polyploidized relatives (Mayrose *et al.* 2011; Scarpino *et al.* 2014). These finding correspond to the expectation of the high extinction risk in newly formed poplyploids, which are presumed under the intensive competition with diploid progenitors at many aspects (Parisod *et al.* 2010; Arrigo & Barker 2012; Ramsey & Ramsey 2014). Meanwhile, there are some evidences

implying that polyploids better survive than diploids in certain circumstances. Among extant angiosperm clades, there is a burst of ancient polyploidization events occurring within the time period between the Late Cretaceous and the Early Tertiary, and these polyploidizations seem to be coincided with KT mass extinction, when the severe environmental changes caused a global extinction of ~60% plant species (Fawcett *et al.* 2009; Vanneste *et al* 2014 a, b). Regarding to recent polyploidizations, (neo-)polyploids taxa in Europe and North America have been found with a higher proportion in the areas with vegetation strongly affected by Pleistocene glaciation than those without (reviewed in Ramsey & Ramsey 2014). Collectively, these imply a relation of polyploidy evolution to certain historical factors (Ramsey & Ramsey 2014). Although the formation rate of unreduced gamete can be related to environment factors, the link between polyploidy formation rates and eviromental changes in these historical events is still unclear (Ramsey & Schemske 1998; Ramsey & Ramsey 2014). Instead, the hypothesis of increased success for polyploid establishment under changing enviroment rather than the explanation directedly linking polyploidy with historical factors has received more discussions. It has been hypothized that the geological/climatic events generate new niches by disruption of original environments, and, thus, these disturbing areas provide available habitats for polyploid taxa to escape exctinction due to sympatric competition with their diploid proginetors (Arrigo & Barker 2012; Ramsey & Ramsey 2014).

The historical factors facilating polyploid establishments have also been implied for European ferns, in where the fern flora might have been affected by the Pleitocen glaciation (Vegel *et al.* 1999). However, no previous case elucidated the historical factor linking to fern polyploid establishment in East Asia region, and the Pleistocene glaciation seems less affect the flora in East Asia, especially in Pacific regions, comparing to that in Europe and North America (Qian & Ricklefs 2000; Harrison *et al.* 2001; Tiffney & Manchester 2001). As the first detailed case, in this thesis, I proposed that the sea barrier formation isolating East Asia Archipelago during the Early Pleistocene (2.0-1.55 Ma; Osozawa *et al.* 2012) could be an important historical factor initiating the successful establishment of polyploid lineages in *Deparia lancea*. Specifically, the geographical process isolating this island chain is hypothesized to generate habitats unable to be accessed by the diploid, which is revealed

with limitation of oversea population establishment ability. Thus, these newly released niches provide the "refugia" for recently formed polyploid lineages preventing from the competition with their diploidy progenitors. Then, these refugia can be rapidly occupied by polyploids since their formation are always accompanied with an increase of colonization ability. This hypothesis can be also supported by the dated phylogeny and divergence time estimates, which suggest that the polyploid lineages were formed during 1.84-0.28 Ma at time period of geographical barrier formation, and diverged within 1.3 Ma after geographical barrier formed. Similar cytogeographic pattern had be suggested in many other East Asian fern species, in which their conspecific diploids are restrictedly distributed but recently formed polyploids are widely distributed across many isolated regions (Shinohara *et al.* 2006; Lin & Iwatsuki 2010; Yamamoto *et al.* 2010; Hori *et al.* 2014).

Biogeography of Deparia lancea *polyploid formation/establishment*

In this thesis, I demonstrated the cytogeography and phylogeography of successfully established polyploids in *Deparia lancea*, including sexual tetraploids and hexaploids, and found that they are parapatricaly or allopatrically distributed with the diploids. At least for hexaploids, it is most likely that formation/polyploidization events of these polyploids have been taken place in Taiwan Main Is., where the only area diploids have been found (see Chapter 3, 4, and 6). Regardless of multiple origins revealed in both these tetraploids and the widespread line hexaploids, their current populations with highest genetic diversity, however, were found distant to the distribution center of diploid population. Regarding to such distribution patterns, I proposed the biogeographic scenario for natural establishment of these polyploids, and this scenario was similar to source-to-sink speciation process (Goldberg *et al.* 2011). Thus, these polyploids were initially sympatrically distributed with their diploid progenitors as the consequence of their formation/polyploidizations, and, then, dispersed to and established allopatric population in the other regions. The subsequent extinctions of the sympatric population in polyploids were caused by intensive competitions from the diploids, and finally these resulted in the allopatry toward distribution for current polyploid population. Based on these, the natural selections reacted on the processes from sympartic formation (i.e. source) to allopatric population establishment (i.e. sink) in polyploidy evolution.

In addition to the accompanied increase of inbreeding tolerance resulted from duplicated homoeologs in polyploidy genome, the historical event of sea barriers formation isolating East Asia Archipelago might be an important factor facilitating successful establishments of *D. lancea* polyploids (see the previous section). For the widespread line hexaploids, the inbreeding tending gender expression should be also a critical trait with selective advantage favoring their polyploidy establishment. In addition to historical and reproductive factors, the ecological niche shifts and differentiations might be selected for the allopatric population establishment in H12-14 line hexaploids, for which their populations were mostly found in the mountain region > 1000m of Taiwan Main Is. and maladapted to lowerland environments (Kuo *et al.* unpublished).

In the case of source-to-sink speciation (see example in Goldberg *et al.* 2012), the allopatric and parapatric speciation resulting in a new taxon requires a high dispersal rate from core (i.e. source) to marginal (i.e. sink) population. This high amount of dispersals reduces allopatric extinction risk of marginal population, and, thus, elevates the success of an allopatric speciation. Similarly, the successful establishment of a polyploid taxon might require multiple times of formation/polyploidization, for which polyploidy fern taxa have been revealed with multiple origins and continuous range expansion (see in Chapter 3). In addition, these explain why occasional long-distance dispersal events, which carry founder from single or few origins, are not always associated with polyploidy evolution as revealed in the historical biogeography of genus *Deparia* upon species level phylogeny (see in Chapter 2; also see Linder & Barker 2014). This proposed biogeography scenario can also explain cytogeography of other fern polyploids, such as *Deparia petersenii* subsp. *petersenii* and *Cytormium falcatum* complex (Matsumoto 2003; Shinohara *et al.* 2006), but the detailed mechanism involving in these successful polyploid establishements are required further studies in the future.

References

Arrigo N, Barker MS (2012) Rarely successful polyploids and their legacy in plant genomes. *Current Opinion in Plant Biology*, **15**, 140–146.

Fawcett JA, Maere S, Van de Peer Y (2009) Plants with double genomes might have had a better chance to survive the Cretaceous-Tertiary extinction event. *Proceedings of the National Academy of Sciences of the United States of America*, **106**, 5737–5742.

Goldberg EE, Lancaster LT, Ree RH (2011) Phylogenetic inference of reciprocal effects between geographic range evolution and diversification. *Systematic Biology*, **60**, 451–465.

Harrison SP, Yu G, Takahara H, Prentice IC (2001) Diversity of temperate plants in east Asia. *Nature*, **413**, 129–130.

Hori K, Tono A, Fujimoto K *et al.* (2014) Reticulate evolution in the apogamous *Dryopteris varia* complex (Dryopteridaceae, subg. Erythrovariae, sect. Variae) and its related sexual species in Japan. *Journal of Plant Research*, **127**, 661–684.

Lin SJ, Iwatsuki K (2010) A new sexual diploid of *Dryopteris erythrosora* complex (Dryopteridaceae) from Oki Islands, Japan. *Bulletin of the Faculty of Life and Environmental Science, Shimane University*, **15**, 11–13.

Linder HP, Barker NP (2014) Does polyploidy facilitate long-distance dispersal? *Annals of Botany*, **113**, 1175–1183.

Matsumoto S (2003) Species ecological study on reproductive systems and speciation of *Cyrtomium falcatum* complex (Dryopteridaceae) in Japanese archipelago. *Annals of the Tsukuba Botanical Garden*, 1–141.

Mayrose I, Zhan SH, Rothfels CJ *et al.* (2011) Recently formed polyploid plants diversify at lower rates. *Science*, **333**, 1257.

Osozawa S, Shinjo R, Armid A *et al.* (2012) Palaeogeographic reconstruction of the 1.55 Ma synchronous isolation of the Ryukyu Islands, Japan, and Taiwan and inflow of the Kuroshio warm current. *International Geology Review*, **54**, 1369–1388.

Parisod C, Holderegger R, Brochmann C (2010) Evolutionary consequences of autopolyploidy. *New phytologist*, **186**, 5–17.

Qian H, Ricklefs R (2000) Large-scale processes and the Asian bias in species diversity of temperate plants. *Nature*, **407**, 12–14.

Ramsey J, Ramsey T (2014) Ecological studies of polyploidy in the 100 years following its discovery. *Proceedings of the Royal Society B: Biological Sciences*, **369**, Doi: 10.1098/rstb.2013.0352.

Ramsey J, Schemske DW (1998) Pathways, mechanisms, and rates of polyploid formation in flowering plants. *Annual Review of Ecology and Systematics*, **29**, 467–501.

Scarpino SV, Levin DA, Meyers LA (2014) Polyploid formation shapes flowering plant diversity. *The American Naturalist*, **184**, 456–465.

Shinohara W, Hsu TW, Moore SJ, Murakami N (2006) Genetic analysis of the newly found diploid cytotype of *Deparia petersenii* (Woodsiaceae: Pteridophyta): evidence for multiple origins of the tetraploid. *International Journal of Plant Sciences*, **167**, 299–309.

Tiffney BH, Manchester SR (2001) The use of geological and paleontological evidence in evaluating plant phylogeographic hypotheses in the northern hemisphere Tertiary. *International Journal of Plant Sciences*, **162**, S3–17.

Vanneste K, Baele G, Maere S, Peer Y Van de (2014a) Analysis of 41 plant genomes supports a wave of successful genome duplications in association with the Cretaceous-Paleogene boundary. *Genome Research*, **24**, 1334–1347.

Vanneste K, Maere S, Peer Y Van de (2014b) Tangled up in two: a burst of genome duplications at the end of the Cretaceous and the

consequences for plant evolution. *Philosophical Transactions of the Royal Society B*, **369**, Doi: 10.1098/rstb.2013.0353.

Vogel J, Rumsey F, Schneller J, Barrett J, Gibby M (1999) Where are the glacial refugia in Europe? Evidence from pteridophytes. *Biological Journal of the Linnean Society*, **66**, 23–37.

Yamamoto K, Murakami N, Ebihara A (2010) The distribution of *Dryopteris caudipinna* (Dryopteridaceae), a sexually reproducing counterpart of the apogamous D. erythrosora, in Japan. *Acta Phytotaxonomica et Geobotanica*, **61**, 109–114.

Protocol 1. A modified CTAB method for DNA extraction of silica-dry/fresh materials in ferns

3X CTAB buffer <autoclaved and keep under room temperature>:

0.1 M Tris HCl pH 8.0
1.4 M NaCl
0.02 M EDTA
30 mg/mL CTAB

PCI solution <for DNA use keep in 4℃ avoid light>:

Phenol: Chloroform: IAA, 25:24:1 mixture in pH 7.5-8.0

CI solution <keep in 4℃ avoid light>:

Chloroform: IAA, 24:1 mixture

Steps

1. Estimate 1 mL 3X CTAB buffer for each sample.
2. Add 5 μL β-mercaptoethanol and 4 mg PVPP for per mL of 3X CTAB buffer just before use.
3. Squeeze appropriate amount of frond samples from specimen in N_2(l).
4. Mixture 1 mL of CTAB solution with sample powder immediately, and transfer into 2.0 mL eppendof.
5. Incubate samples in 65℃ for 30 mins.
6. Add 500 μL PCI solution into each sample then shake them in inverted manner for 2-3 hours under room temperature. <Using CI solution to replace PCI is better for some taxa in this step>
7. LUNCH! <optional>
8. Apply samples into table centrifuge under 13000 rpm 10 mins.
9. Transfer the aqueous part (upper layer) into a new 2.0 mL eppendof with 500 μL CI solution, and shake samples in inverted manner for 0.5-1 hour under room temperature.
10. Apply samples into table centrifuge under 13000 rpm 10 mins.
11. Repeat step 8-9 again, but substitute the CI solution for Chloroform (99%).
12. Transfer the aqueous part into new 1.7 mL eppendof(s) and mix with 2/3 (1/2 if

sample is in dark color) volume of isopropanol.

13. Apply samples into table centrifuge under 13000 rpm 10 mins.
14. If pellet appear, remove solution part. Then, spin down and remove all solution completely. <if pellet not appear add more isopropanol and/or keep in -20℃ for two hours, and go back to step 11>
15. Dry the pellet by vacuum centrifuge for 10 mins.
16. Apply 100 μL ddH_2O to dissolve pellet at 65℃ on heater for 10mins or longer.
17. Store the extracted DNA solution in -20℃.

Related references

Varma A, Padh H, Shrivastava N (2007) Plant genomic DNA isolation: an art or a science. *Biotechnology Journal*, **2**, 386－392.

Protocal 2. A modified CTAB-Qiagen column for DNA extraction in ferns

3X CTAB buffer <autoclaved and keep under room temperature>:

0.2 M Tris HCl pH 8.0
1.4 M NaCl
0.02 M EDTA
30 mg/mL CTAB

PCI solution <for DNA use keep in 4℃ avoid light>:

Phenol: Chloroform: IAA, 25:24:1 mixture in pH 7.5-8.0

CI solution <keep in 4℃ avoid light>:

Chloroform: IAA, 24:1 mixture

Qiagen DNeasy Plant Mini Kit

Steps

3. Estimate 1 mL 3X CTAB buffer for each sample.
4. Add 5 μL β-mercaptoethanol and 4 mg PVPP for per mL of 3X CTAB buffer just before use.

For fresh/silica-dry material <3.1>

3.1 Squeeze appropriate amount of frond samples from specimen in N_2(l).

For specimen material <3.2>

3.2 Apply specimen fragments ≤ 20 mg into 2.0 mL tube with beads for homogenizer.

In the following steps, filter tips are recommend to use.

18. Mixture 1 mL of CTAB solution with sample powder immediately, and transfer into 2.0 mL eppendof.
19. Incubate samples in 65℃ for 30 mins.
20. Add 500 μL PCI solution into each sample then shake them in inverted manner for 2-3 hours under room temperature. <Using CI solution to replace PCI is better for some taxa in this step>
21. LUNCH! <optional>
22. Apply samples into table centrifuge under 13000 rpm 10 mins.
23. Transfer the aqueous part (upper layer) into a new 2.0 mL eppendof with 500 μL

CI solution, and shake samples in inverted manner for 0.5-1 hour under room temperature.

24. Apply samples into table centrifuge under 13000 rpm 10 mins.
25. Repeat step 9-10 again, but substitute the CI solution for Chloroform (99%).
26. Transfer the aqueous part into new eppendof(s) and mix with 5 times volume of Qiagen binding buffer (buffer AP3). <the following steps are slightly modified from Qiagen protocol>
27. Transfer appropriate volume of the mixture into DNA binding column (DNeasy Mini spin column) with 2 ml collection tube, then apply samples into table centrifuge under ≥ 8000 rpm 1 min. Discord the flow-through.
28. Repeat step 11 for remaining mix solution.
29. Add 500 μl washing buffer (buffer AW) to DNA binding column, and then centrifuge under ≥ 8000 rpm 1 min. Discord the flow-through. <if the flow-through or membrane of DNA binding column show colored, recommend repeat this step until the color becomes disappear or diluted. 95-100% ethanol can be used to substitute washing buffer for more efficient clearing>
30. Dry the DNA binding column under 13000 rpm 5 mins in table centrifuge.
31. Discard the collection tube, and apply DNA binding column to a new 1.5 ml eppendof.
32. Dry the DNA binding column in vacuum centrifuge for 10 mins.
33. Apply 50 μL ddH_2O onto DNA binding column at 65℃ for 2-3 min, and then centrifuge under ≥ 8000 rpm 1 min.
34. Repeat step 17 again, discord the DNA binding column and store the extracted DNA in -20℃.

Related references

DNeasy Plant Handbook — October 2012.
http://www.qiagen.com/resources/download.aspx?id=95dec8a9-ec37-4457-8884-5dedd8ba9448&lang=en

Varma A, Padh H, Shrivastava N (2007) Plant genomic DNA isolation: an art or a science. *Biotechnology Journal*, **2**, 386－392.

Protocol 3. A modified Beckman protocol to estimate ploidy level and nuclear DNA content in ferns

Chopping buffer <keep in 4℃>:

1.0% TritonX-100

50 mM Na_2SO_3

50 mM Tris-HCl (pH7.5)

RNase solution < keep in -20℃>:

10mg/mL

PI solution < keep in 4℃ in dark>:

2.04g/mL

Steps

1. Preparing 1.5 mL of Chopping buffer per sample (or standard).
2. Add 0.04g PVP-40, 5 μL β-mercaptoethanol, 1 μL RNase (10mg/mL) per mL of chopping buffer just before use.
3. Add 500 μL of buffer to every glass petri dish.
4. Add ~400 mm^2 of material (young leave usually better) per sample (or standard) to each petri dish, and chop by a razor. <This step keep on ice>
5. After chopping, placed the sieve (50 mm nylon mesh) onto the 2.0 mL eppendorf, and transfer mixture of buffer/material into the sieve.
6. Add additional chopping buffer for each sample/standard until total volume larger or around 1 mL, and remove the sieve.
7. Invert gently several times, and incubate in 37℃ for 15 mins.
8. Invert gently several times, and transfer 500 μL of each sample (or standard) into a new 2.0 mL eppendorf. The remaining sample (standard) keep in 4℃.
9. Add 10μL PI solution (2.04g/mL) for each sample (or standard), and invert them gently several times.
10. Keep in dark 4℃ for 1 hour for staining.

For the using of internal standard

11. After first round for estimation of nuclear particle concentration of each sample

and standard.

12. Invert the sample and standard (the remaining one of step 8) gently several times, and transfer the appropriate volume of sample mix with appropriate volume of standard.
13. Add 1μL PI solution (2.04g/mL) for per 50 μL of sample/standard mixture.
14. Keep in dark 4℃ for 10-20 mins for staining.

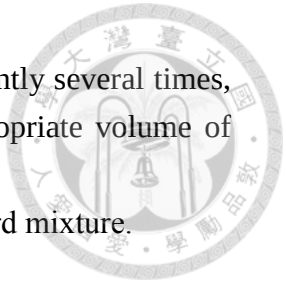

Related References

Doležel J, Greilhuber J, Suda J (2007) Estimation of nuclear DNA content in plants using flow cytometry. *Nature Protocols*, **2**, 2233－2244.

Doležel J, Greilhuber J, Suda J (2007) Flow Cytometry with Plant Cells: Analysis of Genes, Chromosomes and Genomes. Publisher: Wiley-VCH Verlag GmbH & Co. KGaA.

Ebihara A, Ishikawa H, Matsumoto S *et al.* (2005) Nuclear DNA, chloroplast DNA, and ploidy analysis clarified biological complexity of the *Vandenboschia radicans* complex (Hymenophyllaceae) in Japan and adjacent areas. *American Journal of Botany*, **92**, 1535－1547.

Johnston JS, Bennett MD, Rayburn AL, Galbraith DW, Price HJ (1999) Reference standards for determination of DNA content of plant nuclei. *American Journal of Botany*, **86**, 609－613.

Protocol 4. Single Strand Conformation Polymorphism applying for AE-6290 (ATTO, Tokyo, Japan)

Gel preparation for SSCP analyses:

1. Mix MDE solution **5 mL**, 10×TBE **1 mL**, ddH_2O **13.2 mL** and 50% glycerin **0.8 mL** (2%) by stir, and cover the container by membrane when mixing.
2. Prepare the gel makers.
3. Add TEMED **8 μL** and 10% ammonium peroxodisulfate **80 μL** into solution. Mix for a while, and then transport mixed solution into gel maker. Insert the comb and wait for gel solidification for more than **2 hours**.

Electrophoresis and cooling system setup:

1. Subject the solidified gel with gel maker into electrophoresis system which is filled with 0.5×TBE and flush the wells on gel.
2. Setup the cooling system and pre-run the system (**350V, 20℃**) for **30 min**.

DNA sample preparation and electrophoresis:

1. For each sample, mix formamide:BPB solution (9:1) **18 μL** with DNA amplicon **2 μL** in 0.2 μL PCR eppendorf for **5 min** denaturing at **94℃** in heat block. **Freeze** samples on cooler **2 min**.
2. Load **5μL** for each sample and DNA ladder into wells. Electrophoresis at **350V** under at constant temperature **20℃** for **14 hours**.

Related references

Gasser RB, Hu M, Chilton NB, Campbell BE et al. (2006) Single-strand conformation polymorphism (SSCP) for the analysis of genetic variation. *Nature Protocols*, **1**, 3121－3128.